Adaptive Mechanisms of the Heart to Ischaemic Stress

Lockie, Tim

Awarding institution:
King's College London

Adaptive Mechanisms of the Heart to Ischaemic Stress

Version 1.3

Timothy Paul Emrys Lockie

Kings College London
Cardiovascular Division
Rayne Institute, BHF Centre
4th Floor Lambeth Wing
St Thomas' Hospital
London, SE1 7EH

Submitted for the

Degree of Doctor of Philosophy

To the University of London

2012

ABSTRACT

Background

The response of the human heart to ischaemic stress is not uniform and adaptive mechanisms play a role in attenuating myocyte damage and improving performance. The mechanisms of such adaptations are poorly understood and likely multifactorial. The main aim of this thesis was to examine these mechanisms using the models of exercise induced myocardial ischaemia and acute myocardial infarction

Methods

Using a specially adapted supine ergometer, we used invasive physiological measurements and high-resolution cardiac magnetic resonance imaging to assess changes in coronary blood flow, central haemodynamics and transmural myocardial perfusion during exercise. In a separate group, we sought to examine the role of *post-conditioning* as a potential therapeutic tool in a randomised controlled trial involving patients undergoing primary percutaneous revascularisation for acute myocardial infarction.

Results

We were able to demonstrate that the reduction of ischaemia seen on second exercise in patients with stable coronary artery disease is associated with synergistic changes in central and coronary haemodynamics, with a fall in myocardial microvascular resistance and enhanced vascular-ventricular coupling. High-speed CMR perfusion imaging using *k*-t acceleration is a feasible tool to investigate these differences, with sufficient spatial resolution to detect transmural flow heterogeneity. The data from the postconditioning study did not show a difference in infarct size between the groups but numbers were small.

Conclusion

The mechanisms of adaptation of the heart to ischaemic stress are complex and likely multifactorial. These results suggest that synergistic changes in systemic and coronary circulations as part of a generalised reactive hyperaemic vasodilatory response to exercise results in improved myocardial perfusion and overall

performance. Transmural flow redistribution to the subendocardium is likely to play an important role in attenuating myocardial ischaemia on repeat exercise although we await the results of ongoing work. Innate myocardial protection, such as that afforded by postconditioning remains a possibility, although the results from this study are inconclusive.

ACKNOWLEDGMENTS

I would like to thank my supervisors, Professor Simon Redwood and Professor Sven Plein for their inspiration and expertise throughout the period of my research. I am also deeply indebted to Professor Michael Marber. The clinical studies in this thesis were a challenge to get going as all had to be practically started from scratch, especially those relating to the exercise bikes that were specially developed for the catheterisation lab and the MRI scanner. They all required endless meetings to convince, cajole and eventually complete and without the enthusiasm and support of my supervisors this project would certainly have fallen short at any of the innumerable hurdles that arose along the way.

On this note I would also like to thank the staff of the cath labs at St Thomas' who would let out a groan as I wheeled my research kit into the lab for another study, but without whom these studies could not have been completed and whose suggestions and advice were invaluable in the evolution of the final clinical protocol. I am also grateful to the skills and patience of the CMR radiographers in the Rayne Institute for expertly optimising and assisting in the CMR studies.

I would like to thank all my fellow research fellows for their important help in recruitment of patients and volunteers. I am also very grateful to Dr. Maria Siebes and her team at the AMC Hospital in Amsterdam for their generous support with data analysis and world-class expertise in the intricacies of coronary pressure and flow measurements.

I would like to acknowledge all the beautiful places around the world where my family has spread, including Malabar (Australia), Unterphüret (Austria), El Trapiche (Spain) and Alissos (Greece). I was lucky enough to go and spend time in each one over the last year and as well as the warmth and familiarity provided by all my loved ones I was able find a small corner with my lap-top and complete the writing of this thesis.

I am also deeply grateful to my wife Nadia, who was a constant source of support and love without whom I could not have completed this work. It is to her that I dedicate my thesis.

This Thesis was kindly supported by a Fellowship from the British Heart Foundation

TABLE OF CONTENTS

LIST OF FIGURES

1 BACKGROUND

Coronary atherosclerosis is endemic in the Western world and is the principle cause of morbidity and mortality[1]. The classical symptoms of angina have long been described in the medical literature[2] yet our understanding of their origins are poorly understood.

"But there is a disorder of the breast marked with strong and peculiar symptoms, considerable for the kind of danger belonging to it, and not extremely rare, which deserves to be mentioned more at length. The seat of it, and sense of strangling, and anxiety with which it is attended, may make it not improperly be called angina pectons. They who are afflicted with it, are seized while they are walking, (more especially if it be up hill, and soon after eating) with a painful and most disagreeable sensation in the breast, which seems as if it would extinguish life, it it were to increase or to continue; but the moment they stand still, all this uneasiness vanishes."

William Heberden **(1795)**

Figure 1. Dr Heberden who first described classical angina pectoris [*from Medical Transactions, Royal College of Physicians in London, 1795*][2]

1.1 Anatomy and Physiology of the Human Circulation

1.1.1 The Coronary Circulation

The coronary circulation can be divided into three compartments: arteries, microcirculation, and veins. The microcirculation can be further split into arterioles, capillaries and venules. The epicardial compartment includes vessels ranging from 0.5mm-5mm. The predominant function of these vessels is to provide capacitance and under normal conditions they offer minimal resistance to flow. The small arteries then branch out into pre arterioles, which are 200µm -500µm in diameter and are located on the epicardial surface of the heart. These vessels maintain pressure at the entrance to the arterioles and are able to compensate for changes in flow. These develop into arterioles less than 200µm, which can be further divided into three sub compartments, each characterised by their size, function and predominant regulatory mechanism. There is a significant overlap between the mechanisms that regulate the flow of blood into the microcirculation. There is a tendency for each domain of microvessel to have a predominant regulating mechanism, and in the event that one mechanism becomes dysfunctional or is inhibited, then other mechanisms become active to compensate. The largest of these arterioles are 100µm -200µm in diameter. Kuo et al. demonstrated that endothelial dependent dilation was most prominent in larger arterioles and least effective in the smallest vessels[3]. In these vessels, an increase in flow rate causes vasodilatation and a reduction in flow causes vasoconstriction. The medium sized arterioles are 40µm - 100µm in diameter and the main regulating mechanism is dependent on intraluminal pressure changes in the vessels. Intraluminal pressure is detected by vascular smooth muscle cell stretch receptors, which respond to increased intraluminal pressure by causing vasoconstriction. Conversely a reduction in intraluminal pressure causes compensatory vasodilatation due to smooth muscle relaxation. This pressure sensitive mechanism is known as myogenic control[4]. Endothelial dependent mechanisms are also present in medium sized arterioles, although the dominant mechanism is myogenic mediation. The smallest arterioles (<30 µm) are regulated by changes in metabolic activity, whereby an increase in

metabolic activity leads to vasodilatation[3]. Therefore in the microcirculation, an increase in metabolic activity initially causes the tiny vessels to dilate. This causes a secondary reduction in pressure upstream in the medium sized vessels causing myogenic dilation, leading to increased flow further upstream in the larger arterioles causing endothelial dependent dilation[5]. This self-regulating mechanism allows for an integrated sequential activation from the smallest vessels to the largest arterioles in response to increased metabolic demand. These mechanisms are discussed in further detail below.

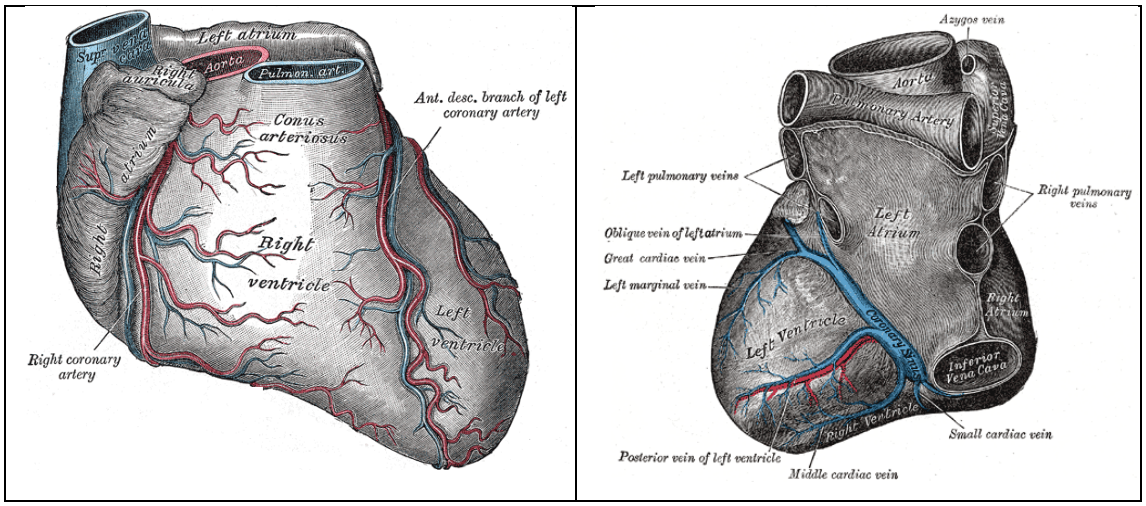

Figure 2. Anatomy of the heart showing the major epicardial coronary arteries [*taken from Gray's Anatomy, fig 491, p371, Philidelphia, 1918*]

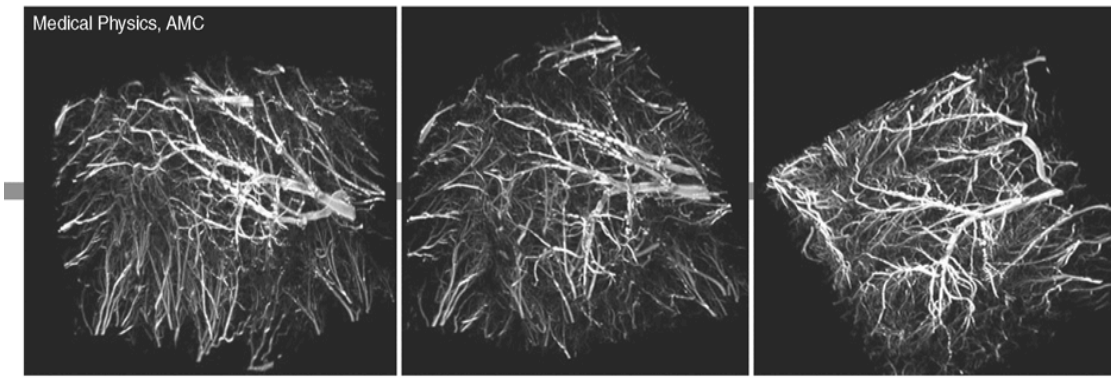

Figure 3. 3-Dimensional reconstruction of cryomicrotome images taken of the coronary microcirculation illustrating the dense web of vessels [*images courtesy of Jos Spaan, AMC Hospital, Amsterdam, Netherlands*[6]]

1.1.2 Coronary Blood Flow and Exercise: In the Normal Heart

The heart is primarily dependent on oxidative phosphorylation for energy production. This means that any increase in cardiac activity is dependent on rapid, almost instantaneous, parallel increases of oxygen availability. In contrast to skeletal muscle, that has very low metabolic requirements during rest periods, the resting oxidative requirements of the myocardium are far higher. In order to sustain such activity the myocardial tissue maintains a very high level of oxygen extraction so that 70-80% of available oxygen is extracted from the arterial blood supplying it. This compares to skeletal muscle where the extraction fraction is closer to 30-40%[7]. Such levels of oxygen extraction in the myocardium are made possible through high capillary density, typically in the region of 3,000-4,000/mm^2, as opposed to 500-2,000/mm^2 in skeletal muscle[8]. Because of such highly efficient oxygen extraction during basal conditions, when metabolic demands on the myocardium are increased (such as during exercise) these needs are met principally by augmenting coronary blood flow rather than further oxygen extraction[9].

1.1.2.1 Increased Myocardial Oxygen Demand

Exercise is the most important physiological stimulus for increasing myocardial oxygen demand. The increase in metabolic requirements of the exercising skeletal muscle necessitates a corresponding increase in blood flow that is met by vasodilatation of the resistance vessels largely located in the skeletal muscle. Such vasodilatation requires an increase in cardiac output, facilitated by an increase in arterial pressure. Such haemodynamic changes result in an increase in each of the key determinants of myocardial oxygen demand, *heart rate* and *contractility* and *ventricular work*[10].

Heart Rate

Studies using rapid pacing as a stimulus have suggested that up to 30-40% of the increase in coronary blood flow during exercise can be attributed to increases in heart rate[11]. However, such studies do not offer a surrogate for exercise-stress as the increased heart rate produced by pacing alone actually causes a *reduction* in the ventricular work of each beat through a decrease in end-diastolic volume and stroke

volume, thereby underestimating myocardial oxygen consumption[12]. Overall, the increase in heart rate during exercise is thought to contribute around 60% of the increased myocardial oxygen consumption[13].

Contractility

Beta-adrenergic activation as well as the direct positive inotropic effect of heart rate cause the increased contractility observed during exercise[14]. In studies that used propanolol to block beta-adrenergic receptors and rapid pacing to maintain a steady heart rate it was estimated that the contribution of increased contractility to the increase in oxygen consumption during exercise was in the region 15-25%[15, 16]. The effect of beta-blockers in reducing left ventricular systolic pressure and stroke volume and consequently left ventricular work per beat also needs to be considered[11].

Ventricular Work

Left ventricular work goes up during exercise in proportion to the increased afterload that is primarily formed by increases in systolic arterial pressure. It is also related to the increase in left ventricular end-diastolic volume[17, 18]. External work increases as a result of the augmented stroke volume and hence smaller end-systolic volume caused by the increased contractility resulting in an overall increase in ventricular work. This accounts for around 15-25% of the increased myocardial oxygen demand during exercise[19].

1.1.2.2 Increased Myocardial Oxygen Supply

The increased oxygen demands of the myocardium during exercise are primarily met through an augmentation in coronary flow. The increase in coronary blood flow results from a combination of coronary vasodilatation, with a reduction in coronary vascular resistance, and an increase in mean arterial pressure[20-22].

Coronary Blood Flow

Resting left ventricular coronary blood flow in humans is in the range 0.5-1.5ml/min/mg myocardium[23-26]. Dynamic exercise increases coronary blood flow in proportion to the heart rate, with peak values during maximal exercise typically 3 to

5 times the resting level[26, 27]. This relationship is amazingly similar across different species with a strong correlation on regression analysis of left ventricular blood flow against heart rate[13, 28, 29].

Oxygen-carrying Capacity

Unlike other species where oxygen delivery may be improved by a rise in haemoglobin[20, 30], the haemoglobin concentration in humans increases by no more than 15% in response to upright exercise[31] This is largely as a result of a reduction in plasma volume resulting from extravasation of fluid from the capillaries during exercise[32]. In addition, arterial oxygen tension and saturation are generally unchanged during different grades of exercise in normal humans[31].

Myocardial Oxygen Extraction

In many species the increase in oxygen delivery to the heart does not meet demand thereby requiring an increase in oxygen extraction. In humans this increase is relatively small due to the high levels of basal extraction attained at rest[31, 33]. The decrease in blood pH resulting from lactate production by working skeletal muscle has been reported to cause a rightward shift of the haemoglobin oxygen dissociation curve thereby facilitating oxygen delivery to the myocardium, with an observed 8% drop in coronary venous oxygen content, but minimal change in coronary oxygen venous tension during exercise[27, 34]. Although the vast majority of increased oxygen demands are met through increased blood flow, several mechanisms are thought to contribute to this need for increased oxygen extraction. Adrenergic-mediated vasoconstriction may attenuate the maximal increase in coronary blood flow during exercise and hence contribute to the need for increased oxygen extraction. Studies using α-adrenergic blocking agents showed an increase in myocardial blood flow during exercise with a corresponding fall in myocardial oxygen extraction[35, 36].

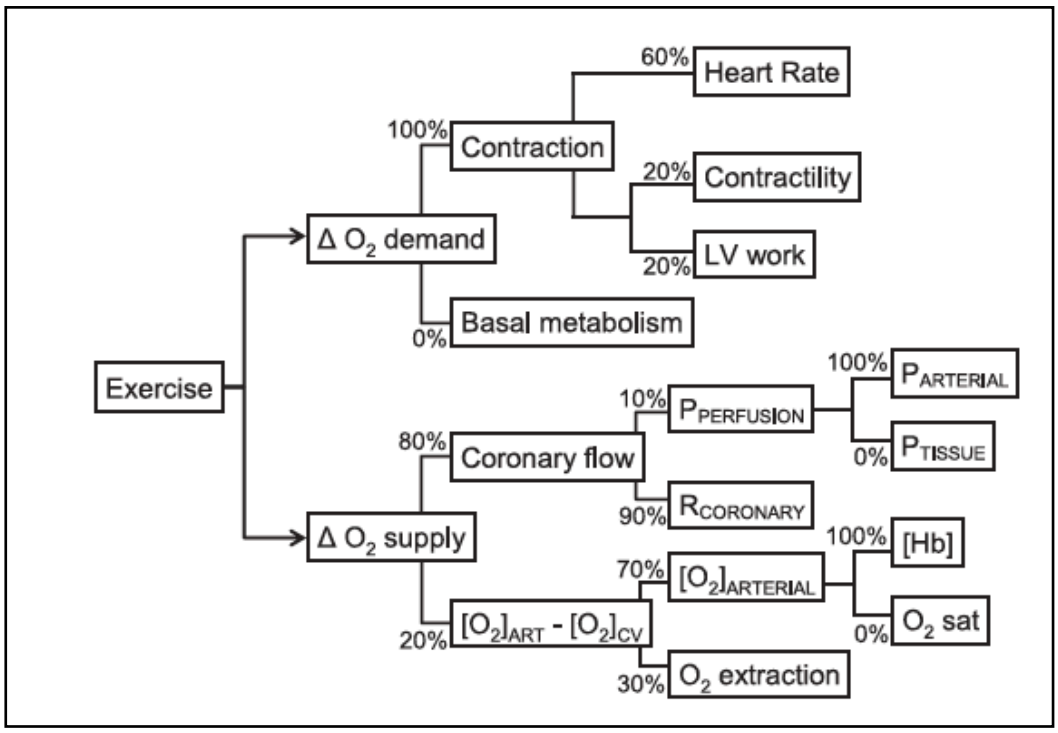

Figure 4. A schematic overview of the effect of exercise on myocardial oxygen balance. Shown are the contributions of the variables to the exercise-induced increase in myocardial oxygen demand (ΔO_2 demand) and supply (ΔO_2 supply). $P_{PERFUSION}$ =coronary perfusion pressure; $R_{CORONARY}$ =coronary vascular resistance; P_{TISSUE} =intramyocardial tissue pressure; $[O_2]_{ART}$ =arterial oxygen content; $[O_2]_{CV}$ =coronary venous oxygen content; [Hb] =haemoglobin content; O_2 sat =oxygen saturation. [*Adapted from Dunker et al, p.1012*[37]]

1.1.2.3 Determinants of Coronary Blood Flow

Autoregulation

Autoregulation is defined as the capacity to maintain constant blood flow in the face of a change in perfusion pressure (with constant metabolic needs). In the myocardium so-called autoregulation curves demonstrate this phenomenon. When coronary perfusion pressure is decreased, but still within the physiological range, progressive vasodilatation of the resistance vessels ensures that coronary flow is maintained. The plateau of the autoregulation curve shifts upwards with an increase in metabolic demand. At a given perfusion pressure, coronary flow reserve (CFR, the ratio of maximum to basal coronary blood flow) can be determined from the difference in flow as dictated by the pressure-flow lines in the presence of autoregulatory mechanisms and maximal vasodilatation.

Coronary Vascular Resistance

While the increased blood flow to the heart is in part due to the increased effective perfusion pressure the majority of increase in coronary blood flow is mediated through a reduction in coronary vascular resistance. Total coronary resistance is the sum of both passive (structural) and active (smooth muscle tone) components. In the completely vasodilated bed, flow to the different regions of the heart is determined by the cross-sectional area of the vessels, the length of the vasculature, and the number of parallel vessels that supply a defined perfusion territory. Blood flow has 3 major resistance components: the epicardial vessel (R1), the small arteries and arterioles (R2) and the intramyocardial capillary system (R3). When coronary reserve is normal these 3 resistances are assumed to be functioning normally. In patients without atherosclerosis, the large epicardial vessel resistance (R1) is trivial. Arteries with diameter >400µm have only minimal resistance. It is suggested that 90% of the adjustment of coronary resistance that controls autoregulation resides in the small (<400µm) resistance vessels, due to the integrated response of several mechanisms.

The *myogenic response* describes the property of these small resistance vessels to respond to a change in transmural pressure by changing tone, resulting in a diameter change in a direction opposite to the pressure stimulus[38, 39]. When the vasodilatory capacity of these vessels is exhausted and vasomotor tone is absent during ischaemic heart disease or following administration of vasodilators, then the vessels react passively to changes in intraluminal pressure and their diameter changes in the same direction as intraluminal pressure[40, 41].

Flow dependent dilatation refers to the property of endothelial cells to respond to an increase in blood flow by releasing nitric oxide (NO), which relaxes smooth muscle tone and induces vasodilatation. Endothelial dependent hyperpolarizing factor (EDHF) may act as a reserve for the NO-mediated flow-dependent dilatation mechanism[42].

1.1.2.4 Transmural Redistribution of Myocardial Blood Flow

There is abundant proof that coronary perfusion is impeded by cardiac contraction, a process known as coronary systolic flow impediment (CSFI)[43, 44]. This means that

during basal conditions coronary arterial blood flow occurs predominantly during diastole.

However, during heavy exercise due to high heart rates there is a progressive increase in systolic flow such that up to 40-50% of coronary blood flow may occur during systole[20, 45]. This has important implications for the transmural distribution of blood flow, where the effects of ventricular extravascular compression have a disproportionate effect on the subendocardium. During exercise there is a redistribution of blood away from the subendocardial region towards the epicardium[46].

The Effect of Extravascular Compressive Forces

The pressure drop across the coronary vascular bed determines its effective perfusion pressure, with the proximal pressure equal to central aortic pressure. The effective backpressure, however, cannot be simply derived from right atrial pressure because of the extravascular forces exerted on the compressible intramural coronary vessels by the surrounding myocardium. The *"vascular waterfall"* and model addresses the interaction between the intravascular distending pressure and the extravascular compressive forces that occur during systole[43, 44, 47, 48]. It assumes that the radial stress in the ventricular wall generates a tissue pressure that varies over the myocardial wall, from LV pressure at the endocardium to thoracic pressure at the epicardium. It further assumes that this tissue pressure acts on the outer surface of the intramural vessels as a fluid pressure. If tissue pressure happens to exceed coronary arterial pressure, then coronary flow would cease altogether. With a lower tissue pressure only intramural veins would collapse locally and at this point intramural pressure would equal tissue pressure. Flow, therefore, would be equal to the difference between arterial and tissue pressure divided by the vascular resistance between coronary main artery and the point of collapse. Thus, during systole, the contracting myocardium generates a high level of intramyocardial pressure that compresses the microvasculature resulting in the attenuation of flow. Conversely, during diastole, intraventricular pressures transmitted into the left ventricular wall exert a small compressive force on the intramural vascular network,

creating the so-called "waterfalls" at the level of the arterioles and venules[47, 49]. While the vascular waterfall model provides a good framework to explain transmural flow heterogeneity it ignores the variations in resistance during the cardiac cycle and cannot account for retrograde systolic blood flow[50]. The *"intramyocardial pump"* model is probably the best model to incorporate the dynamics of the cardiac cycle. It includes the compliance of the intramural vessels and attributes systolic-diastolic variations in coronary flow to an active intramyocardial pump and not resistances varying over the cardiac cycle[43]. The phasic variation in coronary flow and pressure during the cardiac cycle is complex and will be discussed in greater detail in Chapter 5.

Coronary Pressure-Flow Relationship During Exercise

The observation that coronary blood flow during exercise can be further augmented with a pharmacological or ischaemic vasodilator stimulus suggests that, in the normal heart, maximal exercise does not the result in the exhaustion of coronary vasodilator reserve. Studies have demonstrated in dogs and swine a reactive hyperaemia to brief episodes of coronary occlusion resulting in an increase in blood flow during maximal exercise[51, 52]. Similarly, intravenous administration of adenosine resulted in a 15-26% increase in myocardial blood flow during maximal exercise in swine despite a fall in arterial pressure[45, 53]. It has been demonstrated that such pharmacological induced increases of coronary blood flow during exercise can enhance contractile function (known as the Gregg effect)[7, 44].

Overall the increase in extravascular compressive forces during exercise is unlikely to be of physiological significance in the normal coronary circulation because of the fact that coronary vasodilator capacity reserve persists even during maximal exercise[46, 53, 54]. However, when the oxygen-carrying capacity of the blood is reduced by anaemia or hypoxia or when obstructive atherosclerotic coronary disease reduces vascular calibre and reactivity then the increased vascular forces produced by exercise can produce significant restriction of coronary flow rates.

1.1.3 Coronary Blood Flow and Exercise: In the Presence of Coronary Stenoses

1.1.3.1 Functional Effect of an Epicardial Stenosis on Coronary Flow

Normally the large epicardial coronary "conductance" vessels contribute little to total coronary resistance. However, autoregulation becomes clinically important when vessels become narrowed due to atherosclerotic disease. Such stenoses may result in a variety of shapes and forms and may be rigid or compliant[55]. The haemodynamic effect of a particular stenosis can be determined by the equation (see p.16 KT), where Q is the flow through the lesion and A, B and C are constants that depend on the geometry of the lesion and the viscous properties of the blood; where all are critically dependent on the inverse fourth power of the diameter of the stenosis[56]. The first term of the equation corresponds to the law of Poisuille and describes the pressure drop because of the viscous friction exerted on the blood stream by the stenotic wall. The second non-linear term refers to the pressure loss caused by the convergence and divergence of flow as it enters and leaves the stenosis respectively. According to the law of Bernoulli, velocity is increased and therefore pressure must be decreased as the blood flow enters the stenosis. At the exit, because of the increase in area flow velocity drops and this is accompanied by a partial pressure recovery, but some energy is permanently lost due to flow separation and eddy formation at the downstream end of the stenosis. Because of these, pressure-drop increases quadrantically with flow (version of figure 2.9 KT p.16 and also one of flow diagram of stenosis). A direct result of this is that stenosis resistance ($\Delta P/Q$) is flow dependent.

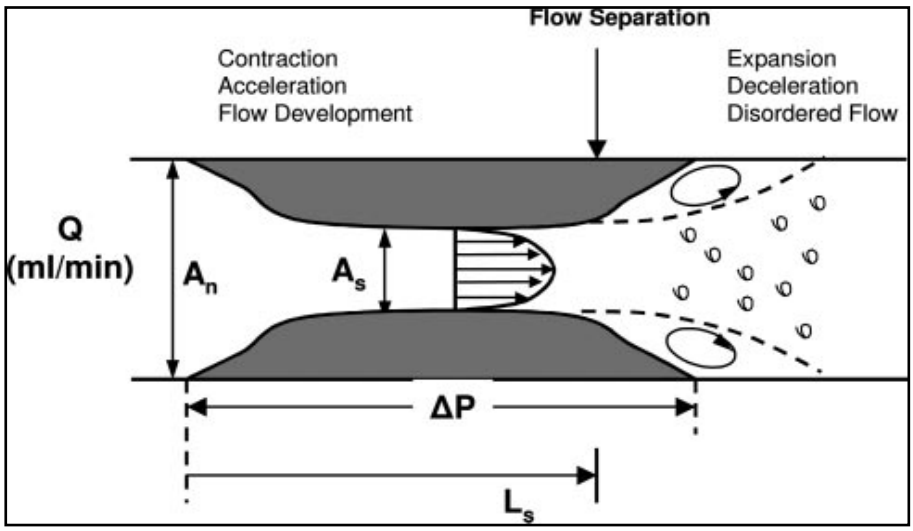

Figure 5. A schematic of a coronary stenosis showing the two main sources of pressure loss as blood flows through the stenosis. 1) frictional loss, and 2) inertial loss stemming from the sudden expansion at the exit of the stenosis causing flow separation and eddies [*adapted from Kern et al figure 1 p.1323*[57]].

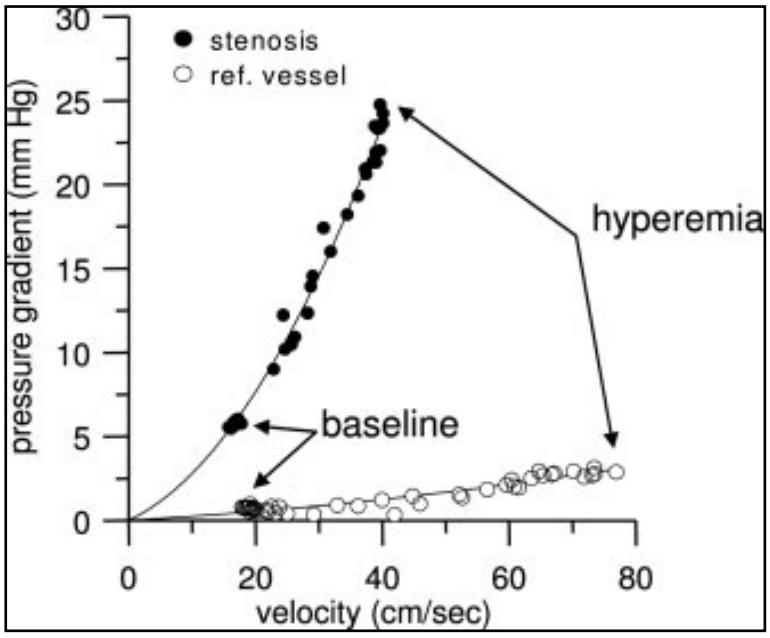

Figure 6. The quadratic nature of the stenosis pressure drop-velocity relationship illustrated by data obtained in a vessel of a patient with a moderate coronary stenosis (shown in closed circles) and in a normal reference vessel (open circles) using a dual sensor guidewire. Data points represent mean values of consecutive beats, from baseline to hyperaemia induced by i.c. adenosine injection [*adapted from Kern el at figure 2 p.1323*[57]]

When the narrowing reaches over 50% of the luminal diameter, the increase in proximal resistance causes a decrease in distal coronary perfusion pressure. In this

situation, autoregulation can preserve coronary blood flow, but maximum coronary blood flow (such as measured during intracoronary infusion of adenosine) is reduced. Consequently CFR, is reduced. When a diameter stenosis becomes so severe as to reduce distal perfusion pressure to below 40mmHg during resting conditions, then endogenous vasodilator reserve becomes exhausted resulting in myocardial hypoperfusion and subsequent ischaemia[58, 59].

1.1.3.2 Subendocardial/Subepicardial Coronary Perfusion

When autoregulation is intact then flow distribution between these different layers is maintained in a relatively homogenous manner[60]. This is achieved by the appropriate adjustment of vascular resistance at a local level and, provided that the vasodilatory capacity of the resistance vessels in the subendocardium is sufficient, demand and supply can still be matched in this myocardial layer.

Coronary Steal

Autoregulatory reserve, however, is not distributed evenly across the LV wall and perfusion to the subendocardium is more impeded by myocardial contraction than subepicardial flow[43]. This causes the lower limb of the autoregulatory curve to be shifted to the right compared to that in the subepicardial layers as is illustrated in the figure below. This also demonstrates the phenomenon of "*coronary steal*". In this situation, intracoronary infusions of adenosine (or dipyridomole) in the presence of a severe stenosis where the subendocardial vasodilatory reserve is exhausted results in enhanced subepicardial flow, thereby increasing the pressure gradient across the stenosis and further attenuating subendocardial flow through the consequent reduction in distal perfusion pressure[59, 61].

When myocardial exercise oxygen consumption increases during exercise then the autoregulatory curve will be shifted upwards (see figure above). During exercise, the increased heart rate causes more systolic blood flow and results in an increase in average myocardial tissue pressure, particularly in the subendocardial layers. This explains why a subcritical coronary lesion can have little or no effect during resting conditions but can result in selective subendocardial hypoperfusion during exercise stress.

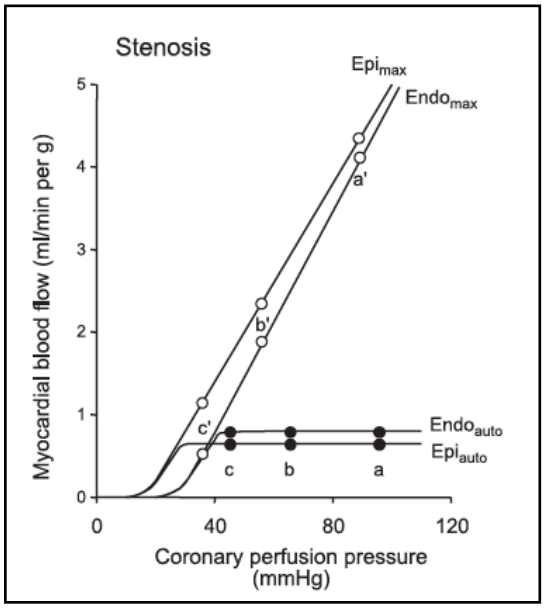

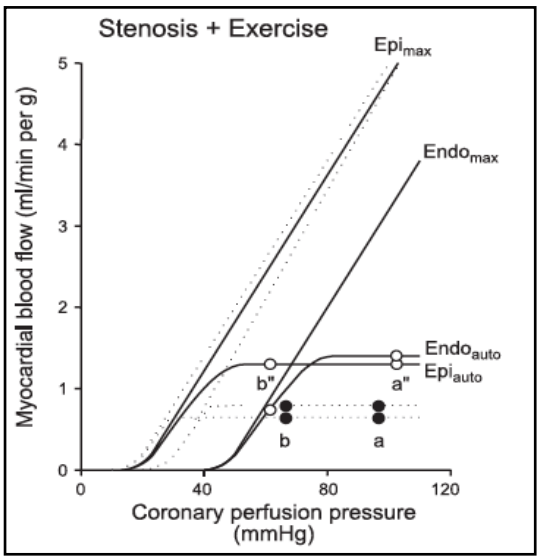

Figure 7. Coronary pressure-flow curve in the subepicardial (Epi) and subendocardial (Endo) layers during autoregulation (auto) or during maximal hyperaemia with adenosine (max), at rest (top panel) and during exercise stress (bottom panel). The panel on the top shows myocardial blood flow during resting conditions in the presence of a normal coronary vessel (*a* and *a'*), with a moderate stenosis (*b* and *b'*) and with a severe coronary stenosis (*c* and *c'*). Note that the distal perfusion pressure decreases with increasing stenosis severity with a reduction in coronary flow reserve (CFR). Coronary steal occurs in *c* where subepicardial perfusion is enhanced at the further expense of the subendocardial layer. The bottom panel shows blood flow in a normal vessel (*a* and *a"*) and the presence of a moderate stenosis (*b* and *b"*). Exercise causes an upward shift of the autoregulatory plateau and in the presence of a stenosis, the rightward shift of the subendocardial pressure-maximal flow relation causes flow to decrease in this layer while subepicardial blood flow shows a normal response [*adapted from figure 27 p.1049 Duncker et al*[37]].

The Influence of Diastolic Time Fraction on Subepicardial Perfusion

Coronary blood flow occurs predominantly during diastole[62] and is therefore critically dependent on diastolic duration. Diastolic time fraction (DTF) is the relative duration of diastole with respect to the cardiac cycle and decreases with increasing heart rate both in healthy humans and in patients with obstructive coronary artery disease[63]. In the absence of coronary stenosis and myocardial hypertrophy, coronary blood flow increases proportionally as diastolic perfusion time decreases during stress tests[64, 65]. This is primarily due to a reduction in coronary vascular resistance through vasodilatation, which maintains uniform net transmural perfusion

even if there is a marked reduction in diastolic perfusion time or higher heart rate[60, 66]. In the presence of significant coronary artery disease, however, during stress these autoregulatory mechanisms are exhausted[67, 68] and subendocardial perfusion becomes inversely dependent on heart rate and decreases with decreasing DTF, whereas subepicardial perfusion is minimally affected[60, 66, 69]. Importantly, while diastolic perfusion time was found to be closely related to stenosis severity at the onset of stress-induced myocardial ischaemia in humans, no correlation was found between DTF and heart rate at the ischaemic threshold[70]. At a given heart rate, the decrease in DTF at the ischaemic threshold was more marked in supine rather than in upright exercise and more notable in exercise than in atrial pacing. This variation reflects differences between the stressors that result from changes in left ventricular loading conditions and sympathetic nervous system activity that have been shown to influence *systolic duration* and consequently diastolic perfusion time, especially at the onset of ischaemia[71-73]. By accounting for the amount of diastole (i.e. supply) relative to that of systole (i.e. demand), this would explain why DTF is a much better parameter for predicting subendocardial ischaemia than heart rate alone.

There is thought to be an inverse nonlinear relation between DTF and intracoronary pressure and flow suggesting a possible protective mechanism whereby DTF increases when coronary perfusion is impaired distal to a stenosis[74]. Such a mechanism may explain the clinical benefit of betablockers where the administration of urapidil, a selective α_1-blocker, following coronary angioplasty resulted in a significant prolongation in the DTF that was independent of heart rate[75].

Is Coronary Vasodilatation Maximal During Myocardial Ischaemia?

It is known from the descriptions of coronary steal that vasodilatory reserve can exist in the subepicardium in the presence of a coronary stenosis causing subendocardial ischaemia, but what is more uncertain is whether residual coronary reserve exists within these ischaemic subendocardial regions. It has been traditionally assumed that ischaemic stress induces maximal vasodilatation, overriding any persistent and opposing vasoconstrictor control. Studies, however, have shown that this is not the

case with recruitable subendocardial vasodilator reserve still present even under conditions of stress-induced ischaemia due to a flow-limiting coronary stenosis[76-79]. When the coronary pressure distal to the stenosis was maintained at a constant level, an intracoronary adenosine infusion was found to increase subendocardial flow by 50% and subsequently enhance contractile function[79]. Such recruitment has been shown to be most significant under conditions of increased sympathetic drive, in particular during treadmill exercise[80]. This is consistent with the finding that residual vasomotor tone during ischaemia has been found to reside within the small arteriolar resistance vessels of the subendocardium suggesting that this reserve is under the influence of α-adrenoreceptor stimulation that is not under local metabolic control[81].

1.1.4 Systemic Arterial Blood Flow

1.1.1.1 Central vs. Peripheral Blood Pressures

Traditionally, blood pressure is measured by cuff sphygmomanometry at the brachial artery. However, there is variation in blood pressure throughout the arterial tree, with systolic blood pressure increasing towards the periphery, while diastolic and mean arterial pressures remain relatively constant. The overall effect is the amplification of pulse pressure from the aorta to the brachial artery. Therefore, blood pressure obtained peripherally is not representative of central blood pressure[82]. It has been demonstrated that during exercise, aortic systolic blood pressure may be overestimated by as much as 80 mmHg if only brachial systolic blood pressure is considered[83]. The variation in pulse pressure throughout the arterial tree is likely to be clinically important because the heart, coronary and carotid arteries are influenced by central, not peripheral blood pressure. Indeed, it is central blood pressure that determines left ventricular workload[84] and correlates with carotid artery intima-media thickness[85], both of which are independent predictors of mortality. Moreover, central blood pressure is a stronger predictor of all-cause mortality in high-risk patients with cardiovascular disease than peripheral blood pressure[86]. However, the difference between central and peripheral pressure varies with a number of factors, including age, gender and heart rate[87].

1.1.4.1 Propagation and Reflection of Pressure Waves

Central pressure waves generated during the cardiac cycle are propagated along the arterial tree and return as reflected waves to interact with the out-going incident waves. This results in characteristic waveform morphology, which is subject to modification by various homeostatic and environmental factors and changes with increasing distance from the heart. A typical central pressure waveform is shown in Figure 8 below.

1.1.4.2 Changes in Arterial Pressure in Response to Exercise

Reduced Pressure Augmentation

Arterial pressure during exercise is largely dependent on the function of large elastic and muscular arteries. Exercise induces marked changes in the arterial waveform, similar to those changes induced by nitrovasodilators[88] with a reduction in augmentation of the central and peripheral pulse waveforms and a reduction in central systolic pressure and central pulse pressure to a greater degree than peripheral pressure[88, 89]. These effects are thought to be due to a reduction of pressure wave reflection from peripheral to central arteries by vasodilatation of muscular arteries. The changes in arterial waveform increase with increasing intensity of exercise and persist for up to 60 minutes into recovery. These changes appear to be independent of heart rate and other changes in ventricular ejection characteristics that occur acutely during exercise as the changes in waveform morphology are observed well after the heart rate has returned to baseline.

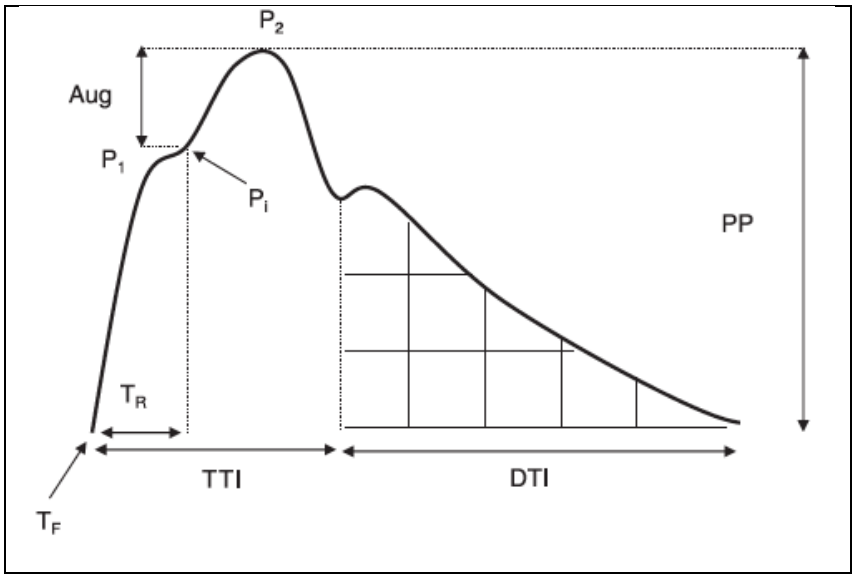

Figure 8. Typical resting ascending aortic waveform in a healthy middle-aged man. Two systolic peaks are labeled P1 and P2. Augmentation index (AIx), a measure of systemic arterial stiffness[90], is calculated as the difference between the second (P_2) and first (P_1) peaks expressed as a percentage of the pulse pressure (PP). Timing of the reflected pressure wave (T_R) is determined as the time between the foot of the pressure wave (T_F) and the inflection point (Pi)[91]. The T_R denotes the round-trip travel time of the pulse wave to peripheral reflecting sites and its return to the heart. It has been shown to correlate strongly with aortic pulse wave velocity[92, 93] and is an indicator of aortic stiffness. The area under the aortic systolic (tension time index; TTI) and diastolic (diastolic time index; DTI) portions of the pressure wave is determined by the area under the waveform during systole and diastole, respectively. The TTI relates to myocardial oxygen demand and DTI to coronary perfusion[94].

Increased Pulse Wave Velocity and Aortic Stiffness

Exercise also produces a loss of aortic vessel wall compliance, i.e. increases vessel stiffness [89, 95]. During exercise, increases in aortic pulse wave velocity accompany an increase in mean arterial pressure, a key determinant of arterial stiffness. The concomitant increase in heart rate is unlikely to contribute as previous data indicate that when heart rate is incrementally raised with cardiac pacing, there is no change in T_R or mean arterial pressure[87]. The relationship between these two variables has relevance because, as mean pressure increases, there is a change in the type of fibres that sustain vessel-wall stresses. At low mean pressures the more compliant elastin fibres predominate, but collagen fibres are progressively recruited with mounting pressure[96], effectively 'stiffening' the large central elastic arteries, resulting in increased pulse wave velocity.

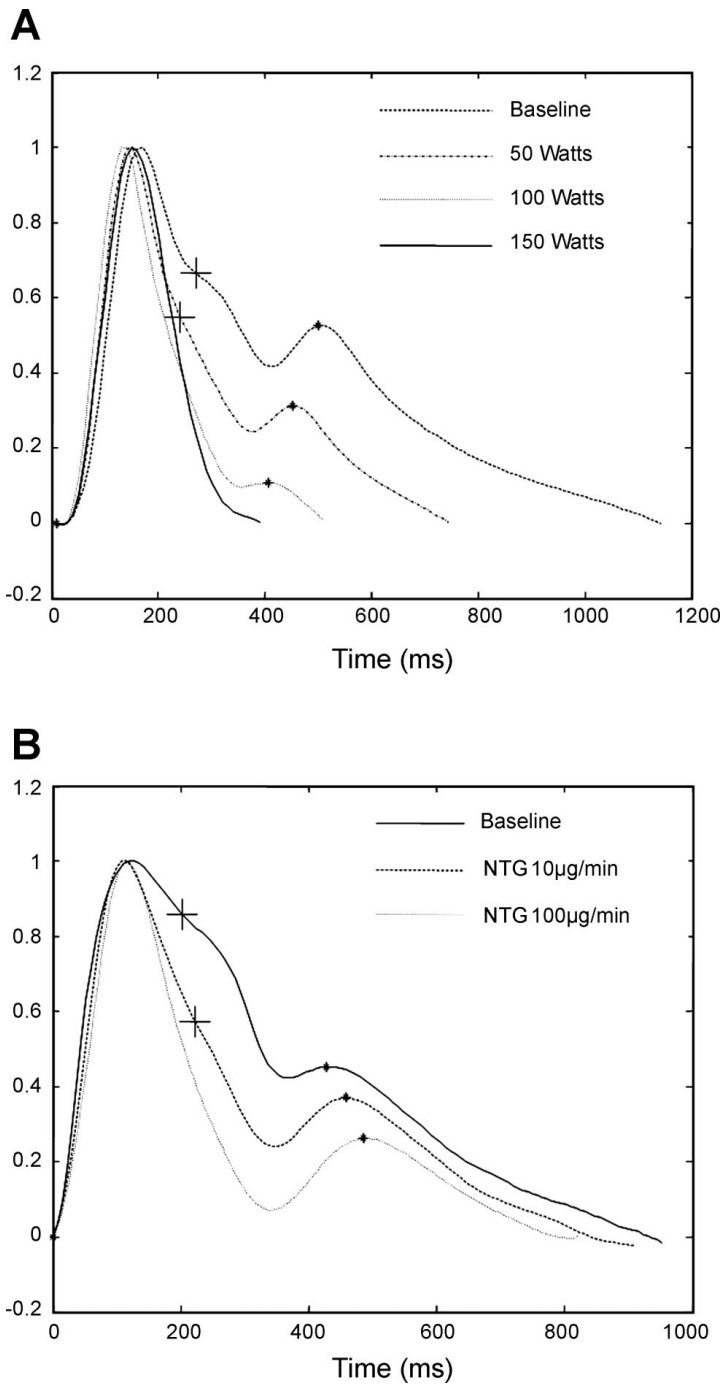

Figure 9. A) Pressure waveforms obtained at baseline and during exercise using a Finapres digital monitor. Waveforms are ensemble averages of 10 cardiac cycles and are shown normalized to the same diastolic and systolic pressures to demonstrate the change in morphology. Exercise resulted in a reduction or abolition of late systolic augmentation (+) and diastolic augmentation (♦); B) similar changes in pulse wave morphology in response to nitroglycerin (NTG) infusion at rest. [*Adapted from Munir et al Fig. 2 p. H1646*[88]]

1.2 Ischaemic Heart Disease

1.2.1 Warm-Up Angina

The variable relation between exercise and angina has been recognised for more than 200 years[2]. The terms “first effort”, “warm up”, or “first-hole” angina, have been used to describe the ability of some patients to exercise to angina, rest, and then continue exertion with reduced symptoms or none at all. In the experimental

setting, the salient observation is that at the accumulated work (exercise duration) causing max ST-segment depression on first exercise, on second exercise there is less ST depression, chest pain and dysrhythmia[97]. The traditional view is that angina is the result of an imbalance between the supply and demand of the myocardium for blood[98, 99]. However, the mechanisms underlying the warm-up phenomenon are still poorly known and somewhat controversial. Potential causes of the warm-up phenomenon include: (1) an improvement of blood flow, which, in turn, may be caused by stenosis dilation, collateral recruitment or myocardial perfusion redistribution[100-102]; (2) an adaptation of the myocardium to ischaemia, such as that caused by ischaemic preconditioning[98, 103-105]; and (3) peripheral effects causing a slower increase of cardiac workload, such as seen during training[106] or changes in central blood pressure[107]. Initial results from our own department suggest that changes in collateral flow have little influence[97].

Previous Studies

Okazaki et al[104] suggested that the benefits observed during the warm-up phenomenon were due to changes in regional myocardial oxygen consumption rather than increases in blood flow. The investigators, however, relied on great cardiac vein catheterisation to assess flow through thermodilution which has been shown to be inaccurate and highly dependent on the position of the catheter[107]. In addition, because it only assesses global LV myocardial flow this method cannot determine the changes that may occur in a particular vessel or the redistribution of flow between the different myocardial layers which may have a very important role[108]. Williams et al[103] performed a similar protocol but relied on rapid right ventricular pacing, a non-physiological surrogate for exercise, to induce tachycardia stress in a small group of stable coronary disease patients with exertional symptoms but not necessarily warm-up angina. Only 7 out of their cohort of 9 patients actually exhibited warm-up angina clinically. They also relied on great cardiac vein sampling to determine global coronary flow and similarly concluded to the Okazaki group that warm-up angina could not be explained by an increase in coronary flow alone. See chapter XX for further discussion.

1.2.1.1 Preconditioning

Ischaemic preconditioning (IPC), is the term used to describe the increased myocardial resistance to ischaemia that follows a brief episode of ischaemia[109, 110]. In animal models it protects against infarct size and arrhythmias[111] and has shown to have a similar beneficial effect in human studies[97, 112]. Patients with coronary artery disease have been observed to exercise longer before developing angina and may develop less angina and ischaemia during a second exercise test compared with a first test when these tests are separated by a brief rest period[104, 113]. It has been suggested that the clinical observation of the warm-up phenomenon may represent one aspect of IPC in humans[105]. IPC, like warm-up angina is also unexplained by a down-regulation of contractile function or an increase in collateral myocardial perfusion induced by initial exercise[114, 115]. Warm-up angina, however, does not seem to be mediated by adenosine or by cardiac adenosine triphosphate-sensitive potassium channels[116, 117] suggesting that it is mechanistically distinct from classic ischaemic preconditioning.

1.2.1.2 Subendocardial Perfusion and Microvascular Function

The transmural distribution of myocardial blood flow from endocardium to epicardium is critical during exercise and was discussed in the previous section. Because the contractile forces within the heart have a disproportionate effect on the subendocardial layer it renders it much more sensitive to ischaemia[43]. When coronary blood flow control mechanisms are intact, the flow distribution across the myocardium is relatively uniform through local autoregulation with vasodilatation of the myocardial resistance vessels[60]. When this vasodilatory capacity is exhausted (such as during exercise), subendocardial conductance becomes inversely dependent on heart rate and is decreased as the diastolic time fraction (DTF) shortens. Subepicardial perfusion, in contrast, is generally unaffected by these changes[69]. DTF is the relative duration of diastole with respect to the duration of the heart cycle and decreases with increasing heart rate. In the presence of a coronary stenosis, the autoregulatory mechanisms regulating myocardial blood flow are exhausted at an earlier stage during exercise (or even at rest) rendering the subendocardial layer even more critically dependent on the DTF[118]. Changes in DTF have been found to

reduce microvascular resistance and improve perfusion[69]. It has been suggested that an increase in diastolic duration during ischaemia may therefore be an important mechanism for matching coronary supply and demand of oxygen by simultaneously decreasing demand and increasing supply. It is possible that such changes contribute to the protective effects of serial exercise observed during warm-up angina.

1.2.1.3 Global Ventricular Work and Myocardial Stunning

It has been suggested that the reduction in ischaemia seen on second exercise in patients with warm-up angina can be explained by enhanced vaso-ventricular coupling caused by a reduction in augmentation index (AI)[88] as discussed in the previous section. Peripheral vasodilatation causes attenuation of wave reflection with a resultant lowering of central systolic blood pressure thereby reducing global cardiac work and subsequent ischaemia. To date, this work has not been carried out but remains an exciting possibility.

Myocardial stunning occurs when ischaemic insult to a region of myocardium results in the transient reduction of contractile function in that territory and has also been suggested as a potential mechanism for warm-up. With less contraction in that region, oxygen requirements are reduced and hence the ischaemic threshold raised. However, work has shown that stunned areas of myocardium *do not* have lower rates of oxygen consumption and are just as sensitive to myocardial infarction[119]. In addition, contractile dysfunction has not been shown to correlate with warm-up[115, 116].

1.2.1.4 Conclusion

The mechanisms of the phenomenon warm-up angina remain elusive. Warm-up shares many characteristics with ischaemic preconditioning but also maintains distinct differences, which suggest that other factors may predominate. During repetitive exercise, differences in ventricular afterload, subendocardial perfusion and microvascular resistance that relate to the propagation of waves within the aortic and coronary circulation may play an important role and form one of the major investigative areas of this thesis.

1.2.2 Myocardial Infarction and "No Re-Flow"

Myocardial infarction and subsequent heart failure constitute a leading cause of death in the UK[120]. Prognosis after AMI is related to the extent of myocardial injury occurring around the time of coronary occlusion[121, 122]. It is known that patients with extensive myocardial infarction are at risk of post-infarction remodeling and heart failure[123]. Early restoration of TIMI III blood flow through the infarct related artery is the main goal of modern treatment[124]. This has led to reduction of infarct size, preservation of left ventricular (LV) function and improved survival[125-127]. Primary angioplasty is superior to thrombolysis in restoration of TIMI III flow[128]. Although the restoration of epicardial blood flow does improve the myocardial perfusion of the affected area, the process is not homogenous. In fact 25-40% of patients have severely impaired flow at tissue level despite restoration of TIMI III flow in the infarct related artery (IRA)[129]. This "no-reflow" or "low-reflow" phenomenon has been documented in the endocardial portion of the LV wall. Electron microscopic studies of tissue within the no-reflow region reveal severe microvascular damage and obstruction by swollen endothelial cells and other necrotic debris[130]. It has been demonstrated that progressive microvascular impairment and myocyte damage continues after coronary artery recanalisation[131]. This increase was found to occur over and above infarct size augmentation during the same period. While the early reperfusion of the heart is essential to prevent further tissue injury and cell necrosis, it may be that the reintroduction of blood flow expedites the death of vulnerable, but still viable, myocardial tissue.

1.2.2.1 Reperfusion Injury and Cardiac Protection

Lethal myocardial reperfusion injury is defined as the death of myocytes, alive at the moment of reperfusion, as a direct result of one or more events initiated by reperfusion itself[132]. Numerous experimental studies have provided compelling evidence as to its existence as an entity and animal models suggest that 50% of final infarct size may be a result of reperfusion injury[133]. Hearse et al. first introduced the so-called "oxygen-paradox" when they noted significant cardiac muscle enzyme release and alterations in ultra structure when isolated hearts were reoxygenated after a period of hypoxic perfusion[134, 135]. It is believed that many different

mechanisms are involved in reperfusion injury in a highly complex process that occurs in both the intracellular and extracellular environments[136]. This complexity is reflected in the diverse array of physiological sequelae that arise including endothelial and microvascular dysfunction, metabolic and contractile dysfunction, arrhythmias, cellular necrosis and apoptosis[137]. Novel therapies to attenuate these processes may reduce final infarct size and improve outcome. Ischaemic preconditioning has long been regarded as the gold standard of "cardiac protection". It is a phenomenon whereby brief periods of myocardial ischaemia offer protection during subsequent prolonged ischaemia. There is a large body of experimental data from perfused isolated, and in situ animal hearts with preconditioning resulting in substantial reductions in volume of myocardial infarction[109]. Studies on ischaemic preconditioning have demonstrated that cell death cannot be seen as a mere consequence of energy deficiency; preconditioning does not alter the progression of ischaemic injury but, rather, modifies the consequences of reperfusion by switching the cell fate from death to survival[138, 139]. Preconditioning has proven clinical benefits in settings where the ischaemia can be predicted such as in elective percutaneous coronary intervention (PCI), cardiac surgery and the phenomenon of warm-up angina[140] (*See chapter 5)*. The unpredictable nature of AMI, however, means that one cannot pre-empt the event and initiate an intervention prior to it occurring.

1.2.2.2 Postconditioning

Postconditioning is defined as rapid intermittent interruptions of blood flow in the early phase of *reperfusion*. Zhao et al first demonstrated the cardioprotective effects of postconditioning using a canine model of 1 hour coronary occlusion and 3 hours of reperfusion[141]. After 30 seconds of reperfusion the artery was occluded again for 30s with the cycle repeated 3 times. Compared to the control group, postconditioning resulted in significantly reduced infarct size. This cardioprotective effect was associated with an improvement in endothelial function, a reduction in tissue superoxide generation, a reduction in cardiac apoptosis, and a decrease in microvascular injury. In fact, the infarct reduction was similar to that observed in a group who had undergone ischaemic preconditioning. Subsequent studies have confirmed a similar infarct size reduction in other species with the duration of the

alternating periods of reperfusion and ischaemia varying from species to species[142-144]. Common to all is the time-dependent manner in which postconditioning must be applied if cardioprotection is to be achieved and post-ischaemic injury reduced. If the first interruption of blood flow was applied more than 1 minute after the onset of reperfusion then the infarct sparing effect was not observed[143]. There are many cellular and molecular events involved in the pathogenesis of myocardial infarction occurring during the early moments of reperfusion that are thought to be modulated by postconditioning, including the activation of survival kinases principally known to attenuate the pathogenesis of apoptosis and possibly necrosis[145]. It has been suggested that this may represent an innate final common pathway of cardiac protection shared with ischaemic preconditioning[137]. Post-ischaemic dysfunction, or myocardial stunning, is the mechanical dysfunction that persists after reperfusion despite the absence of irreversible damage and despite restoration of normal or near-normal coronary flow[119]. Myocardial stunning is thought to be partly caused by reperfusion injury but also partly by damage sustained during the ischaemic insult and therefore less amenable to therapies to reduce reperfusion injury[146]. Contrasting to its beneficial effects on reducing overall myocardial infarction postconditioning does not protect against myocardial stunning in dogs and rabbits[147]. Staat et al were the first group to assess the benefit of post-conditioning at the time of primary angioplasty for AMI in humans[148]. Compared to a control group who underwent angioplasty alone they demonstrated a 36% reduction in infarct size as determined from creatinine kinase release over 72 hours following reperfusion. In addition, myocardial blush grade, an angiographic marker of myocardial perfusion, was significantly increased in postconditioned compared to control subjects suggesting an improvement in microvascular integrity. This was also suggested by Laskey who demonstrated improved ST segment shift and improved Doppler-derived coronary flow in a postconditioned group of patients[149]. Several other clinical studies have been carried out since using varying postconditioning protocols in patients at the time of reperfusion of AMI and a consistent reduction in infarct size of around 30% has been demonstrated. Yang[150] used SPECT at 1 week to show a 27% reduction in infarct size. Ma[151] also found reduced infarct size based on

CK release and improved wall motion scores on echo. Although this early work is encouraging, both clinical and animal studies examining postconditioning to date have concentrated on early time points following reperfusion. It has been suggested that many of the mechanisms leading to myocyte necrosis occur some time after reperfusion[152] and that post-ischaemic injury is an ongoing process with infarct expansion continuing for at least 24 hours following onset of reperfusion[131, 144, 153]. Early determination of infarct size may therefore lead to inaccuracies with an underestimate of final infarct volume. Miki et al[154] found in a rabbit model of acute MI using the diffusible antioxidant MPG, that protection assessed with early TTC staining was seen in the rabbits treated with MPG following reperfusion. When the experiment was repeated, however, with infarct size determined at a later time point after reperfusion no such differences could be found compared to control.

Whether postconditioning results in a long-term sustained attenuation of post-ischaemic injury and infarct reduction rather than simply a delay in inevitable injury is a question still to be determined. The demonstration of such an effect would add significantly to the argument of the existence of intrinsic cardiac protection in ischaemic heart disease patients, where the promise of such a phenomenon based on laboratory studies has perhaps failed to live up to expectations in the clinical setting. A randomised clinical trial investigating the potential beneficial effect of postconditioning in patients presenting with acute myocardial infarction forms one of the major chapters of this thesis; it also complements the clinical investigation of the other cardioprotective phenomenon, warm up angina.

1.3 Non-Invasive Techniques to Investigate Ischaemic Heart Disease

1.3.1 Detection of Reversible Myocardial Ischaemia

The detection of reversible myocardial ischaemia has formed a cornerstone for the investigation and treatment of patients with stable coronary disease[155]. Studies involving thousands of patients have shown that in the absence of inducible ischaemia, patients with coronary artery disease (CAD) have an excellent prognosis with an adverse event rate of less than 1% p.a., which is nearly as low as the general population[156-158]. Large perfusion defects and defects in multiple coronary territories, however, suggest a poor prognosis[159-161]. In addition, those with a low burden of ischaemia have been found to gain little benefit from coronary revascularisation compared to optimal medical therapy[162]. Conversely, the CASS registry suggests that those with a high burden of ischaemia are at risk of adverse events if left without revascularisation, with a mortality of around 5% per annum in the medically treated arm with a strongly positive exercise tolerance test (ETT) compared to a mortality rate of less than 1% p.a. in those medically treated patients without inducible ischaemia[163].

Testing for reversible ischaemia requires the induction of some marker of myocardial ischaemia (such as ECG ST-segment shift, a new regional LV wall motion abnormality or a myocardial perfusion defect) during conditions of exercise or pharmacological stress. A variety of different techniques may be employed for this, ranging from the simple exercise ECG, through echocardiography, PET and SPECT imaging and cardiac magnetic resonance. Because of the limits of this thesis, we will concentrate on ischaemia detection and perfusion imaging provided by cardiac magnetic resonance imaging which will be covered in the following section.

1.3.1.1 Pharmacological Stress

Adenosine, dipyridamole and, dobutamine are three agents currently used in pharmacological stress testing. Dobutamine is a synthetic sympathomimetic amine. Like exercise, dobutamine increases myocardial oxygen demand by increasing

myocardial contractility[164]. CFR is therefore increased indirectly by creating a greater flow demand. Direct exercise and dobutamine can therefore provoke ischaemia due to their effects in increasing oxygen demand and flow.

Adenosine and dipyridamole are vasodilators and induce hyperaemic flow directly by dilating the coronary microcirculation. Adenosine binds and activates A_2 receptors on smooth muscle cells causing relaxation and thus coronary vasodilatation[165]. Dipyridamole inhibits cellular uptake of adenosine thus increasing the interstitial adenosine concentration which results in active hyperaemia and vasodilatation[166]. Caffeine inhibits the effects of dipyridamole and adenosine and thus should be avoided 24 hours before a stress test[167].

Direct vasodilatation of the coronary arteries provokes blood flow heterogeneity in patients with CAD because areas of stenosis receive relatively reduced flow in comparison to areas without stenosis. This heterogeneity of flow may present as a perfusion defect during stress testing with myocardial perfusion imaging (MPI). Such perfusion defects correlate strongly with clinical endpoints and are thought to represent regions of inducible myocardial ischaemia[160, 161].

1.3.1.2 Exercise Stress

In most cases, exercise stress testing would be the ideal method for assessing CAD because it is the most physiological stimulus for increasing myocardial oxygen demand and therefore coronary blood flow. Vasodilating agents increase coronary flow directly, independent of endothelial function, and without increasing cardiac work and so may therefore be inappropriate in demonstrating reduced CFR. However, exercise stress testing is not always possible or may be inappropriate. Apart from monitoring ECG, it is difficult to actually acquire data *during* exercise therefore such acquisition must occur almost immediately after peak exercise stress is achieved as heart rate depreciates rapidly after cessation of exercise. It may be difficult to perform an exercise test in the immediate vicinity of the scanner, be it ultrasound, nuclear or MRI imaging for practical reasons. In addition, pharmacological stress testing is usually preferred in the elderly or those with physical disabilities that do not allow them to exercise to adequate diagnostic or

prognostic levels. Caution must be used in patients with recent myocardial infarction or those with severe valvular heart disease.

1.3.2 Cardiac Magnetic Resonance Imaging

1.3.2.1 Basic Principles

Magnetic resonance (MR) images depend on the distribution and concentration of hydrogen nuclei in the body and on the physical and chemical environment of those nuclei. It is beyond the scope of this introduction to explain the detailed physics behind the acquisition of MR images but there are numerous reviews where excellent and clear descriptions can be found[168-170]. When a patient enters the core of the magnet within a scanner, hydrogen nuclei align with and *precess* about the axis of the magnetic field. This precession can be altered by application of additional small magnetic field pulses. The application of these pulses in a controlled manner (in the form of *pulse sequences*) means that signals can be received and processed to produce an image of the spatial distribution of the spins or protons within the body. Multiple types of pulse sequences can be used for different imaging protocols to define cardiac structure, tissue characterisation, or measurement of cardiovascular function; all can be employed within a single study. The unique ability to provide such a comprehensive assessment of cardiac form and function, together with the lack of exposure to ionising radiation to patients makes CMR a very useful non-invasive imaging modality[171].

1.3.2.2 Different CMR Techniques

Cine Imaging

The assessment of global and regional left ventricular (LV) and right ventricular (RV) function by CMR is typically based on a cine data set aligned in the true LV short axis that covers the heart in 10-12 consecutive two-dimensional slices[172]. Alternatively, three-dimensional cine data sets covering the entire heart in a single breath-hold can be acquired[173, 174]. In addition to its high tissue contrast, the main advantage of CMR over other imaging modalities is that imaging planes can be freely and reproducibly defined. Consequently, CMR is the most accurate and reproducible imaging modality

for the assessment of global ventricular volumes and function [175, 176]. In addition, regional contractile function can be assessed either by visual interpretation of cine loops[177, 178] or by measuring wall motion, thickening and strain using myocardial tagging methods[179, 180]. Myocardial tagging during low dose dobutamine stress has been used to measure parameters of diastolic dysfunction such as the time to peak untwist which may identify coronary stenosis[181,182]. Following AMI, low dose dobutamine cine CMR can be used to predict viability and functional recovery[183-186]. High dose dobutamine stress CMR has high diagnostic accuracy to identify inducible LV wall motion abnormalities indicative of flow-limiting coronary stenosis[187-189].

First Pass Myocardial perfusion

Current first pass myocardial perfusion CMR methods track the passage of a bolus of a T1-shortening contrast agent injected into a peripheral vein[190, 191]. Data acquired during intravenous vasodilator-stress (most commonly with adenosine) delineate relatively underperfused regions associated with myocardial ischaemia. The spatial resolution of CMR myocardial perfusion imaging of 2 to 3 mm is vastly superior to other imaging modalities, so that subendocardial ischaemia can be more reliably identified. Recent developments have seen further improvements in spatial resolution to around 1 mm in the imaging plane[192] and acquisition at 3-Tesla promises improved signal to noise ratio and diagnostic yield[193, 194]. Both of these developments should continue to enhance the value of CMR perfusion assessment. The interpretation of CMR myocardial perfusion studies in clinical practice is most commonly visual, but quantitative approaches that measure characteristics of myocardial signal intensity profiles are available[191, 195-198] and have been validated against x-ray angiography, SPECT and PET[199-201]. The recent MR-IMPACT study in 234 patients reported improved detection of coronary stenosis by CMR compared with SPECT in the first multi-centre, multi-vendor comparison[156]. In the context of ACS, myocardial perfusion CMR imaging can be used to delineate microvascular obstruction and ischaemia, as described in subsequent sections. See Figure 10 below.

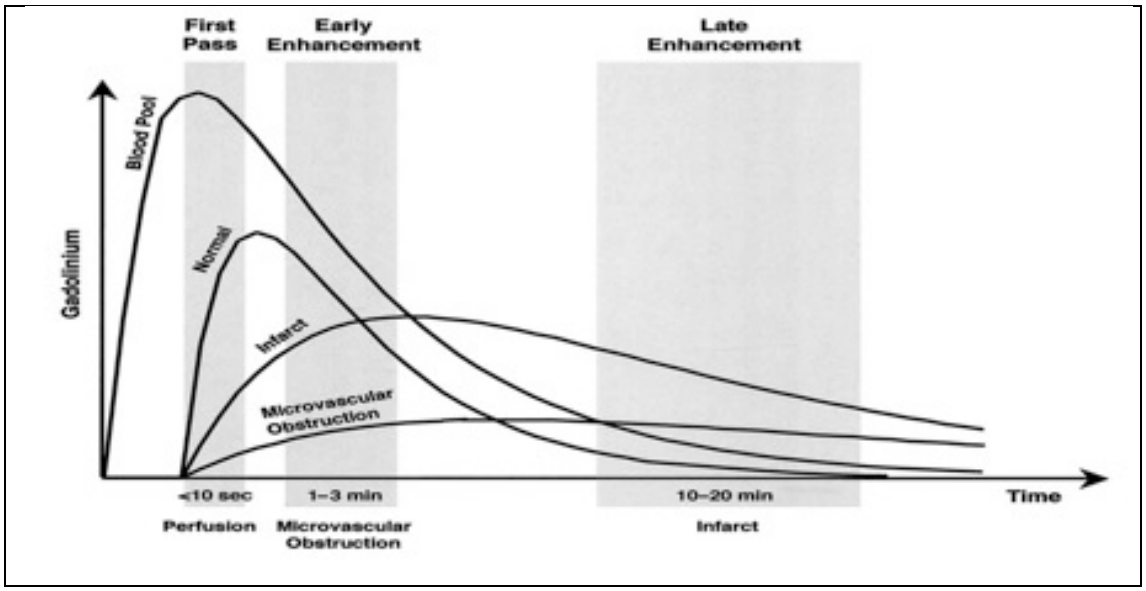

Figure 10. Kinetics of gadolinium during the 3 different acquisition periods. [Taken from Pennell, 2004, figure 1, p.27[202]]

Early and late gadolinium enhancement

Because normal myocardium is uniformly tightly packed with muscle, and gadolinium is a hydrophilic extracellular contrast agent, there is uniformly low signal in the normal heart. Following acute ischaemic injury, the myocardial distribution volume of extra-cellular gadolinium-based contrast agents is increased because of the presence of sarcrolemmal disintegration and abnormal washout kinetics. In chronic myocardial infarction, the presence of fibrotic tissue increases the distribution volume of the contrast agents. The resulting differences in contrast distribution between normal and injured myocardium can be delineated with T1-sensitive inversion-recovery CMR methods. Imaging within the first few minutes after contrast administration is the method of choice to delineate microvascular obstruction (MVO), which prevents contrast delivery to the infarct core and thus results in low signal on T1-weighted imaging[203]. Acutely injured and chronically infarcted tissue without MVO on the other hand retains contrast agent and therefore appears bright[204-207]. The preferred imaging time for scar is between 10 and 20 minutes after contrast agent administration, when the differences between scar, normal myocardium and blood pool are maximal. This method is referred to in the literature variably as late gadolinium enhanced CMR (the currently preferred term), late-contrast enhanced, delayed contrast-enhanced or hyperenhancement

CMR. It has become the reference standard for the in vivo assessment of myocardial viability because of its very high spatial definition and high contrast to normal myocardium, which allows a detailed assessment of the spatial distribution of scar. Because of its high spatial resolution late gadolinium enhanced CMR can detect infarction in as little as 1ml of tissue, substantially less than other in vivo methods. The technique has been extensively validated in animal models showing excellent agreement with histology and has been applied in numerous recent human studies[203-208]. Most notably, it was shown that CMR is more sensitive in detecting subendocardial MI than SPECT or PET and in chronic CAD that the extent of scar on CMR predicts the potential for functional recovery after revascularisation [209-211].

T2-weighted imaging

Myocardial edema is a feature of many forms of acute myocardial injury that are associated with inflammation. Edema alters myocardial T2-relaxation and can therefore be detected with T2-weighted CMR imaging[212]. Following acute myocardial infarction, T2-weighted CMR can be used to delineate the ischaemic risk region, which typically extends beyond the scar (See Figure 11). This is discussed in greater detail later. However, both the relatively small contrast-to-noise ratio between edematous and normal myocardium (around 2 to 3) and artefacts from slow flowing blood at the subendocardial border can make interpretation of T2-weighted images more challenging than other CMR methods, although recent methodological developments promise to improve these limitations[213].

1.3.2.3 CMR and the Detection of Reversible Myocardial Ischaemia

CMR offers great potential in the detection of myocardial ischaemia and recent studies have suggested a high degree of accuracy compared to other more established non-invasive techniques[214]. The MR-IMPACT study has been mentioned above and was a multi-centre, multi-vendor study involving 234 patients with suspected IHD comparing CMR perfusion to SPECT imaging for the detection of significant coronary disease. CMR was found to be as good as SPECT in the considered patients, and performed better than SPECT when the entire SPECT

population was considered[156]. CMR also holds certain advantages over other non-invasive techniques such as ETT, stress echo or SPECT imaging because of its high

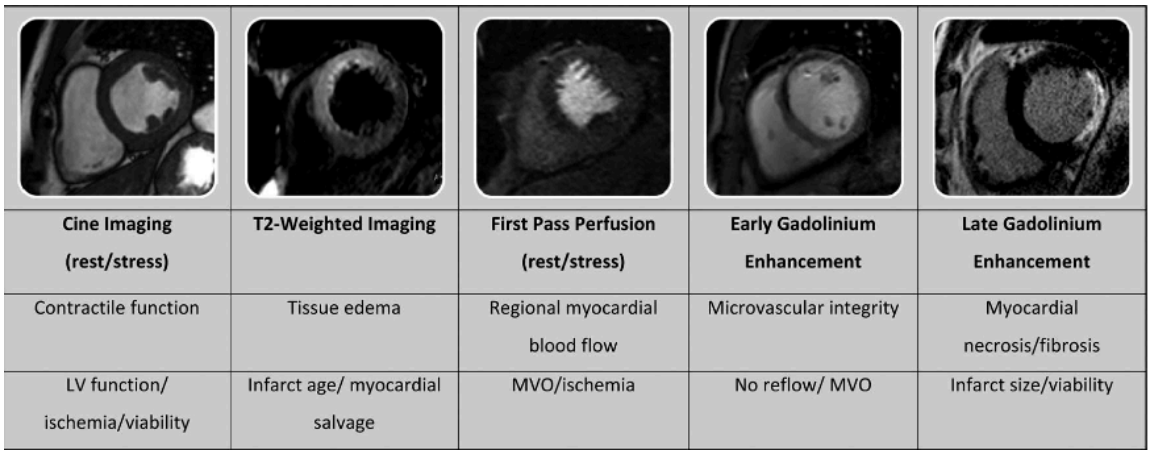

Cine Imaging (rest/stress)	T2-Weighted Imaging	First Pass Perfusion (rest/stress)	Early Gadolinium Enhancement	Late Gadolinium Enhancement
Contractile function	Tissue edema	Regional myocardial blood flow	Microvascular integrity	Myocardial necrosis/fibrosis
LV function/ ischemia/viability	Infarct age/ myocardial salvage	MVO/ischemia	No reflow/ MVO	Infarct size/viability

Figure 11. Different CMR imaging methods. The figure shows short axis views (of different patients) illustrating the different imaging techniques used, their morphological correlates main clinical application *[Adapted from Lockie et al Circulation 2009*[215]].

resolution, lack of ionising radiation and tissue characterisation. CMR perfusion involves the tracking of a bolus of gadolinium (Gd)-containing contrast agent as it diffuses through the myocardium. Recent improvements in temporal resolution have allowed the acquisition of several slices of the heart within one cardiac beat. Such dynamic multislice imaging allows the detection of perfusion defects within the myocardium during hyperaemic stress following the administration of intravenous vasodilator agents such as dipyridamole or more commonly adenosine. Such perfusion defects correlate with obstructive coronary disease on invasive coronary angiography[216] and against fractional flow reserve with a sensitivity and specificity of 91% and 94% respectively using visual analysis of CMR perfusion to detect haemodynamically significant coronary stenoses[217]. Overall, the performance of CMR perfusion to detect myocardial ischaemia according to a recent meta-analysis of 12 trials involving 1,183 patients demonstrated a sensitivity of 91% (95% CI 88-94) and specificity of 81% (95% CI 77-85)[214]. Despite these figures the majority of the studies included in this meta-analysis used perfusion abnormalities based on a patient basis, rather than a specific perfusion territory and used coronary angiography alone as the "gold standard". The localisation of a perfusion defect to a specific coronary territory is important in determining the optimal revascularisation

strategy in patients with multi-vessel disease and requires high-resolution scanning capacity. In addition, functional coronary measurements such as fractional flow reserve (FFR) should be used to determine the haemodynamic significance of a coronary lesion as angiography alone correlates poorly with the presence of ischaemia[218]. This is discussed in further detail in the following sections.

1.1.4.3 The Influence of higher field strength

MR imaging at 3-T potentially provides a substantial improvement of tissue contrast in T1-weighted imaging techniques relying on gadolinium-based contrast material enhancement[219]. In a systematic comparison between CMR perfusion using 3-T and 1.5-T, Cheng et al found the perfusion at 3-T to be superior to that at 1.5-T[194]. They suggest that the significantly higher diagnostic accuracy of 3-T perfusion could be attributed to a combination of higher SNR (signal-to-noise ratio), allowing detection of subendocardial perfusion defects (the most sensitive parameter for a reduction of overall coronary blood flow) and reduced occurrence of dark rim artefacts. These are an acknowledged problem with 1.5-T perfusion imaging and can often be mistaken for real perfusion defects, potentially explaining the lower specificity seen at 1.5-T.

1.3.2.4 K-t SENSE Encoding

Standard CMR first-pass perfusion methods are limited by the need for acquisition of the complete data set in a single shot with a limited portion of each cardiac cycle. This limits the maximum resolution attainable by perfusion imaging compared to other sequences such as late Gd-enhancement or cine imaging which may be acquired over several heartbeats. New acquisition strategies that simultaneously take advantage of coil encoding and spatiotemporal correlations, such as *k*-space and time sensitivity encoding (*k*-*t* SENSE), allow considerable acceleration of CMR data acquisition[220]. These methods are based on the premise that the raw data in dynamic images exhibit correlations in *k*-space and in time and that it is sufficient to acquire only a reduced amount of data and recover the missing portion afterwards[220]. Such correlations can be obtained from a set of training images that are obtained beforehand and by exploiting this prior information it is possible to vastly accelerate data sampling. Such acceleration can be invested in improved

spatial resolution leading to in-plane spatial resolution approaching $1mm^2$, which is far superior to conventional methods where a maximum spatial resolution of 3-$5mm^2$ is possible. This is accompanied by a reduction in dark rim (susceptibility) artefacts, which may be problematic in other perfusion sequences with less spatial resolution, especially in the assessment of subendocardial perfusion defects. Previous studies have suggested that there is improved signal to noise ratio (SNR) and image quality using *k-t* perfusion at higher field strength (i.e. at 3-T rather than 1.5-T) due to the potential loss of SNR that can occur due to acquisition of data at higher spatial resolution and with the use of spatiotemporal under-sampling[216]. *K-t* has proved accurate in the detection of coronary disease as determined anatomically by a 50% stenosis on the coronary angiogram[221]. However, to date there have been no studies comparing the performance of *k-t* perfusion to FFR to detect haemodynamically significant coronary disease.

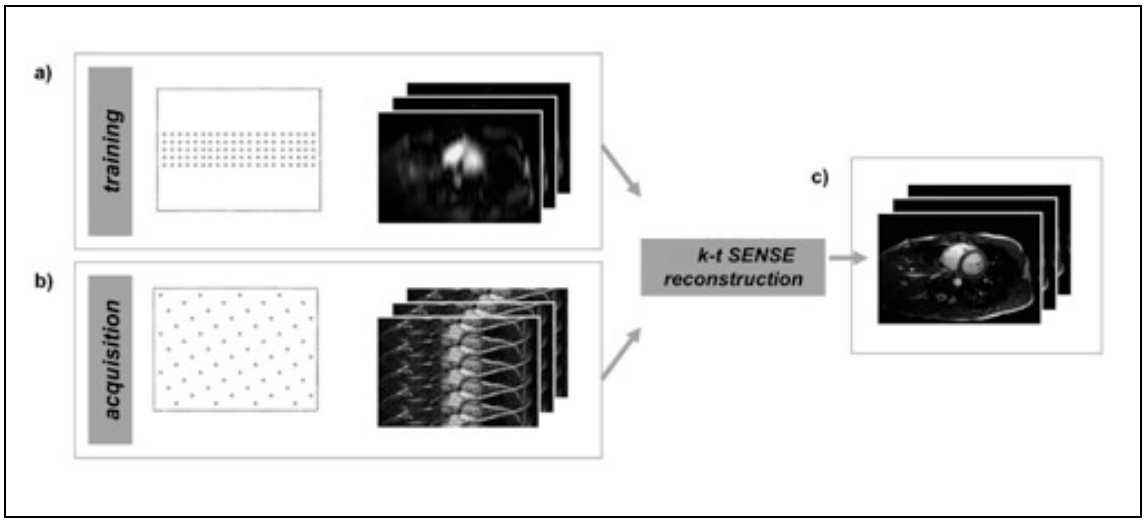

Figure 12. Summary of the *k-t* SENSE method. *k-t* SENSE involves the reconstruction of images. First a low-resolution scan is performed to provide training data (a). An estimate of the expected signal intensities of the moving object is obtained based on this data. During the data acquisition stage, under-sampling is applied, creating multiple foldover in the images (b). Training data and acquisition data are then both combined and reconstructed using *k-t* SENSE to produce high-resolution images (c). [*Adapted from Korezeke and Tsao, 2004, figure 7, p.165*[222]]

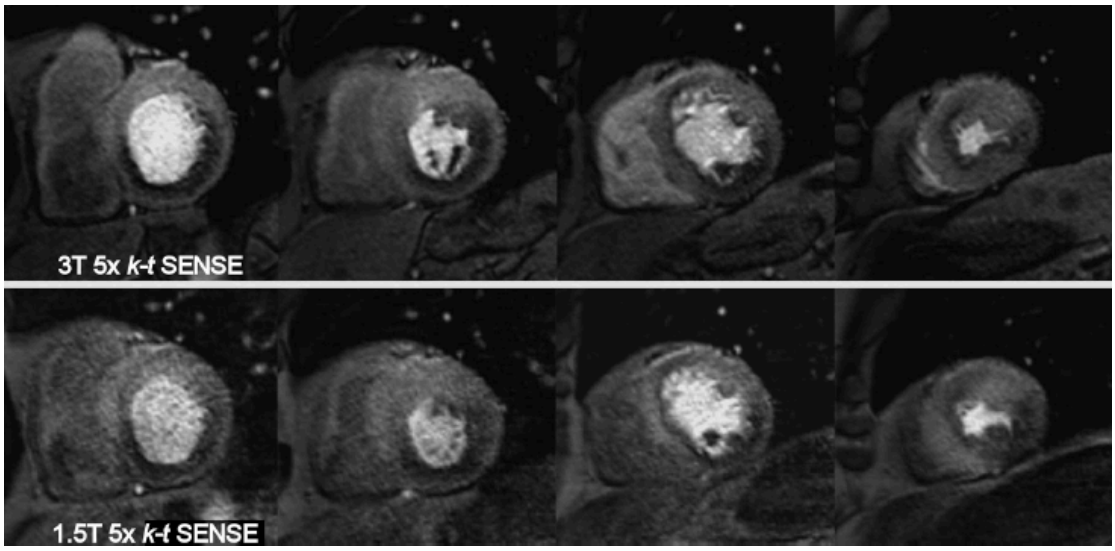

Figure 13. Fivefold *(5x)* k-t SENSE–accelerated adenosine-induced stress 3.0- and 1.5-T perfusion MR images in a 65-year-old patient suspected of having coronary artery disease. Four sections in the double-oblique short-axis orientation from base (left) to apex (right) were acquired. Both data sets have similar diagnostic content, but image quality at 3.0 T is superior. Data sets show inferior and lateral ischaemia in basal and midcavity section and anteroseptal ischaemia in apical sections. [*adapted from Plein et al Radiology 2008*[223]*]*.

1.4 Invasive Techniques to Investigate Ischaemic Heart Disease

1.4.1 X Ray Coronary Angiography

Coronary angiography is defined as the radiographic visualization of the coronary vessels after injection of radio-opaque contrast media, usually with specialist catheters. The purpose of coronary angiography is to define the coronary anatomy and the degree of luminal obstruction of the coronary arteries. It is most commonly used to determine the presence and extent of obstructive coronary artery disease (CAD) and to assess the feasibility and appropriateness of revascularisation either surgically or by percutaneous intervention (PCI).

In 1844 the French physiologist Claude Bernard (1813-1878) first coined the phrase "cardiac catheterization" and used catheters to record intracardiac pressures in animals. The next step forward did not occur until 1929 when Werner Forsmann (1904-1979) performed the first documented human cardiac catheterization in Eberswald, Germany. This he did by inserting a cannula into his own antecubital vein, through which he passed a catheter for 65 cm and then walked to the X-ray department, where a photograph was taken of the catheter lying in his right atrium. He went on to win the Nobel Prize for medicine or physiology in 1956, sharing the honours with André Frédéric Cournand (1895-1988) and Dickinson W. Richards (1895-1973) who first employed the cardiac catheter as a diagnostic tool. They utilised techniques to measure cardiac output, in the assessment of valvular heart disease and for the detection and diagnosis of congenital defects. They were also able to investigate pulmonary diseases through cannulation of the pulmonary arteries. In 1958 F. Mason Sones of the Cleveland Clinic performed the first selective coronary arteriogram. This was inadvertently obtained during an aortic root injection in a 26 year old patient with rheumatic heart disease. The catheter prolapsed into the ostium of the right coronary artery, which was directly injected with contrast thus providing the first selective coronary angiogram.

50 years later, with its excellent resolution (<1mm) selective coronary angiography remains the gold standard for the visulalisation of the coronary arteries. It maintains a prominent role in the diagnosis and treatment of coronary disease[224]. However, the two dimensional anatomical representation of the highly complex form of a coronary stenosis that is obtained by standard techniques may be misleading and the use of quantitative coronary angiography (QCA) alone may be inaccurate in the determination of haemodynamically significant coronary disease[218].

1.4.2 Invasive Coronary Physiology

1.4.2.1 Epicardial Lesion Assessment

The use of invasive indices of coronary flow and pressure may overcome some of the inadequacies of QCA by providing more physiological lesion assessment. The **fractional flow reserve** (FFR) using a distal pressure wire under hyperaemic conditions is widely used in the presence of normal myocardium to assess the severity of an epicardial stenosis[225]. It predicts the fraction of maximal flow that can still be achieved in the presence of a stenosis compared with the case if the stenosis were absent and is based on the assumption of a constant minimal microvascular resistance at hyperaemia that is independent of the severity of the epicardial stenosis[226, 227]. FFR correlates well with clinical end points and non-invasive measures of ischaemia[228]. However, it has been demonstrated that there is variability in the assumed minimal microvascular resistance that is dependent on the perfusion pressure of the distal coronary artery with a reduction found following PCI to the epicardial stenosis[229]. This has led some to challenge the concept of a uniformly distributed microvascular resistance and dispute the use of the FFR as an independent variable[229, 230]. When evaluating FFR, only the ratio of distal to aortic pressure at maximal vasodilatation is taken into account, regardless of the flow that passes through the stenosis or of the microvascular resistance. It has been described that FFR may indicate a false-negative result (above threshold) in cases of low maximal flow due to microvascular disease[231]. Conversely, FFR may indicate a false-positive result (below threshold) in the case of a higher pressure gradient caused by a high-flow rate through the stenosis in the presence of a low microvascular

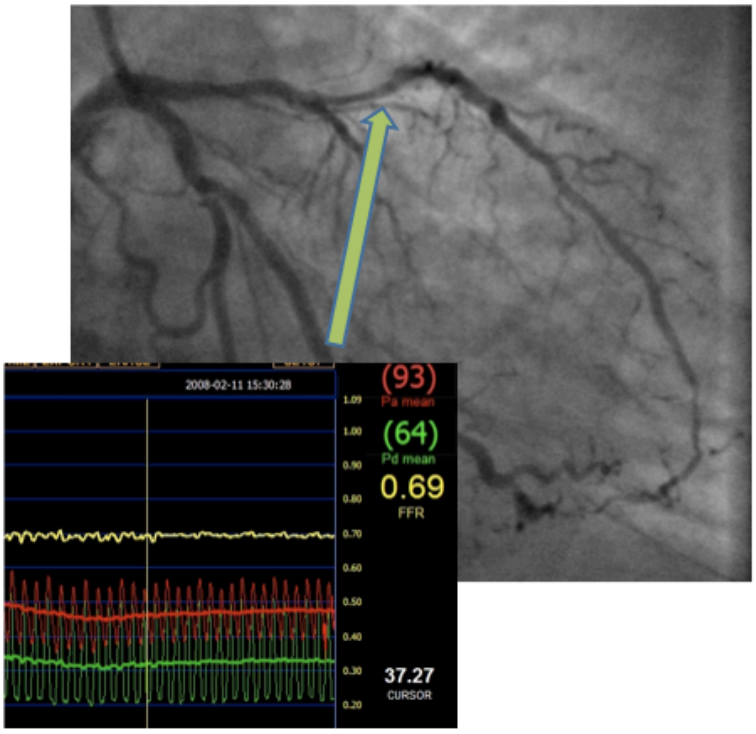

Figure 14. Pressure wire tracing from an LAD containing a moderate mid-vessel stenosis showing the distal coronary pressure (Pd) in green and proximal aortic pressure (Pa) in red. The ratio of the two during adenosine-induced hyperaemia is the fractional flow reserve (FFR). An FFR of 0.69, (normal >0.8) suggests a highly haemodynamically significant lesion that would benefit from revascularisation [*adapted from Lockie et al, Circulation, 2009*[215]].

resistance[232]. **Coronary flow reserve** (CFR) can be measured in the vessel either using Doppler or thermodilution[233]. It represents the ratio of maximal-to-baseline flow velocity distal to the stenosis and like FFR correlates well with non-invasive indices of ischaemia[234]. However, CFR is sensitive to haemodynamic conditions[235] with poor reproducibility and it cannot discriminate between the potential effects of an epicardial stenosis or a damaged microcirculation on coronary flow[236, 237]. The **hyperaemic stenosis resistance index** (SR) has been introduced as a more powerful predictor of reversible perfusion defects by incorporating both pressure and flow[238]. It involves the ratio between stenosis pressure drop and the distally measured flow velocity at maximal hyperaemia $(P_a - P_d)/V_d$ and therefore acts as a measure of stenosis severity that can be separated from the effect of microvascular resistance. Recent technological advances mean that such measurements can be made with a single combined flow/pressure wire. SR has been shown to be the best predictor of reversible perfusion defects as determined by SPECT compared to FFR or CFR[238]. The

difference was greatest with intermediate lesions where a large variability between FFR and CFR was seen, probably reflecting differences in microvascular resistance during maximal vasodilatation that affect CFR and FFR in opposite directions[229].

1.4.2.2 Microvascular Assessment

Simple coronary angiography measurements such as TIMI flow grade (TFG), corrected TIMI frame count (cTFC) and myocardial blush grade (MBG) provide some information on the state of the coronary microcirculation but such methods are inaccurate and poorly reproducible[239]. Coronary sinus thermodilution can be used to measure global myocardial blood flow, yet the most useful invasive tools are the dual sensor pressure and flow wire (Combowire™, Volcano®) and the temperature sensitive pressure wire (RADI®). The Combowire has a tiny piezoelectric crystal embedded near the tip of the wire together with a pressure transducer, either also situated at the tip of the wire or offset by 30mm[240]. The temperature sensitive pressure wire has a high fidelity sensor embedded near the tip, allowing for simultaneous measurement of temperature and pressure. The shaft of the wire acts as the proximal thermistor by monitoring changes in electrical resistance that are temperature dependent. The limitations of CFR have been discussed above. Because CFR is a measure of combined epicardial and microvascular resistance and thus cannot discriminate between them independently, in practical terms CFR is only a useful measure of microvascular function if there is no epicardial disease. The other indices that have been introduced are the **index of microcirculatory resistance** (IMR)[241] and coronary **microvascular resistance index** (MR)[229]. IMR is calculated by using the temperature-sensitive coronary pressure wire and modified software to calculate the mean transit time of room-temperature saline injected down a coronary artery. The inverse of the hyperemic mean transit time has been shown to correlate with absolute flow. IMR is then obtained by dividing distal coronary pressure by the inverse of the hyperemic mean transit time. MR is calculated using the dual sensor Combowire as the ratio of mean distal pressure to average peak blood flow velocity (APV). Both of these give an index of minimal microvascular resistance during maximal hyperaemia and because both pressure and flow are incorporated they may be used in patients with epicardial disease. However, both

techniques attract controversy, such as the uncertain effect of coronary collaterals and coronary steal and there is ongoing debate as to which is the more representative of true myocardial microvascular resistance[230].

1.5 Aims and Outline of this Thesis

The main aim of this thesis was to examine the adaptive mechanisms of the heart to ischaemic stress, using the models of exercise induced myocardial ischaemia and acute myocardial infarction. In the former, we sought to use invasive physiological measurements and high-resolution cardiac magnetic resonance imaging to assess changes in coronary blood flow, central haemodynamics and transmural myocardial perfusion in patients with symptomatic coronary arterial disease. In the latter, we sought to examine the role of *post-conditioning* as a potential therapeutic tool in a randomised controlled trial involving patients undergoing primary percutaneous revascularisation for acute myocardial infarction. The results of the post-conditioning trial are presented in Chapter 3.

The principle tools required for the studies involving stable IHD patients were high-speed and high-resolution CMR imaging and invasive dual-sensor coronary measurements in the cardiac catheterisation lab. Both of these involved the development of a specially adapted supine ergometer that would be used to exercise the patients to provoke myocardial ischaemia. The development of the catheter lab exercise protocol as well as the different analytical techniques used are described in the methods section in Chapter 2 and the results of these studies in Chapter 5. For the CMR protocol, data sampling had to be very fast, not only to allow imaging at high heart rates such as during peak exercise but also to allow high-resolution imaging required to determine differences in endo- and epicardial patterns of perfusion. A novel *k*-t SENSE perfusion protocol was used (see Methods) and imaging was undertaken using a dedicated 3-T magnet at the Rayne Institute. 3-T offers better signal-to-noise ratio with a reduction in artefacts compared to 1.5-T. Because there have been only few studies using *k*-t perfusion at 3-T a validation study was first required comparing it's diagnostic accuracy with the invasively measured fractional flow reserve (FFR). The results of this are presented in Chapter 4. Once the perfusion sequence was validated, it was tested in volunteers undergoing exercise stress and novel quantification methods were used to

determine differences in transmural myocardial blood flow. The results of these studies are presented in Chapter 6.

Key Hypotheses Under Investigation in this Thesis

1. The reduction of ischaemia seen on second exercise in patients with coronary artery disease can be explained by changes in central haemodynamics, especially a reduction in central blood pressure causing a reduction in ventricular afterload and enhanced vascular-ventricular coupling.
2. Warm up angina is associated with reduced microvascular resistance and an improvement in subendocardial perfusion and on second exercise
3. Postconditioning causes a reduction in infarct size through activation of innate myocardial protective mechanisms

2 METHODS AND TECHNIQUES USED IN THIS THESIS

2.1 Introduction

This chapter outlines some of the specific techniques used in this thesis. A general description of many of these has been given in the previous chapter and detailed derivations of certain indices and quantification methods will be referenced rather than presented in full. Such derivations will be presented, however, if they are of relevance to the results and discussion of the particular experiments in which they were used.

This chapter will also cover the development of the novel techniques used in this thesis and include some of the preliminary data that were obtained for internal validations and reproducibility purposes and to fine-tune methods prior to their use in the main studies.

2.2 Catheter Lab Derived Data

2.2.1 Assessment of Coronary Pressure and Flow

2.2.1.1 Dual-Sensor Pressure and Flow Measurements

Simultaneous pressure and flow measurements are required to distinguish the relative effects of microvascular or epicardial resistances in patients with coronary disease. The measurement of coronary flow reserve (CFR) can be assessed either by using a Doppler sensor probe mounted on an intracoronary guide wire, or using coronary thermodilution where the transit time of a room temperature bolus of saline is tracked as it passes down a coronary artery. When a thermistor is attached to a pressure sensor-tipped guide wire the thermodilution technique can be used to obtain simultaneous pressure and flow measurements that can be used to assess microvascular resistance[241]. While robust and reliable, CFR_{thermo} correlates well with Doppler-derived CFR[242]. However, there are some concerns about the physiological derivation of this index as well as the effect of collateral flow on such measurements in patients with significant epicardial stenosis[230]. In addition, for more detailed information regarding instantaneous velocity measurements at specific time points within the cardiac cycle a Doppler flow signal is required. Catheter-based Doppler systems were first introduced in the 1970s and have since undergone many improvements[243]. Until the development of the dual-sensor Combowire® (Volcano Therapeutics™, USA), see Figure 15, the only way to measure simultaneous pressure and flow measurements was using two separate wires, one mounted with a piezoelectric Doppler probe and the other tipped with a pressure sensor. As well as being inconvenient and unwieldy there was evidence that the very presence of the second wire had a significant effect on the measurements taken with the other[41]. The development of the Combowire therefore greatly facilitated the collection of such data and it has been successfully used in numerous clinical studies investigating the microcirculation[41, 238, 240]. In addition, simultaneous pressure and velocity measurements are necessary for the estimation of arterial wave speed at a single site[244] which has allowed the development of wave intensity analysis, an exciting

new method of assessment of travelling waves within the coronary circulation (see next section)[245].

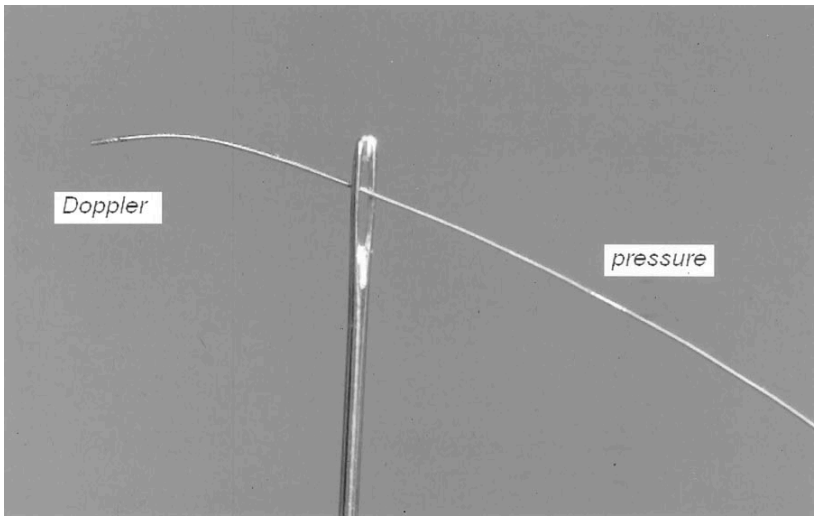

Figure 15. 0.014" Dual-sensor guide wire, Combowire® (Volcano Therapeutics™, USA). On this version of the wire (model 9515), the pressure sensor is offset by 30mm from the Doppler sensor which is situated at the tip if the wire. Another version is available (model 9500) where both sensors are situated at the tip, although this can be more difficult to manipulate in tortuous vessels or across tight lesions.

Figure 16. Screenshop from the ComboMap™ console showing simultaneous pressure and flow measurements.

2.2.1.2 In-House Data on Reproducibility and Variance of Invasive Catheter Techniques

Before embarking on studies involving invasive coronary pressure and flow measurements it is important to assess repeatability and variance of the measurements using the dual-sensor Combowire®. In order to do this 8 consecutive patients being considered for percutaneous coronary intervention (PCI) and pressure wire assessment were selected and consented into the study*. As in standard clinical use the wire was introduced into the coronary artery and the lesion was crossed with a 0.014" ComboWire® (Volcano® Theraputics, USA) and the tip positioned in the distal vessel. 3 baseline measurements of pressure and flow were recorded. The patient was then given a bolus of 36µg intra-coronary adenosine and a further set of measurements taken during peak hyperaemia. The values were allowed to return to baseline before this was repeated a further two times. All tracings were recorded for off-line analysis using dedicated software (StudyManager©)[240].

Analysis

Baseline average peak velocity (APV) was measured as the average instantaneous peak velocity (IPV) taken over 3 cardiac cycles. These values were also recorded at peak hyperaemia. At peak, the pressure measurements in the distal coronary (P_d) and aorta (P_a) were also recorded. From these values fractional flow reserve (FFR= P_d/P_a), coronary flow reserve (CFR= APV_{peak}/APV_{base}), hyperaemic stenosis resistance index (SR=P_a-P_d/APV_{peak}) and index myocardial resistance (MR=P_d/APV_{peak}) as previously described. All arterial pressure values were corrected to venous pressure measurements taken from a catheter in the right atrium. As is consistent with other similar studies, from the 3 sets of values recorded for each vessel (base and peak measurements) the outlier was excluded and the statistical analysis performed on the 2 closest sets of values. Variability was calculated as the standard deviation (SD)

*This number was based on previous similar validation studies240. Siebes M, Verhoeff BJ, Meuwissen M, de Winter RJ, Spaan JA, Piek JJ. Single-wire pressure and flow velocity measurement to quantify coronary stenosis hemodynamics and effects of percutaneous interventions. *Circulation*. 2004;109:756-762.

divided by the mean and expressed as a percentage. Bland-Altman plots were then used to record the mean difference and standard error.

Results

14 vessels in 8 patients were examined in the study. Measurements were successfully taken in 13 vessels (5 LAD, 5 Cx and 3 RCA). One set of data was unusable due to poor quality of the traces.

	Absolute mean±SD	**Variability (%)**	**Mean absolute difference**	**95% CI**	**Standard Error**
Base APV	19±7.9	7.8	2.16	0.3-4	2.2
Peak APV	33.5±11.5	7.3	3.43	1.1-5.8	3.2
P_a	73.3±11.8	2.5	2.56	0.1-5	3.3
P_d	58±10.7	2.9	2.57	0.2-2.9	2.9
FFR	0.79±0.16	1.7	0.02	-0.004-0.05	0.05
CFR	1.8±0.6	8.4	0.2	0.03-0.3	0.17
SR	0.67±1	12.3	0.05	0.006-0.1	0.27
MR	2±0.72	7.3	0.21	0.02-0.4	0.2

Table 1. Table of results for Combowire measurements taken from 3 sequential data sets taken from 13 vessels in 8 patients. Variability was calculated as the standard deviation (SD) divided by the mean and expressed as a percentage. APV = average peak velocity, P_a = mean aortic pressure, P_d= mean distal coronary pressure, FFR =fractional flow reserve, CFR =coronary flow reserve, SR =hyperaemic stenosis resistance index, MR =index of myocardial resistance, SD =standard deviation.

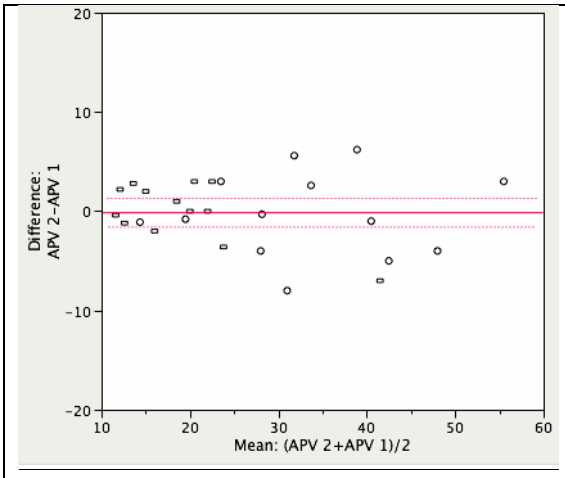
Difference:
APV 2-APV 1
Mean: (APV 2+APV 1)/2

A

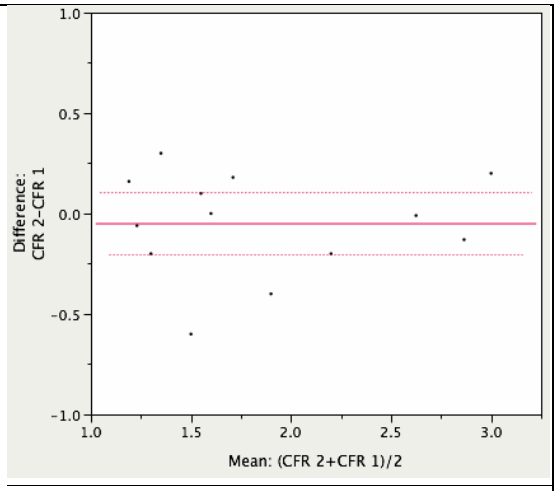
Difference:
CFR 2-CFR 1
Mean: (CFR 2+CFR 1)/2

B

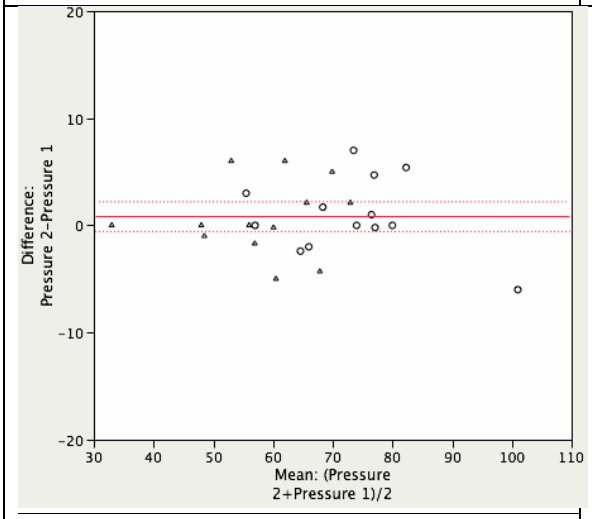
Difference:
Pressure 2-Pressure 1
Mean: (Pressure
2+Pressure 1)/2

C

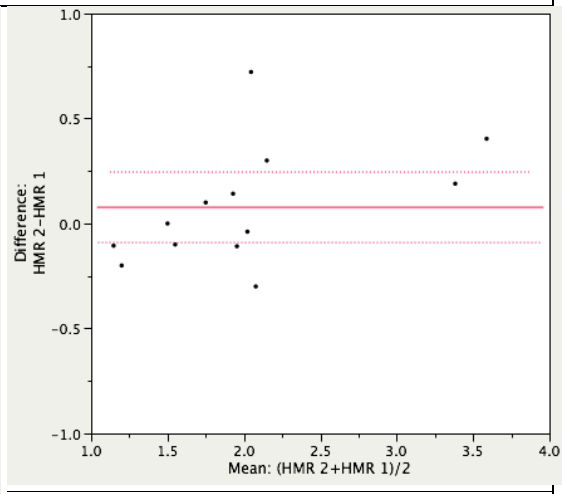
Difference:
HMR 2-HMR 1
Mean: (HMR 2+HMR 1)/2

D

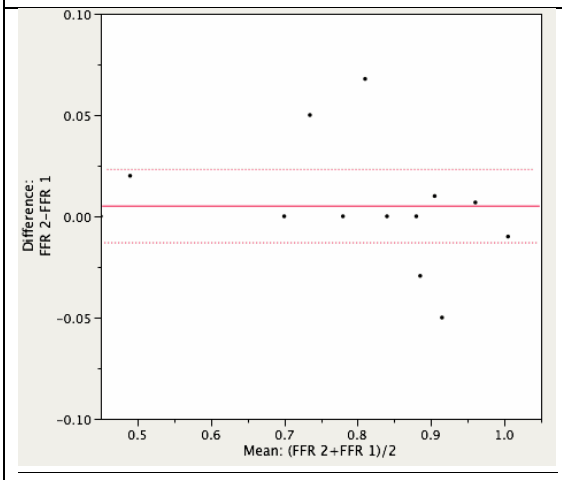
Difference:
FFR 2-FFR 1
Mean: (FFR 2+FFR 1)/2

E

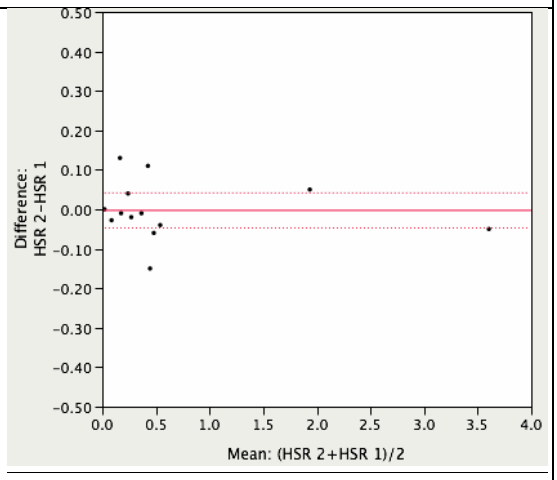
Difference:
HSR 2-HSR 1
Mean: (HSR 2+HSR 1)/2

F

Figure 17. Bland-Altman Plots showing mean difference and standard error (SE) for A) Average peak velocity (APV), B) coronary flow reserve (CFR), C) Pressure measurements, D) index myocardial resistance (MRv), E) fractional flow reserve (FFR), and F) hyperaemic stenosis resistance index (SRv).

These data suggest a high degree of repeatability with low variance for Combowire measurements in our institution that compare well to results from other centres published in the literature[240].

2.2.2 Pulse Wave Analysis

Assessment of the arterial pulse has been a major part of medical assessment and investigation since the earliest times. The arterial pulse is of complex shape, varies with age, differs in different arteries, and changes markedly with physiological and pharmacological interventions. However, advances in pulse wave interpretation have only been possible since the development of accurate high-fidelity instruments for invasive and non-invasive pressure wave recording, and for a deeper understanding of arterial hemodynamics to be achieved. This occurred with the introduction of catheter-tip manometers in the 1970s, and with the development of methods to characterize and analyze the arterial pulse in the frequency as well as the time domain[246].

2.2.2.1 Peripheral Vs. Central Measurement of the Aortic Pressure Waveform

In the majority of studies, limitations in the direct measurement of central aortic systolic pressure mean that such measurements are usually estimated using a radial-aortic transfer function, such as that incorporated into a peripheral applanation tonometer[88, 89, 247, 248]. This transfer function has been validated to estimate reliably central systolic blood pressure (and pulse pressure) at low workloads[249] but has not been validated at higher heart rates/workloads which would limit it's use in the proposed studies for this thesis. Transfer functions do change during exercise [250], and therefore this technique may have limitations with respect to precise estimation of central pressure at high heart rates/workloads. Limitations on the accuracy of estimation of central pressure may also be imposed by calibration of peripheral arterial waveforms by brachial cuff pressure[251] and by brachial-to- radial

amplification[252]. Because of these, we sought to develop a protocol whereby central aortic pressure would be measured directly using a high fidelity pressure-sensor tipped wire. The development of this protocol is described in more detail in Section 2.2.4 below

2.2.2.2 Physiological Parameters Derived from the Central Aortic Pressure Waveform

A typical central pressure waveform is shown in Figure 8 above. T_F marks the foot (start) of the pressure waveform. The time between two consecutive T_F is the cardiac cycle, or pulse, duration. P_1 is the pressure at the "first shoulder" ("inflection") that represents the non-augmented systolic pressure that is devoid of the effects of the reflected waveform. P_2 is the maximum height of the waveform and represents the central systolic blood pressure (cSBP). T_R is the time between T_F and P_i that denotes the round-trip time taken for pressure waveform to be propagated from the central aorta to the site of reflection and back again, which results in pressure augmentation. The difference between P_1 and P_2 quantifies this phenomenon (Aug). The lowest point of the pressure waveform is the central diastolic blood pressure (cDBP, not shown), and the difference between cSBP and cDBP is the central pulse pressure (cPP). Systolic (ejection) duration is defined as the time between T_F to the dicrotic notch; the latter corresponding to the global maximum of the second derivative of the pressure waveform between the systolic peak and the end of the pressure waveform. Diastolic duration is the time from the dicrotic notch to the foot of the next wave. The diastolic time fraction (DTF) is the diastolic duration expressed as a fraction of the pulse duration. The area under the waveform (pressure-time integral) during systole is the tension time index (TTI) and that during diastole is the diastolic time index (DTI, hatched), which are indices for myocardial oxygen consumption and supply respectively[89]. TTI and DTI divided by the systolic and diastolic durations respectively constitute the mean systolic and diastolic pressures.

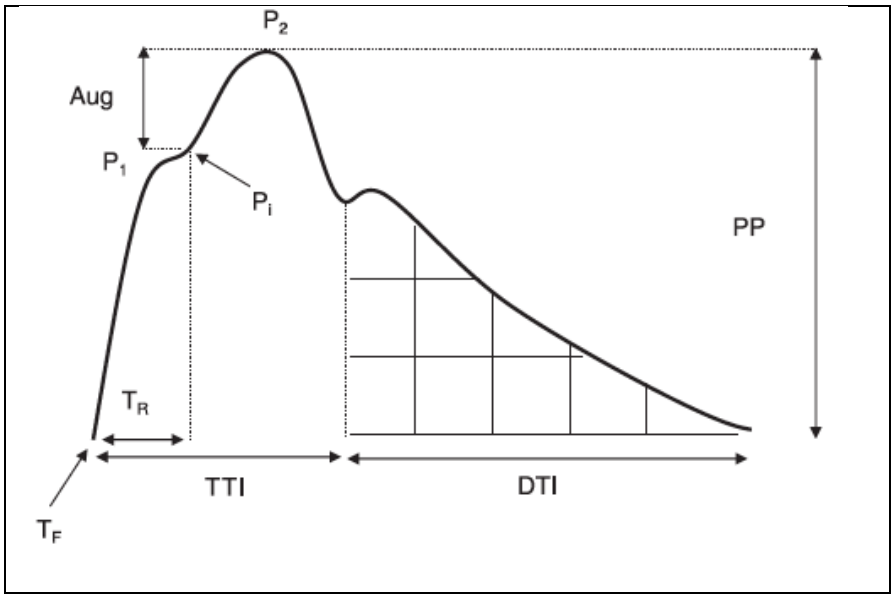

Figure 18. Typical resting ascending aortic waveform in a healthy middle-aged man. Two systolic peaks are labeled P1 and P2. The area under the curve (AUC) during systole is the tension time index (TTI), and AUC during diastole is diastolic time index (DTI). TR is defined as the time between the foot of the wave (TF) and the inflection point (Pi).

2.2.3 Wave Intensity Analysis

The majority of resistance within the coronary circulation takes place in the proximal arteriolar resistance vessels. However, assessment of microvascular resistance using epicardial measurements may be confounded by more distal (capillary and venous) effects. Wave intensity analysis (WIA) is a technique that evaluates the proximal (arteriolar) part of microvascular resistance more or less separately of these downstream effects.

2.2.3.1 Theoretical Background

The shape of a pressure or flow waveform during a cardiac cycle results from the interaction of successive forward and backward wave fronts. Wave travel in any given direction carries information about its initiating event. WIA is based on the *method of characteristics*, a mathematical technique for solving partial differential equations and widely used in gas dynamics. Kim Parker and co-workers first addressed the problem of wave propagation in elastic arteries[253] and their theoretical groundwork has subsequently be applied to a variety of vascular beds. WIA is a time-domain method and assumes that every wave can be reconstructed by the superposition of an infinite number of wavefronts. No assumption regarding the

periodicity of the interrogated signals or the linearity of the system under study is necessary. The full mathematical derivation of WIA is not presented here but can be found in the paper by Parker et al referenced above. WIA has dimensions of power per unit area and refers to the power carried by the waves travelling in the blood stream and not to the waves propagating in the vessel wall. It allows separation of upstream from downstream originating events based on a single set of measurements at an accessible site remote from where the waves were initiated[244, 254].

WIA is uniquely suited to investigate events in the coronary circulation, where forward waves originate in the left ventricular cavity and are transmitted to the coronary vessels via the aorta, and backward waves originate in the small vessels within the contracting or relaxing myocardium and are damped by the proximal resistance arteries[254]. WIA can identify the origin and nature (acceleration or deceleration of blood flow) of these overlapping waves and cast light on how the complex interaction of ventricle, coronary artery, and myocardial microcirculation produces the recognisable coronary pressure and flow profiles. These new concepts have recently been applied to normal coronary vessels in animals[255, 256] and humans[245].

2.2.3.2 The Pattern of Coronary Waves Generated Throughout the Cardiac Cycle

The application of WIA to the human coronary circulation was first carried out by Davies et al[245] and the description below is adapted from their observations of waves during the cardiac cycle.

Waves Occurring During Ventricular Contraction

The early backward-traveling pushing wave (labelled 1 in Figure 19) originates from the microcirculation in early systole before opening of the aortic valve, when small vessels that permeate throughout the myocardial beds are compressed by the contracting ventricle, as described by Spaan et al[43] in the intramyocardial pump model. This pushing wave propagates backwards along the coronary artery toward the coronary ostium. Because of the severe impedance mismatch between the coronary artery and the aorta, a large proportion of this wave is reflected back into

the coronary artery (as a suction wave, because this is an “open-ended” reflection). This reflection is seen almost simultaneously because of the very short distance between the proximal coronary artery (where the measurements are made) and the coronary ostium. Both of these waves decelerate blood flow velocity within the coronary artery. The dominant forward-traveling pushing wave (labelled 2 in Figure 19) occurs early in systole and is caused by ventricular ejection. The wave is transmitted from the lumen of the contracting ventricle into the aorta and thence into the coronary artery. This wave continues along the coronary artery until it meets a reflection site, such as a bifurcation or a microvascular bed, where a proportion of the wave is reflected back toward the coronary ostium, to contribute to the late backward-traveling pushing wave (labelled 3 in Figure 19). The other contributor to this wave is compression of the distal coronary microcirculation. Although both of these waves occur during ventricular contraction, the dominant forward-traveling pushing wave accelerates coronary blood flow, whereas the late backward-traveling pushing wave acts to decelerate coronary blood flow velocity.

Waves Occurring During Ventricular Relaxation

The next wave in the coronary artery circulation begins as the rate of contraction of the ventricular lumen is decreasing. This deceleration results in increasing “separation” tensions within the moving column of blood in the heart and aorta. Soon these tensions build sufficiently to form a detectable wave, which is transmitted along the aorta and into the coronary artery. This forward-traveling suction wave (labelled 4 in Figure 19) has a suction action at the proximal end of the coronary artery and slows coronary artery blood flow velocity. Continuing ventricular relaxation eases the compressive forces on the small vessels lying within the myocardium, which decreases the resistance of the microcirculation and lowers the pressure at the distal end of the coronary artery. This initiates a suction wave—the dominant backward traveling suction wave (labelled 5 in Figure 19)—causing blood to be accelerated forwards. There is a tug-of-war between these 2 competing suction waves originating from opposite ends of the artery, overlapping in time.

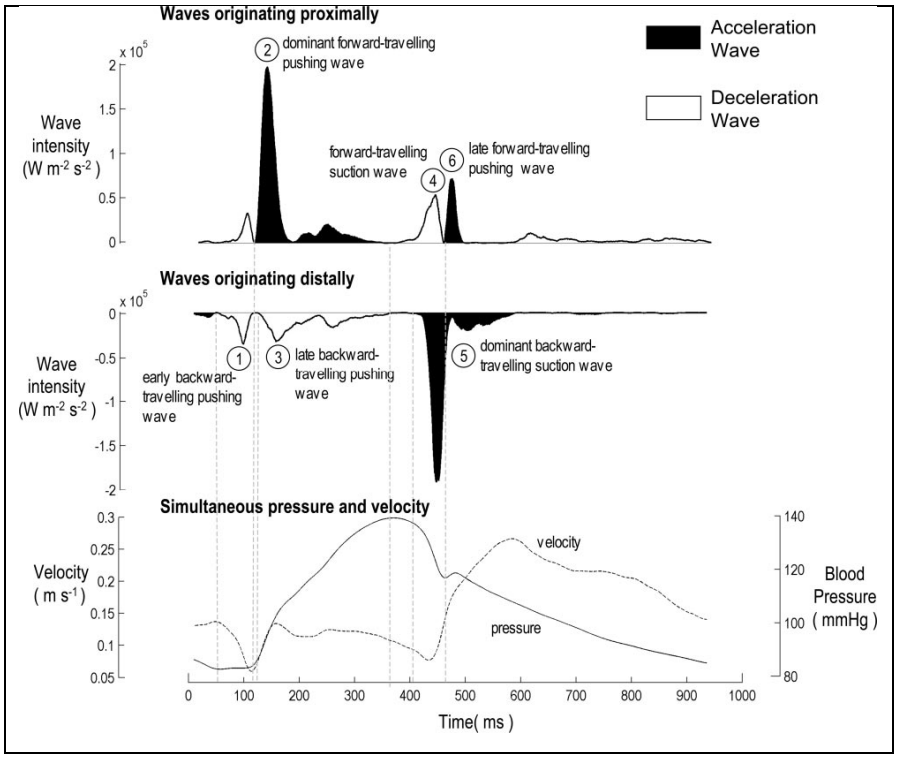

Figure 19. Identification of waves in the human circumflex artery, waves originating proximally (WI, upper panel), wave originating distally (WI, middle panel). Coronary artery flow velocity and pressure is shown in the lower panel. Dashed line shows the onset of each wave *[Adapted from Davies et al, Circulation 2006]*[245].

At first, the forward-traveling suction wave predominates, but later the dominant backward-traveling suction wave becomes dominant as the myocardium ceases to compress its small vessels. The dominant backward-traveling suction wave continues as the heart continues to relax, remaining the dominant wave until it is briefly interrupted by the late forward-traveling pushing wave (labelled 6 in Figure 19). This wave originates from the proximal end of the artery, coinciding with closure of the aortic valve, when aortic pressure is briefly augmented. This proximal originating wave accelerates blood still further, augmenting the actions of the distal acceleration wave in the coronary artery. This wave is short-lived, as the dominant backward-traveling suction wave once again becomes the dominant wave in the coronary artery.

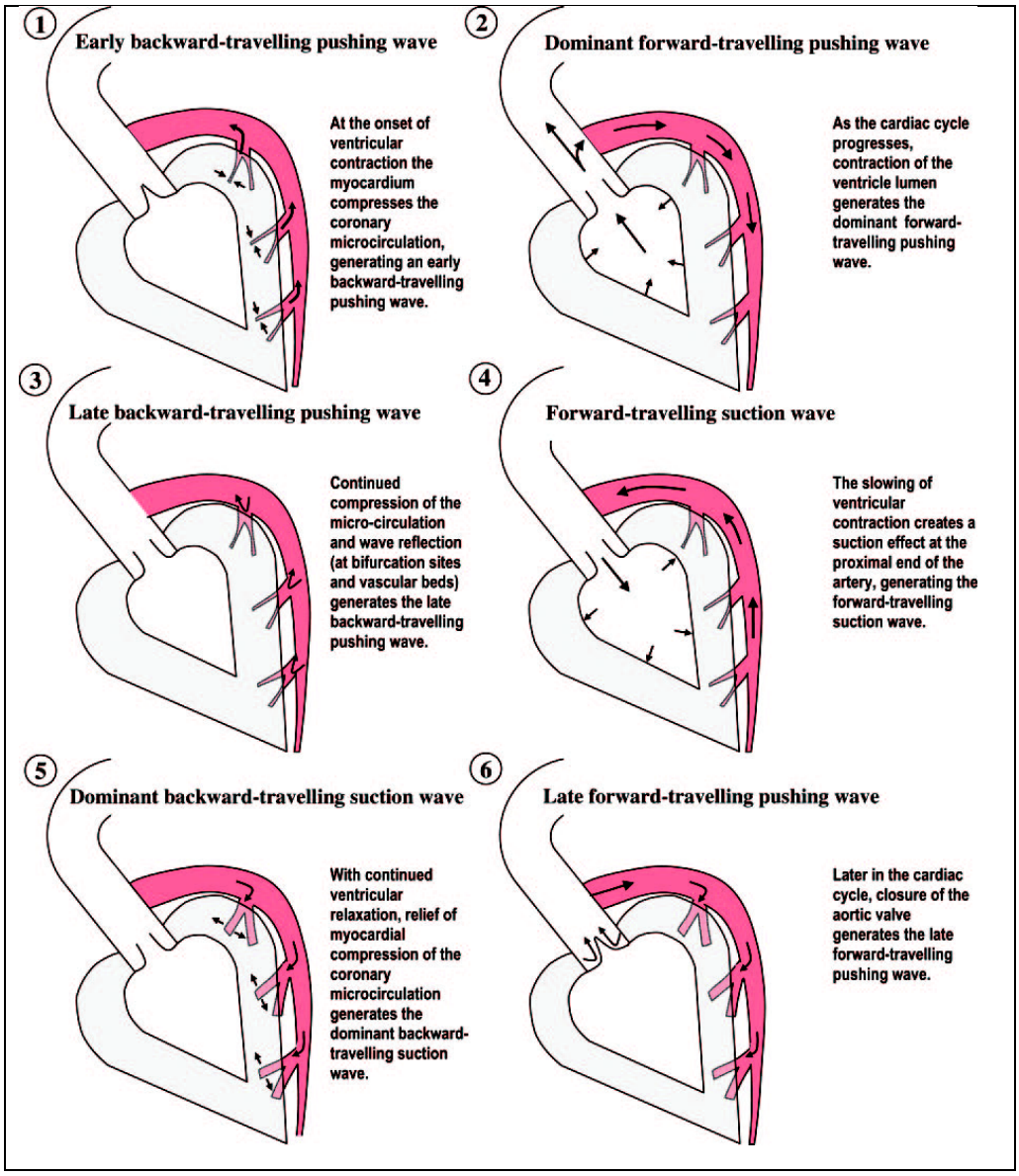

Figure 20. Sequence of energy waves in the human coronary artery during the cardiac cycle. Arrows represent direction of wave motion rather than direction of blood flow *[Adapted from Davies et al Circulation 2006]*.

2.2.3.3 Details of WIA carried out for these studies

Net wave intensity (dI) represents the flux of energy carried by the wave per cross-sectional area of a vessel and is determined as the product of changes in pressure (P) and velocity (U) at a single location [253]:

$$dI = dP \times dU \quad (1)$$

dI can differentiate between upstream (dI_+) and downstream (dI_-) traveling contributions:

$$dI = dI_+ + dI_- \tag{2}$$

Forward waves (FW, dI_+) travel in the direction of blood flow and are positive and backward waves (BW, dI_-) travel in the opposite direction and are negative.

The separated forward and backward contributions are defined as[257]:

$$dI_\pm = \frac{1}{4\rho c}\left(\frac{dP}{dt} \pm \rho c \frac{dU}{dt}\right)^2 \tag{3}$$

As discussed in the section above waves are also characterized by their effect on the blood mass: compression waves increase pressure and expansion waves decrease pressure. Thus, waves can be classified into four types: Forward compression wave (FCW), forward expansion wave (FEW), backward compression wave (BCW) and backward expansion wave (BEW).

In the coronary circulation, FWs arise from the left ventricular cavity and enter coronary vessels via the aorta, and BWs originate in the small vessels that are embedded within the contracting or relaxing myocardium[258]. Figure 21 below shows the net coronary wave intensity and the separated forward and backward contributions. The compression waves occur during contraction and the expansion waves during the early relaxation phase of the cardiac cycle.

WI analysis was performed using a custom-made program written in Delphi. After Savitzky-Golay filtering and ensemble averaging of the respective selected beats, net coronary wave intensity was calculated as

$$dI = dP_d/dt \times dU/dt \tag{4}$$

in order to normalize for the sampling rate[257]. The separated forward and backward contributions were then derived based on Eq. 3. The energy carried by each of the

four dominant waves was obtained by integrating the area under the respective wave.

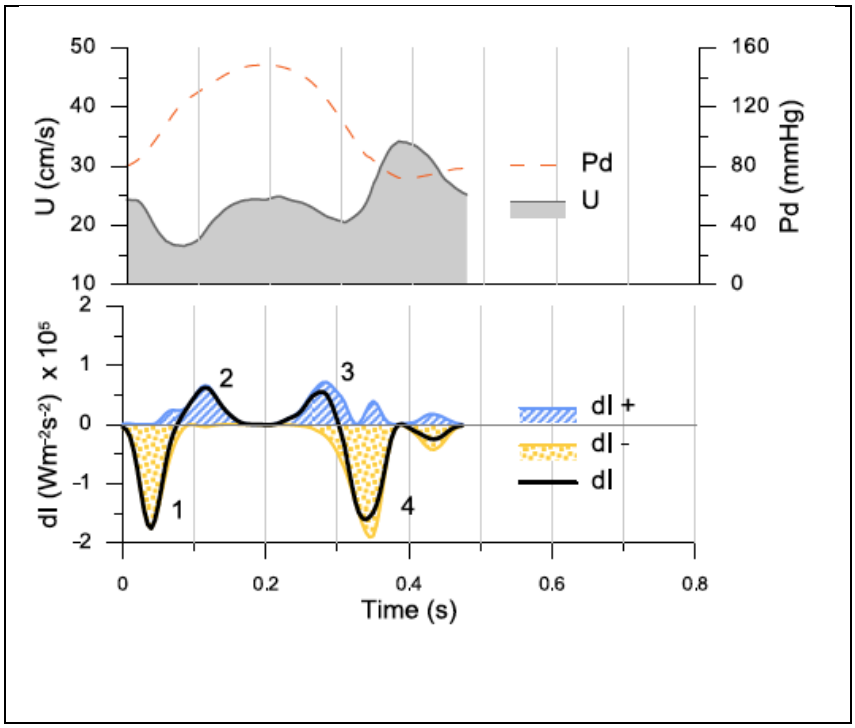

Figure 21. Coronary net wave intensity (dI) and the corresponding forward and backward contributions. The coronary pressure (Pd) and flow velocity (U) waveforms used to calculate dI are shown on top. BCW and BEW (1 and 4) come from the microcirculation; FCW and FEW (2 and 3) come from the coronary ostium.

2.2.4 Assessment of Invasive Coronary Pressure and Flow During Exercise Stress

2.2.4.1 What are the advantages of using exercise stress?

Exercise stress plays a unique role in the assessment and investigation of patients with cardiac disease. A reduction in exercise capacity is often the first manifestation of underlying cardiac problems and a knowledge of the complex local and systemic haemodynamic adaptations that result from exercise are key to understanding how and why these patients develop symptoms, and importantly how such symptoms may be relieved through therapy. The metabolic requirement of exercising skeletal muscle is met by an increase in cardiac output and subsequent increase in myocardial oxygen demand as a result of increased heart rate and myocardial stroke work. The onset and severity of symptoms in a patient will result from a complex interaction of myocardial microvascular resistance, coronary stenosis severity, coronary perfusion pressure and diastolic interval. Vasodilators such as adenosine

and dipyridamole, or inotropes such as dobutamine are used in everyday practice as pharmacological stressor agents in a wide range of cardiac investigations, including echocardiography, nuclear perfusion and in the catheter lab to measure fractional flow reserve (FFR). In research, rapid cardiac pacing has been advocated as an additional, alternative stressor and while it reduces diastolic interval it may actually *reduce* cardiac work by diminishing diastolic filling and hence stroke volume[12]. While the effect of these different methods can simulate some of the haemodynamic components of exercise, none can recapitulate its full effects and therefore such methods do not provide an accurate impression of what is actually happening at the time of onset of symptoms in the patient.

Exercise stress testing using either a treadmill or bicycle is widely used in the non-invasive sphere of cardiac investigation and research. In the catheter laboratory, however, impracticalities have limited its use despite an increase in the interest and utilization of invasive physiological measurements, both in the clinical assessment of coronary disease[259] and as a research tool. The development of a combined pressure and flow intracoronary wire [240] has further improved our capability to interrogate the intricate haemodynamic events occurring at a coronary and microvascular level. Vasodilator agents (primarily adenosine) are generally used to induce maximal blood flow, or hyperaemia, either delivered locally or systemically. While the administration of such agents may be sufficient to induce minimal microvascular resistance or invoke a pressure drop across a coronary stenosis, such effects bear little resemblance to the intense systemic haemodynamic impact of strenuous exercise on the circulation. The effects of exercise on large artery haemodynamics are also thought to play a key role in the manifestations of cardiac disease. Pulse wave analysis[88] of the central aortic pressure trace as well as wave intensity analysis of combined central pressure and flow measurements[260] have the potential to take our understanding further but rely on high fidelity signals obtained invasively during exercise. To date, there have been no published data examining the effects of exercise stress on invasively-acquired aortic and coronary pressure and flow data obtained during cardiac catheterisation.

Our purpose was to develop a protocol where invasive aortic and intracoronary physiological measurements could be obtained during strenuous exercise stress in patients undergoing cardiac catheterisation.

2.2.4.2 Development of the experimental protocol

The requirement for the development of this protocol was that measurements be actually recorded *during* exercise stress rather than immediately before or after. Under some circumstances bicycle stress is used immediately before measurements of pulmonary artery pressure during right heart catheterisation via the brachial vein[261]. However, in most patients there is a rapid decrement in peak heart rate that occurs after the cessation of exercise[262] and in our study with the time that would be taken to position the patient, intubate the coronary artery and pass the sensor wire into the diseased vessel, this would not be possible. In addition, we wanted to record the full range of data throughout exercise from baseline through incremental increases in workload until peak stress and then through recovery.

Study Patients

Patients were recruited from routine waiting lists for percutaneous coronary intervention (PCI) for single vessel coronary disease. Exclusion criteria were unstable symptoms, previous myocardial infarction/CABG, impaired left ventricular (LV) function, severe co-morbidities, and inability to exercise.

Supine ergometer

A variety of methods to induce exercise stress were considered. Handgrip repetitive exercise is simple and allows trans-femoral arterial access. However, it only utilizes the small muscles in the hand and forearm and does not induce the large haemodynamic changes that accompany lower limb bulk muscle exercise[89]; hence it is difficult to reach the ischaemic threshold in patients with coronary disease. Straight leg-raising is another option, but is difficult to standardize and ensure consistency of workload. Again it is difficult for patients to reach their ischaemic threshold through this technique alone. After due deliberation, a specially adapted supine cycle ergometer (Ergosana®, Germany) was selected (see Figure 22 below) which allows a standardized and incremental increase in workload, as well as

allowing leg movements familiar to most patients. Supine cycle ergometers are commonly used in other settings, such as stress echocardiography, where the patients exercise to their ischaemic threshold. A special clamping mechanism to allow the bike (which weighs in excess of 60 kilograms) to be firmly attached to the catheter laboratory table was designed and built by the engineering department at our institution as well as a mechanism for its rapid fitting to, and removal from, the table. The device was then thoroughly tested by the local health and safety team to ensure it complied with all safety regulations and did not hinder the movement of the table or interfere with the ability of the team to carry out the catheter procedure or deal with its rare acute complications.

Figure 22. Supine cycle ergometer (Ergosana®, Germany) with purpose made mechanism to and from, and to attach to, the catheter lab table.

Supine Vs. Upright Exercise

For the purposes of this study where the intention was to record invasive physiological data in the catheterisation lab actually during exercise, we were obliged to use supine exercise. Supine exercise has been used in numerous previous physiological studies[104, 263, 264]. In one such study, Sowton et al measured hemodynamic changes in a group of young subjects (some with pulmonary valve disease) during both upright and supine exercise[263]. The alteration in posture from lying supine to sitting erect on the bicycle ergometer was accompanied by a mean fall in cardiac output of 25 per cent; the stroke volume fell by 36 per cent and there was a 12 per cent increase in the heart rate. These changes are in agreement with

previous reports[265] and the authors emphasized the necessity for the body position during the control measurements to be accurately stated (and then maintained). In the current study all measurements refer to the supine body position during exercise, with patients acting as their own controls and without movement in between, therefore we do not envisage body position having any impact on these data comparisons. In addition, supine bicycle exercise electrocardiography has been shown to be significantly more sensitive, yet equally specific for the detection of coronary ischaemia when compared with upright treadmill exercise[266].

Catheter laboratory protocol

Patients were positioned on the catheter lab table in the standard fashion and a vacuum cushion containing small polystyrene balls placed beneath their shoulders to keep their position and prevent cranial migration during cycling. They were familiarized with the bike and had a short practice session to ensure they were comfortable cycling and at ease. Their legs were then removed from the pedals and they were draped in the usual fashion. Extension manometer lines were used to allow the equipment from the manifold to reach around the bike to the radial artery access site. Patients were catheterized via the right radial artery using a standard 6F arterial sheath. 3000u heparin and 1 milligram Isoket® were injected into the sheath. Right and left coronary angiograms were then taken using standard diagnostic catheters. A standard 6F guiding catheter was then introduced and positioned in the aortic root. A dual sensor pressure-flow 0.014" intracoronary wire (Combowire®, Volcano Therapeutics®, USA) was then connected to the ComboMap® console (Volcano® Therapeutics, USA) and positioned at the tip of the guide. A single sensor 0.014" pressure wire (Brightwire®, Volcano Therapeutics®, USA), which provides a high fidelity proximal pressure signal (P_a), was attached to the aortic input port on the ComboMap via an analogue transducer (SmartMap®, Volcano Therapeutics®, USA) and zeroed to gravity. It was then positioned alongside the Combowire at the tip of the guide and the pressure trace (P_d) on the Combowire was normalized to the pressure wire trace. The guide was then inserted into the coronary ostium and the Combowire passed distal to the stenosis in the target coronary artery and the wire manipulated until a good Doppler flow trace was obtained. Intracoronary nitrates

were not given, to maintain as close to real life conditions as possible. At this point the guide was disengaged, carefully avoiding displacing the Combowire, and the pressure wire was passed into the aortic root and a stable pressure signal obtained (see Figure 23 below). Finally, a servo-controlled finger pressure cuff (Finometer, Finapres Medical Systems®) was positioned and used to record the peripheral pressure waveform. All data were recorded at 100 Hz and stored on a disk for off-line analysis.

Exercise protocol

When the set-up was complete the patient's feet were fitted into the pedals on the bike and baseline measurements were taken before the patient underwent 2 periods of exercise (see Figure 24 below). The exercise protocol is a standardised incremental programme based on the patients weight and age, typically starting at 25W and increasing by 20W each minute. Exercise was continued until any of the following occurred, 1) ST depression >3mm, 2) maximum age-related heart rate, 3) severe chest pain, 4) physical exhaustion, 5) occurrence of adverse conditions such as hypotension, severe arrhythmia or dyspnoea.

Coronary flow and pressure data, ECG, central aortic pressure and peripheral pressure waveforms were recorded continuously throughout exercise and recovery. At intervals throughout the exercise protocol the aortic root was screened to ensure the correct position of the wires and the guide. At the end of the study protocol the patient underwent their planned percutaneous revascularization procedure.

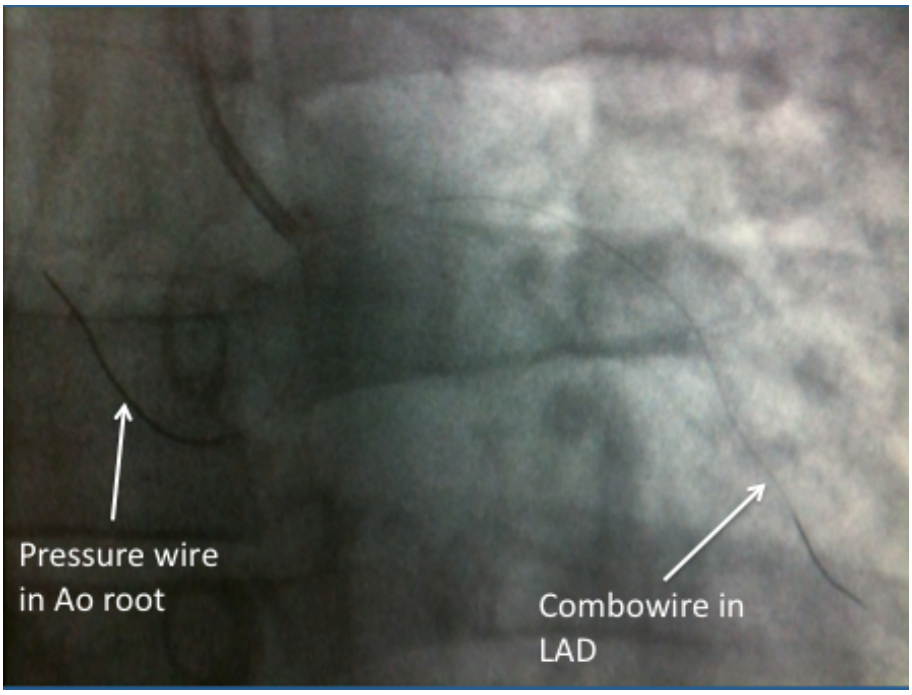

Figure 23. Still image showing a 6F guiding catheter with a dual sensor pressure-flow wire (Combowire) positioned in the left anterior descending artery (LAD) and a pressure wire positioned in the aortic root.

Intracoronary and large artery measurements

A full interrogation of the pressure waveforms from within the arterial tree: from the distal coronary artery to central aortic pressure to the peripheral circulation, was obtained throughout dynamic exercise as well as simultaneous flow measurements from the distal coronary artery . The data were then imported into Matlab™ (The MathWorksInc®, USA) and an average signal obtained across each minute during exercise and recovery and used for further analysis. Haemodynamic data recorded at baseline and peak exercise are presented as mean ± standard deviation (SD). Paired student's t-tests were used to compare group means at rest and peak stress. $P<0.005$ suggested statistical significance.

Ethics

The study protocol was approved by the local research ethics committee (08/H0802/136) and all participants signed a written consent form. They completed a feedback questionnaire following the study detailing every aspect of their experience.

Figure 24. The set-up in the cath lab during an experimental exercise protocol. The patient is cycling while catheterized via the right radial artery with the Combowire down that LAD and a pressure wire in the aortic root. The Combomap console is visible to the left of the picture.

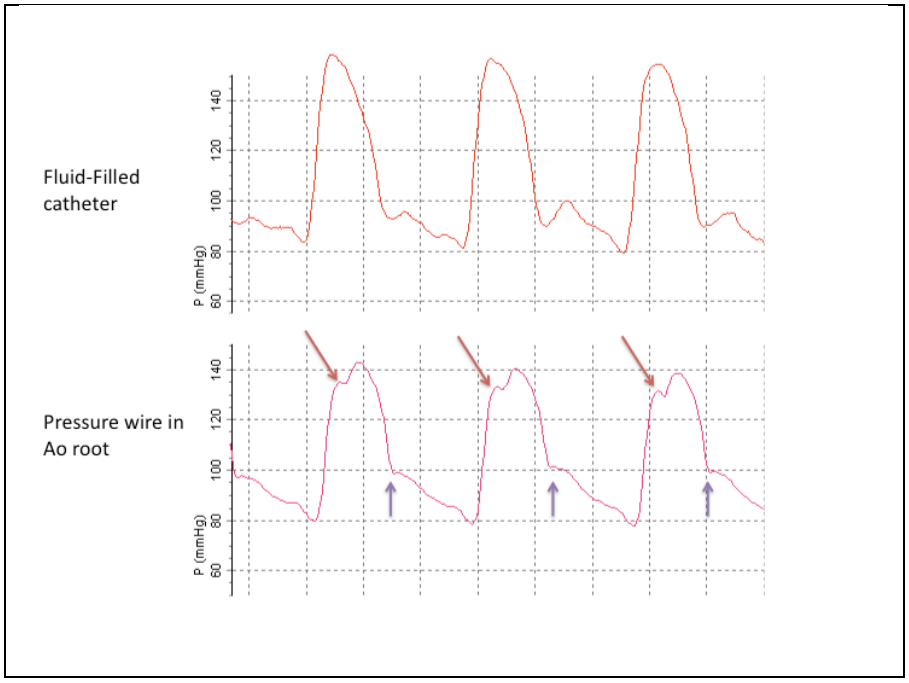

Figure 25. Arterial pressure tracings taken at peak exercise showing the superior quality of the central aortic pressure tracings obtained from the high fidelity pressure wire in the aortic root compared to the standard tracings obtained from the fluid-filled catheter from the tip of the guide. The arrows demarcate the first shoulder (necessary to calculate pressure augmentation, for example) and the dicrotic notch respectively.

2.2.4.3 Results

5 patients (4 male, age 54±7.5 years) who fulfilled the inclusion criteria were recruited into the study. Details of each case are given below. All successfully completed the protocol, exercising for 6.4±0.5 minutes with an increase in heart rate from 72.8±8.1 baseline to 120.6±8.9 ($p<0.0001$) peak and rate pressure product (RPP, $mmHg.min^{-1}$) from 95.8±17.9 x 10^3 to 200.3±33.6 x10^3 ($p=0.001$). Coronary average peak velocity (APV) went from 18.7±6.5 to 31.4±5.8 $cm.sec^{-1}$ ($p=0.002$). There were no complications. All data were of sufficient quality for further analysis. Full haemodynamic data are presented in Table 2.

Case 1

66 year old male with a background of hypertension and exertional angina with an equivocal ETT. Angiogram showed a moderate lesion in the LAD with a 50% diameter stenosis and mild atheromatous disease in the other vessels. The patient underwent the full protocol with the Combowire in the LAD. He exercised for 6.5 minutes and stopped as target heart rate was achieved. He had no chest pain or ECG changes.

Case 2

51 year old male with a background of smoking and dyslipidaemia and exertional angina with a dobutamine stress echo suggesting a small area of apical ischaemia. Angiogram showed diffuse disease in the mid-LAD with a severe stenosis at the ostium of a small diagonal. The patient underwent the full protocol with the Combowire down the LAD. He exercised for 7 minutes and stopped because of chest pain and some ST depression. There was no pressure gradient along the LAD but a relatively modest flow reserve suggested some potential microvascular dysfunction.

Case 3

55 year old male with a background of hypertension and exertional chest pain and a positive ETT. Angiogram showed a moderate lesion in the RCA. The patient underwent the full protocol with the Combowire in the RCA. He exercised for 6.9 minutes and stopped because he reached his target heart rate. There were some minor ECG changes but no he did not suffer chest pain. Again, a modest flow reserve suggests microvascular dysfunction.

Case 4

52 year old male with a background of hypertension, smoking and a strong family history presented with exertional angina. Angiogram showed a moderate lesion in a large dominant RCA with a 60% diameter stenosis. The patient underwent the full protocol with the wire in the RCA and exercised for 5.8 minutes before stopping due to leg tiredness.

Case 5

48 year old female with a background of diabetes and dyslipidaemia and exertional angina. Angiogram showed a severe lesion in the LAD with an 80% diameter stenosis. She underwent the full protocol with the Combowire in the LAD and managed 6 minutes before she had to stop because of chest pain and significant ST depression on the ECG.

	Baseline									
	HR	SBP	DBP	P_a	P_d	RPP	APV	P_d/P_a	SR	MR
Pt 1	72.3	152.5	91.8	127.6	118.7	110.2	29.7	0.9	0.3	4.0
Pt 2	81.9	122.4	80.9	98.6	96.3	100.2	13.4	1.0	0.2	7.2
Pt 3	75.3	172.5	84.7	130.6	128.1	129.9	15.1	1.0	0.2	8.5
Pt 4	59.5	121.7	79.9	103.7	94.9	72.4	18.3	0.9	0.5	5.2
Pt 5	61.0	145.0	43.8	94.4	90.6	88.4	16.6	1.0	0.2	5.5
Mean	70.0	142.8	76.2	111.0	105.7	100.2	18.7	1.0	0.3	6.1
SD	9.5	21.5	18.7	16.9	16.6	21.8	6.5	0.0	0.1	1.8
	Peak									
	HR	SBP	DBP	P_a	P_d	RPP	APV	P_d/P_a	SR	MR
Pt 1	126.3	207.0	114.8	153.5	148.3	261.5	38.5	1.0	0.2	4.8
Pt 2	124.5	176.6	98.5	135.0	126.2	219.8	29.7	0.9	0.3	4.3
Pt 3	119.0	177.5	97.9	150.6	143.9	211.3	24.4	1.0	0.3	6.0
Pt 4	127.7	159.9	102.9	129.1	112.8	204.1	36.0	0.9	0.5	3.1
Pt 5	125.2	189.5	57.4	123.2	96.0	236.9	28.3	0.8	1.0	3.4
Mean	124.5	182.1	94.3	138.3	125.4	226.7	31.4	0.9	0.4	4.3
SD	3.3	17.5	21.7	13.3	21.8	23.0	5.8	0.1	0.3	1.1
p value	0.0	0.0	0.0	0.0	0.0	0.0	0.0	0.2	0.3	0.1

Table 2. Haemodynamic data from the 5 study patients recorded at baseline and peak exercise. HR = heart rate, beats per minute; SBP = central systolic blood pressure, mmHg; DBP =central diastolic blood pressure, mmHg; P_a = mean central arterial pressure, mmHg; P_d= distal coronary pressure, mmHg; RPP = rate pressure product (=HR x SBP), $mmHg.min^{-1}$; APV= average peak velocity (distal coronary), $cm.sec^{-1}$; SR =stenosis resistance (ΔP/APV); MR=microvascular resistance (P_d/APV). *paired student's T-test.

2.2.4.4 Discussion of technique and modifications

This study demonstrates that exercise stress can be used in the catheter laboratory to obtain useful and good quality invasive physiological data. The protocol is complex but became more practicable with each case. The 5th case (6 minutes exertion) added about 30 minutes to the usual procedure duration. There were no complications during this early feasibility study and all patients, given sufficient preparation and encouragement, managed to complete the protocol with a good increment in workload as suggested by RPP. Although all the patients recruited had exertional angina and background risk factors for IHD, only case 5 had angiographically and functionally significant disease with an apparent pressure drop across the stenosis that became significant with exercise. Interestingly, the addition of i.c. adenosine at the end of the case to confirm the functional severity of the lesion demonstrated an FFR of 0.51[*], much lower than the P_d/P_a ratio of 0.78 obtained at peak exercise. This suggests that even during conditions of ischaemia there was still some vasodilatory reserve within the perfusion territory of this vessel; perhaps mediated by the vasoconstrictor effects of adreno-receptor stimulation during exercise. Such effects have been demonstrated in animal studies[78]. While cases 2 and 3 did not have severe epicardial disease an attenuated flow reserve suggested some microvascular dysfunction which may have been contributing to their symptoms.

Each iteration in the development of the protocol merited careful consideration with paramount concern for the safety of the study participants. There was some anxiety about the potential traumatic effect of the guide tip on the coronary ostium during

[*] By definition FFR can only be determined under confirmed conditions of maximal hyperaemia or minimal microvascular resistance, such as during administration of adenosine.

exercise. This was mitigated by disengaging the guide and leaving the tip well away from the coronary ostium throughout exercise. In addition, the use of the second wire in the aortic root helped prevent the guide from accidently re-engaging with the coronary ostium. By using a pressure wire for this purpose it allowed high-fidelity pressure tracings far superior to those that would have been obtained from a fluid-filled catheter alone (see Figure 25). The quality of the signal from the pressure wire was sufficient for pulse wave analysis to determine systolic augmentation, wave reflection, diastolic time fraction and other variables that would not be possible using the highly filtered trace from the fluid filled catheter.

2.2.4.5 Conclusion

It is feasible to obtain good quality, invasive intracoronary and central aortic physiological data during strenuous exercise stress in patients undergoing cardiac catheterization. The protocol develop during these preliminary studies was used in the main study and the results can be found in Chapter 5.

2.3 Cardiac Magnetic Resonance Imaging Methods

2.3.1 Determining Infarct Size and Microvascular Obstruction

Cardiac magnetic resonance (CMR) has emerged as a powerful tool in the assessment of ventricular function, perfusion and viability in AMI. Many studies using CMR have tracked the complex changes that occur in ventricular structure and function post AMI in both animal models and humans[267]. Its high spatial resolution and reproducibility make it an excellent tool for assessing ventricular function over time[268] and allow discernable differences between groups with small study populations[269]. The first-pass administration of gadolinium-DTPA (Gd-DTPA), myocardial perfusion can be assessed both at rest and with stress. Hypo-enhanced areas in the first few minutes after the gadolinium injection correlate very closely with regions of microvascular obstruction documented by radioactive microspheres and histological staining of post mortem specimens with thioflavin[205]. Delayed hyper-enhancement (10-20 min) after gadolinium injection enables precise localisation of myocardial infarction (acutely) and scar (chronically) over the full range of infarct size[204]. See The pathophysiology of infarct healing and LV remodeling has been studied in a canine model of AMI using Gd-DTPA enhanced CMR[270]. Infarct healing seemed to be an ongoing process, with early infarct expansion followed by infarct resorption, scar formation, and late wall thinning. Necrotic myocytes, interstitial oedema, hemorrhage, and inflammatory cells are resorbed and replaced by collagenous scar tissue. During the phase of initial infarct expansion it has been shown that flow within the infarct region is non-uniform with MVO continuing to progress for up to 48 hours following reperfusion[131]. Gadolinium enhancement has been used to track the changes in infarct morphology over time in humans. Following reperfusion of AMI there was about a 30% reduction in infarct volume at 5 months with some recovery of function[271]. Segments containing little MVO showed good recovery, with improved wall thickening and function. Segments containing MVO became thinned and scarred at 5 months and showed minimal recovery. Such microvascular perfusion defects are widespread and can be demonstrated in a large proportion of AMI patients despite excellent angiographic

results after primary PCI[272]. The presence of severely delayed microvascular reperfusion is predictive of impaired LV systolic function independently of the transmurality of infarction and is a strong predictor of adverse cardiovascular complications even after control for infarct size[273]. CMR has been shown to be safe in patients within 24 hours of stent placement in patients undergoing primary angioplasty for AMI[272].

In the present thesis CMR was used to determine infarct size, as well as the burden of MVO at baseline and at 3 months in the postconditioning study (see Chapter 3). Its low variability and excellent reproducibility reduce the sample size to detect differences in such studies[268, 269] and make it the ideal choice for comparing these endpoints both across subjects initially and within subjects at follow-up. Standard infarct and MVO detection sequences were used. For further specific details regarding these, as well as the quantification methods used, see Chapter 3.

2.3.2 Dynamic Contrast Enhanced Perfusion Methods

MR first pass perfusion imaging has become a valuable clinical tool for the assessment of myocardial perfusion[274]. The development of high spatial resolution perfusion techniques holds great potential to examine the changes in endo- and epicardial blood flow during exercise. We intended to develop a protocol to investigate this using a specially adapted cycle ergometer. First we had to validate the high-resolution *k*-t perfusion sequence at 3T, initially in healthy volunteers, and, then in patients with ischaemic heart disease (see Chapter 4). We then sought to examine whether the perfusion and quantification methods used could identify the physiological changes in endo-epicardial perfusion ratios that would be expected to occur during adenosine hyperaemia (see Chapter 6). Unlike with standard adenosine perfusion methods where typically only two contrast injections are used (i.e. at rest and during hyperaemic stress), during the proposed exercise protocols at least three contrast injections would be used (i.e. rest, exercise 1 and then exercise 2 after a period of rest to look for any warm-up effect).

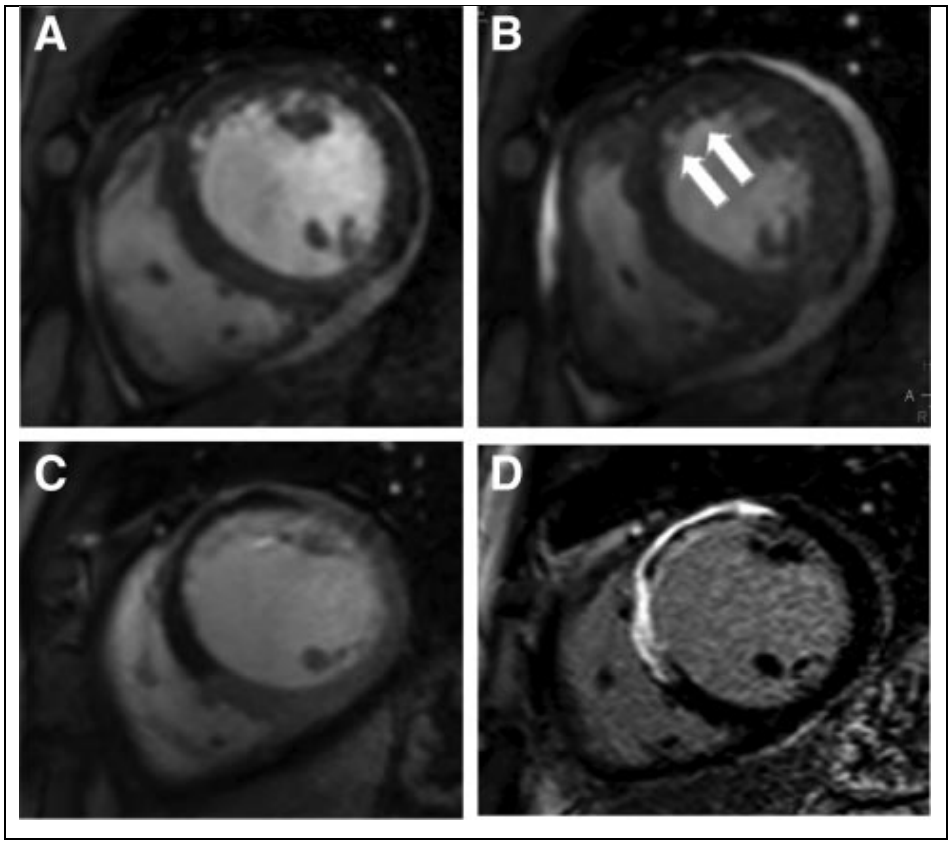

Figure 26. Diastolic (A) and systolic (B) frame from a cine CMR study acquired at the midventricular level in the short-axis orientation in a patient with a recent anterior wall acute ST-elevation MI. The arrows in B demonstrate the akinetic anterior wall with no systolic thickening compared with the other myocardial segments. C, An early gadolinium enhancement image taken 2 minutes after injection of a gadolinium-containing contrast agent shows a large region of MVO (dark areas) in the anterior wall. The late gadolinium enhancement image acquired 15 minutes after contrast application in D shows an extensive region of infarction as demarcated by the bright white regions of hyperenhancement with a core of MVO still visible. Such extensive transmural infarction with a high burden of MVO suggests that functional recovery in this region is unlikely [*adapted from Lockie et al. Circulation 2009*[215]].

A potential impact of this would be the accumulation of contrast within the myocardium with a resultant attenuation of signal and the effect this may have on quantification of myocardial blood flow. We therefore performed T1-weighted mapping studies to examine this effect and there was a need for it could be corrected for in subsequent calculations (see Section 2.3.3.4 below).

The next stage was to develop a cycle ergometer protocol similar to the one used in the catheter lab (outlined in Section 2.2.4 above). Once this was set up then a series of preliminary studies were performed on healthy volunteers both to establish the

optimum perfusion sequence, and then ensure that the data produced was of sufficient quality that it could be analysed, both to examine overall changes in myocardial blood flow, but also, and crucially, differences in flow to the endo- and epicardium. The results of these studies are presented in Chapter 6.

2.3.2.1 Principles of Dynamic CMR Perfusion

Dynamic CMR typically exploits the first-pass kinetics of conventional T_1-enhancing extracellular gadolinium chelates. The magnetic resonance contrast medium, typically Gadolinium-DTPA (Gd-DTPA) enters the microvasculature and also starts to diffuse within the interstitial space during the first pass[274-277]. As a result, the signal intensity of the myocardium increases, the rate of which is linked to the perfusion status of the tissue. Accordingly, normally perfused myocardium demonstrates a fast signal increase per unit time in the vasodilated state, whereas signal increase is delayed in myocardium supplied by, for example, a flow-limiting coronary stenosis. The first pass lasts only a few seconds and therefore in such dynamic studies it is crucial to acquire good quality data during this period to allow subsequent analysis (see below). Respiratory and cardiac motion are the two main potential sources of artefact. The data acquisition can be completed within a breath-hold, which efficiently eliminates respiratory motion; in addition, the MR data collection is electrocardiography (ECG)–triggered, which eliminates cardiac motion. Together, breath holding and ECG-triggering allow a high spatial resolution for perfusion data of around 1.5 to 2.5 mm x 1.5 to 2.5 mm. This excellent spatial resolution allows for discrimination of perfusion deficits that are limited to the vulnerable subendocardial layer of the left ventricular myocardium[191, 278].

To increase the sensitivity of the pulse sequence to detect changes in the contrast as it diffuses through the myocardium, the magnetisation may be prepared before data readout occurs. In the past an inversion recovery preparation was most often used, providing a large dynamic range of signal response. However, in practice the delay time from preparation to readout required 300 to 400 milliseconds of waiting time, thus precluding true multislice imaging. Therefore the currently accepted preparation is a saturation recovery approach, which renders the signal response

independent of heart rate variations and further shortens the waiting time down to 100 to 200 milliseconds[191, 201, 279]. Selection of the optimum delay time should not only optimise signal response for the expected changes in the contrast bolus concentration during the first pass but also locate the window for data readout into phases of the cardiac cycle where motion is minimal. Data acquisition in late systole is ideal as during this phase the myocardium is at it's thickest and facilitates subsequent perfusion analysis.

Data Post-Processing Strategies

It is important to ensure maximum coverage of the LV myocardium in order to detect and quantify perfusion defects accurately. In addition, to obtain signal intensity–time curves from which perfusion parameters (see below) can be derived, a temporal resolution of 1 stack covering the left ventricular myocardium being acquired every 1 to 2 RR intervals is recommended[279, 280]. To satisfy these conditions very fast data acquisition for perfusion imaging is crucial. Echoplanar imaging (EPI), which describes the acquisition of a full k-space (required to reconstruct 1 single image) after a single radiofrequency excitation is one such fast approach. In contrast, with a conventional fast gradient echo approach, 1 radiofrequency excitation is required for every line in k-space. Single shot EPI is very fast, but its relatively long echo time renders the sequence prone to susceptibility artifacts[281]. Therefore a hybrid-EPI approach appears to be ideal, in which 4 to 8 k-lines per radiofrequency excitation are acquired[279, 282]. Steady-state free precession pulse (SSFP) sequences preserve magnetization and are particularly promising with respect to a high signal-to-noise ratio (SNR) but may suffer from other disadvantages because of the relatively long acquisition windows[280]. Alternatively, parallel imaging techniques, such as SENSE (SENSitivity Encoding) can be combined with perfusion imaging[283]. These are based on the fact that receiver sensitivity generally has an encoding effect complementary to Fourier preparation by linear field gradients. Thus, by using multiple receiver coils in parallel, scan time in Fourier imaging can be considerably reduced. These techniques acquire data from folded fields of view and resolve wraparound artifacts by taking into account the different spatial sensitivities of various coil elements[284]. In general, parallel imaging techniques trade the SNR for

speed of acquisition. These parallel imaging approaches can be combined with techniques that exploit spatiotemporal correlations in *k*-t–space, which results in even higher acceleration factors. Techniques such as *k*-t SENSE (discussed in previous chapter) and *k*-t BLAST (Broad-use Linear Acquisition Speed-up Technique) achieve high acceleration factors but with higher susceptibility to motion and could smooth temporal information[220]. The suitability of these different perfusion post-processing strategies for use in the studies contained in this thesis is discussed below.

2.3.2.2 CMR Perfusion Quantification Methods

Qualitative and Semi-quantitative Perfusion Analysis

The simplest method for interpreting CMR perfusion is to view the study in cine-loop format for regions of relative hypoperfusion. Such a qualitative approach yields high diagnostic accuracy when compared with invasive angiography[214] and is the method most widely used in everyday clinical practice to interpret CMR perfusion scans. Semi-quantitative analysis of a CMR perfusion scan involves firstly mapping the endo- and epicardial borders of a myocardial slice at rest and then at stress to form a sampling grid (see Figure 27 below); from this the mean signal intensity within a region of interest over time, or "signal intensity (SI) curve" is extracted (see Figure 28 below). From these curves the maximum upslope or initial area under the SI curve have been used as indexes of regional flow[285] and correlate well with flow measurements based on microsphere analysis[286, 287]. Semi-quantitative analysis has been shown to improve diagnostic accuracy over visual analysis alone[198, 288]. The MR-IMPACT multi-centre study indicates the prognostic significance of CMR perfusion with a higher incidence of cardiac death or nonfatal myocardial infarction in patients with an abnormal scan than those with a normal scan[289].

Although qualitative and semi-quantitative methods either used separately or together are useful clinical tools to detect relative areas of hypoperfusion it was felt that for the more detailed analysis required for the studies in this thesis we should pursue full quantification of myocardial blood flow. Having said that, given its widespread use in everyday clinical practice we did use qualitative assessment of the

perfusion scans as one of the end points in the *k*-t perfusion validation study presented in Chapter 4.

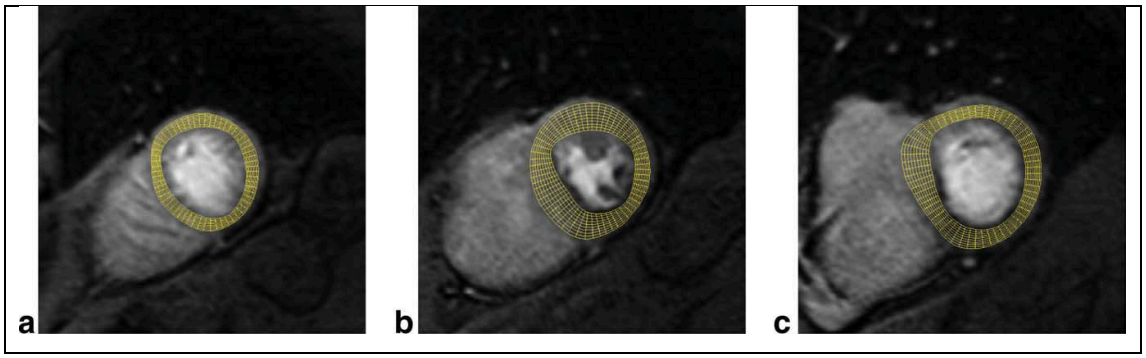

Figure 27. Examples of the sampling grid used to extract SI curves from apical (a), mid (b), and basal (c) slice of a SA perfusion CMR series [*adapted from Hautvast, Chribiri, Lockie et al, MRM 2011*[290]]

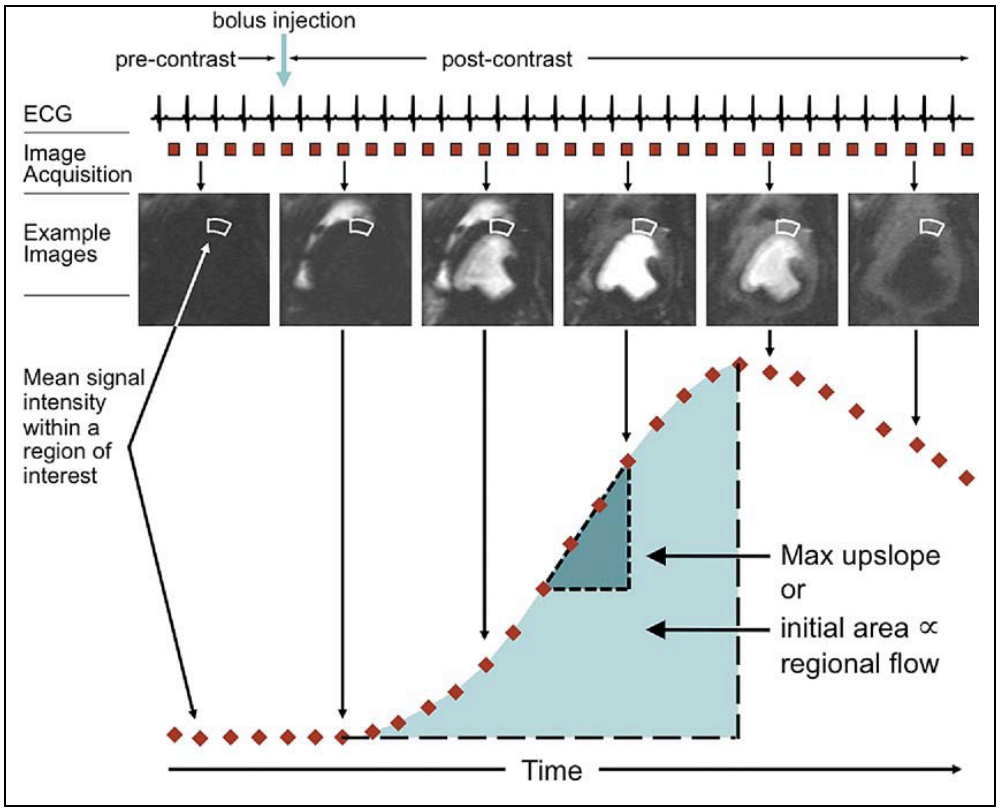

Figure 28. The heart is imaged every cardiac cycle during the first passage of gadolinium-based contrast agent. The resulting 30- to 40-frame image stack can be viewed in cine-loop format for qualitative assessment of regional flow deficits. Semi-quantitative flow analysis involves measuring the mean signal intensity over time for a region of interest and calculating the peak upslope or area under the curve as an index of regional flow [*adapted from from Lee et al. Circulation 2004* [291]].

Absolute Perfusion Quantification

In contrast to qualitative, which rely on the comparison of regions of relative hypoperfusion with regions of "normal" myocardium, and semi-quantitative methods, which allow the calculation of a myocardial perfusion reserve, it is also possible to quantify absolute myocardial blood flow. These are similar in derivation to those employed in quantitative PET and computed tomography perfusion as well as thermodilution estimation of cardiac output. Flow models use the myocardial and left ventricular (LV) blood pool SICs to estimate absolute myocardial blood flow. Two major classes of models exist: linear, shift-invariant (LSI) models and compartment models. Each class of model has its own assumptions that must hold or at least approximately hold for the model to produce meaningful and valid estimations of flow. We tested both of these models to see which was the most suitable for use in the further studies in this thesis.

The *LSI models* are generally more widespread in the calculation of absolute flow values than compartment models. The LSI models assume the cardiac circulatory system is linear and temporally invariant in its response. In other words, if two contrast boluses are injected, then the myocardial uptake is the linear sum of the uptake had each bolus been injected separately; and if the injection of a bolus is delayed by a certain amount of time, then its uptake is delayed (shifted) by the same amount of time. These two assumptions allow for a powerful and complete description of the system by its so-called "transfer function." Characteristics of the transfer function reflect properties of its system, the most relevant of which is absolute myocardial blood flow. The output from an LSI system (the myocardial SI curve) is equal to the input to the system (the tracer bolus, measured from the LV SI curve) merged with the transfer function by a mathematical process known as convolution (see Figure 29 below). Convolution folds two curves together via a shift-scale-and-add process similar to cross-correlation in statistics. To obtain the transfer function, the input and output curves must undergo the reverse process of deconvolution. Unfortunately the process of deconvolution is very sensitive to noise, so that small errors in the input data can lead to large differences in the resulting transfer function. Therefore, additional constraints need to be imposed to obtain a

physiologic solution. The most popular method for "constrained" deconvolution demands that the transfer function take a certain shape and is known as the **Fermi function**[292]. It can be shown that the maximum value of the Fermi transfer function equals absolute myocardial blood flow[196] and has been validated in both animals[293, 294] and patients with coronary artery disease[295, 296].

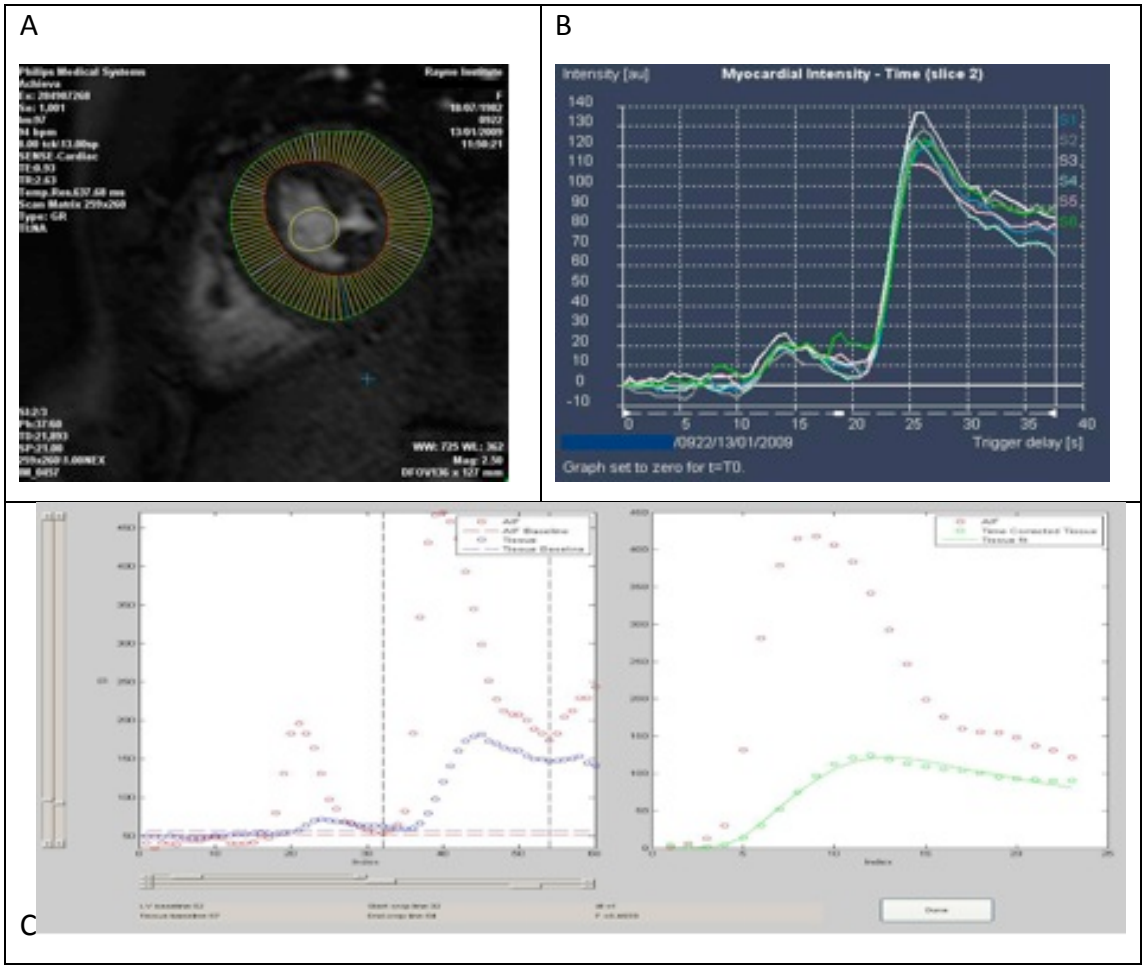

Figure 29. a) Mid-ventricular slice from an adenosine-stress CMR perfusion scan showing mapping of the endo-and epicardial boarders scan, (b) associated signal intensity curve, (c) associated deconvoluted signal intensity curve.

Compartment models divide the cardiac circulatory system into distinct spaces (intravascular, interstitial, and intracellular). The Gd-DTPA concentration varies among these compartments over time as molecules move from one space to another. Rate constants describe the movement between any two compartments. Such models determine compartment concentrations and the individual rate

constants from the summed SI curve of all compartments[297]. Clinically approved Gd-DTPA -containing contrast agents leak from the intravascular compartment into the interstitial compartment along an osmotic gradient but do not enter the intracellular compartment. Thus, a 2-compartment model (intravascular and interstitial) has been used to model its transit through the cardiac circulatory system[294]. There are two parameters to the 2-compartment model's transfer function. Unlike the LSI model, for which the maximum amplitude of its transfer function is equal to absolute myocardial blood flow, the maximum amplitude of the 2-compartment model transfer function is equal to the product of absolute flow and the myocardial extraction efficiency of the contrast agent. Their product is conventionally referred to as "k1" (the first-order rate constant). If the extraction efficiency is known or can be estimated, then blood flow can be determined. However, this adds an extra assumption to the model for quantifying perfusion. Thus, an advantage of the LSI model is that blood flow can be calculated explicitly, provided the transfer function can account for the extravascular leakage of contrast. The 2-compartment model also depends on linearity of signal response, so the previous comments about ensuring linearity in the blood pool and myocardium apply as well.

In Europe, the most common method for full quantification of myocardial blood flow is using the Fermi deconvolution and this was chosen as the main quantification tool for our studies. For the results of the repeatability and reproducibility data in volunteers as well as the full data from the validation against the invasively measured FFR see Chapter 4. The results of the Fermi derived absolute blood flow in exercise volunteers can be found I Chapter 6. In addition to the Fermi deconvolution technique, we also had the advantage of the expertise of Dr. Masaki Ishida, a visiting fellow from Japan, who has experience of using the **Patlak plot model** of quantification of absolute myocardial blood flow[298]. The Patlak plot method is based on a two-compartment model and describes the k1 of one-way transfer of contrast material from the LV blood to the myocardium. Patlak plot analysis is performed using a blood SI curve as an input function and a regional myocardial SI curve as an output function[297, 299]. Myocardial blood flow can then be calculated as k1 divided by the extraction fraction of Gd-DTPA, using extraction fraction values from the

literature[300, 301]. See Figure 30 below. We therefore also evaluated the use Patlak plots in the quantification of flow during exercise (see Section 2.3.3.5).

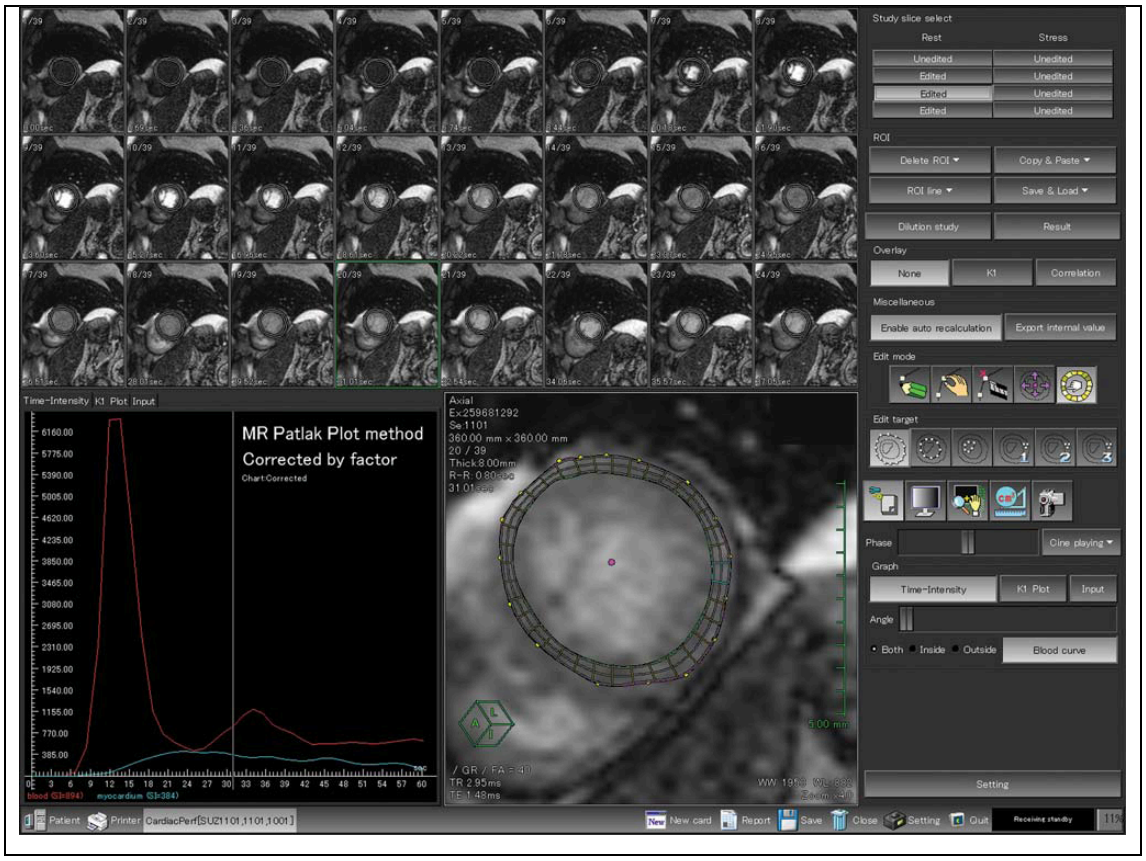

Figure 30. Quantitative analysis of myocardial perfusion magnetic resonance images using the Patlak plot method. Similar software was used for the quantification of myocardial blood flow in this thesis. Epicardial and endocardial contours of the left ventricular (LV) myocardium are manually determined to generate myocardial signal intensity (SI) curves. A region of interest is placed in the LV chamber to generate a blood SI curve. Patlak plot analysis is performed using blood input function and myocardial output functions [*adapted from Kurita, Ishida et al. EHJ 2009*][298].

2.3.3 Development of an Exercise-Stress CMR Perfusion Protocol

The development and validation of a robust method to quantify transmural myocardial blood flow at peak stress after large muscle exercise was an important aspect of this thesis, as changes in subendocardial flow on repeat exercise may be an important cardioprotective mechanism in warm-up. To develop such a model is an ambitious undertaking and there are no previous reports from the literature that this has been previously successfully achieved. There are 3 main limitations:

1. Undertaking large muscle exercise within the immediate confines of the MR scanner

2. Obtaining good quality perfusion data at high heart rates
3. Overcoming the potential obstacles of breathing and other movement artefact

We also needed to determine the effect of repeated Gd-DTPA doses on background myocardial saturation levels might have on subsequent quantification, and whether or not this would need to be corrected for.

2.3.3.1 Development of the CMR-Compatible Cycle Ergometer

The reasons why it is preferable to use large-muscle exercise stress, as opposed to other pharmacological methods are discussed in Section 2.2.4.1 above. There are various ways to induce exercise stress in the MR scanner environment. Handgrip exercise is straightforward and can provoke modest increases in heart rate and cardiac output although the limitations of this and other forms of small-muscle exercise are also discussed above. Studies have been undertaken with MR compatible cycles, or ergometers, although these tend to focus either on aortic and lower limb blood flow[302, 303] or SVC and pulmonary blood flow[304]. In all of these cases, either the cycle has either been distant to the MR scanner, so at peak exercise the subject must get off the bike and walk across to the scanner, or the patient is lying in the scanner but with the bike adapted to undertake a pumping leg exercise, rather than the usual circular motion with the pedals. Neither of these is ideal. In the first instance, walking across to the scanner would not be feasible in patients with chest pain and other symptoms, or who may be older and less mobile. This may add a considerable delay in getting the scan underway during which time the heart rate and cardiac output rapidly fall away from peak[89]. Keeping the subject in the scanner to minimise such delays and using the alternative lower-limb exercise is also not optimal as subjects struggle to reach their peak target heart rates with such an unfamiliar task[305]. Semi-quantitative perfusion analysis was obtained in a group of healthy volunteers using an MR compatible treadmill that was within the MR scanner room, but again involved the subject having to walk across to the scanner after exercising to peak stress[306]. In this study, scanning was commenced after a mean of 45 seconds from peak exercise which is impressive although these were a

young and mobile group of volunteers, and even then there were problems with regaining the correct position on the scanner (very important as the reference images for the perfusion sequence rely on this), and problems with re-attaching i.v lines and the radiofrequency coil and other leads in a hurry. This group did use a vacuum mattress (Vac Lok™, CIVCO® Medical Solutions, USA) to help maintain the correct position on the scanner table, and after contacting them we ordered a similar one to use in our protocol. This turned out to be extremely useful.

After trying various alternatives, we elected to use an MR-compatible cycle ergometer (Lode® Medical Systems, UK) that we specially adapted to use with the 3T scanner in the Rayne Institute at St Thomas' campus, KCL. To minimise delays between scanning, and also to ensure that position on the scanner table was maintained and the patients would not have to move between the bike and the scanner, we decided to exercise the patients just outside the scanner, but remaining on the table, with i.v lines, ECG leads and the RF coil etc. all in position. At peak exercise we would then rapidly slide the subject back into the scanner. After several further adaptations we came up with the final design and successfully tried it on our first healthy volunteer (see Figure 31 below). Heart rate and blood pressure were monitored throughout via cables that reached into the control room. The use of the vacuum cushion together with straps for the subject to hold onto minimised the tendency for cranial migration that we found occurred during the cycling, especially as the effort increased. A supervisor remained in the scanner room at all times both during the period of exercise and the subsequent scan. Consistent with other studies (and in particular in our initial volunteers who were young and fit), we observed that heart rate would fall rapidly after cessation of exercise; by the time scanning started, even if it was less than 1 minute from the end of the exercise, there was a substantial reduction in heart rate compared to peak. We found that continuing to squeeze a soft ball, during the duration of the scan was a good way to maintain the heart rate and slow the rate of decline.

Figure 31. Image of the MR compatible cycle ergometer specially developed for the 3T scanner at the Rayne Institute, St Thomas' campus, KCL. The subject is mostly out of the scanner allowing him full range of movement to undertake conventional supine cycle ergometry. The radiofrequency coil, ECG, BP cuff and all i.v lines remain in situ throughout. The patient is lying on a vacuum cushion to minimise movement and is holding onto straps to reduce to tendency to drift up the table during exercise, especially as the workload increases.

2.3.3.2 The Challenge of Scanning at High Heart Rates

Scanning at high heart rates makes almost every aspect of dynamic perfusion imaging difficult. Acquisition speed is a crucial factor. Good quality perfusion images require an acceptable balance between temporal resolution, or coverage of the myocardium achievable within each R-R interval, spatial resolution and the signal to noise ratio (SNR)[190]. It may be possible to get good coverage of the LV myocardium but at the expense of special resolution; or good spatial resolution but with poor SNR. At high heart rates, where the scanning time available for each beat is even less than usual, all of these are compromised. Jekic et al, for example, using a steady state free precession (SSFP) perfusion sequence at 1.5 T with standard SENSE acceleration were able to reduce the shot duration to 57.8±3.4 milliseconds but with an in-plane spatial resolution of only 2.9 x 3.7mm, with no ECG gating[306]. Such a

relatively poor spatial resolution would not allow examination of transmural flow differences that are crucial for the purposes of our proposed studies; spatial resolution approaching 1mm was what we were aiming for. Scanning at 3T gave us significant advantage, allowing greater SNR with the potential for faster scanning[219].

It was felt that to start with we should try and use standard SSFP perfusion sequences similar to the one above, but to try and utilize the advantages of scanning with the 3T magnet to improve spatial resolution. There were other reasons that we thought that standard SSFP might actually be advantageous over other more complex sequences even though they had the potential for even faster data acquisition (see below). However, despite using various adaptations in the initial 10 exercise volunteers including the use of WET pre-pulses, linear half-scan, TFE perfusion sequences, alteration of the M0 flip angles, and increasing the SENSE factor, it was not possible to obtain decent images that were suitable for further analysis. Movement and dark rim artefacts seemed to be the major issue, and it was key to try and reduce the shot duration, which despite all the above remained at around 100ms. Another problem that we encountered was through the use of ECG gating to optimise the timing of the scan to mid-systole where the myocardium is the thickest, which greatly facilitates subsequent data analysis. The increased field strength of the 3T magnet has a tendency to interfere with the ECG even under optimum conditions and with the additional factors of high heart rates, plus the subject moving around during the exercise this could be problematic. In one or two studies we lost the ECG trace altogether and thus lost much of the data from the scan. To overcome this, we also fitted a pulse finger probe (PPU) that can be used to gate the perfusion sequence. Although not ideal (as it is hard to time systole with this) it served as a useful backup should the ECG fail and we fitted the probe to all our subsequent subjects.

k-space and time sensitivity encoding (*k-t* SENSE) has been discussed in previous sections (XXX). It simultaneously exploits coil encoding and spatiotemporal data correlations to allow acceleration of data acquisition, which is crucial during dynamic MR perfusion[222]. This acceleration can be used to improve temporal and spatial

resolution of perfusion CMR especially at 3T where there is a greater SNR[223]. It is also associated with a reduction in dark rim artefacts, which are caused by the interface between the low flow velocity of the myocardium and the high flow velocity of the left ventricular blood pool[193]. We found these dark rim artefacts to be particularly troublesome at high heart rates with the standard perfusion techniques; consequently a lot of these early data were not suitable for quantitative analysis. Using *k*-t made an immediate impact of the shot duration, dropping to around 80ms and consequently resulted in a great improvement in the quality of the images (see Figure 32 below).

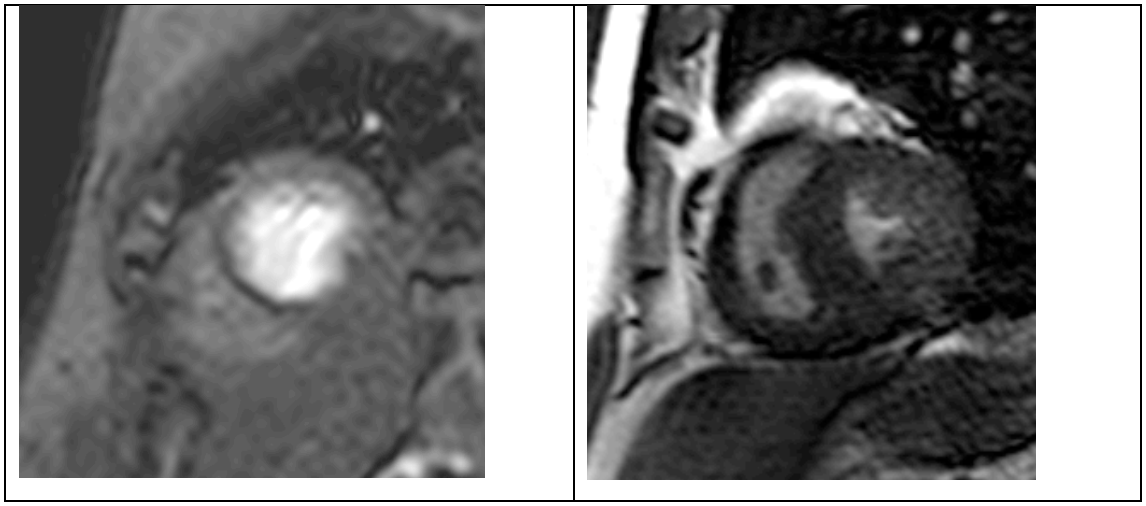

Figure 32. Images taken from the volunteer exercise CMR studies. The images are of different subjects but both taken at peak exercise. The image on the left is a standard PFE perfusion image taken early on in the protocol development. It illustrates the problems of movement and respiratory artefact with blurring of the endo- and epicardial boarders. There is also a large dark-rim artefact in the anterior wall, again a result of slow acquisition speeds. Such data was not suitable for quantification analysis. The image on the right is one take after optimisation of the protocol with the use of *k*t-acceleration methods to speed up acquisition time to reduce the dark rim artefacts in particular. This technique was still susceptible to respiratory motion artefacts in particular, but with good breath holding nice pictures could be obtained that were suitable for further analysis.

2.3.3.3 Minimising Breathing and other Movement Artefact

Motion-induced artefacts, either from respiratory or cardiac motion, are one of the main obstacles in obtaining high quality CMR first-pass perfusion images[221, 307]. Breathing artefact, in particular after intense exercise was envisaged to be a particular problem in our proposed studies. Reducing the scanning duration to a single breath hold was a minimum requirement. It would seem that using the fastest available scanning technique therefore would be the most suitable. However,

despite the advantages of faster scanning using *k*-t outlined above it also presents some potential drawbacks; as a result of the spatiotemporal under-sampling it is particularly vulnerable to breathing and other movement artefact. By relying on the consistency of spatiotemporal correlations obtained in the training images taken beforehand, any movement results in the substantial loss of data in the subsequent reconstruction[222]. This was the rationale to try and start with standard perfusion sequences that did not rely so crucially on the subject being able to hold their breath throughout the scan. Unfortunately, as outlined above it was not possible to get data of sufficient spatial resolution and quality without resorting to *k*-t. We therefore had the pay-off between much better images overall, but if the subject took a breath at any point during the scan, especially during the first pass of the Gd-DTPA contrast bolus, then the images were almost un-useable. After several meetings and review of the data of the first 20 volunteers scans, roughly half standard perfusion and half *k*-t, it was felt that overall we should proceed with the *k*-t scanning protocol and concentrate on preparing the subjects carefully and emphasizing the importance of holding their breath during the scan; if they had to breath at all then to do so gently towards the end of the scan, when the initial contrast bolus had already passed. This proved successful by and large, and we were able to proceed with the initial evaluation of quantitative analysis in the next batch of volunteers.

2.3.3.4 Myocardial T1 Mapping to Determine the Effect of Repeated Contrast Bolus Injections during CMR Perfusion Imaging

The first stage in the development of a CMR protocol to investigate the effects of repeat exercise on myocardial perfusion was to examine the impact of repeat injections of Gadolinium (Gd-DTPA)-containing contrast agent. In standard rest-stress perfusion scan protocols there are only two contrast injections required. However, in our proposed protocol there would be at least three. The increased spin-lattice relaxation rate 1/T1 and dynamic signal enhancement following the intravenous injection of Gd-DTPA has been shown to be a linear function of local gadolinium concentration[276]. However, studies in rat myocardium revealed that the enhancement may reach a plateau, which would inhibit the deduction of reliable kinetics from observed signal intensity-time curves[308]. The purpose of this

preliminary study was to determine the effect of repeated injections of Gd-DTPA on background myocardial saturation. If a saturation effect is found then this would need to be accounted for in quantification of perfusion scans involving multiple injections of Gd-DTPA. The myocardial T1 values were measured at multiple points in time during the study and compared with a reference, i.e. the expected T1 extrapolated from the previously published washout kinetic tables of Gd-DTPA following a single injection[277].

Methods

All experiments were performed on a clinical 3T scanner (Achieva®, Philips Medical Systems) equipped with a 32-element cardiac coil array. Experiments were conducted in 10 healthy adult volunteers with no history of cardiac disease. 1-2 injections of a 10% dilute (Scan 0, 0.025mMol/kg) were given to optimize the perfusion sequence timing. Three subsequent contrast injections (Scans 1-3, dose=0.25 mMol/kg) were given at an approximate temporal spacing of 15 mins, and a fourth injection (Scan 4, 0.25mMol/kg) was given immediately after the third. Myocardial T1 was measured before the respective contrast injections using an ECG-triggered "Look Locker" inversion recovery sequence. The scan parameters were as follows: FOV=300x300mm², measured voxel size=2.5x2.16x10mm³, inversion-prepared T1 weighted FFE-EPI, flip=10°, EPI factor=3, 9 excitations per phase, 16 phases distributed over 2 RR intervals (phase interval 100ms). One pause interval was employed in between inversion pulses to allow for magnetization recovery. The total scan duration was one breathhold (9 RR intervals). T1 was measured in a ROI in the septum wall (position adjusted in each phase to cope with cardiac motion). T1 values were calculated using a plug-in tool comprising a 3-parameter exponential fit with Look-Locker correction implemented in an open source DICOM viewer (OSIRIX®). The measured T1 values were compared with the expected values extrapolated from the previously published Gd-DTPA concentrations found in blood serum after intravenous contrast injection, where a fixed blood volume fraction in myocardium and equal relaxation times of Gd-DTPA in blood and myocardium were assumed. The molar concentration of contrast agent in blood was assumed to be a

linear addition of the existing concentration at the given delay from the previous injection, and the actually injected dose.

Results

The T1 values measured prior to the respective contrast injections are summarized for all volunteers in Table 3 below. A minor decrease in myocardial T1 was observed after the injection of the 0.025mMol/kg dilute. A marked decrease of myocardial T1 was observed following all 0.25mMol/kg injections. A saturation effect, i.e. a plateau of T1 after subsequent injections, could not be observed at the given doses. A moderate variance was observed for some T1 values, which can in part be attributed to the slight variations in time at which the values were measured. A plot of the measured myocardial T1 versus the expected values obtained from the previously described model is shown for one volunteer in Figure 33 below. The timing and given doses were taken into account for the calculation of the T1 model (solid arrows). A good agreement between the expected and measured values was observed.

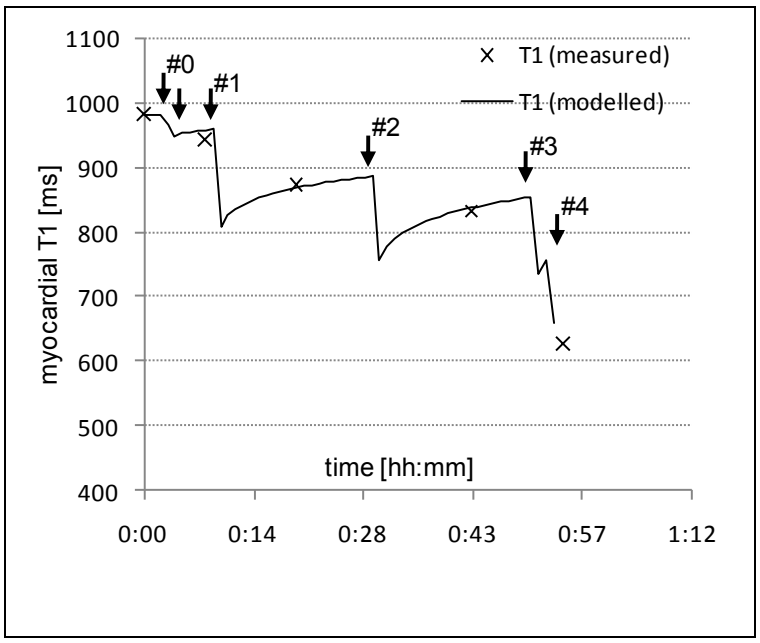

Figure 33. Plot of measured myocardial T1 vs. expected values extrapolated from previously published contrast washout kinetics. A good agreement between the model and the measured values was observed. *Courtesy Dr Christian Stehning.*

Injection Number	T1 (ms)
Baseline	971±73
(0) After 0.025mMol/kg	950±105
(1) After 0.25mMol/kg	833±47
(2) After 0.25mMol/kg	787±33
(3) After 0.25mMol/kg	728±33
(4) After 0.25mMol/kg	552±58

Table 3. Summary of measured T1 values over all volunteers. Data presented as mean ± standard deviation [*Courtesy Dr. Christian Stehning*].

Discussion

For the doses employed in the present study, no plateau of myocardial T1 could be observed after subsequent contrast injections. A decrease of T1 was observed following each individual 0.25mMol/kg injection, which indicates that contrast-enhanced perfusion studies can be conducted with multiple contrast injections. The measured myocardial T1 correlates well with the expected values extrapolated from the excretion characteristics of Gd-DTPA[277]. Although the currently available data points are relatively sparse, is seems that the contrast kinetics in myocardium after multiple injections can be modeled with sufficient accuracy using a simple superposition of the logarithmic contrast washout behavior. According to the model, an oscillation around an equilibrium T1 value, which is determined by the individual dose, injection interval, and excretion rate, could be expected if further contrast injections were given.

Conclusion

Based on these observations we suggest that perfusion studies can be conducted with multiple contrast injections, and myocardial T1 can be approximated from a model with sufficient accuracy to translate signal intensities into contrast agent concentrations.

2.3.3.5 Assessment of Physiological Flow Reserve in Normal Volunteers Undergoing Exercise Stress Using Patlak Plots

Having established that *k*-t SENSE was the optimal perfusion sequence for the exercise studies the next stage was to determine whether the data that we acquired was of sufficient quality to obtain myocardial flow data that was consistent with the physiological data from the literature. On the basis of previous experience and more widespread availability of the software we had decided that we would use the Fermi deconvolution methods outlined in Section 2.3.2.2 above. Fermi deconvolution is also the only technique validated in the assessment of differences in transmural flow distribution[293]. However, we also had the opportunity to analyse this data with the Patlak plot method, which would allow a useful comparison with the data obtained from the Fermi deconvolution. The results from the Fermi analysis are included in Chapter 6. The Patlak data is presented below.

Methods and Analysis

8 healthy volunteers (age 25-35 years) underwent a standardised exercise protocol (increments of 20W each minute for 6 minutes at a rate of 60 rpm) using a specially adapted supine cycle ergometer that was attached to the sliding table inside the CMR scanner; the subject could exercise without leaving the table and scanning could occur almost immediately after peak exercise. Rate pressure product (RPP) calculated as peak systolic blood pressure x peak HR was recorded at peak exercise. *k*-t SENSE accelerated perfusion CMR was performed on a 3T Philips Achieva® system using 0.025mmol/kg/min Gd-DO3A-butrol and the following pulse sequence: saturation recovery gradient echo, repetition time/echo time 3.0ms/1.0ms, flip angle 15°, 5x k-t SENSE acceleration, 11 interleaved training profiles, WET pre-pulse (angles 120°, 90°, 180°, 140°); delay 100ms, spatial resolution 1.8x1.8x10mm3, 3 slices at each RR interval, 40 dynamic images. For blood pool saturation correction MR images with diluted Gd-DO3A-butrol injection (0.0025mmol/kg) were also acquired. The mid-slice was used in each subject for further analysis. After correcting for saturation of the blood signal, arterial input and myocardial output time-intensity curves were analyzed with a Patlak plot method to quantify global myocardial K1 at rest and stress. Then, absolute global myocardial blood flow (MBF) at rest and stress

and myocardial perfusion reserve (MPR) were calculated from the K1 measurement using the extraction fraction (EF) of the Gd contrast agent, where EF=0.5 at rest, EF=0.3 at stress. The local ethics board approved the study and all subjects signed a consent form beforehand. Data are presented as mean ± standard deviation (SD).

Results

All subjects successfully completed the exercise protocol. Full data are presented in Chapter 6. Resting MBF was 89.8±10 ml/min/100g compared to stress of 302.1±141.1ml/min/100g (P<0.008), giving an MPR of 3.3±1.4. RPP was 17556 ± 1209 indicating equivalent workload across all subjects.

Discussion and Conclusions

k-t SENSE can be used to acquire perfusion CMR data during ergometer stress and analysis with Patlak plots can be used to determine global myocardial perfusion reserve in healthy volunteers. The value of 3.3 for the MPR is consistent with physiological values from the literature[306, 309]. Also see Chapter 6, where the mean MPR derived from the Fermi deconvolution was very similar 3.3±0.5; obtaining the same values from two different quantification methods is reassuring and suggests consistency of the data. We did not use Patlak plots to examine differences in transmural flow distribution as the technique is not validated for this purpose.

More studies are required to determine regional flow distribution but this technique holds potential for the functional assessment of patients with cardiac disease.

	K1 measurement (ml/min/100g)		Myocardial Blood Flow (ml/min/100g)		Myocardial Perfusion Reserve (MPR)
	Rest	*Stress*	*Rest*	*Stress*	
Volunteer 1	47.9	182.2	95.8	607.3	6.3
Volunteer 2	41.4	98.5	82.8	328.3	3.9
Volunteer 3	38.4	64.3	76.8	214.3	2.8
Volunteer 4	54	84.5	108	281.7	2.6
Volunteer 5	44.6	74.7	89.2	249	2.7
Volunteer 6	45.4	70.1	90.8	233.7	2.5
Volunteer 7	42.8	60.5	85.6	201.7	2.4
Volunteer 8	88.6	103	177.2	343.3	1.9
Mean	50.3	92.3	89.8	302.3	3.3
SD	16.1	39.4	10	141.1	1.4

Table 4. Results of the first 8 volunteers showing blood flows at rest and peak exercise as calculated using Patlack plots.

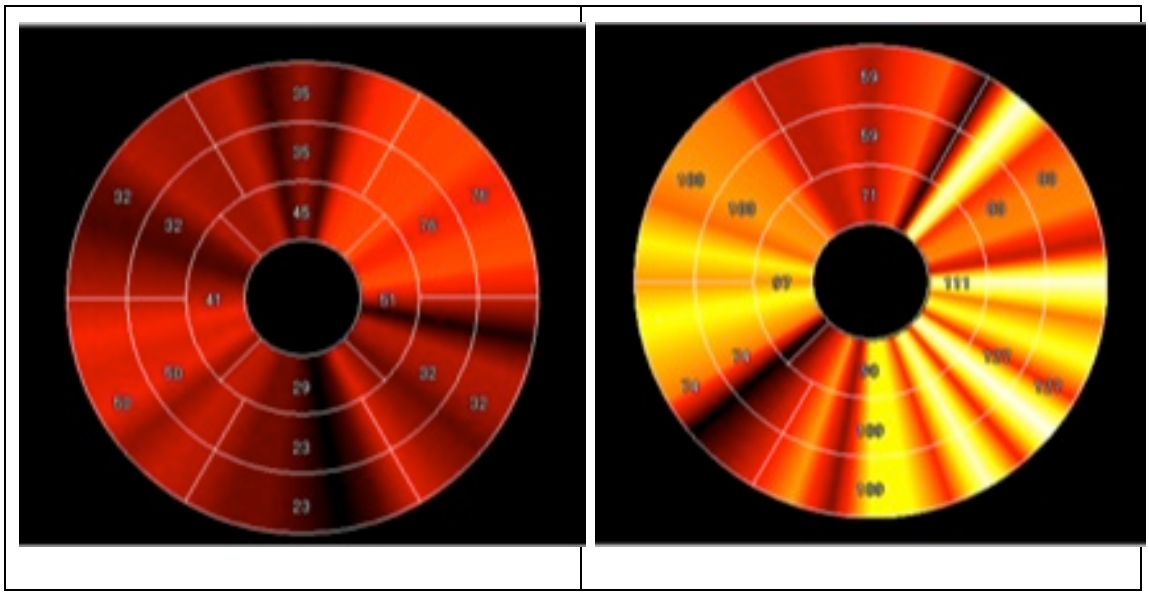

Figure 34. Patlack plots in a volunteer; the left hand panel is at rest, and, the right hand panel, during maximal exercise stress showing globally increased k1 measurements [*slide courtesy of Dr. Masaki Ishida*].

2.4 Acknowledgements

I am most grateful to Mick Kelly and his team in the Works Dept., St Thomas' Hospital for his valuable assistance with the many adaptations required to both the catheterisation lab and MRI ergometers. His endless enthusiasm and innovative ideas were crucial to the project. I am also grateful to all the staff in the cath lab and MRI suite who endured the many frustrations and delays through the early development stages of both exercise protocols, again without whom this project would not have been possible. I would like to thanks Masaki Ishida for his help with the Patlak plot analysis, and Christian Stehning for his work on the T1 plots and modeling to look at background contrast saturation. Thanks to Dr. Maria Siebes and her team at the Academic Medical Centre, Amsterdam, the Netherlands, for their help with the WIA of data used in this thesis.

3 A CLINICAL TRIAL EXAMINING *POSTCONDITIONING* OF THE MYOCARDIUM FOLLOWING MYOCARDIAL INFARCTION: INNATE CARDIAC PROTECTION?

Tim Lockie[1], Ian Webb[1], Divaka Perera[1], Amedeo Chiribiri[2] Sven Plein[2, 3], Eike Nagel[2], Simon Redwood[1], Mike Marber[1]

[1]Cardiovascular Research Division, The Rayne Institute, St Thomas' Hospital, KCL, London UK

[2]Division Imaging Sciences, The Rayne Institute, St Thomas' Hospital, KCL, London, UK

[3] Academic Unit of Cardiovascular Medicine, University of Leeds, UK

3.1 Abstract

Background

Postconditioning (PC) is a novel strategy to reduce reperfusion injury following myocardial infarction through graded restoration of blood flow. Cardiac magnetic resonance (CMR) imaging provides unique tissue characterization.

Methods

Patients undergoing primary percutaneous coronary intervention (PPCI) were enrolled into a prospective randomised control pilot study to evaluate the feasibility of early CMR imaging to examine the effect of PC. Following restoration of TIMI 3 flow the PC protocol involved 4 x 1 minute serial balloon inflations at 4-6 atm to re-occlude the artery, with 1 minute between each inflation. Patients in the control arm were stented after 8 minutes of unhindered reperfusion. CMR was then performed <36 hrs to determine the extent of infarction by late gadolinium enhancement (LGE). Microvascular obstruction (MVO) was represented by areas of low signal on the early gadolinium enhanced image. Results are presented as mean ± standard error (SE). Student's t-test was used to compare the groups. CMR data were blinded for analyses.

Results

33 patients were randomised into the study of which 19 patients completed the protocol (3 haemodynamic instability, 5 IABP insertion, 2 thrombectomy, 4 no-reflow post stent (2 control, 2 PC)) and 14 underwent a successful CMR scan (8 PC, 6 control) <36 hrs. Baseline characteristics were similar as was the pain-to-balloon time (mins) (137±24 con; 183±45 PC, NS). ST segment resolution (mm), a marker of reperfusion, was significantly improved in the PC group (3.3±0.3 vs. 1.3±0.3, p<0.004). Peak CK release (IU) was not different between the groups (2319±540 con vs. 2010±336 PC, NS) nor was the area under the curve of CK release over 36 hours. There was no significant difference in the area of LGE(cm^3) (25.4±4.9 con vs. 36.8±7.1 PC, NS) nor was there a difference in MVO(cm^3) (4.18±1.9 con vs. 6.6±3.6 PC, NS). There were no MACE reported in any study patients at 9 months.

Conclusions

A CMR scan early after PPCI is feasible and provides high quality data. Initial data suggest improved perfusion by PC but no infarct reduction.

3.2 Background

The consequences of acute myocardial infarction (AMI) are a major cause of morbidity and mortality. Primary percutaneous intervention (PPCI) aims to restore myocardial blood flow rapidly but there is evidence that this process in-itself may precipitate cell death, microvascular obstruction (MVO) and tissue dysfunction through reperfusion injury. Postconditioning is a novel strategy to reduce reperfusion injury through graded restoration of blood flow[148]. More detailed background is given in Section 1.2.2.2. Preliminary clinical trials have suggested that postconditioning at the time of reperfusion results in an early reduction in infarct size. Our proposed prospective, randomised, controlled study will compare PPCI alone to PPCI with a postconditioning protocol. We aim to study the effects of post conditioning on late infarct volume and left ventricular (LV) segmental and global performance using delayed Gadolinium-enhanced cardiac magnetic resonance imaging (CMR). We suggest that postconditioning will result in reduced late infarction at 5 months with improved LV wall thickening and overall improved function. We suggest that MVO within the infarct zone in the 24 hours following AMI will be reduced by postconditioning and will predict LV recovery. MVO will be measured by early first-pass Gadolinium hypoenhancement CMR imaging.

To date there have been no clinical studies using CMR imaging to assess the effects of postconditioning at the time of primary PCI. CMR provides unique tissue characterisation of the myocardium with high resolution and reproducibility and without the use of ionising radiation. It is able to determine function, perfusion, viability and scar characteristics that are not possible through other imaging modalities. Although other studies[148, 150, 310] have suggested that postconditioning provides a significant reduction in early infarct volume they have generally relied on

enzyme release to infer infarct size with only the recent Yang paper utilising SPECT imaging at 1 week. Although CK release profile has been used previously as a marker of infarct size it is very crude and prone to error. The process of postconditioning itself may affect the dynamics of enzyme release and such a rise alone gives little indication of the processes occurring at a microvascular level. It is also known that interventions can reduce necrosis at the expense of increased oncosis/apoptosis, a process not associated with immediate CK release[311]. By relying on CK release one cannot be sure that such interventions are not simply delaying the progression to infarction rather than representing a sustained anti-infarct effect. Robust, serial imaging modalities are therefore required to assess the long term sustained effect of postconditioning in reducing infarct size. SPECT imaging has many well-recognized limitations. The poor resolution of the technique, which cannot distinguish subendocardial from transmural myocardial infarction, means that it may significantly underestimate infarcts where there is not full thickness involvement. In a heterogeneous study population with a large range of infarct sizes this may be very significant. To compound this myocardial stunning and acute abnormalities in microvascular perfusion may result in the well reported overestimation of infarct size in certain groups with the possibility that late recovery of the myocardium may alter the measurement[312]. The large radiation dose from each study means that serial examinations are not feasible. A much more accurate means of tracking changes in infarct size and LV function is using Gd-enhanced CMR, a well-validated and robust modality. CMR is safe, reproducible and does not result in excess radiation doses to patients undergoing repeated examinations. The latest CMR navigation and tracking sequences allow highly accurate comparisons to be made over time[313]. To show whether early infarct reduction is maintained the patients in the proposed study will be rescanned at 5 months which is the time when it is considered the scar has achieved its final form[314]. No studies to date have published such data. Recovery of LV function following AMI is directly related to clinical outcome[121]. Improvements in function at 5 months compared to baseline will form the primary endpoint of the study. Crucial to the recovery of wall motion is the presence of MVO within infarcted segments as it is highly predictive of poor recovery

compared to dysfunctional segments at time of reperfusion that do not contain MVO[271]. CMR will be able to track both changes in LV segmental wall thickening and the presence of MVO. It is suggested that by ameliorating the deleterious effects of reperfusion injury in the first minutes following restoration of coronary flow postconditioning will reduce MVO and promote LV recovery over and above the reduction in infarct size alone. To assess microvascular function the postconditioning studies to date have either relied on the myocardial blush grade (MBG), a crude angiographically derived marker of perfusion, or coronary flow reserve, also unreliable and highly dependent on loading conditions and residual epicardial coronary disease. In addition, they were measured almost immediately after PCI; this may simply represent post-PCI hyperaemia and does not account for the well described dynamic nature of MVO continuing to evolve beyond reperfusion[315]. In our study we will assess microvascular function through accurate and validated measures at 24-48 hours following reperfusion. The purpose of this study is to use contemporary CMR techniques to confirm that the described short-term benefits of postconditioning are followed by long-term improvements in LV performance. So far, studies have relied on unreliable markers of infarct size or imaging modalities early after tissue reperfusion and therefore the sustained positive effects of postconditioning have yet to be determined.

3.3 Aims

1. To establish the existence and potential therapeutic role of postconditioning in the setting of primary angioplasty for acute myocardial infarction in reducing anatomical infarct size through a prospective, randomised, controlled clinical study.
2. To investigate whether the early reduction in infarction volume with postconditioning is maintained at 5 months and results in improved wall motion scores and global LV performance
3. To establish whether postconditioning reduces microvascular obstruction acutely in the infarct zone which in turn predicts improved LV recovery

3.4 Study Design

3.4.1 Inclusion criteria

Patients with AMI defined by chest pain ≥30 minutes and ≤12 hours, ST elevation ≥0.1mV in 2 contiguous limb leads or ≥0.2mV in ≥2 contiguous precordial leads or new LBBB. There must be TIMI 0/1 flow in the infarct related artery (IRA) at diagnostic angiogram.

3.4.2 Exclusion criteria

Contra-indications to MRI, pregnancy, concomitant illness, culprit left main stem disease, thrombolysis, Q-waves in territories without ST elevation, previous CABG, spontaneous recanalisation (TIMI 2/3 flow in the IRA) or extensive collateralisation (Rentrop Score ≥1) at diagnostic angiogram.

3.4.3 Randomisation

Was carried out after the coronary angiogram confirmed TIMI 1/0 flow in the infarct related artery and was via an envelope to either postconditioning or control group.

3.4.4 Interventional Protocol

All procedures were carried out by the interventional cardiologists at St Thomas' Hospital. The infarct related artery (IRA) and culprit lesion were identified, lesion crossed and flow restored with a single balloon inflation. Those patients with TIMI 2/3 flow after this first balloon inflation were randomized to (1) routine PCI or (2) PCI followed by the postconditioning protocol. This process is time-dependent and there must not be more than 1 minute between the restoration of flow to the IRA and the start of the postconditioning protocol. Patients who required multiple balloon inflations to achieve satisfactory flow were excluded. The postconditioning protocol involved 4 x 1 minute serial re-inflations of the pre-dilatation balloon at low atmospheres (e.g. 4-6 atmospheres) in order to re-occlude the artery with a period of 1 minute left between each inflation. Occlusion of the artery was confirmed by either further ST elevation on the electrocardiograph or a short contrast injection with the balloon inflated to ensure no distal flow. If there was evidence of flow then

the balloon was inflated further or up-sized. The protocol was commenced after 1 minute of initial reperfusion and at the same intra-coronary site. The lesion was then stented as per usual. Patients in the control arm were stented after 8 minutes of unhindered reperfusion (see figure below). The loading of patients with aspirin and clopidogrel and the use of adjuvant glycoprotein IIb/IIIa inhibitors as suggested by guidelines was allowed, however, the use of thrombus aspiration or haemodynamic instability that required temporary pacing or the use of an intra-aortic balloon pump or other inotropic support meant the patient was excluded from the study

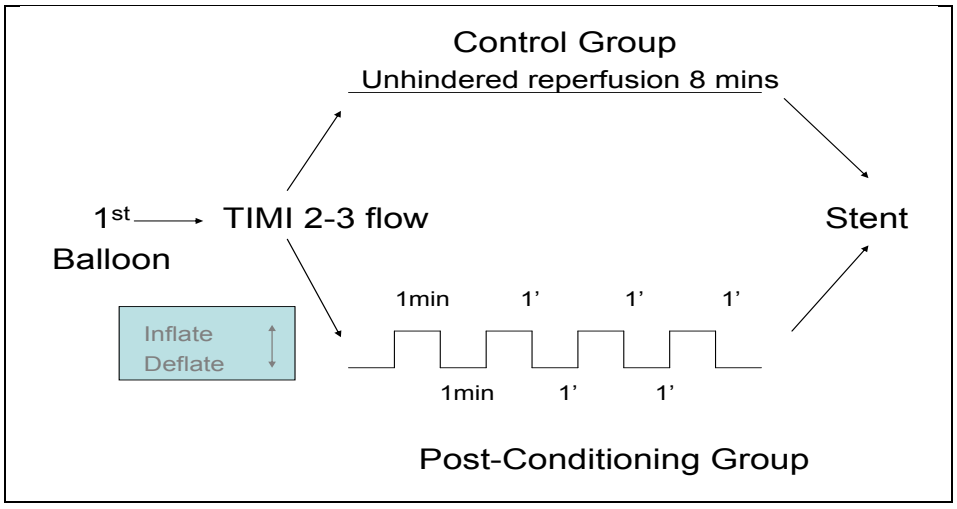

Figure 35. Study protocol for the cardiac catheterisation laboratory after the diagnostic coronary angiogram confirming an occluded vessel (TIMI 0 flow) in patients being treated with PPCI for acute STEMI.

3.4.5 Cardiac Magnetic Resonance Imaging

Imaging was carried out on a Philips Intera CV 1.5T dedicated research MR scanner. The imaging protocol consisted: a plan scan; a SENSE reference scan; cine SSFP short axis LV function scan (app. 12 slices, 40 phases of the cardiac cycle); a 1st pass Turbo Field Echo dynamic perfusion scan (3 slices per cardiac cycle, resolution (better than 2.5 mm x 2.5 mm x 8 mm) using Gd-DTPA (0.1 mmol/kg); 3D Inversion Recovery (IR) myocardial viability late enhancement scans in short and long axis views, resolution (2 mm x 2 mm x 10mm) at 2 minutes (for hypo-enhancement) and 15-20 minutes (for hyper-enhancement) following Gd-DTPA injection (additional 0.3 mmol/kg). End systolic volume (ESV) and end diastolic (EDV) were quantified by drawing endocardial and epicardial contours on the short axis series of the cine-MRI images

and ejection fraction (EF) was calculated as: (EDV-ESV)/EDV x 100%[271]. The 17-segment model of the LV was used for regional wall motion assessment[316]. LV segmental thickening (%) at baseline and at 5 months was compared to regions of remote myocardium that are unaffected by significant coronary disease. Myocardial perfusion was evaluated per segment and scored as: 1, normal perfusion (homogeneous enhancement of myocardium); 2, mild perfusion defect (subendocardial layer of hypo-enhancement); and 3, severe perfusion defect (30% transmural extent of hypo-enhancement)[271]. Infarct mass was determined by multiplying delayed enhancement volume by 1.05g/ml as previously described[271]**.** The dynamic increase in infarct size in the hours beyond reperfusion has been well documented with continued tissue oedema, inflammation and myocardial stunning that may last for several days[131, 273]. Subsequently, there is little recovery in wall motion in the days following reperfusion[317]. The early CMR scan within 24 hours of reperfusion representing baseline function is, therefore, likely to reflect the extent of myocardial ischaemia through contractile dysfunction caused by both irreversible, and reversible (stunning), injury.

3.4.6 Power Calculations and Sample Size

A standard (two-tailed) t-test was used to assess sample size to detect a mean improvement in LV function in the control and intervention groups. We use a standard formula for sample size determination[55]

$$N = 2(\sigma/\delta)^2(z_{1-\alpha/2} + z_{1-\beta})^2 + (z_{1-\alpha/2})^2/4$$

Where N is the sample size, α is the significance level, 1-β is the study power required, σ is the inter-study standard deviation, δ is the difference in ejection fraction to be detected and z_x is the x-th percentile of a standard normal distribution. Using α=0.05, 1-β=0.9, σ=5.1 (derived from published data[36] as well as in-house observations) and δ= 3 (a 36% reduction in infarct size suggested by Staat et al[27] would equate to an approximate improvement in EF of 6% from post MI longitudinal studies[40]; an improvement of 3% EF will be sought to allow for smaller infarct sizes), N= 15 using the above values. With potential patient dropout we aimed to

recruit 20 patients per group. This will also compensate for assumptions regarding a known standard deviation and using a standard normal, rather than t critical values.

3.4.7 Ethics

Full ethical approval was obtained (COREC Ref 06/Q0702/67). Consent was a two-stage process with the patient giving verbal consent to the postconditioning protocol prior to going to the catheter lab and then written consent to the rest of the study afterwards. Both stages of the consent were taken by either TL or IW. A study safety and event monitoring committee met regularly and assessed the patients recruited to the study. At a pre-specified point after the recruitment of 20 patients into the study a full interim analysis of data recorded so far was undertaken to assess safety of the protocol and the usefulness of continuing.

3.5 Results

These results reflect the interim analysis performed after 14 patients successfully completed the entire study protocol.

3.5.1 Baseline characteristics

33 patients were randomised into the study of which 19 patients completed the catheter lab protocol. 3 were excluded due to haemodynamic instability during the initial wiring of the vessel, 5 required intra-aortic balloon insertion, 2 required thrombectomy because of heavy thrombus load, in 4 patients there was no-reflow after stent insertion requiring multiple further balloon inflations (2 occurred in the control arm and 2 in the PC arm). In total, 14 (13 male, 1 female) underwent a successful CMR scan (8 post con, 6 control) within 36 hrs and of these 9 underwent a successful follow-up scan at 5 months. The full details of the study population and recruitment are listed in Table 5. Data are presented as mean ± standard deviation. There were no differences regarding baseline characteristics, other than the PC population tended to be slightly older with a higher proportion of left anterior descending (LAD) infarcts. Otherwise, background medication, incidence of prior ischaemic heart disease and cardiovascular risk factors were similar other than a

higher proportion of diabetics in the control arm. The pain-to-balloon times showed that these were longer in the PC group at 183±45 minutes compared to the control group at 137±24 minutes although these differences were not statistically significant and were skewed by one subject in the PC arm who arrived at the lab after 420 minutes of pain.

3.5.2 Coronary Angiography and Primary PCI

Out of the 33 patients randomised into the study it can be seen from the above flow chart that there was a high proportion of patients who dropped out of the study with 8 being excluded in the PC arm and 6 excluded in the control arm before the cath lab protocol was completed or if completed before the patient left the lab and was safely back on the coronary care unit (CCU). The causes for this are listed above and were evenly distributed between the groups. There was no suggestion that the PC protocol of re-occluding the vessel with serial balloon inflations was associated with procedural complications and was tolerated very well by the patients. Any form of instability, however, meant that in the interests of the safety of the patient he or she had to be taken out of the study to receive therapy such as intravenous inotropic support agents, temporary pacing, thrombus aspiration or the insertion of an IABP all of which, in addition, may have confounded the results of the study. The use of GP IIb/IIIa inhibitors is standard in our institution and the use of such agents was equal between the groups. All the patients recruited into the study had TIMI 0 flow at the time of the first diagnostic pictures and in the PC group the protocol was commenced within the first minute in all cases. There was a spread of infarct related arteries between the groups with slight preponderance for LAD involvement in the PC arm.

	Post Con (n=8)	**Control (n=6)**
Male (%)	8 (100)	5 (83)
Age (years)	51.1±6.8	49.5±7.3
Diabetic (%)	1 (13)	4 (66)
Raised cholesterol (%)	3 (38)	3 (50)
Family history IHD (%)	2 (25)	1 (17)
Renal dysfunction (%)	0	0
Previous MI (%)	0	0
Known IHD (%)	2 (25)	1 (17)
Aspirin	3 (38)	2 (33)
Statin	3 (38)	3 (50)
ACEi/ARB	4 (50)	2 (33)
Beta-blocker	2 (25)	2 (33)
Infarct related Artery		
• LAD	4 (50)	2 (33)
• Cx	1 (13)	2 (33)
• RCA	3 (38)	2 (33)
TIMI 0 flow at presentation	7 (88)	6 (100)
Pain to balloon time (mins)	183±45	137±24
GP IIb/IIIa used	7 (88)	6 (100)
Final TIMI 3 flow	8 (100)	5 (83)

Table 5. Baseline characteristics of study patients

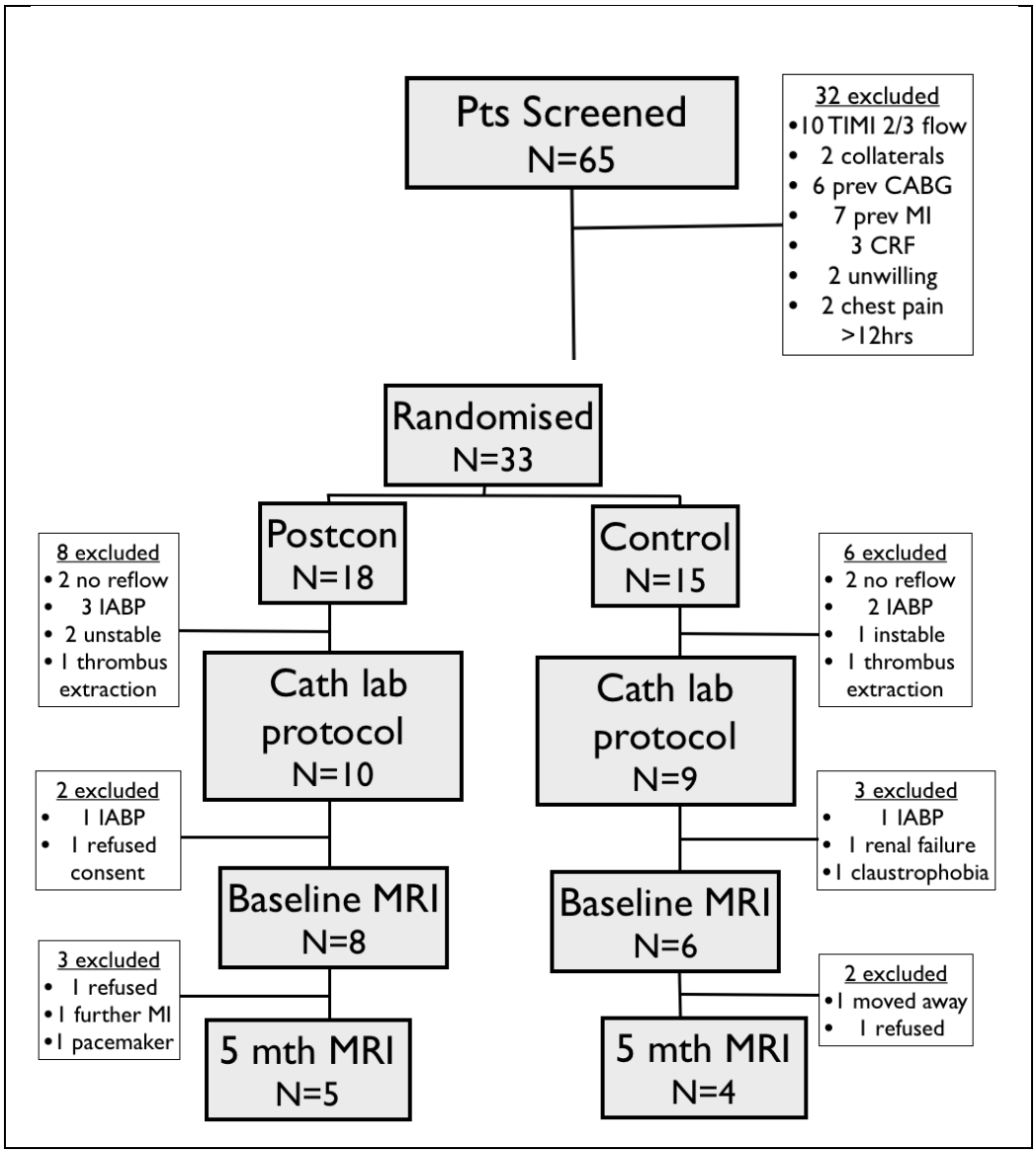

Figure 36. Flow diagram showing recruitment to the study. IABP = intra-aortic balloon pump

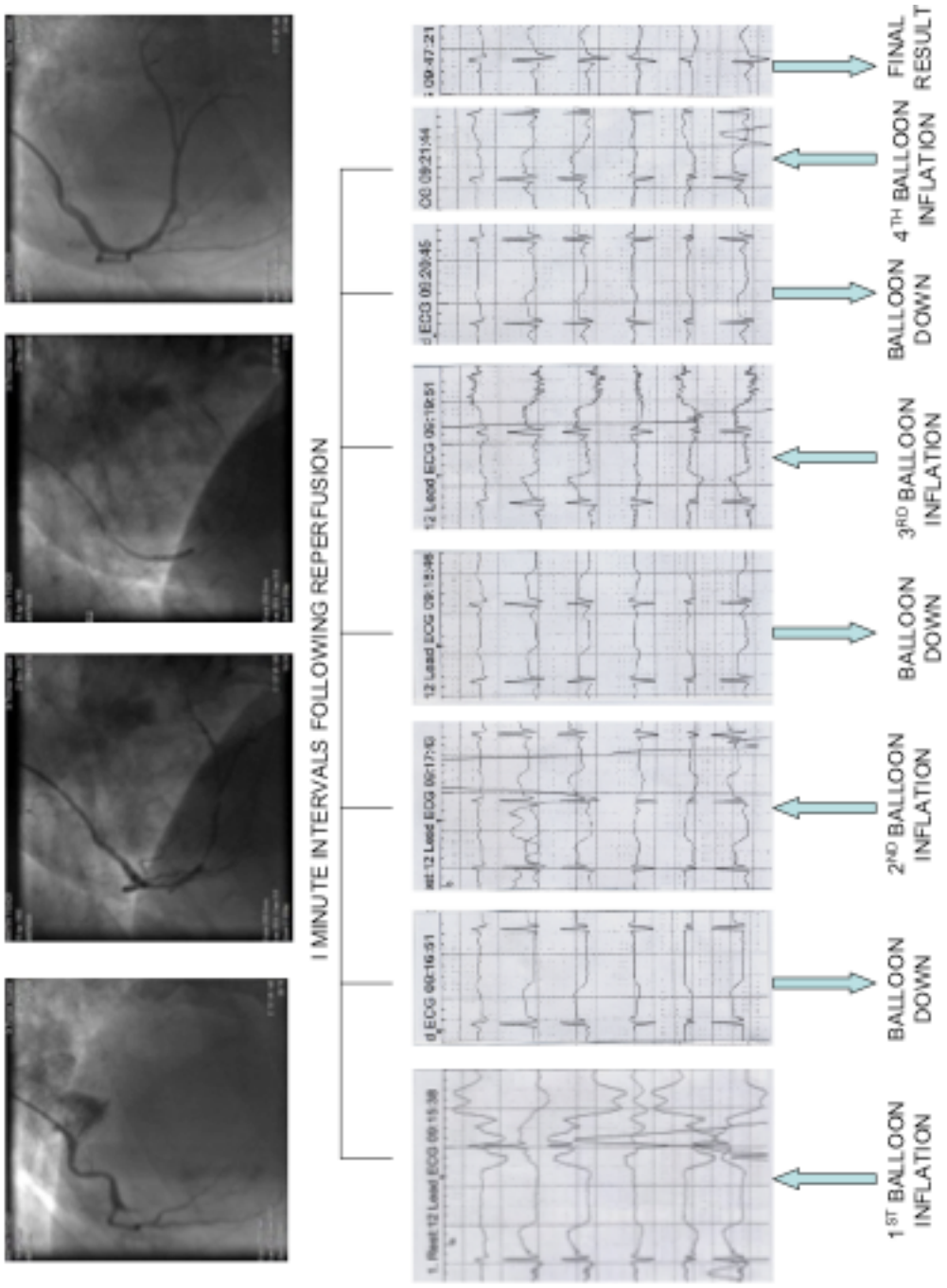

Figure 37. Post conditioning protocol in a patient with an inferior STEMI. Sequential balloon occlusion of the artery following reperfusion at minute intervals causing brief episodes of ischaemia as evidenced by further transient ST segment elevation

3.5.3 Enzymatic Infarct Size

Peak CK release (IU) was not different between the groups (2319±540 control vs. 2010±336 PC, NS) nor was the area under the curve of CK release over 36 hours. See Figure 38 below. Peak Troponin T measured 12 hours after admission was also not

different between the groups (7.3±1.3 control vs. 5.4±1.1 PC, NS). See Figure 39 below.

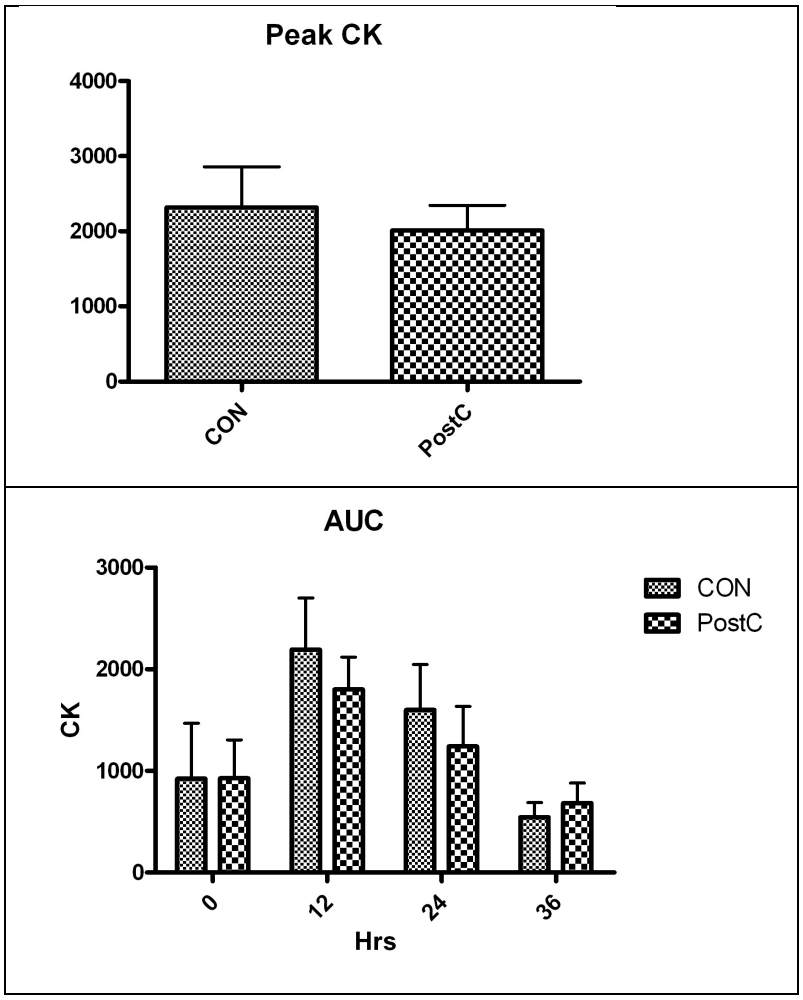

Figure 38. Figure showing peak release of CK (IU) and the release over the first 36 hours after presentation. Differences not significant.

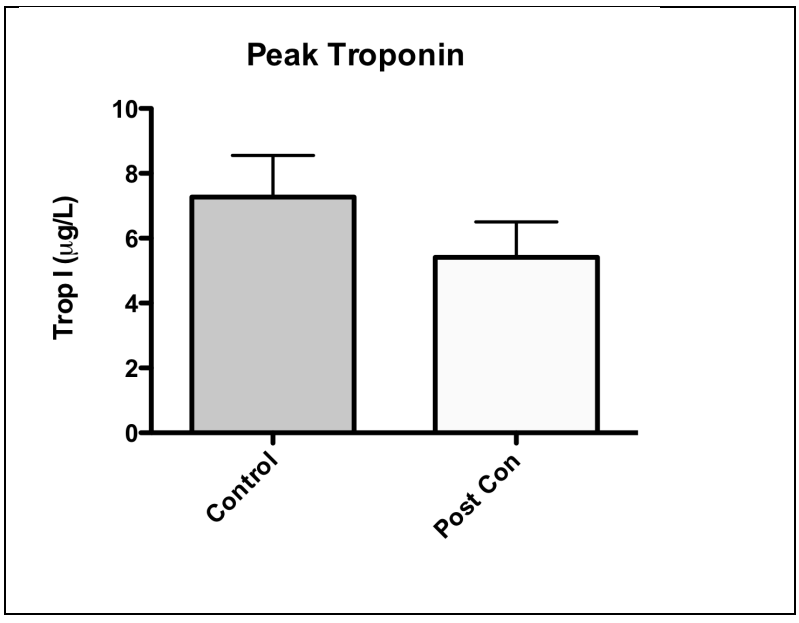

Figure 39. Showing peak Troponin I (μg/L) at 12 hours after presentation. Differences not significant

3.5.4 ST-Segment Shift

ECG ST-segment resolution (mm), a marker of reperfusion, was significantly improved in the PC group (3.3±0.3 vs. 1.3±0.3, p<0.002).

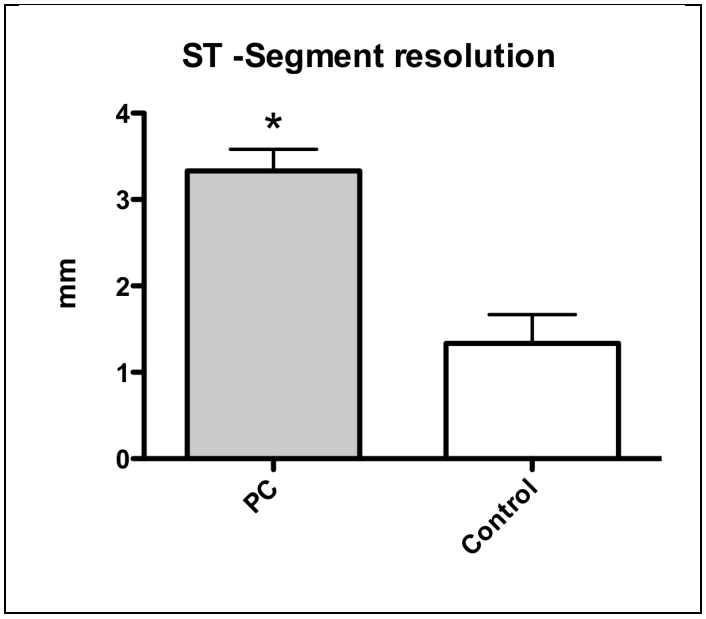

Figure 40. Showing ST-segment resolution on ECG following primary PCI. *P<0.002.

1.1.5 Cardiac Magnetic Resonance Imaging

Early CMR imaging was carried out on all subjects successfully within 36 hours of presentation (mean 23 ±13.3 hours), apart from one patient in the control arm who suffered claustrophobia at the beginning of the scan meaning that no data could be collected. The mean scanning time was 51±18 minutes and all images were of sufficient quality for analysis.

Baseline CMR Scan

There was no difference in LV size (cm^3), which was 128.5±29.8 in the PC group compared to 151.6±25.8 in the control group, or, mass (g) where the corresponding values were 133.6±31 in the PC group vs. 157.6±26.8 for the control. The volume of late gadolinium enhancement was not different between the groups, either when expressed as a absolute measurement (cm^3) (35.6±16.4 in the PC group compared to 26.1±9.8 control), or as a percentage of the LV myocardium as a whole (26.9±9.3 PC vs. 17.4±6.3 control).

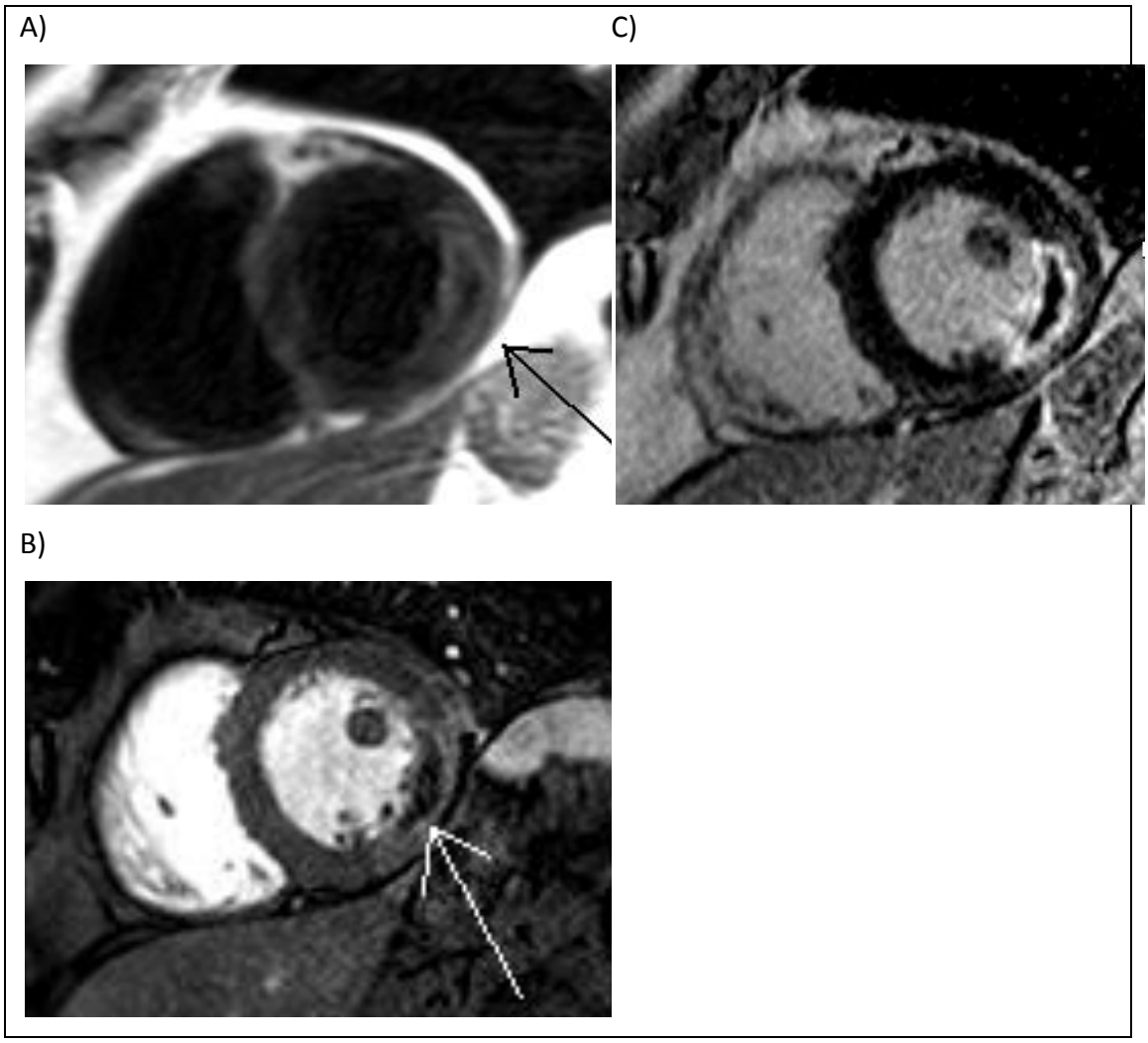

Figure 41. CMR images taken at 36 hours from a study patient presenting with a lateral STEMI due to an occluded left umflex coronary artery. A) T2-weighted scans showing increased tissue oedema in the lateral wall, B) Gd-enhanced perfusion images demonstrating dark areas at the endocardial border representing microvascular obstruction (MVO), and, C) T1-weighted images demonstrating areas of late gadolinium enhancement representing early infarct size with a dark core of MVO that corresponds to the early perfusion images

Microvascular obstruction (MVO) was defined by the dark regions of hypo-enhancement within the infarct zone and again there was no significant difference between the groups either when expressed as an absolute value (6.2±8.5 PC vs. 4.2±0.2 control) or as a percentage of the total infarct area (12.3±9.3 PC vs. 13.4±8.6 control), which consisted of the regions of hyper and hypo-enhancement added together (see Figure 42 below).

CMR scan at 5 months

5 further patients dropped out before the second CMR scan could be performed, including one patient who had a cardiac defibrillator fitted meaning he could no

longer undergo a scan. The full details of the data are presented in the table above but there remained no differences in any of the major endpoints at 5 months between the groups.

3.6 Discussion

The main results of the interim analysis of this randomised, prospective study examining the benefits of postconditioning compared to control in a population of patients undergoing primary PCI for acute ST-elevation MI suggest an improvement in tissue perfusion, but no reduction in infarct size. These results must be treated cautiously as they are not powered to determine any significant differences due to low numbers.

Although Staat et al[148, 318] showed that postconditioning can reduce infarct size, other similar small, single-centre studies have been disappointing and more

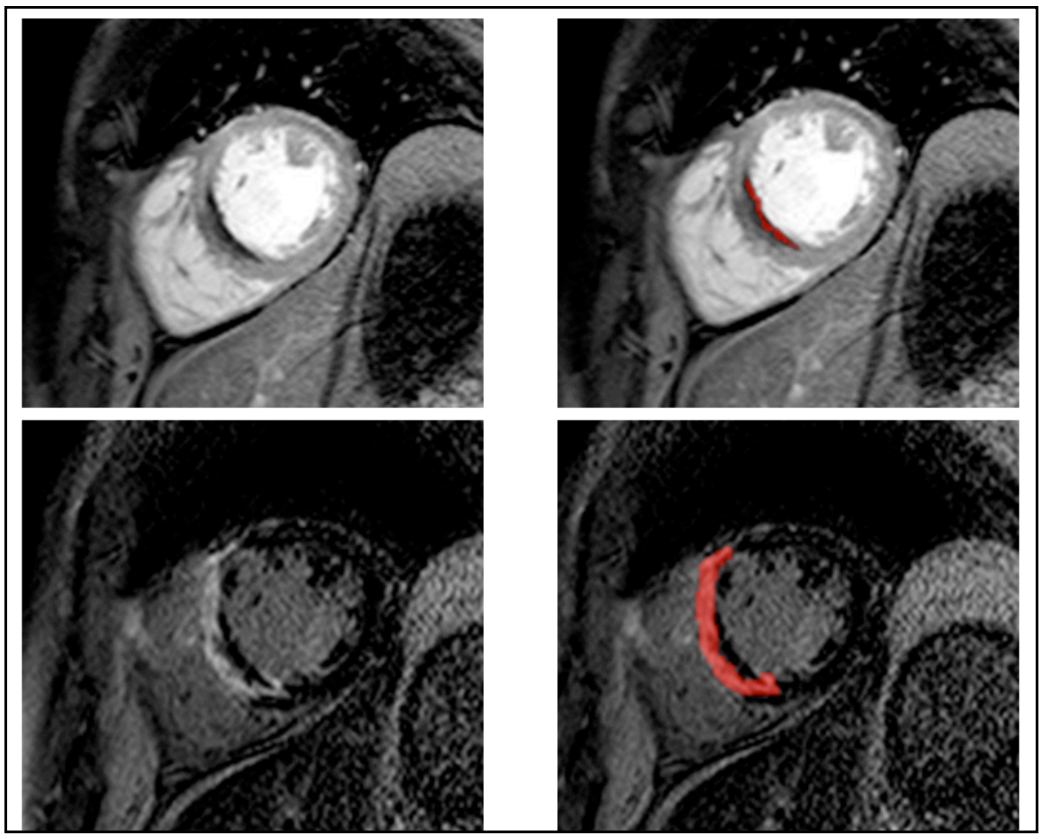

Figure 42. Showing mid slice short axis CMR images in a patient 21 hours after presenting with an acute anterior ST-elevation MI. The top images show T1-weighted images early after injection of a gadolinium (Gd) containing contrast agent. The dark endocardial area indicates microvascular obstruction (MVO), which can be quantified using planimetry computer software as seen in the right-hand panel. The images below are late enhancement images taken 15 minutes after contrast injection with the myocardium nulled to optimise the signal to noise between the bright areas signifying acute injury and the dark areas that represent normal myocardium. Within the infarct zone at the endocardial border, however, the intensely black areas represent MVO where the contrast agent is not able to reach. Total infarct size is calculated by adding together the areas of early hypo-enhancement seen in the early images and late hyper-enhancement seen in the later images.

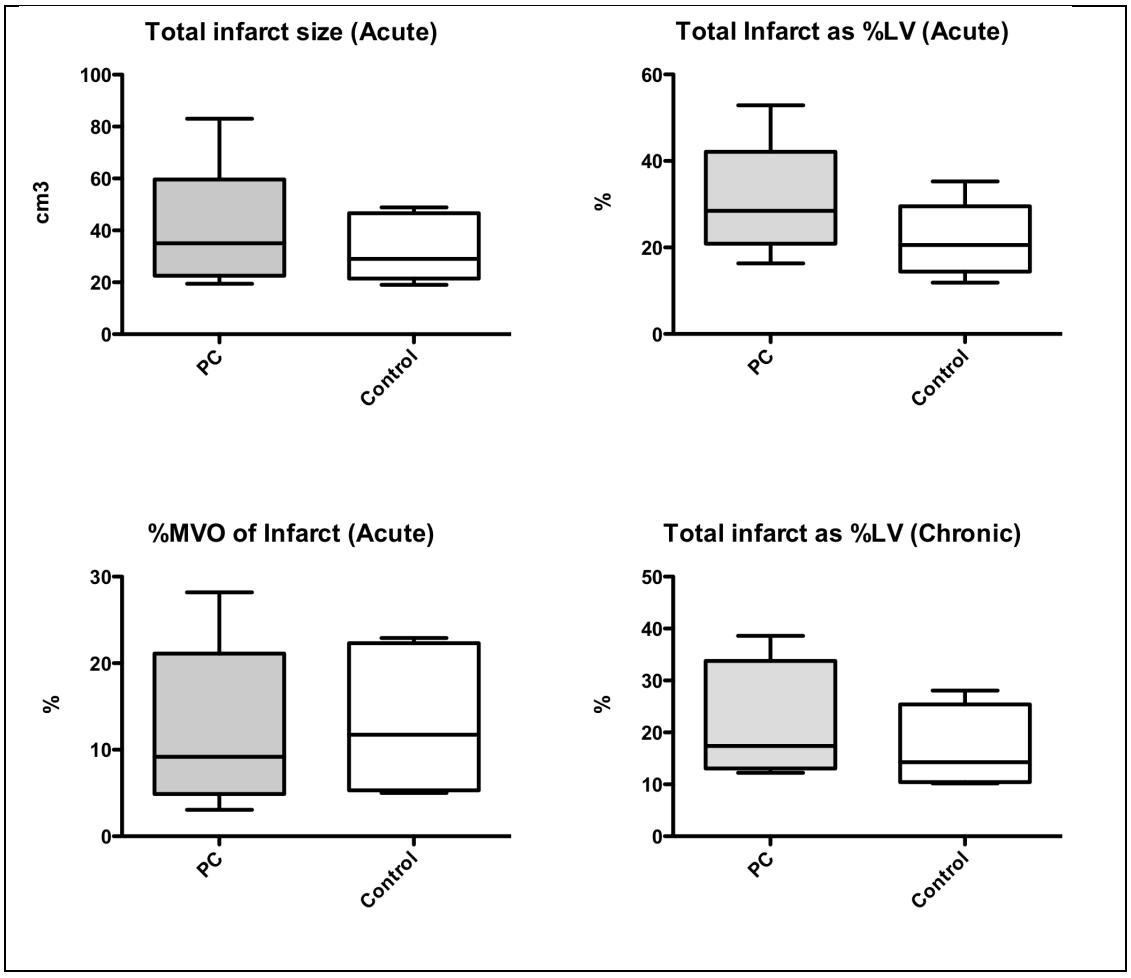

Figure 43. Showing illustrating the main MRI data. LV= left ventricle, MVO= microvascular obstruction, PC= postconditioning arm

consistent with the findings from the present study. Recently, in a study of 72 patients being treated with PPCI Masotti et al[319] failed to demonstrate a benefit from postconditioning in limiting infarct size and, on the contrary, found a significant reduction in myocardial salvage in the postconditioning group compared to control. A trend toward increased infarct size was seen in the current study but this is likely to be due to the preponderance of LAD infarcts in the postconditioning arm, rather than an adverse effect of the postconditioning protocol itself although this must be considered given these recent data. Other similar studies have also been presented, all showing a lack of clear benefit from mechanical postconditioning delivered in this fashion. Despite these negative results there is still possible that some form of postconditioning can be used to attenuate re-perfusion injury in patients with acute

Baseline Scan	**Post Con (n=8)**	**Control (n=6)**	
LV volume (cm^3)	128.5±29.8	151.6±25.8	NS
LV mass (g)	133.6±31	157.6±26.8	NS
LGE volume (cm^3)	35.6±16.4	26.1±9.8	NS
LGE %	26.9±9.3	17.4±6.3	NS
MVO volume (cm^3)	6.2±8.5	4.2±0.2	NS
MVO % of infarct	12.3±9.3	13.4±8.6	NS
Total Infarct size (cm^3)	41.32±23.4	33±12.9	NS
Infarct as % of LV	31±12	21±8.7	NS
5 month Scan	**Post Con (n=5)**	**Control (n=4)**	
LV volume (cm^3)	143±35.9	137.1±29.3	NS
LV mass (g)	148.7±37.4	142.6±30.4	NS
LGE volume (cm^3)	29±14.1	23.5±15	NS
LGE %	21±13.9	16±8.3	NS
MVO volume (cm^3)	0.5±0.7	0.2±0.4	NS
Total Infarct size (cm^3)	29.4±14.6	23.7±14.8	NS
Infarct as % of LV	22.1±14.3	16.7±8.2	NS

Table 6. Table showing the baseline MRI data. LV= left ventricle, LGE =late gadolinium enhancement, MVO= microvascular obstruction, total infarct size =LGE area + MVO area. Data are expressed as mean ± standard deviation (SD).

myocardial infarction, perhaps using different methods to deliver the postconditioning stimulus. The direct mechanical method i.e. the direct interruption of blood in the coronary artery supplying the infarcted myocardium is relatively complicated and limited by the availability of local expertise and particularly by the time-dependent manner in which the postconditioning stimulus needs to be applied following re-perfusion means that this technique is likely to be always limited by these factors. Similarly the increased use of thrombectomy devices prevents comparison with a control group of unhindered reperfusion. Interest has been shown in other ways to tap this "new wine from the old bottle"[137] of cardiac protection. Remote preconditioning where an ischaemic stimulus such as a ligature around an arm or leg has been shown to confer cardiac protection in patients

undergoing cardiac surgery[160] and early evidence suggests a similar protective benefit with remote postconditioning[320-322]. Trials are underway to evaluate role the role of remote postconditioning in acute myocardial infarction where it has the advantage of being able to be applied in the ambulance by the paramedics almost immediately and as such can potentially yield the maximum benefit. Interest is also being shown in pharmacological agents such as glucagon-like-peptide[323], erythropoietin[324], atorvastatin[296], atrial naturetic peptide[295] and cyclosporin[325] which have all been shown to have a cardioprotective effect and are undergoing further evaluation in larger clinical trials. Again these agents have the advantage of being easily and rapidly administered at an early stage so that their effect will be apparent as soon as anterograde blood flow is restored and they are able to take advantage of that golden moment after reperfusion when there is some chance of conferring cardio-protection and increasing myocardial salvage.

3.7 Study Limitations

Clinical studies involving patients presenting with acute myocardial infarction are a notoriously difficult group to study due to the inherent clinical instability and unpredictability of their presentation. It is often difficult to gain an accurate history from patients about both the duration and severity of their symptoms and past medical history; in addition, patients are naturally anxious about consenting into clinical trials when they are scared and uncertain about what is happening to them. In addition, there are those patients in whom anterograde flow is already present when the diagnostic pictures are taken or have evidence of extensive multi-vessel disease with collateralisation or previous myocardial infarction all of which are exclusion criteria for the study. As can be seen from the recruitment flow chart, even if they are randomised then there is still a high chance of the patient being excluded from the study with the inherent complications that are present in a high proportion of PPCI cases, such as no-reflow or haemodynamic compromise requiring additional LV support. All of the above conspired to a slower than predicted recruitment rate.

From a protocol perspective this was well tolerated in the cath lab and the early MRI scan was feasible and produced good quality data. With its excellent tissue characterization and accurate evaluation of infarct size and area of MVO, CMR should become the investigation of choice for such trials in the future. There is the potential for inadvertent bias due to the fact that the interventionalist was not blinded to whether the patient was either in the postconditioning or control arm. To ameliorate this possible bias, analysis of ECG and blood enzyme levels as well as all the CMR data collection and analysis were undertaken in a blinded fashion by researchers who were unaware of the intervention received by the patient.

With the problems encountered in the recruitment of patients into the present study together with the lack of any positive signal from the pre-specified interim analysis and the publication of similar (albeit better powered) single-centre trials which also failed to elicit a positive result, it was decided by the study steering committee that it was not worth continuing with the present study for reasons of futility. Future studies need to be directed in the form of multi-centre large trials to establish the benefits of postconditioning using hard clinical endpoints, and possibly utilising less invasive methods such as pharmacotherapy or remote postconditioning.

3.8 Conclusion

In this small, single-centre pilot we examined the role of postconditioning in reducing infarct size in patients undergoing PPCI for acute ST-elevation MI. The study was attenuated by slow recruitment and high drop-out rates and while a pre-specified interim analysis suggested better tissue perfusion in the postconditioning group as evidenced by better ST-segment resolution, there was no reduction in infarct size or reduction in MVO as determined by cardiac enzyme release and CMR imaging. These data need to be interpreted cautiously because of the lack of statistical power.

3.9 Acknowledgements

I would like to thank all the staff at St Thomas' hospital cardiac catheterisation labs and coronary care unit in particular for their support. I would also like to thank Dr Chiribiri for his analysis of the MRI data and Prof Nagel and Dr. Plein for their expertise in optimising the sequences. I am also grateful to all the interventional consultants at St Thomas', in particular Prof. Redwood and Dr. Perera and to Prof Marber for his help in the conception and over-seeing of the study. I would also like to thank the BHF for their funding for this project. Dr. Siobhan Crichton from the Dept. of Medical Statistics, KCL, provided statistical support, in particular with respect the sample size calculation.

4 *K-T* ACCELERATED MRI PERFUSION TO DETECT CORONARY ISCHAEMIA

Tim Lockie[1] , Masaki Ishida[2] , Divaka Perera[1] , Amedeo Chiribiri[2] , Sebastian Kozerke[2] , Mike Marber[1] , Eike Nagel[2] , Simon Redwood[1] , Sven Plein[2, 3]

[1]Cardiovascular Research Division, The Rayne Institute, St Thomas' Hospital, KCL, London UK

[2]Division Imaging Sciences, The Rayne Institute, St Thomas' Hospital, KCL, London, UK

[3] Academic Unit of Cardiovascular Medicine, University of Leeds, UK

4.1 Abstract

Background

Cardiac magnetic resonance (CMR) myocardial perfusion is an evolving technique for the detection of significant coronary artery disease (CAD). New acquisition strategies may enable high spatial resolution CMR perfusion images but requires further clinical validation.

Objectives

To compare visual and quantitative analysis of high spatial resolution CMR perfusion at 3 Tesla against fractional flow reserve (FFR) determined in the cath lab.

Methods and Results

42 patients (33 male, age 57.4±9.6 years) with known or suspected CAD underwent a k-t SENSE accelerated adenosine-stress perfusion CMR scan at 3T achieving in-plane spatial resolution of 1.2 x1.2 mm2. In the catheter laboratory, FFR was measured in all vessels with >50% severity stenosis. FFR < 0.75 was considered haemodynamically significant. 2 blinded observers visually interpreted the CMR data, which was further fully quantified to determine the myocardial perfusion reserve (MPR). In total, 126 coronary territories were examined and 52 major vessels underwent pressure wire assessment. Of these, 27 lesions had an FFR <0.75 and 25 lesions had an FFR ≥0.75. Sensitivity and specificity of visual analysis of CMR perfusion to detect coronary stenoses at a threshold of FFR <0.75 was 0.82 and 0.94 ($p<0.0001$) respectively with an area under the curve (AUC) of 0.92 ($p<0.0001$). From quantitative analysis, the optimum MPR to detect such lesions was 1.58 with a sensitivity of 0.80 and specificity of 0.89 ($p<0.0001$) and an AUC 0.89 ($p<0.0001$).

Conclusions

High-resolution CMR perfusion MR at 3T accurately detects flow-limiting coronary artery disease as defined by FFR, using both visual and quantitative analyses.

4.2 Background

Cardiac magnetic resonance (CMR) myocardial perfusion imaging offers great potential for the non-invasive detection of myocardial ischaemia due to its high resolution, lack of ionising radiation and additional tissue characterisation. Recent studies have suggested a high degree of accuracy of CMR compared to other non-invasive techniques[156, 214]. New CMR acquisition strategies that simultaneously take advantage of coil encoding and spatiotemporal correlations, such as *k*-space and time sensitivity encoding (*k*-*t* SENSE), allow considerable acceleration of CMR data acquisition[220]. Such acceleration can be invested in further improved in-plane spatial resolution approaching 1mm^2. The introduction of 3 Tesla CMR scanners is a further improvement in perfusion CMR due to the intrinsically high signal to noise ratio (SNR) compared with 1.5 Tesla. Combined, high spatial resolution and high SNR at 3 Tesla may offer a step change in the performance of myocardial perfusion CMR. High-resolution myocardial perfusion CMR at 3 Tesla has been proved accurate in the detection of coronary disease as determined anatomically by a 50% stenosis on the coronary angiogram[223]. However, coronary angiography alone is known to be inaccurate in the determination of haemodynamically significant coronary disease[218]. Fractional flow reserve (FFR) determined invasively by measuring the pressure gradient across a coronary stenosis during hyperaemia correlates well with clinical end points and non-invasive measures of ischaemia based on a dichotomous cut-off of 0.75[225, 326]. FFR is highly reproducible under a range of haemodynamic conditions and considered by many to be the "gold standard" to determine functionally significant coronary stenoses that would benefit from revascularisation. To date there have been no studies comparing the performance of high resolution CMR myocardial perfusion CMR at 3 Tesla to FFR in the detection of haemodynamically significant coronary stenosis.

4.3 Objectives

- To validate CMR *k-t* perfusion and quantification methods in a set of normal volunteers
- To compare visual and quantitative analysis of high spatial resolution CMR perfusion at 3 Tesla against fractional flow reserve (FFR) determined in the catheterisation lab.

4.4 Methods

Ethics approval for the patient and volunteer studies was obtained from the local ethics committee (REC Study No: 07/Q0704/16). As part of the consent process, all patients were provided with an information sheet and signed a written consent form.

4.4.1 Volunteer Recruitment

To validate the quantitative perfusion methods 8 normal subjects aged less than 40 years with no history of previous coronary artery disease and with no other underlying medical problems or contraindications to CMR scanning were approached and consented into the trial. They were asked to abstain from any caffeine-containing products for 24 hours before the scan.

4.4.2 Patient Recruitment

Patients were selected who either had confirmed coronary artery disease and were awaiting revascularisation, or those who had a high suspicion of coronary artery disease and had been booked in for a coronary angiogram with a view to proceed if a significant coronary stenosis was detected. Exclusion criteria for the study were contraindications for CMR; known allergies or a contra-indication to Gd-chelates; significant cardiac arrhythmia; pregnancy; previous myocardial infarction; previous coronary artery bypass grafting (CABG); unstable angina pectoris (CCS IV) or acute

coronary syndrome (ACS); impaired LV function (EF<40%); asthma, or obstructive pulmonary disease.

4.4.3 CMR Protocol

Myocardial perfusion CMR was performed on a 3T Philips Achieva® system using a 6 channel cardiac phased array receiver coil for signal reception and a vectorcardiogram for triggering and gating. Subjects had a peripheral cannula inserted in both antecubital fossae, one for administration of a contrast agent and the other for the infusion of adenosine. All perfusion data were acquired in the true short axis of the LV at end-inspiration to minimise respiratory artefacts. The perfusion pulse sequence consisted of a saturation recovery gradient echo method with a repetition time/echo time 3.0ms/1.0ms and flip angle 15°; 5x *k-t* SENSE acceleration was used with 11 interleaved training profiles providing an effective acceleration of 3.8x and a spatial resolution of 1.2x1.2x10mm^3. 3 slices were acquired at each RR interval. The first slice was acquired immediately following the R-wave on the ECG. In order to acquire data during cardiac phases with minimal bulk cardiac motion, mid-systole and mid-diastole were identified on cine images and the trigger delays for slice two and three set so that acquisition occurred in these cardiac phases. Data were acquired during adenosine-induced hyperaemia (140µg/kg/min) and after a 15 minute delay at rest using a dose of 0.05mmol/kg Gd-DTPA (Magnevist®, Shering, Germany) at a rate of 4ml/minute followed by a flush of 20ml Saline. Blood pressure and heart rate were monitored throughout, as was the subject's response to adenosine to ensure that hyperaemic conditions were achieved. In patients, standard dual inversion recovery late gadolinium enhancement images were acquired after 15 minutes to ensure there were no significant areas of scar that may interfere with the analysis.

4.4.4 Cardiac Catheterisation Lab Protocol

In the cardiac catheterisation lab arterial access was secured in the right femoral artery with a 6F sheath. A 7F sheath was inserted into the right femoral vein to record right atrial pressure via a multipurpose catheter[327]. Diagnostic images were taken using standard Judkins catheters in at least 2 orthogonal views to determine

the maximum visual vessel diameter stenosis. For PCI a guiding catheter was inserted into the coronary ostium and 500µg nitrates were injected intracoronary to ensure maximal dilatation of the epicardial vessel. A 0.014" coronary pressure sensor-tipped wire (Volcano®) was passed into any vessel with a >50% diameter stenosis. A vessel with a <50% diameter stenosis was not considered to be haemodynamically significant. Fractional flow reserve (FFR) was measured in all vessels with a >50% diameter stenosis and calculated as $(P_d – P_v)/(P_a - P_v)$, where P_a, P_v and P_d are simultaneous aortic, right atrial and distal coronary pressures measured during an intravenous infusion of adenosine at 140µg/kg/min. An FFR reading of <0.75 was considered to be haemodynamically significant[6]. If serial stenoses were present then a pullback was performed with the pressure wire and the lowest FFR measurement was used. Following the FFR measurement the vessel was then stented as appropriate at the discretion of the operator. Quantitative coronary angiography (QCA) was calculated for all lesions using off-line software (Medcon™) by an observer blinded to the FFR and CMR data.

4.4.5 CMR Perfusion Analysis

Visual analysis

In the patient cohort, 2 experienced observers blinded to the clinical background undertook the analysis using a dedicated off-line analysis workstation (ViewForum®, Philips Medical Systems). The LV myocardium was divided into 3 perfusion territories correlating to each of the major coronary vessels (left anterior descending, LAD, circumflex, Cx and right coronary artery, RCA) according to the modified standardised nomenclature for tomographic imaging of the heart[328]. Defects were reported for each perfusion territory by visual analysis using a scale from 0 to 3 (0=normal, 1=probably normal, 2=probably abnormal, 3=abnormal). Abnormal perfusion was reported if contrast enhancement in a segment was delayed relative to that of a remote segment, or if a transmural enhancement gradient was seen. If any LGE was present then the observers identified only perfusion defects outside of the areas of LGE. In case of disagreement, arbitration from a third observer was sought.

Quantitative analysis

Data was analysed off-line by means of a commercially available dedicated software package (MASS®, Medis, Leiden, the Netherlands) by two separate experienced observers who were blinded to the results of the visual perfusion analysis and both the coronary angiogram and FFR data. Subendocardial borders and subepicardial borders were positioned on each slice with a region of interest (ROI) placed in the LV cavity. The LV myocardium was divided into 6 equiangular segments per slice according to the modified standardised nomenclature for tomographic imaging of the heart[9]. Data generated in MASS were imported to a Fermi Function deconvolution algorithm implemented in Matlab® (The MathWorksInc®, USA)[196]. The Fermi deconvolution provided estimates of absolute myocardial blood flow (ml/g/min) following correction for baseline and timing offsets between the input and tissue response functions. Inter-and intra-observer variability was calculated. Myocardial perfusion reserve (MPR) was calculated by dividing the peak stress flow by resting flow. The segments were then assigned to the respective perfusion territory[9] and the mean value of the two lowest scoring segments for each perfusion territory was used for further analysis. Although the observers were blinded to the coronary angiogram and hence information relating to the dominance of the coronary artery, if a large perfusion defect was present relating to a presumed dominant RCA that spilled over into the segments assigned to the Cx artery then these data were regarded as being within the RCA perfusion territory and vice-versa.

4.4.6 Statistical Analysis

Continuous data were expressed as the mean ± standard deviation (SD). Group means were compared using paired and unpaired Student *t*-test as appropriate. Discrete data were expressed as percentages. Statistical significance was considered for $P<0.005$. Receiver operating characteristic (ROC) analysis was used to determine the diagnostic accuracy of visual analysis to detect haemodynamically significant coronary stenoses with an FFR≤0.75 and also to determine the optimal myocardial perfusion reserve (MPR) to determine significant coronary disease using a dichotomous FFR cut-off of 0.75. Areas under the curve (AUCs) with 95% confidence intervals (95% CI) were determined from ROC analysis and used to compare the

diagnostic accuracy of the two methods. Linear regression was used for correlation of MPR with FFR and QCA, which were compared using Seiger's Z-test. The inter- and intra-observer variability was calculated using the Cohen kappa (*k*) statistic for the discrete visual analysis data and for the continuous quantitative analysis data observers were compared using the method described by Bland and Altman[329]. Coefficient of variability was calculated as standard deviation of differences between the measurements divided by the mean value of the two observations or studies. Because three coronary territories were examined per patient the intra-class correlation coefficient (ICC) was calculated to determine the design effect and the need to adjust these data for clustering [323]. Statistical analysis, including generation of the ROC curves was performed using SPSS (IBM®, Statistics, Version 19) software.

4.5 Results

4.5.1 Volunteer Studies

In the 8 volunteers (6 male, 32 ±8.3 years) all subjects experienced mild, transient, typical symptoms with the administration of adenosine suggesting adequate hyperaemia. There were no complications from the adenosine. Full quantitative analysis was possible with all studies. The MPR was 2.64±0.63 with a mean intra-observer difference of 0.1±0.57 (p=0.68) and a coefficient of variability of 21%. Inter-observer difference was 0.3±0.28 (p=0.13) with a coefficient of variability of 18%. Full results are shown in Table 7 below.

	Absolute Flow (mls/g/min)		
	Rest	***Stress***	***Reserve (MPR)***
Intra-observer			
Mean ± SD	1.72±0.4	4.46±1.06	2.64±0.63
Mean difference ± SD	0.09±0.22	0.21±0.6	0.1±057
Coefficient of variability %	14	12	21
P value	0.33	0.44	0.68
Inter-observer			
Mean ± SD	1.99±0.6	4.7±1.4	2.47±0.74
Mean difference ± SD	0.53±0.38	0.5±0.88	0.3±0.28
Coefficient of variability %	16	18	18
P value	0.06	0.22	0.13

Table 7. Intra- and inter-observer variability for full quantitative analysis for the volunteer cohort.

4.5.2 Patient Studies

44 patients (33 male, age 57.4±9.6 years) were recruited. 2 patients were excluded from the final analysis: 1 because they did not tolerate the CMR scan due to claustrophobia; 1 because of technical problems with the FFR measurement. 126 coronary territories in 42 patients were thus available for analysis. Full background demographics of those included are shown in Table 8 below.

Parameter	Data (n=42)
Male (%)	33 (78.6)
Age (years)	57.4±9.6
Previous PCI (%)	8 (19)
DM (%)	8 (19)
Previous stroke (%)	1 (2.3)
PVD (%)	3 (7.1)
Smoker (%)	9 (21.4)
Family history IHD (%)	11 (26.1)
Medications	
• Statin (%)	31 (73.8)
• Betablocker (%)	20 (47.6)
• Aspirin (%)	35 (83.3)
• Clopidogrel (%)	22 (52.3)
• Nitrate (%)	17 (40.4)
• Calcium channel blocker (%)	10 (23.8)

Table 8. Baseline demographics of patient cohort. DM =diabetes melitus, PVD =peripheral vascular disease, LAD =left anterior descending artery, Cx =circumflex, RCA =right coronary artery, FFR =fractional flow reserve. Data presented as mean ±SD.

CMR Data	
Resting BP (MAP mmHg)	78±11
Stress BP (MAP mmHg)	70±15
Resting HR (bpm)	71±15
Stress HR (bpm)	87±25
Scanning time (mins)	56±13
Late Gadolinium Enhancement (%)	
• Full thickness	0 (0)
• Partial thickness	2 (4.7)
Adenosine symptoms	42 (100%)
Adenosine complications	0 (0)

Table 9. Details of CMR scanning carried out in study patients. BP =Blood pressure; HR = heart rate. Data are presented as mean ± SD.

Angiographic Data	
Time from CMR scan (days)	2.5±4.9
No. pts with ≥1 lesion (>50% visual diameter stenosis)	38 (90%)
No. vessels FFR measured (per pt)	1.3±0.8
Vessels with FFR >0.75	25 (0.89±0.06)
Vessels with FFR≤0.75	27 (0.53±0.17)
• LAD	17
• Cx	3
• RCA	7
QCA in vessels with FFR >0.75 (% diameter stenosis)	47±15.4
QCA in vessels with FFR <0.75 (% diameter stenosis)	81.8±16.3

Table 10. Angiographic data from study patients. FFR = fractional flow reserve; LAD = left anterior descending artery; Cx = circumflex artery; RCA = right coronary artery; QCA = quantitative coronary analysis. Data are presented as mean ± SD.

Coronary Angiography

Coronary angiography was performed 2.5 ± 4.9 days after CMR. The findings are summarised in table 1. Out of the 126 vessels examined 53 (42.1%) contained a visual stenosis >50% diameter. Of these, 52 vessels underwent a pressure wire study with 1.3±0.6 vessels examined per patient. One vessel contained a chronic total occlusion and was thus not assessed. Of those assessed, 27 lesions had an FFR <0.75 and 25 lesions had an FFR ≥0.75, with mean values of 0.53±0.17 and 0.89±0.06 respectively (p<0.0001). In the vessels with an FFR <0.75 there was an 81±16.3% diameter stenosis on QCA, while in those vessels with an FFR≥0.75 the diameter stenosis was 47.1±15.4% (p<0.0001). In the vessels angiographically assessed as normal the diameter stenosis was 10.7±14.5%. There was a good degree of correlation between FFR and diameter stenosis (r=-0.76 [95%CI -0.83-to-0.66], P<0.0001). See Figure 44 below.

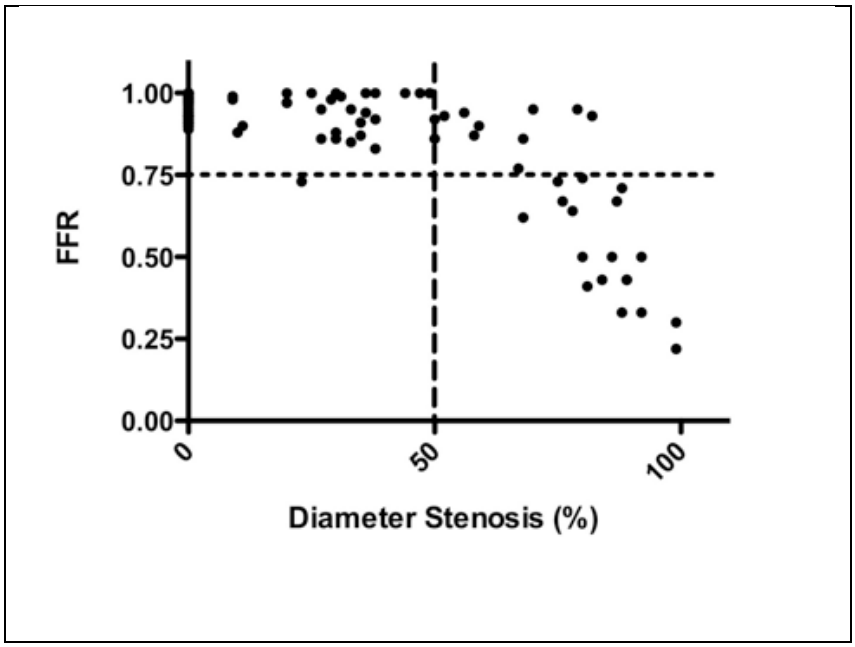

Figure 44. Comparison of FFR and diameter stenosis (%) with reference lines indicating an FFR of 0.75 and diameter stenosis of 50%. Pearson correlation co-efficient was r=-0.76 [95%CI -0.83-to-0.66], P<0.0001) indicating a good degree of correlation.

CMR imaging

Mean scanning time was 56±13 minutes and all patients experienced mild, transient, typical symptoms with the administration of adenosine. There were no complications from the adenosine. There was an appropriate fall in the mean arterial blood pressure (MAP) from 78±11mmHg to 70±15mmHg (p=0.001) and an increase in heart rate from 71±10 beats per minute to 87±18 beats per minute (p<0.0001) suggesting that adequate hyperaemia was achieved. 2 (4.7%) patients had evidence of subendocardial scar based on the gadolinium late enhancement images; none had evidence of full thickness transmural scar.

Visual Analysis vs. FFR

Perfusion was reported as abnormal for 30 coronary territories (23.8%) and normal for 96 territories. Examples of normal and abnormal perfusion scans are shown in Figure 45 below. The inter-observer reliability was *k*=0.79 [95% CI 0.69-0.91] (p<0.0001). FFR in vessels with a visually detected perfusion defect was 0.59±0.22 and was 0.93±0.09 (p<0.0001) in those with visually normal perfusion. Conversely, 22 out of the 27 territories with an FFR<0.75 had a perfusion defect on visual CMR analysis. 5 perfusion defects were reported in 99 vessels that were angiographically normal or had an FFR ≥0.75. Sensitivity of CMR perfusion to detect coronary

ischaemia at a threshold of FFR<0.75 was 0.82 [95% CI 0.61-0.93], specificity 0.94 [95% CI 0.87-0.98] p<0.001, positive predictive value 0.83 [95% CI 0.65-0.94] and negative predictive value 0.94 [95% CI 0.88-0.98]. The likelihood ratio was 16 with an AUC of 0.92 [95% CI 0.85-0.99], p<0.0001. See Figure 46 below. The agreement between visual analysis and FFR was *k*=0.76 [95% CI 0.63-0.89], (p<0.0001).

Quantitative analysis of CMR perfusion

In four patients, quantitative analysis of CMR perfusion data was not possible because of imaging artefacts affecting the upslope of the myocardial signal intensity profile at stress. Full quantitative analysis was thus carried out for 114 perfusion territories in 38 patients. MPR in the 24 territories with an FFR≤0.75 was 1.35±0.5. In the 90 territories where FFR was >0.75 MPR was 2.2±0.5 (p<0.0001). ROC analysis revealed that the optimum MPR was 1.58 to detect functionally significant coronary disease based on a dichotomous FFR cut-off of 0.75, which yielded a sensitivity of 0.80 [95%CI 0.0.58-0.94] and specificity of 0.89 [95%CI 0.8-0.95], p<0.0001. This gave a likelihood ratio of 9.3 and AUC of 0.89 [95%CI 0.8-0.98], p<0.0001. The positive predictive value of an MPR cut-off of 1.58 to detect flow-limiting disease was 0.73 [95%CI 0.54-0.88] and negative predictive value was 0.95 (95% CI 0.88-0.98]. The agreement between MPR and FFR was *k*=0.70 [95% CI 0.54-0.86], (p<0.0001). The coefficient of interobserver variability for MPR was 18%. See Figure 48 below.

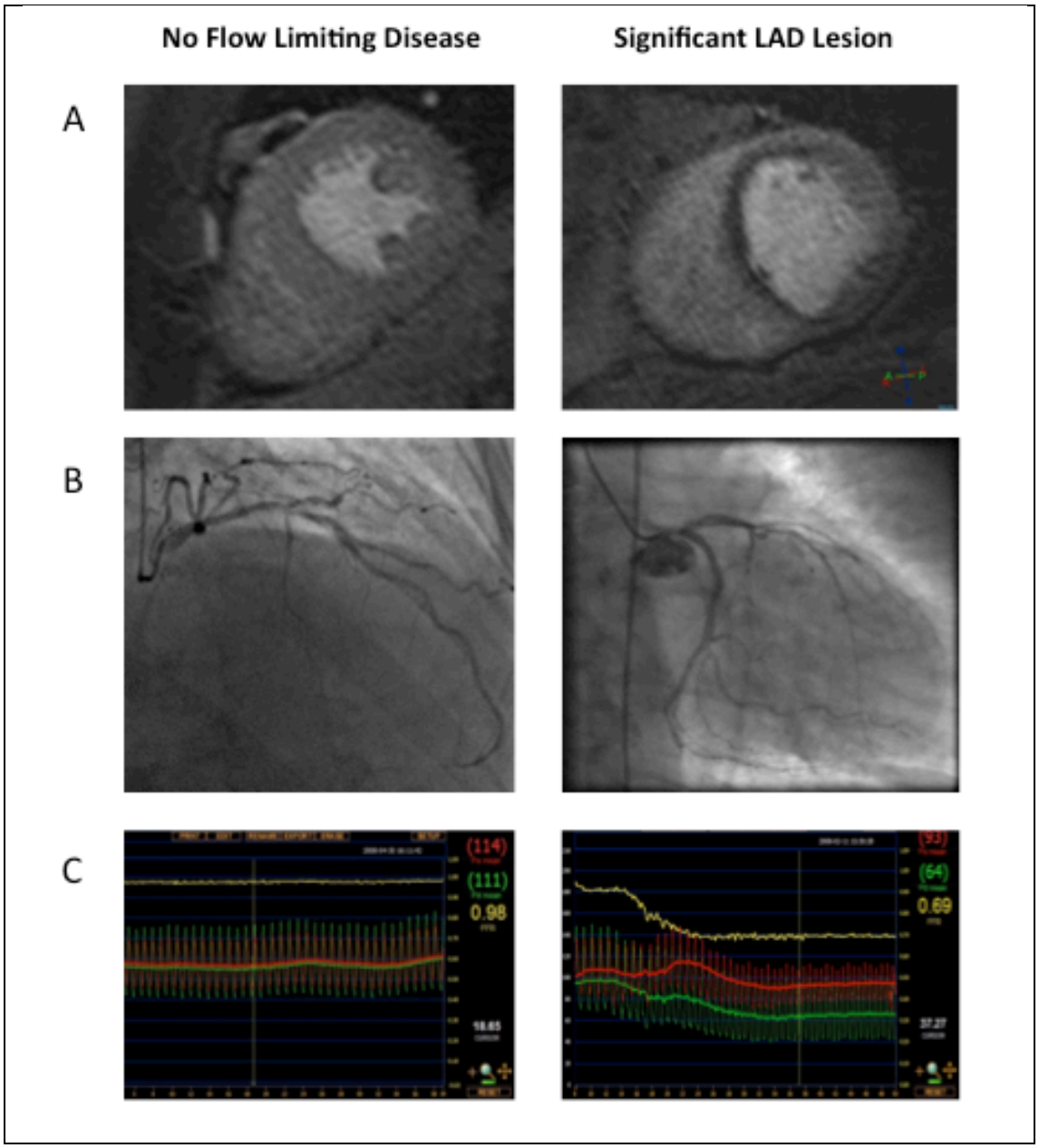

Figure 45. Effects of flow limiting and non-limiting stenoses on FFR and CMR perfusion images. Patient in the left-hand column showing a) normal perfusion scan, b) moderate lesion by visual analysis in the left anterior descending (LAD) coronary artery and a non-dominant circumflex vessel, and c) an FFR trace from the LAD during adenosine hyperaemia showing a reading of 0.98 signifying a non-flow limiting lesion. The right-hand column is from a patient who has a) a clear anterior wall sub-endocardial perfusion defect, b) a tight lesion in the proximal LAD and c) an FFR of 0.69 suggesting a flow-limiting lesion.

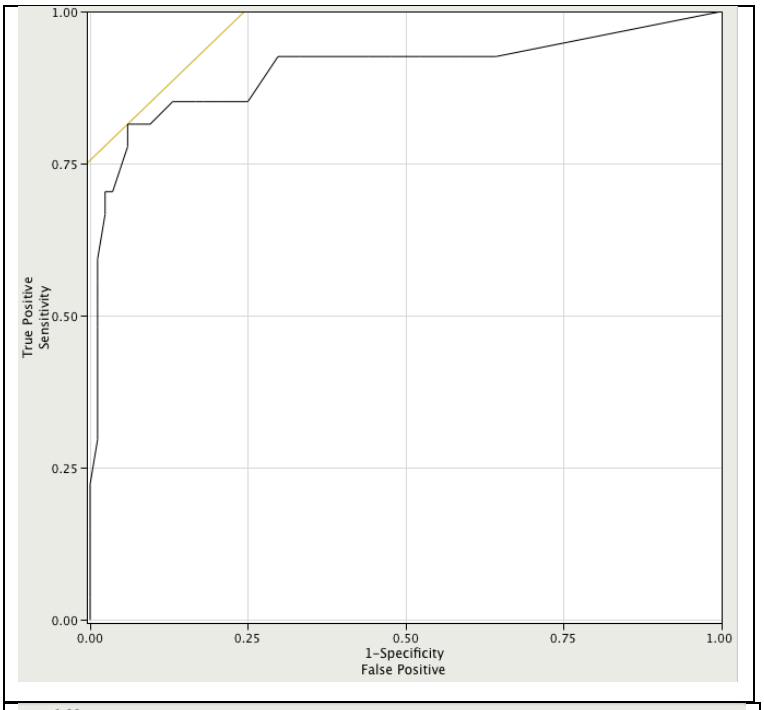

Figure 46. Receiver Operator Curve (ROC) showing the sensitivity and specificity of MR perfusion visual analysis to detect a haemodynamically significant coronary stenosis using a dichotomous value of 0.75 for fractional flow reserve (FFR). The area under the curve (AUC) was 0.922.

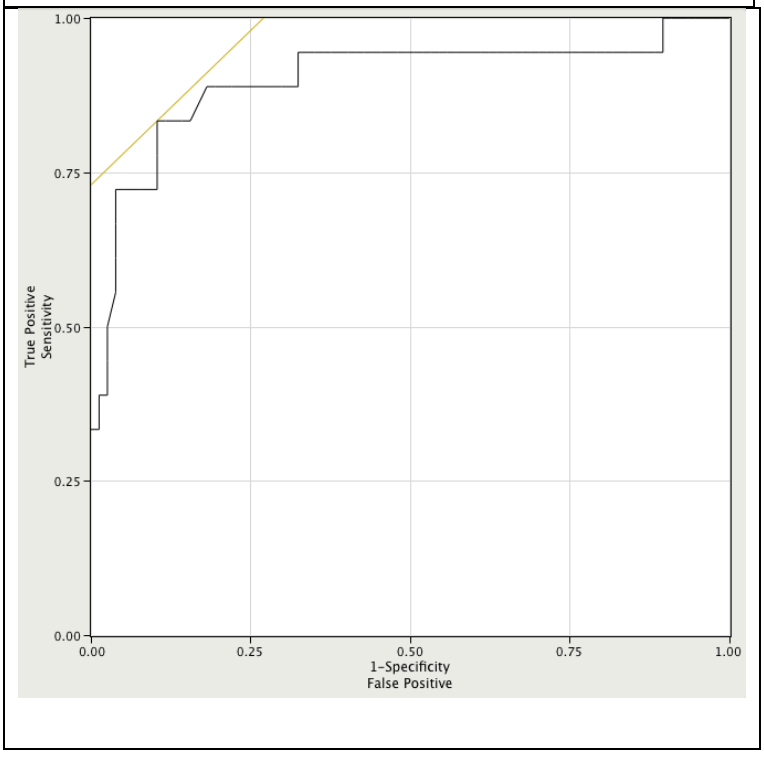

Figure 47. Receiver Operator Curve (ROC) showing the sensitivity and specificity of MPR to detect a haemodynamically significant coronary stenosis using a dichotomous value of 0.75 for fractional flow reserve (FFR). The area under the curve (AUC) was 0.89.

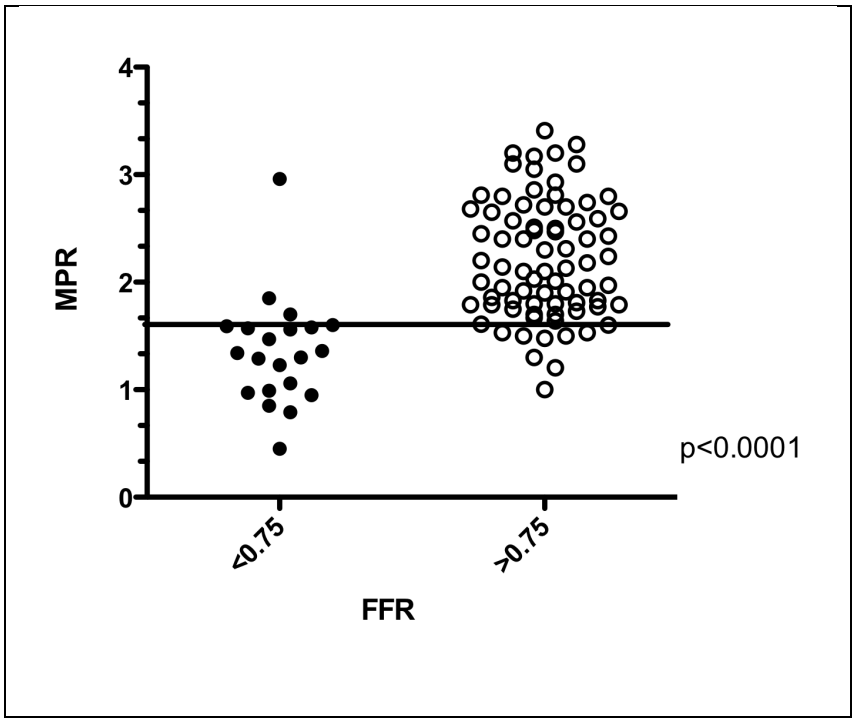

Figure 48.
Scatter plot showing the distribution of MPR values according to FFR using a dichotomous cut-off of 0.75 to signify a significant lesion. The cut-off of 1.58 for the MPR has been marked that yielded the optimum sensitivity and specificity to detect a significant lesion as determined by FFR.

Linear Regression

Linear regression analysis showed a closer correlation between MPR and FFR (r=0.59 [95% CI 0.43-0.71] p<0.0001) than between MPR and QCA (r=-0.47 [95% CI -0.61—0.29] p<0.0001), Z=4.73 (p<0.0001). ICC was low (r_1= 0.03 [95% CI -0.19-0.771], p=0.6) with a design effect *D*= 1.06 where cluster size *m*=3. See Figure 49 below.

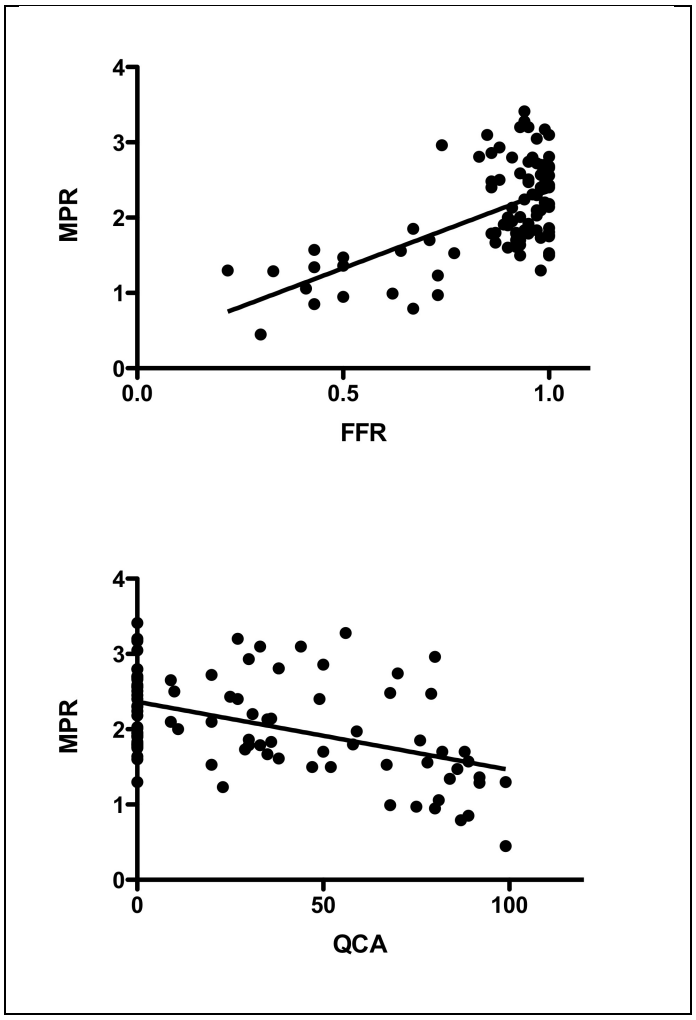

Figure 49. Correlation between MPR and FFR r=0.59 (95% CI 0.43-0.71) p<0.0001 and between MPR and QCA MPR with QCA r=-0.47 (95% CI -0.61—0.29) p<0.0001. The closer correlation between MPR and FFR reflects the fact that both are functional tests rather than QCA that defines a lesion purely on an anatomical basis. QCA =quantitative coronary analysis and refers to diameter stenosis (%).

4.6 Discussion

This study has shown that high resolution myocardial perfusion CMR imaging accurately detects functionally significant coronary artery stenosis as determined by FFR using both visual and quantitative analysis. CMR-based measurements of myocardial blood flow correlated better with FFR than with QCA.

Myocardial perfusion CMR imaging holds great promise as a non-invasive tool in the detection of haemodynamically significant coronary stenosis. *k-t* SENSE accelerated imaging at 3T allows faster acquisition and thus very high spatial resolution of the acquired data at high signal to noise ratio. As shown here, high spatial resolution in turn allows for accurate visual analysis of such images enabling defects to be localised to a particular coronary territory. This is the first study to compare high

resolution CMR perfusion with fractional flow reserve in the detection of functionally significant lesions and it demonstrated that visual analysis of the data was able to identify such lesions with a high degree of accuracy.

The acquired perfusion data were also suitable for full quantification with the MPR obtained per coronary territory correlating well with the FFR measurements. ROC analysis gave an optimal MPR cut-off value of 1.58 to discriminate accurately between haemodynamically significant and non-significant lesions, which is consistent with cut-off values from other studies using CMR perfusion imaging[200, 330, 331]. The majority of these other studies, however, used XCA to determine the lesion severity. It has been discussed previously why a more functional test such as FFR to assess lesion significance is preferable to using anatomically based endpoints alone. The more discriminatory nature of FFR measurements is highlighted in figure 1 in the present study where a significant proportion of the patients with a diameter stenosis >50% had an FFR >0.75 and therefore represent false-positive results. This also explains why MPR was found to correlate more closely with FFR than QCA (see figure 6), reflecting the fact that both are functional tests, rather than QCA that defines a lesion on purely anatomical terms. Rieber et al assessed a standard CMR perfusion sequence at 1.5T for the detection of FFR-determined coronary disease. A semi-quantitative analysis of upslopes of the signal-intensity profiles in 43 patients yielded a sensitivity and specificity of 88% and 90% respectively[330]. Visual analysis was not performed. By comparison, Watkins et al used visual analysis of CMR perfusion alone with FFR in the assessment of 103 CAD patients and were able to detect functionally significant disease with similarly high accuracy[217]. In this later study 25% of the patients had acute coronary syndromes and 23% had evidence of prior myocardial infarction. Although FFR has been used in these settings[332, 333] its applicability remains uncertain and there are concerns about the necessary assumptions of minimal microvascular resistance attained during hyperaemia[230]. In addition, the presence of acutely injured myocardium or variable amounts of scar may have an unpredictable effect on the visual interpretation of myocardial perfusion. For these reasons, such patients were not included in the present study.

No previous study has compared visual and quantitative analysis of myocardial perfusion CMR images. While visual analysis of CMR perfusion is widely used in clinical practice and is quick and convenient, current methods to quantify myocardial perfusion more objectively, either semi- or fully quantitatively, although accurate can be slow and time consuming. The Fermi deconvolution method used has been validated with microsphere techniques and has been shown to be accurate and reproducible[10]. In the present study, despite the potential limitations of an optimised data under-sampling perfusion technique like *k-t* SENSE good quality data were obtained that were amenable to such analysis with an acceptable degree of inter- and intra-observer variability which were similar to previously published values[334]. In terms of diagnostic accuracy, both quantitative and visual analysis yielded high diagnostic accuracy (AUC=0.89 vs. AUC=0.92, respectively) to detect haemodynamically significant disease as determined by FFR. This probably reflects the high quality of the visual images acquired with high spatial resolution and high SNR. It is possible that temporal filtering effects may have rendered the quantitative analysis less accurate. Such effects can be limited with recently proposed improvements of the *k-t* method that were not available at the time this study was performed[335].

4.7 Study Limitations

Consistent with clinical practice, FFR was only measured in vessels with intermediate coronary stenosis. We have studied a population with a very high prevalence of CAD who were already listed for invasive studies so that our data need to be considered preliminary and the reported accuracy is likely to represent a best-case scenario. The applicability of our results to a population with a lower pre-test probability of significant CAD needs to be determined, where the accuracy may well be lower. Artefacts may be a problem with the *k-t* method due to respiratory or cardiac motion and in 4 cases quantitative analysis was not possible because if this. Such problems may be accentuated in patients with tachyarrhythmia or an inability to

breath hold for the scan. Because three perfusion territories were examined per patient there is the potential for data loss through clustering. Although the design effect of this was low due to a small ICC and cluster size, our results may have overestimated data correlations.

4.8 Conclusions

In patients with stable coronary disease, high resolution CMR perfusion at 3 Tesla detects haemodynamically significant coronary stenoses as determined by FFR with a high degree of accuracy, using both visual and quantitative analysis methods. Visual analysis may be an appropriate analysis strategy for the very high quality CMR perfusion images that can be obtained today.

4.9 Acknowledgments

We thank H. Tang and E. Chung for their contributions to the CMR perfusion quantitative analysis and the QCA analysis respectively. Dr. Siobhan Crichton from the Dept. of Medical Statistics, KCL, provided statistical support.

5 SYNERGISTIC ADAPTATIONS TO EXERCISE IN THE SYSTEMIC AND CORONARY CIRCULATIONS THAT UNDERLIE WARM-UP ANGINA

T.P.E Lockie[1], M.C Rolandi[2], A. Guilcher[3], D. Perera[1], S. Plein MD[4, 5], P. Chowienczyk[3], M. Siebes[2], S.R Redwood[1], M.S Marber[1]

[1]King's College London British Heart Foundation Centre of Excellence. The Rayne Institute, St Thomas' Hospital Campus, London, UK; [2]Dept Biomechanical Engineering, Academic Medical Centre, Amsterdam, the Netherlands; [3]Dept. Clinical Pharmacology, KCL, St Thomas' Campus, London UK; [4] Division Imaging Sciences, The Rayne Institute, St Thomas' Hospital, KCL, London, UK; [5]Division of Cardiovascular and Neuronal Remodeling, University of Leeds, UK and NIHR Comprehensive Biomedical Research Centre at Guy's and St Thomas' NHS Foundation Trust.

5.1 Abstract

Background

The mechanisms of reduced angina in patients with coronary arterial disease on second exertion, also known as warm-up angina, are poorly understood. Adaptations by the coronary and systemic circulations have been suggested but never demonstrated *in vivo.* In this study we measured central and coronary haemodynamics during serial exercise.

Methods and Results

16 patients (15 male, 61±4.3 yrs) with a positive exercise ECG and exertional angina completed the protocol. During cardiac catheterisation via radial access they performed 2 consecutive exertions (Ex1, Ex2) using a supine cycle ergometer. Throughout exertions, distal coronary pressure and flow velocity were recorded in the culprit vessel using a dual sensor wire whilst central aortic pressure was recorded using a second wire. Patients achieved a similar workload in Ex2 but with less ischaemia than in Ex1 ($p<0.01$). A 33% decline in aortic pressure augmentation in Ex2 ($p<0.0001$) coincided with a reduction in tension time index (TTI), a major determinant of LV afterload ($p<0.001$). Coronary stenosis resistance was unchanged. A sustained reduction in coronary microvascular resistance resulted in augmented coronary flow velocity on second exertion (both $p<0.001$). These changes were accompanied by a 21% increase in the energy of the early diastolic coronary backward-travelling expansion, or suction, wave on second exercise ($p<0.001$), indicating improved microvascular conductance and enhanced LV relaxation.

Conclusions

On repeat exercise in patients with effort angina, synergistic changes in the systemic and coronary circulations combine to improve vascular-ventricular coupling and enhance myocardial perfusion, thereby contributing to the warm-up effect.

5.2 Background

The variable relation between exercise and angina has been recognised for more than 200 years[2]. The terms “first effort”, “warm-up”, or “first-hole” angina, have been used to describe the ability of patients to exercise to angina, rest, and then continue exertion with reduced symptoms[100]. In the experimental setting, the salient observation is that at the accumulated external work causing maximum ST-segment depression and chest pain on first exercise, on second exercise there is less ST depression, chest pain and dysrhythmia[101]. During effort, coronary microvascular resistance adapts to match the increase in coronary blood flow to the higher oxygen consumption associated with the increase in heart rate[69, 336]. With the onset of effort angina, the adaptation of the microvasculature is exhausted and resistance is thought to be near minimal, beyond the culprit coronary stenosis[37, 60]. It is therefore surprising that symptoms and signs of myocardial ischaemia can improve on second effort. Thus, the phenomenon of warm-up angina was an enigma that attracted the attention of early pioneers of physiological investigation in the cardiac catheterisation laboratory[101-104, 115, 140, 337]. These early studies used relatively insensitive techniques such as coronary sinus thermodilution to estimate coronary blood flow and failed to reach a definitive conclusion. More recently, the warm up phenomenon was proposed to be a manifestation of ischaemic preconditioning[109], but this theory was refuted by subsequent studies[116, 338]. Most recently, it has been suggested that warm up results from reduction in the overall amplitude of the central aortic pressure waveform that has been documented following exercise in healthy volunteers[88, 339]. However such changes, while reducing afterload, would be expected to compromise myocardial perfusion in the presence of a flow-limiting coronary stenosis through a reduction in the coronary driving pressure.

Warm-up angina is not a mere intellectual curiosity since it is observed in patients taking standard anti-anginal medication[98, 102] and reduces ischaemic dysrhythmia as well as chest discomfort and ST segment depression[97]. Therefore, if its underlying mechanism could be better understood and mimicked, further therapeutic strategies could be developed.

The purpose of the present study was to clarify these controversies by invasive measurement of aortic pressure and distal coronary pressure and flow velocity during serial exertion in patients with coronary artery disease causing angina.

5.3 Methods

5.3.1 Study Patients

27 Patients were recruited from routine waiting lists for percutaneous coronary intervention (PCI) with symptoms of exertional angina pectoris and a positive exercise treadmill stress test (ETT). Exclusion criteria were unstable symptoms, previous myocardial infarction/CABG, impaired left ventricular (LV) function, severe co-morbidities, paced rhythm or bundle branch block on ECG or inability to undertake exercise. Patients with chronic total occlusions or significant visible collateral vessels (Rentrop Class 3+) were not included. Oral nitrate preparations, calcium channel blockers and beta-blockers were stopped at least 48 hours before the procedure.

5.3.2 Catheter laboratory protocol

A specially adapted supine cycle ergometer (Ergosana®, Germany) that allows a standardized incremental increase in workload was attached to the catheter lab table. Patients were catheterized via the right radial artery using a standard 6F arterial sheath. Weight adjusted heparin was administered (70u/kg) intra-arterial. Right and left coronary angiograms were then taken using standard diagnostic catheters. Intracoronary nitrates were not used. A standard 6F-guiding catheter was then introduced and positioned in the aortic root. A dual sensor pressure-velocity 0.014" intracoronary wire (Combowire®, Volcano Corp.®, USA)[240] was then connected to the ComboMap® console (Volcano® Corp. USA) and positioned at the tip of the guide. A single sensor 0.014" pressure wire (Brightwire®, Volcano Corp.®, USA) was connected to the ComboMap via an analogue transducer (SmartMap®, Volcano Corp. ®, USA) to provide a high fidelity pressure signal (P_a) that was normalized against aortic pressure measured through the guiding catheter. The pressure wire was then positioned alongside the Combowire at the tip of the guide

and the pressure (P_d) on the Combowire was normalized to the pressure wire signal. The guide was then inserted into the coronary ostium and the Combowire advanced distal to the stenosis in the target coronary artery and manipulated until a good Doppler velocity trace was obtained. At this point, the guide was disengaged and the pressure wire was passed into the aortic root and a stable pressure signal obtained. All signals were sampled at 200 Hz and stored on disk for off-line analysis. The data were imported into the custom-made Studymanager program (Academic Medical Center, University of Amsterdam, The Netherlands) and 20 consecutive beats showing good velocity signals were extracted from each minute of exercise and recovery. Averaged signals over each of these time periods were used in further analyses.

5.3.3 Exercise protocol

Once wires were in place with good quality and stable signals, baseline measurements were taken before the patient underwent 2 periods of exercise. The exercise protocol was a standardized incremental programme[340] based on the patient's weight and age, typically starting at 25W and increasing by 20W each minute. Exercise was continued until any of the following occurred, 1) ST depression >3mm, 2) maximal age-related heart rate, 3) severe chest pain, 4) physical exhaustion, 5) occurrence of detrimental effects such as hypotension, severe arrhythmia or dyspnoea. Coronary flow velocity and pressure, ECG, and central arterial pressure signals were recorded continuously throughout exercise and recovery. After 5 minutes of recovery, or after resting measurements approached baseline, the exercise protocol was repeated. At the end of the study protocol the patient underwent their planned percutaneous revascularization procedure. The full experimental protocol is illustrated in Figure 50 below.

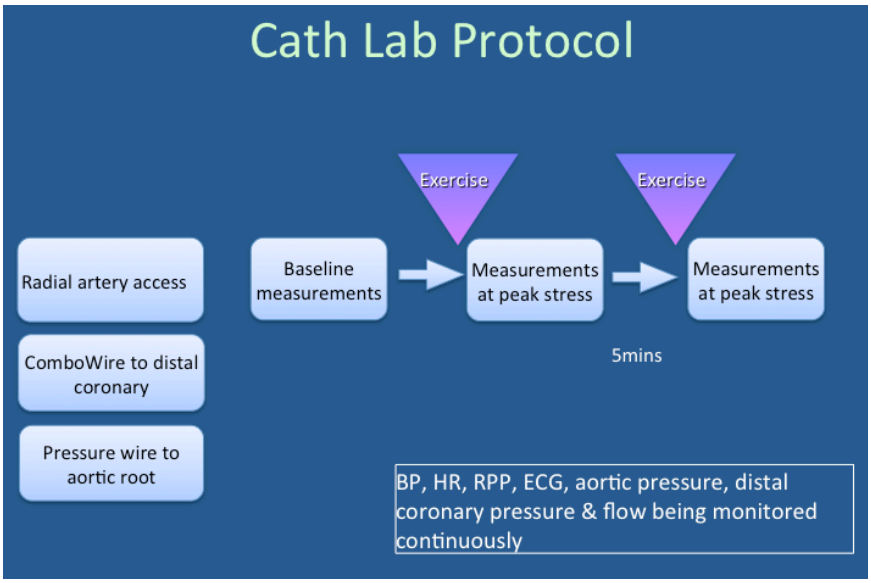

Figure 50. Summary of catheterisation lab exercise protocol.

5.3.4 Ethics

The study protocol was approved by the local research ethics committee (08/H0802/136) and all participants were provided a detailed information sheet prior to obtaining informed consent.

5.3.5 Data Analysis

All patients had continuous 12-lead ECG monitoring throughout exercise that was analyzed in a blinded fashion, off-line. The exercise test was considered positive at first appearance of 1mm (0.1 mV) ST-segment depression (STD) 80ms after the J point compared with the resting ECG just prior to exercise. The time of onset of ECG changes signifying exercise test positivity and the corresponding heart rate-central systolic blood pressure product (RPP) were noted.

Central arterial pressure waveforms were obtained from the pressure sensor-tipped guide wire positioned in the aortic root. A typical aortic pressure waveform is shown in Figure 51A. Pulse wave analysis was performed using custom-made programs (Matlab™ ,The MathWorksInc®, USA). Augmentation index (AI), a measure of central systolic blood pressure augmentation thought to arise from pressure-wave reflection, was calculated as the difference between the second (P_2) and first (P_1) peaks expressed as a percentage of the pulse pressure (PP). Timing of the reflected pressure wave (T_R) was determined as the time between the foot of the pressure

wave (T_F) and the inflection point (P_i). The area under the aortic systolic, or tension time index (TTI), and diastolic, or diastolic time index (DTI), portions of the pressure trace were determined using the dichrotic notch (see Figure 51A).

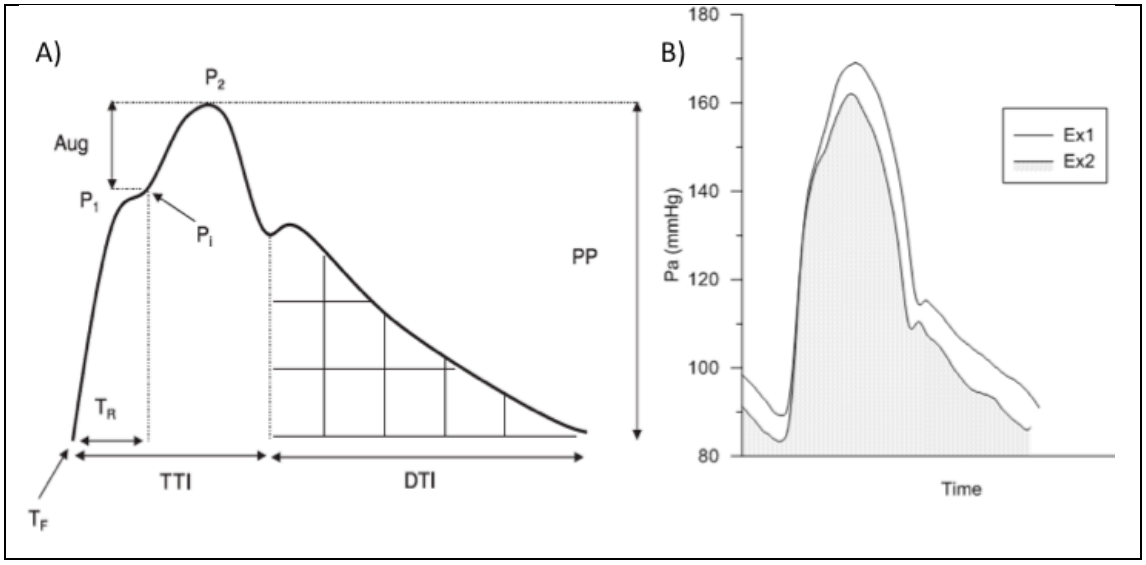

Figure 51. Panel A shows a typical pressure waveform at rest recorded from the ascending aorta in a healthy middle-aged man. Two systolic peaks are labelled P1 and P2. The area under the curve (AUC) during systole is the tension time index (TTI), and AUC during diastole is diastolic time index (DTI). TR is defined as the time between the foot of the wave (TF) and the inflection point (Pi). Panel B shows an example of an aortic pressure trace from one of the subjects taken at the peak equivalent time point showing the striking change in wave morphology between Ex1 and Ex2, with a reduction in the overall amplitude of the wave and specifically a marked reduction in pressure augmentation.

The TTI relates to myocardial oxygen demand[341] and DTI to coronary perfusion[94]. The rate pressure product (RPP) was determined from central systolic blood pressure multiplied by heart rate. Left ventricular ejection time (LVET) was measured from the upstroke of the arterial tracing until the trough of the dicrotic notch. Mean coronary blood flow velocity (U) was determined from the Doppler signal distal to the coronary stenosis. The pressure drop across the coronary stenosis (ΔP) was determined from the mean aortic and distal coronary pressures (P_a-P_d). From these data, an index of microvascular resistance (MR) was calculated as P_d/U[41] and an index of coronary stenosis resistance (SR) was calculated as $\Delta P/U$[240].

Wave intensity represents the rate of energy per unit area transported by travelling waves in arteries and is derived from phasic changes in local pressure and flow velocity[253]. In coronary vessels, backward travelling waves are generated by cardiac

contraction and relaxation at the downstream end, and forward travelling waves arise from changes in aortic pressure at the inlet[245, 254, 342]. Coronary wave intensity hence reflects the interactive effects of cardiac mechanics and coronary conductance on coronary haemodynamics[342]. Wave intensity analysis was performed using custom-made software (Delphi, Embarcadero, San Francisco). The distal pressure and velocity signals were smoothed with a Savitzky-Golay filter to reduce signal noise[343]. Net coronary wave intensity (dI) was calculated from the time-derivatives of ensemble-averaged coronary pressure and flow velocity as $dI = dP_d/dt \times dU/dt$[245, 253]. Since the aim was to examine coronary perfusion during exercise, and coronary blood flow is predominantly diastolic, we focused our investigation on the flow-accelerating wave at the onset of diastole, the so-called backward expansion wave (BEW); generated by relaxation of the myocardium that sucks blood back into microvascular space[245, 342]. The energy carried by the BEW (in $J.m^{-2}.sec^{-2} \times 10^3$) was obtained by the area under the wave and normalized for the sampling interval. The investigators who performed the data analyses were blinded to the sequence of the exercise tests and to the coronary anatomy.

5.3.6 Statistical Analysis

Continuous data are presented as means ± SEM. The study was powered to ensure there were a sufficient number of patients to observe a robust warm up effect on second, compared to first, exertion. This was required as a firm foundation from which to observe associated hemodynamic change. The calculation was based on paired *t*-tests within subjects, using an anticipated difference of 50 seconds between Ex1 compared to Ex2, with a standard deviation of 27, based on previous research[97]. This gave a sample size of 15 subjects with complete data to achieve 99% power with a probability of a Type 1 error of 0.001. We felt it necessary to achieve at least this level of power since it was likely multiple hemodynamic variables contributed to the warm up effect and their variance was possibly greater than that of the ST-segment. Paired Student's *t*-tests were used as indicated. Systemic and coronary parameters were compared between the first and second exertions sessions at each of 4 common time points: baseline ($t_{baseline}$), 1 minute (t_{1min}), 50% of time to peak RPP ($t_{50\%}$) and time of peak RPP (t_{peak}) during first exertion. Repeated measures analysis

of variance (ANOVA) with 2 within-subject factors (exercise and time) were used to compare the common time points between exercise exertions and evaluate the main time trends across exercise periods (IBM® SPSS® Statistics, Version 19). If the overall test for the main effect of exercise exertion reached significance in the ANOVA, we evaluated each separate time point with paired *t*-tests. We did not apply any correction for multiple comparisons, in order to reduce the chance of missing significant associations in this exploratory study (Type II error)[344]. The sphericity assumption, which equates to a compound symmetry correlation structure, was used with the repeated measures ANOVA (IBM® SPSS® Statistics, Version 19). Mauchly's test of sphericity was used to confirm the sphericity assumption. Relationships between variables were investigated with the Pearson correlation coefficient. P-values were two-sided and values of $p<0.05$ were considered significant.

5.4 Results

Out of 27 patients who were consented into the study 16 (15 male, aged 61±8.9 years old) successfully completed the full protocol. Reasons for exclusion were: 4 were found to have left main stem or severe 3-vessel disease on initial angiography; 2 were found to have chronic total occlusions; in 2 patients radial arterial access was unsuccessful; 1 patient developed RBBB during exercise (precluding ECG analysis); 1 patient was unable to cycle; 1 patient developed myocardial ischaemia very early during first exertion and the ECG was slow to return to baseline. Full background demographics and procedural details are shown in Table 11.

Patients exercised for 382±27 seconds during exertion 1 (Ex1) and for 405±28 seconds during exertion 2 (Ex2), p=0.08. The details of exercise performance are summarized in Table 13 below. The maximum external workload attained was similar for both efforts. 15 out of the 16 patients (93%) reached 1mm ST-segment depression (STD) during both periods of exercise. Time to 1mm STD was 53±14 seconds longer in Ex2 than Ex1 (p=0.003) confirming warm-up. In addition, the rate

pressure product (RPP) at 1mm STD was 12% higher for Ex2 than Ex1 (p=0.025) also consistent with a warm-up effect.

Outcomes of haemodynamic variables are summarized in Table 13 below. Despite waiting 8±1.3 minutes for return to baseline after Ex1, heart rate (HR) was higher at the start of Ex2 (p<0.0001), while initial central systolic blood pressure (SBP) was not different. The RPP was correspondingly elevated at the onset of Ex2 compared to Ex1 (p<0.01), although it was not different at t_{peak}. With increasing HR there was a corresponding rise in SBP during both exercise periods, with a fall in left ventricular ejection time (LVET) and augmentation index (AI). At t_{peak} SBP was lower in Ex2 than in Ex1 (p<0.001), while LVET was reduced throughout Ex2 even after accounting for the increase in HR (p=0.0009).

DEMOGRAPHICS (N=16)	
Male (%)	15 (94)
Age	61 ± 8.9 years
Previous PCI (%)	4 (25)
Previous MI (%)	0 (0)
LVEF	65±10%
Diabetes Mellitus(%)	5 (31)
Hypertension (%)	8 (50)
Dyslipidaemia (%)	10 (62)
Family Hx IHD (%)	8 (50)
Smokers (%)	4 (25)
Betablockers (%)	11 (68)
Nitrates (%)	8 (50)

Statin (%)	14 (88)
ACEi (%)	10 (62)
Aspirin (%)	16 (100)
Clopidogrel (%)	15 (93)

Table 11. Baseline characteristics, demographics and procedural details. PCI = percutaneous coronary intervention; MI = myocardial infarction; LVEF = left ventricular ejection fraction; IHD = ischaemic heart disease.

We also observed a 33% reduction in augmentation index (AI) throughout Ex2 compared to Ex1 ($p<0.0001$) and augmentation pressure was correspondingly reduced ($p<0.0001$), also see Figure 51B. Moreover, the degree of warm-up in Ex2 was associated with the change in AI, such that a larger reduction in AI during Ex2 corresponded with a greater increment in RPP at 1mm STD (Pearson r=0.63 95%CI 0.15-0.87, p=0.016). T_R, representing the time for the reflected wave to return to the heart, fell with exercise and remained shorter throughout Ex2 compared to Ex1 ($p<0.0001$). Despite the increase in systolic blood pressure during each exertion, tension time index (TTI), a surrogate of myocardial oxygen demand, did not change due to the decrement in pressure augmentation and the changes in LVET. However, TTI was consistently lower during Ex2 ($p<0.0001$). In contrast, diastolic time index (DTI) fell during both periods with increasing exercise intensity. At the onset of Ex2, the DTI was markedly lower than at the start of Ex1 ($p<0.0001$), although this can probably be accounted for by the differences in HR. Full physiological parameters recorded during the consecutive exercise periods are detailed in Table 14 below.

We observed a progressive fall in microvascular resistance (MR) during Ex1 ($p<0.05$) with a concomitant 27% increase in coronary flow velocity ($p=0.008$). See Figure 54. Despite the resulting trend towards a higher pressure drop across the stenosis (ΔP) during exertions, P_d actually increased, which can be explained by the overall increase in mean aortic pressure ($p<0.001$). In Ex2 the main finding was that MR was consistently lower ($p<0.001$) resulting in a 16% increase in average coronary flow velocity ($p<0.05$) compared to Ex1. The increased flow velocity in Ex2 resulted in a

corresponding increase in ΔP (p=0.0001) and fall in P_d (p<0.005) compared to Ex1. Stenosis resistance (SR) was not different between the two exercise periods suggesting no change in functional stenosis severity.

PROCEDURAL DETAILS	
No. of diseased vessels per pt	1.6 ± 0.7
% stenosis of target lesion	74.6 ± 18.6
Target lesions undergoing PCI (%)	12 (70)
Target Vessel (LAD/Cx/RCA)	9/1/6
Duration of procedure (mins)	67 ± 12

Table 12. Procedural details of the study patients in the catheterisation lab; LAD =left anterior descending artery; Cx = circumflex artery; RCA = right coronary artery. Data are presented as mean ±SD.

Eleven out of the 16 datasets were suitable for WIA due to irregular velocity waveforms caused by motion artifacts during exercise, but there were no differences in characteristics compared to the overall patient group. The energy of all four dominant waves increased during each exercise from baseline to peak. See Table 15 below. There was an overall increase in the *flow accelerating waves*, the backward expansion wave (BEW) and forward compression wave (FCW), during exercise 2 (p=0.001), driven by a 21% increase in the energy of the microcirculatory-originating backward travelling BEW, or suction wave during Ex2 (p<0.001). There was also a small increase in the *flow decelerating waves*, the FEW (forward expansion wave) and BCW (backward compression wave) during exercise 2. This was largely driven by the increase in the BCW, a manifestation of increased left ventricular contractility (p<0.05). There was no difference found between Ex1 and Ex2 for the FEW. Some of these changes are illustrated in Figure 55 below, especially the notable increase in the size of the BEW on second exercise. As might be predicted the changes in the energy of the BEW were significantly related to the concomitant fall in MR between Ex1 and Ex2 (Pearson r =0.46 95% CI 0.14-0.69, p=0.0068).

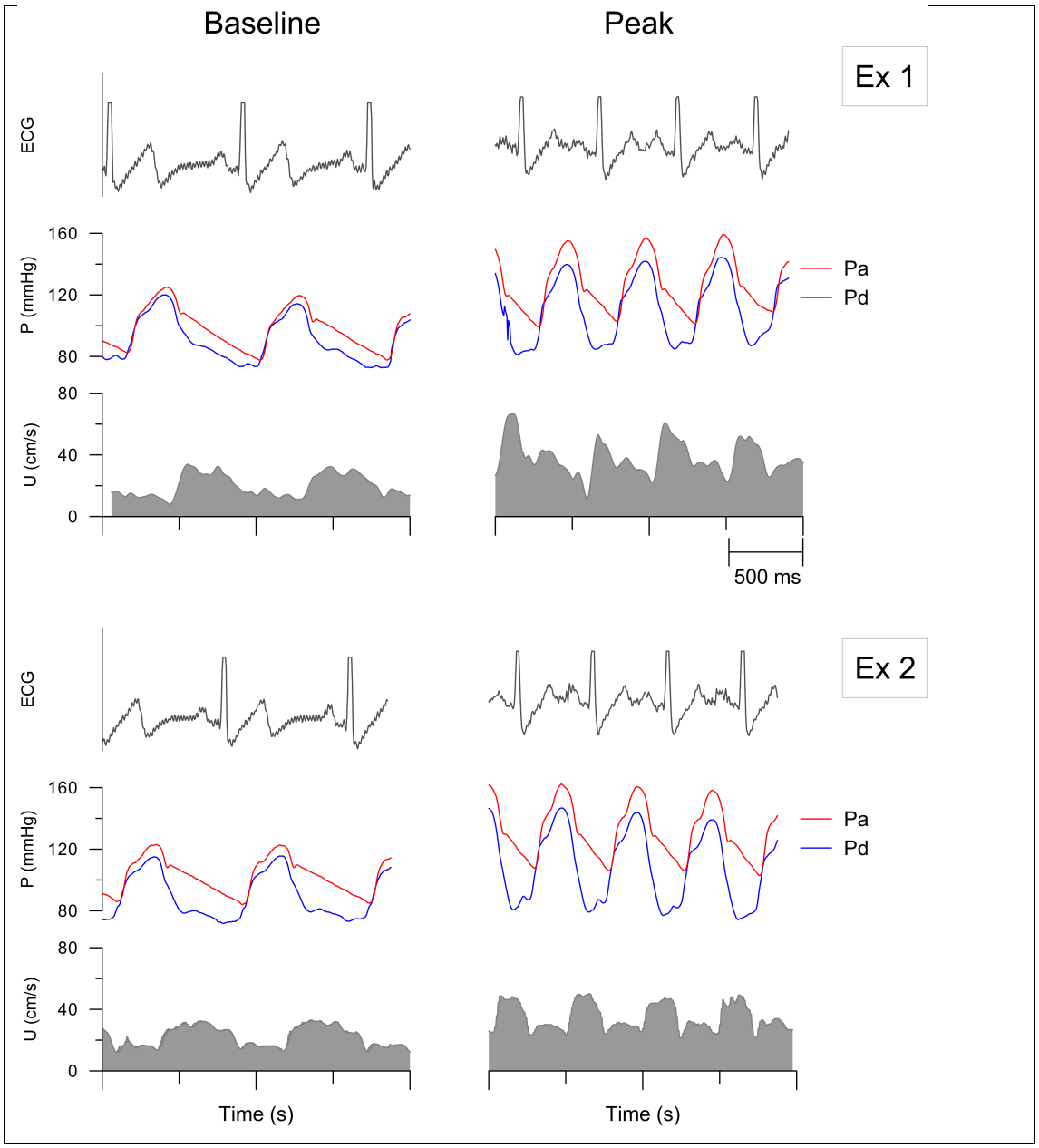

Figure 52. Illustrating an example of flow velocity and pressure signals collected at baseline and at peak equivalent workload during Exercise.1 and Exercise 2 from a sample patient with a significant coronary stenosis. P_a= proximal, or aortic pressure; P_d= distal coronary pressure; U= coronary flow velocity in the distal coronary vessel. The mean flow signals are higher in Ex2 and correspond with a greater ΔP (P_a-P_d) and lower microvascular resistance.

	Ex1	Ex2	p
Duration of Exercise (sec)	382 ± 27	405 ± 28	0.08
Max Workload (watt)	115.6 ±6.8	120.3 ± 7.1	0.13
Pts reaching 1mm STD (%)	15(88)*	15(88)*	
Time to 1mm STD (sec)	260 ± 31	313 ±35	0.003
cRPP at 1mm STD ($mmHg.min^{-1}$) $x10^3$	160.7±13.74	178.4±16.3	0.025

*1 patient not included as went into RBBB during exercise and ECG not readable
§means compared using paired Student's t-test

Table 13. Performance and ST segment change on first (Ex1) and second (Ex2) exercise. STD= ST-segment depression on electrocardiograph; cRPP= central rate pressure product

5.5 Discussion

In our study population of patients with severe coronary disease warm-up was confirmed on second effort (Ex2). Careful analysis of systemic and coronary haemodynamics during first and second exercise reveals a number of highly significant and interdependent alterations that likely contribute to this effect. Most striking amongst these are 1) a reduction in central aortic pressure augmentation, hence reducing left ventricular work; 2) a reduction in coronary microvascular resistance leading to a higher coronary blood flow velocity; and 3) an increased flow-accelerating backward expansion wave at the onset of diastole, reflecting the important interaction of cardiac-coronary coupling and microvascular conduction with respect to enhancing myocardial perfusion. These combined adaptations synergistically served to alleviate the imbalance between myocardial demand and supply and resulted in the improved performance seen on second exercise.

N=16		$t_{baseline}$	t_{1min}	$t_{50\%}$	t_{peak}	$p^{\S}$
HR	*Ex1*	72.9±2.6	86±3.8	97.4±4.3	117.6±4.3	<0.0001
	Ex2	84.2±3.7‡	92.9±3.5†	100.8±3.8	117.3±4	
cSBP	*Ex1*	135.8±5.5	146.8±6.7	157.5±5.4	173.8±6.1	0.0056
	Ex2	137.1±6.3	142.2±6.9	153±6.7	167.7±6.6*	
cRPP	*Ex1*	100±6.4	128.5±9.3	156±10.5	210.3±12.2	NS
	Ex2	117.4±9.7†	134.8±10.7	156.3±13.2	200.3±13.3	
LVET	*Ex1*	0.33±0.008	0.32±0.007	0.3±0.007	0.28±0.005	<0.0001
	Ex2	0.31±0.008‡	0.3±0.007‡	0.29±0.007*	0.27±0.005	
T_R	*Ex1*	0.23±0.006	0.21±0.007	0.2±0.006	0.17±0.003	<0.0001
	Ex2	0.19±0.01‡	0.19±0.006	0.18±0.006	0.17±0.007	
AI	*Ex1*	26.2±3.5	24.8±3.4	22.4±3.2	22.6±2.7	<0.0001
	Ex2	18.5±4.3‡	19±3.7†	16.4±3.5†	16.3±2.8†	
TTI	*Ex1*	40.2±1.5	41.9±1.7	42.6±1.3	42.7±1.1	<0.0001
	Ex2	38.4±1.7	38.5±1.6†	40.3±1.6	39.9±1.4*	
DTI	*Ex1*	45.4±2.6	35.7±1.8	30.4±1.6	25.1±1.5	<0.0001
	Ex2	36.8±2.2‡	30.9±1.3*	28.9±1.5	24.4±1.3	
U	*Ex1*	16.1±1.9	16.5±2.1	21.5±2.8	22.1±2.9	0.0001
	Ex2	19.6±1.9*	20.7±1.9†	22.8±2.7	24.1±3.2	
P_d	*Ex1*	81.4±8.9	85.3±10.2	90.8±9.8	89.6±10.5	0.0003
	Ex2	76.4±9.3	77.1±9.4*	85.4±10.9	84.4±10.8	
ΔP	*Ex1*	24.7±7	28.4±8.7	32.9±7.1	37.8±8.1	0.0001
	Ex2	31.4±7.8†	32.3±9.4	35.8±7.9	39.9±8.7	
MR	*Ex1*	5.4±0.5	5.9±0.8	4.7±0.4	4.5±0.4	<0.0001
	Ex2	4±0.4*	3.7±0.3‡	3.9±0.3	3.8±0.4	
SR	*Ex1*	2±0.9	2.2±0.9	2.1±0.7	2.7±0.9	
	Ex2	1.8±0.5	2±0.7	2.3±0.7	2.8±0.9	

[§]2-way ANOVA with time and Exercise effort the main factors; reported p-value relates to the significance of effort on the variation

Table 14. Physiological parameters measured during the two exercise periods. HR = heart rate (bpm); cSBP = central systolic blood pressure (mm.Hg); cRPP = central rate pressure product (mmHg.min^{-1}x10^3); LVET = left ventricular ejection time (sec); T_R = time for the reflected aortic wave to return (sec) AI = augmentation index (%); TTI = tension time index (mmHg.min^{-1} x10^3); DTI = diastolic time index (mmHg.min^{-1} x10^3); U = coronary flow velocity (cm.sec^{-1}); P_d = mean distal coronary pressure (mmHg); P_a = mean aortic pressure (mm.Hg); MR = microvascular resistance index (mmHg.cm^{-1}.sec); Bonferroni post-hoc test, *p<0.05, †P<0.001, ‡p<0.0001 against corresponding time point during first effort.

N=11		$t_{baseline}$	t_{1min}	$t_{50\%}$	t_{peak}	$p^{§}$
FEW	*Ex1*	3.5±0.5	3.7±0.7	6±1.3	6.4±1.2	0.2
	Ex2	3.8±0.8	04.5±0.9	5.7±1.2	7.6±2	
BEW	*Ex1*	2.7±0.7	1.8±0.6	3.4±0.6†	4.5±1	<0.0001
	Ex2	4±1.06	3.7±0.9	5.8±0.8	6.1±0.9	
FCW	*Ex1*	4.6±1.1	3.8±0.8	5.4±1.2	5.9±1	0.1
	Ex2	4.6±0.8	4.8±0.7	5.5±0.9	7.9±1.8	
BCW	*Ex1*	5.5±1.3	5.7±1.5	8.1±1.9	8.4±1.6	0.02
	Ex2	6.8±1.9	8.4±1.8	9.6±1.8	10.6±2.1	
Flow acc.	*Ex1*	12±2.3	10.9±2*	16.4±3	18.1±2.6	0.001
Waves	*Ex2*	13.4±2.3	14.6±1.9	17.9±2.6	19.6±2.8	
Flow dec.	*Ex1*	10.3±1.9	10.7±1.8	17.1±3.7	15.5±2.5	0.04
waves	*Ex2*	11.7±2.2	14.1±2.3	16.3±2.6	18.3±3.6	

§2-way ANOVA with time and Exercise effort the main factors; reported p-value relates to the significance of effort on the variation

Table 15. Full data from the wave intensity analysis (WIA) displaying the net wave energy in J.m^{-2}.sec^{-2} x10^3. All waves increased with exercise and there was an overall increase in the *flow accelerating waves*, the BEW (backward expansion wave) and FCW (forward compression wave), during exercise 2, driven by a significant increase in the energy of the microcirculatory-derived BEW in particular. There was also a small increase in the *flow decelerating waves*, the FEW (forward expansion wave) and BCW (backward compression wave) during exercise 2. This was largely driven by the increase in the BCW, a manifestation of increased left ventricular contractility.

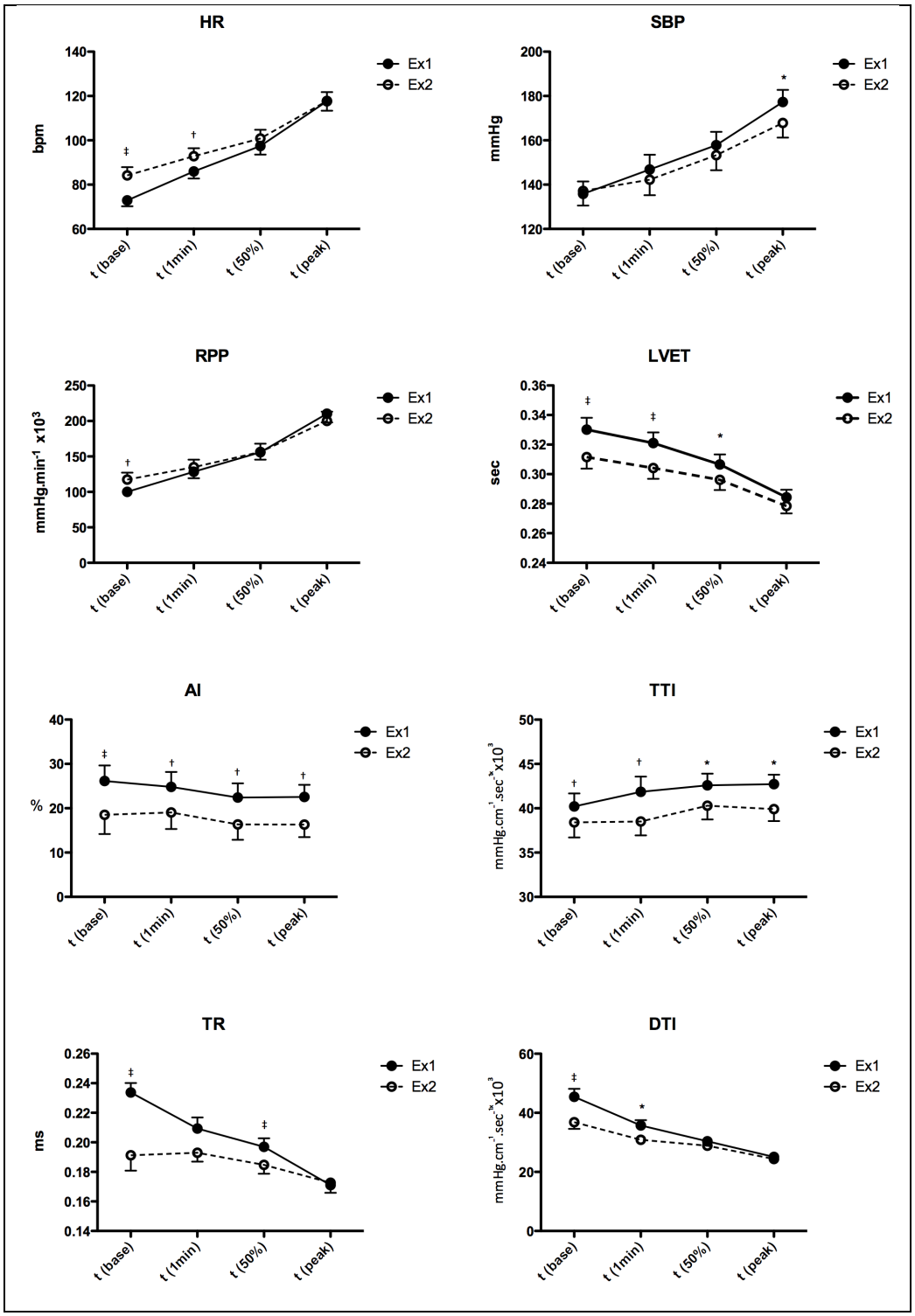

Figure 53. Systemic parameters derived from aortic pressure at different time points for Ex1 and Ex2. Heart rate (HR) and central systolic blood pressure (SBP) increase during each exercise period. At the time of peak exertion during Ex1, SBP is lower in Ex2. Overall there is no change in rate pressure product (RPP) between Ex1 and Ex2. A reduction in augmentation index (AI) and left ventricular ejection time (LVET) during Ex2 results in a reduction in tension time index (TTI), which is lower throughout Ex2. For the same reason there is also a fall in diastolic time index (DTI) at the beginning of Ex2; T_R is the time for the reflected aortic wave to return and is consistently faster in Ex2 suggesting increased wave speed. *p<0.05, †P<0.001, ‡p<0.0001.

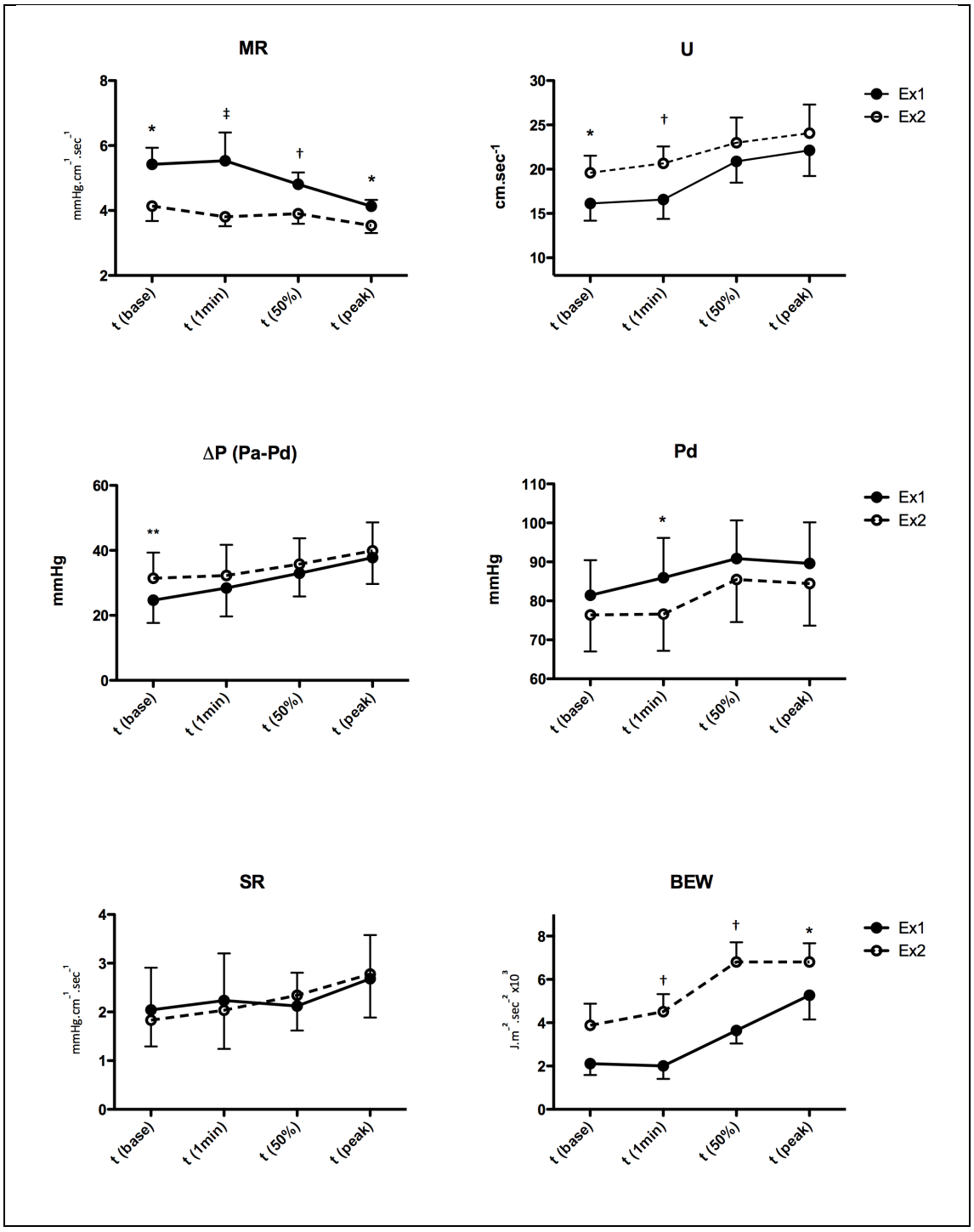

Figure 54. Coronary parameters at different time points for Ex1 and Ex2. In response to the increased myocardial oxygen demand during exercise, coronary flow velocity (U) increases due to a fall in microvascular resistance (MR). Despite the resulting larger pressure gradient (ΔP) across the stenosis, distal perfusion pressure (P_d) a slight increase; most likely due to the increasing mean aortic pressure. At the end of Ex1, MR continues to fall, persisting through recovery and remaining low throughout Ex2, with a consequential increase in coronary flow velocity and ΔP in Ex2. As a result, P_d is slightly lower in Ex2. With wave intensity analysis (WIA) the energy of the net backward expansion wave (BEW) is greater on Ex2, suggesting increased microvascular dilatation and enhanced LV relaxation. *p<0.05, †P<0.001, ‡p<0.0001.

Coronary Blood Flow and Oxygen Consumption

Conceptually and physiologically it is unlikely that increased antegrade blood flow alone is responsible for the beneficial adaptations seen with warm-up[103, 104, 345]. Warm-up is also unexplained by the recruitment of collateral vessels[97]. Instead, it has been suggested that warm-up is due to attenuation of increased regional myocardial oxygen consumption (MVO_2), possibly mediated by adenosine A_1 receptor activation, a signaling system known to improve tolerance to ischaemia[346]. Bogaty et al., however, were neither able to demonstrate a role for the adaptive down regulation of regional myocardial contractile function during exercise, nor for adenosine-initiated adaptation in patients with warm-up angina[115, 116]. Our findings suggest reduced myocardial work during Ex2, with a reduced RPP and TTI at the time point of 1mm STD during Ex1; both TTI and RPP are known determinants of myocardial oxygen consumption.

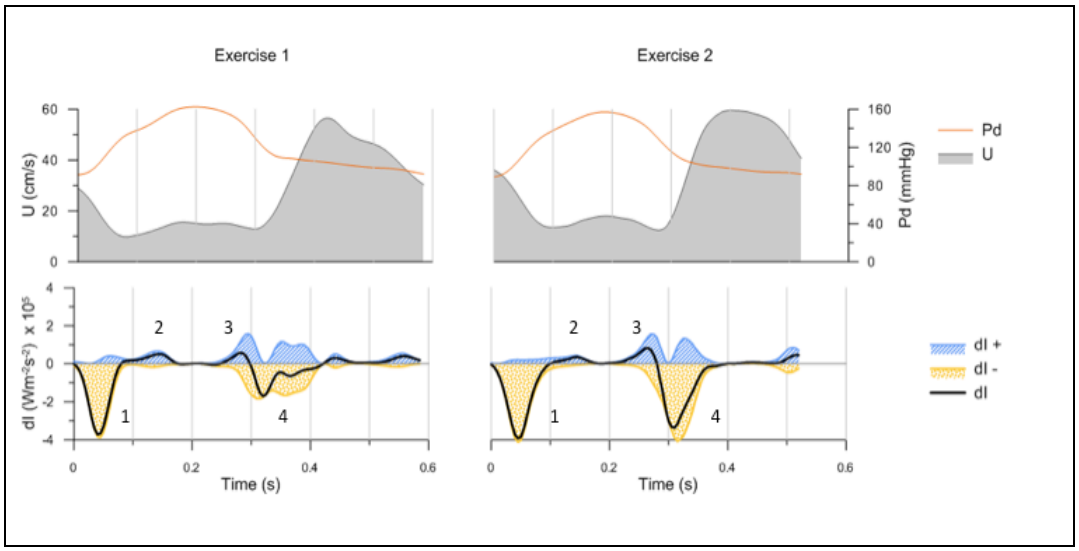

Figure 55. Coronary net wave intensity (dI) and the corresponding forward and backward contributions taken at peak equivalent exercise from one of the study subjects. The coronary pressure (Pd) and flow velocity (U) waveforms used to calculate dI are shown on top. BCW and BEW (1 and 4) come from the microcirculation; FCW and FEW (2 and 3) come from the coronary ostium. The marked increase in energy of the BEW (4) during Ex2 compared to Ex1 can be seen.

Arterial Vasodilation and Changes in LV Afterload

The exercised-induced change to the aortic pressure waveform seen in the present study, i.e. reduced pressure augmentation, is consistent with previous studies[347, 348,

[349]. It results from reduced peripheral wave reflection due to vasodilation of the systemic muscular arteries[88, 95]. At the equivalent time point at peak exercise in Ex2, the augmentation index was 33% lower than in Ex1. These changes are also consistent with more recent studies in healthy volunteers, where exercise provoked a prolonged reduction in pressure augmentation that persisted for up to 60 minutes into recovery despite stroke volume and carotid-femoral pulse wave velocity returning to baseline[14]. This is a similar time-scale to the persistence of the warm-up effect seen after first exertion in other studies[97, 101, 140]. In the study by Munir et al.[88], the reduction in pressure augmentation in the aorta was almost identical to that seen following the administration of nitro-vasodilators, suggesting that the reduced tone of muscular arteries together with a reduction in pressure wave reflection from the lower body is an independent mechanism underlying exercise-induced changes in pulse wave morphology. In the present study, improved ventricular-vascular coupling, induced by the favorable and persistent haemodynamic changes following the first episode of exercise, may have contributed to the beneficial adaptation observed during second exercise by reducing afterload and shortening systole. A reduction in ejection duration is associated with enhanced diastolic relaxation[350]. Exercise-induced peripheral vasodilation has been previously suggested as a potential important mechanism in warm-up[339], but this is the first time it has been demonstrated clinically.

Persistent Decrease in Coronary Microvascular Resistance Index with Exercise

In the presence of a coronary stenosis the subendocardial myocardium is especially sensitive to impedance of blood flow during systole, and maintenance of uniform transmural myocardial flow distribution is very dependent on changes to microvascular resistance during diastole, especially at increased hearts rates, requiring active coronary vasodilatation[60, 336]. It is well established that the subendocardial tissue layer is sensitive to the systolic flow impediment of cardiac contraction, especially in the presence of reduced coronary pressure due to a proximal stenosis[342] and that the resultant hypoperfusion spreads from endocardium to epicardium[37, 336]. Subendocardial flow therefore depends critically on diastolic duration[60, 69]. At increased hearts rates, as the interval of diastole is

reduced, active coronary vasodilatation is required to maintain transmural diastolic perfusion[69, 336]. Exercise produces an intense vasodilatory stimulus on the coronary resistance vessels, which substantially alters the relative distribution of blood flow over the coronary vascular bed [351, 352]. We observed an increase in coronary flow velocity during Ex1 where MR continued to fall, after an initial slight increase at the start, suggesting progressive vasodilation of the coronary vascular bed with increasing workload. It has been shown that persistent vasomotor tone is present throughout the coronary microcirculation even during ischaemia, with substantial vasodilator reserve remaining within the exercising vascular bed of a hypo-perfused region[35, 353]. This is confirmed in the present study, since MR continues to fall after the end of Ex1, through recovery and into the start of Ex2, where the final resistance attained is lower than that which occurred during the myocardial ischaemia induced by peak exercise during Ex1 ($p=0.0002$).

The reduction in coronary microvascular resistance we observed during Ex2 indicates a sustained vasodilatory action. Previous studies have suggested that vasodilation may play an important role in warm-up. Joy[102] and Ylitalo[354] used nifedipine and nisoldipine, respectively, in patients with warm-up angina. In both cases, the addition of these vasodilating agents attenuated the magnitude of warm-up, implying a shared common mechanism. Interestingly, the beta-blocker timolol, which is thought to exert its antianginal effect through reduced myocardial oxygen demand and may cause an increase in α-adrenoceptor mediated coronary vasoconstriction[355], did not attenuate the warm-up response. Bogaty et al. examined the transmural redistribution of coronary blood flow within the myocardium as a mechanism of warm-up using SPECT imaging but was unable to demonstrate any differences, perhaps due to the limited spatial resolution of SPECT[116]. Further studies using high-resolution cardiac magnetic resonance imaging to examine changes in subendocardial perfusion may provide insight.

Coronary-Cardiac Interaction

In the presence of a severe proximal stenosis (and thereby small residual vasodilator capacity) other factors may also influence transmural distribution of perfusion in

response to increased stress. In the setting of myocardial ischaemia it is known that changes in myocardial function, including increased compliance and enhanced LV diastolic relaxation contribute to transmural flow redistribution to the subendocardium[356]. Coronary wave intensity analysis reflects the effects of both cardiac contraction and coronary conductance on coronary blood flow dynamics. In the coronary artery, the effects of LV relaxation generate a dominant backward (via the vasculature) expansion wave. This BEW is a flow-accelerating (suction) wave and plays a prominent role in diastolic coronary blood flow [245, 254]. A higher magnitude of this wave has been observed after a decrease in microvascular resistance through pharmacological vasodilation[342] and also with enhanced LV relaxation due to a decrease in microvascular compression[254]. Similarly, Davies et al found a 30% reduction in the magnitude of the BEW in patients with LV hypertrophy, a group with known impaired microvascular function and LV relaxation when compared to a group of matched controls[245]. In the present study, although the exercise levels were similar, the magnitude of the BEW was 21% greater on second exertion. This important increase in the BEW, together with the beneficial energetics afforded by a reduction in ejection time and LV afterload suggest that enhanced vascular-ventricular coupling, as well as persistent coronary vasodilation and improved cardiac-coronary interaction, play an important role in the improved performance seen on second exertion.

Other Potential Mechanisms

Although the adaptations seen during Ex2 may be a result of the exercise itself, one must also consider the potential role of 1) ischaemic preconditioning (IPC) whereby the ischaemia itself resulted in intrinsic myocardial adaptation; and 2) the contribution of recruitable coronary collaterals. IPC is the term used to describe the increased myocardial resistance to ischaemia that follows a brief episode of ischaemia[109, 110]. It has been suggested that the clinical observation of the warm-up phenomenon may represent one aspect of IPC in humans[105]. IPC, like warm-up angina is also unexplained by a down-regulation of contractile function or an increase in collateral myocardial perfusion induced by initial exercise[114, 115]. The finding, however, that warm-up angina does not seem to be mediated by adenosine

or by cardiac adenosine triphosphate-sensitive potassium channels[116, 117] suggests that it is mechanistically distinct from classic ischaemic preconditioning.

Recruitable coronary collaterals have long been proposed as a mechanism for warm-up and other ischaemic adaptation[100]. While in the present study we excluded those with chronic total occlusions or with significant angiographic collateral vessels, there is[2] the possibility (indeed likelihood) that those included did have some collateral vessels present. Previously, our group has examined this phenomenon specifically and found that there was no relationship between the presence and extent of coronary collaterals and the presence of warm-up, based on a model of coronary vessel occlusion using an angioplasty balloon and measuring collateral flow index[97]. Other studies have also shown ischaemic adaptation to be independent of the presence of recruitable coronary collateral vessels[357, 358]. Although the magnitude of inducible myocardial ischaemia is lower when significant collaterals are present, there is no effect of repetitive ischaemic stress[357]. However, a recent study by Togni et al demonstrated an instantaneous increase in collateral flow index (CFI) in response to dynamic isometric exercise in patients with coronary artery disease[264]. They measured CFI at rest and during the last minute of peak exercise, randomly assigning the patients to either rest or exercise measurements first, to overcome the potential confounder of the initial rest ischaemic stimulation (one minute of balloon inflation) influencing the subsequent exercise measurements. In both cases there was a significant increase in CFI in response to exercise irrespective of which was measured first. Interestingly, when exercise was performed first both the peak exercise CFI and the subsequent resting CFI values were higher, although not statistically significantly, from when the rest measurements were taken first. Although one must be cautious in how one extrapolates such data to the findings from the present study, if collateral vessel recruitment were to play a significant role in warm-up then perhaps one might have expected a higher peak exercise CFI measurement in the group where there had been a preceding ischaemic stimulus; in fact the opposite was true.

In the current study we did not measure CFI. Again, we wanted to preserve the conditions of exercise-induced angina as far as possible in our model and the necessary prolonged balloon inflations for CFI measurement would have substantially altered this. In addition, there is evidence from the literature that even in the presence of exercise-induced coronary ischaemia microvascular resistance is not minimal[35, 353], and this was evidenced in the present study where microvascular resistance continued to fall throughout Ex1 and into recovery. For pressure based CFI measurements, minimal microvascular resistance, as well as central venous pressure measurements are very important as variations in these can have a significant impact on measurements. This is the reason such measurements are usually made following the administration of both intracoronary nitrates and systemic adenosine to minimise such resistances. Again, for these reasons we did not measure CFI in this way. Undoubtedly, however, further work in the response of collateral blood flow to serial exercise exertions would be very interesting, perhaps utilising contrast echocardiography, although again this presents significant technical challenges in itself[264, 359].

Further Work and Potential Therapies?

Endothelin (ET) exerts a constrictor influence on the coronary and systemic circulation through the ET -receptor A, which decreases during exercise thereby contributing to metabolic vasodilation[360]. Mechanisms for this may include exercise-induced increases in adenosine levels, which decrease the sensitivity of the vasculature to ET[361], and, nitric oxide (NO) production that increases during exercise, and can directly modulate the binding of ET to the ETA receptor[362, 363]. These effects were shown to persist after cessation of exercise thereby potentially providing the favorable conditions similar to those seen in the current study, where lasting coronary and systemic vasodilatation through recovery and into the second exertion resulted in reduced ischaemia. In a study in patients with essential hypertension, treatment with the endothelin receptor antagonist BQ-123 was found to increase exercise capacity, with an enhanced peripheral vasodilatory response, especially at higher workloads[364]. Another group found that intensive exercise training resulted in an improvement in endothelium-dependent coronary vasodilatation[352];

nitroglycerin-induced (endothelium-independent) coronary vasodilatation conferred no benefit. Further work is warranted to examine ways to modulate the acute responses to intense exercise seen in the present study, with the goal of "bottling" the beneficial haemodynamic responses that we observed for subsequent exertions. Early studies suggest that metabolic dilation in the systemic and coronary circulation during exercise involves not only increased vasodilator influences but also inhibition of vasoconstrictor influences. Inhibition of endothelin may provide a potential novel target in the treatment of exertional angina.

5.6 Limitations

This was a small, single center study but is the first to examine simultaneously the important changes in aortic pressure waveform, patterns of coronary blood flow, and coronary microvascular resistance during large-muscle exercise in the investigation of warm-up angina. In previous non-invasive studies examining warm-up, an interval of 10-15 minutes was used between the repetitive bouts of exercise. Due to practical considerations this was not possible in the current study and the time between exertions was shorter. Consequently, the lingering effects of Ex1 prevented a return to true baseline conditions at the start of Ex2. We did not measure LV or pulmonary arterial pressures in our study and therefore cannot exclude further differences that may have contributed. We do not expect differences in extra-cellular circulating volumes between Ex1 and Ex2, but previous studies have shown LVEDP to be lower on second exercise, although this did not seem to be related to warm-up[349] . No pharmacological vasodilation was given to keep the environment as close to real-life conditions as possible; minimal resistance was therefore not known. In addition, intracoronary nitrates were not administered at the beginning of the study to avoid the possibility of these exerting a confounding preconditioning effect. There is the possibility that wire induced coronary spasm may have had an effect of the coronary flow and pressure measurements.

5 patients were not suitable for WI analysis, which utilizes the first derivative of pressure and velocity waveforms and is therefore particularly affected by the quality

of the acquired signals. The average systemic and coronary haemodynamic parameters were comparable between the selected group and the entire study group, and hence our findings from this group likely apply to the whole study population.

5.7 Conclusions

In patients with coronary artery disease and demonstrable warm-up, exercise induces vasodilatory changes in the systemic and coronary circulations that reduce central aortic pressure and myocardial microvascular resistance. These combine to improve vascular-ventricular coupling and enhance myocardial perfusion, thereby contributing to the warm-up effect seen on repeat exercise.

5.8 Acknowledgments

The study was conceived, designed and carried out by TL, MM, and SR. MCR, AG and MS assisted with data collection and analysis, as did KP. DP, KA, RW and KDS contributed to data collection and patient recruitment. PC and SP provided additional support. Professor J.G.P Tijssen and N. van Geloven (Academic Medical Centre, Amsterdam, The Netherlands) provided statistical support.

6 DETECTION OF TRANSMURAL FLOW HETEROGENEITY USING HIGH RESOLUTION MRI PERFUSION IMAGING

Tim Lockie[1], Kal Asrass[1], Rupert Williams[1], Hanson Tang[1], Masaki Ischida[2], Antoine Guilcher[3], Sebastian Kozerke[2], Eike Nagel[2], Simon Redwood[1], Mike Marber[1], Sven Plein[2, 4]

[1]Cardiovascular Research Division, The Rayne Institute, St Thomas' Hospital, KCL, London UK

[2]Division Imaging Sciences, The Rayne Institute, St Thomas' Hospital, KCL, London, UK

[3]Dept Clinical Pharmacology, St Thomas' Hospital, KCL, London, UK

[4]Multidisciplinary Cardiovascular Research Centre, University of Leeds, Leeds, UK

6.1 Abstract

Background

With increasing heart rate there is redistribution of blood away from the subendocardium due to the compressive forces of the LV during systole. Subendocardial perfusion is therefore critically dependent on the diastolic time fraction (DTF). With high spatial resolution, cardiac magnetic resonance perfusion has the potential to examine important differences in transmural flow distribution.

Purpose

1. To examine the effect of reduced DTF on coronary flow between the subendocardium and the subepicardium at rest and during adenosine stress using high-resolution cardiac magnetic resonance (CMR) perfusion.
2. To assess the feasibility of examining these differences using exercise stress.

Methods

The effect of adenosine on DTF was assessed in 2 patients undergoing percutaneous coronary revascularisation (PCI) using a pressure sensor tipped guide wire in the aortic root. *k*-t SENSE accelerated perfusion CMR was performed on 19 healthy volunteers. Images were acquired at rest, and during adenosine hyperaemia (8 volunteers) or after peak exercise (11 volunteers). 0.05 mmol/kg Gd-DTPA was administered as contrast agent. Ventricular and myocardial signal intensity curves were generated for both studies. The curves were used to quantify myocardial blood flow (ml/min/g), myocardial perfusion reserve and endocardial/epicardial ratios using a Fermi Function deconvolution algorithm.

Results

1) Adenosine: Resulted in a variation in both the diastolic duration (mean difference 151.9±59.6 ms, $P<0.001$) and the DTF (mean difference 0.04±0.01, $P<0.0009$). In volunteers, endocardial flow at rest was higher than epicardial across all segments (2.69±1.07ml/g/min vs. 2.11±0.91 ml/g/min $P<0.0001$) with an ENDO/EPI ratio of 1.34±0.2. During hyperaemia there remained a difference in perfusion with

endocardial flow 5.41±2.33 ml/g/min and epicardial flow 4.7±2.09 ml/g/min respectively (NS) with a reduced ENDO/EPI ratio of 1.16±0.2 (P=0.03 *vs.* rest).

2) Exercise: 7 out of 11 studies suitable for analysis. Resting transmural blood flow was 0.8±0.06 ml/g/min that increased to 2.6±0.4 and 2.5±0.3 ml/g/min during exercise 1 and 2 respectively (*p*=0.001 rest vs. exercise). MPR was 3.3±0.5 for Ex1 and 3.1±0.4 for Ex2. There was an ENDO/EPI flow ratio at rest of 1.29±0.2 that reduced to 1.04±0.2 after Ex1 and 1.07±0.1 after Ex2 (P= 0.02 *vs*. rest).

Conclusion

Using high resolution CMR perfusion we were able to demonstrate *in vivo* that the endocardial/epicardial flow ratio decreases during hyperaemic stress.

6.2 Introduction

6.2.1 Coronary Physiology and Myocardial Perfusion During Exercise

During exercise, demand for oxygen increases in skeletal muscle[37]. This demands an increase in cardiac output and arterial pressure, which is provided by increases in heart rate, contractility, and ventricular work. The increase in activity of the heart augments the demand and consumption for oxygen which is strongly correlated with coronary flow[37]. Increases in coronary flow are met by vasodilatation of the coronary vessels and an increase in mean arterial pressure[365]. Left ventricular myocardial blood flow is 0.8-1.3 ml/min/g at rest in humans[309, 366-368]. Dynamic exercise can increase coronary blood flow by three to five times above the resting level[11 309]. The difference between the maximal blood flow obtained by coronary vasodilatation and blood flow at rest is known as the myocardial perfusion reserve (MPR) and depends largely on the perfusion pressure and the degree of vasodilatation in the microcirculation[44].

The majority of coronary blood flow occurs during diastole[74]. Physical compression and myocardial shortening during the systolic phase cause impediment of coronary blood flow within the intramural vessels[43, 44]. The LV subendocardium is much more

vulnerable to the compressive forces of systolic contraction than the subepicardium and subepicardial flow is roughly twice that of the subendocardium during systole[21]. Subendocardial perfusion is therefore critically dependent on diastolic perfusion; with increasing heart rate and a reduction in the diastolic interval, perfusion is maintained by vasodilatation of the coronary microvasculature[69]. In contrast, subepicardial perfusion is relatively unaffected by changes in the diastolic duration and heart rate[342]. To compensate for these differences, the subendocardium has a greater capillary vascular density with resting endo-epicardial flow (ENDO/EPI) ratios reported between 1.09 and 1.49[21, 278, 293, 369]. However, as heart rate increases and diastolic perfusion time (or diastolic time fraction, DTF) reduces it has been shown that there is a reduction, or even a reversal in this ratio as blood is directed away from the subendocardium[23, 370,11,371].

6.2.2 High resolution CMR Imaging- the Challenges of Exercise Stress

In order to study differences in transmural flow distribution during exercise in the human myocardium any imaging technique must fulfil some essential criteria. Firstly, it must be able to image the heart at high heart rates; it must be of sufficient spatial resolution to distinguish the endo- and epicardial layers; and it must allow full quantification of myocardial blood flow. Cardiac magnetic resonance (MR) has the potential to fulfil all of these requirements, although, such imaging presents a significant challenge. The main challenge relates to the acquisition of data at much higher heart rates than usual, without significantly degrading either the spatial or temporal resolution necessary for quantification of blood flow to the different myocardial layers. Such studies have not been previously carried out.

Through preliminary studies in volunteers we established that the use of *k*-space and time sensitivity encoding (*k-t* SENSE) was preferable to standard first-pass perfusion techniques [see Chapter 2]. *k-t* SENSE simultaneously exploits coil encoding and spatiotemporal data correlations to allow acceleration of data acquisition, which is crucial during dynamic MR perfusion[222]. This acceleration can be used to improve temporal or spatial resolution of perfusion CMR especially at 3 Tesla where there is a greater signal to noise ratio (SNR)[223]. It is also associated with a reduction in dark rim

artefacts, which we found to be particularly troublesome at high heart rates with standard perfusion techniques; consequently a lot of these early data were not suitable for quantitative analysis. However, despite the advantages of faster scanning using *k-t* SENSE it also presents some potential drawbacks: the higher spatial resolution and spatiotemporal under-sampling can result in a loss of SNR, as well as being especially vulnerable to breathing and other movement artefact. The effect of these on quantification of transmural myocardial blood flow remains to be determined.

6.2.3 Rationale for the Proposed Study

The redistribution of coronary blood flow between the different layers of the myocardium is of great importance, especially in patients with coronary artery disease where the subendocardium is particularly vulnerable to the effects of ischaemia and infarction[108, 131]. An increased understanding of such changes in perfusion might allow us to develop interventions or therapies to attenuate such damage. In the previous chapter (Chapter 5) we documented important changes in myocardial microvascular resistance (MR) that were associated with improved performance in patients with obstructive coronary disease and exertional angina. It is known that with increasing heart rate these reductions in MR are associated with enhanced subendocardial blood flow[60]. Although changes in transmural blood flow have been extensively examined in animals, there is comparatively little data in humans because of the difficulties in acquiring such data *in vivo*.

Quantifying myocardial blood flow during exercise stress using CMR is a challenge. Initially it was important to establish that the scanning and quantification methods we were going to use were capable of detecting differences in transmural flow distribution in subjects not undergoing exercise. Adenosine is a vasodilator, lowering central aortic pressure and increasing heart rate; it is safe and widely used and therefore provided a good choice of stimulant to use. The effects of the standard adenosine infusion used in clinical practice (and in the experimental protocol) on DTF are uncertain. This was determined by analysis of the central aortic pressure

waveform in two patients undergoing scheduled percutaneous coronary revascularisation in the catheterisation lab during adenosine infusion.

6.3 Methods

6.3.1 Adenosine Protocol

Catheterisation Lab Protocol

2 patients with obstructive coronary disease in whom percutaneous coronary intervention (PCI) was planned and were undergoing a pressure wire assessment of the lesion, were consented into the study. A pressure wire (Brightwire®, Volcano® Therapeutics, USA) was positioned at the tip of the guide and also connected to the Combomap via a Smartmap® transducer (Volcano® Therapeutics, USA) which provided a high fidelity proximal pressure signal (P_a) and was equalised to the fluid-filled catheter pressure trace from the main Philips Sensis® system in the cath lab. The guide was disengaged from the coronary ostium and the pressure wire was passed into the aortic root. Data were recorded at rest and during an intravenous infusion of adenosine at 140µg/kg/min for 3 minutes to achieve hyperaemic stress. All data were recorded at 1 kHz and stored on a disk for subsequent analysis. The second derivative of the waveform was used to identify the dicrotic notch and the first derivative to identify the maximal point of change of the upstroke of the following beat to determine diastolic duration (see Figure 56 below), using Matlab® (The MathWorksInc®, USA). DTF was then determined by dividing the diastolic duration by the whole pulse duration. The analysis was performed blind to whether the readings were taken at baseline or hyperaemia.

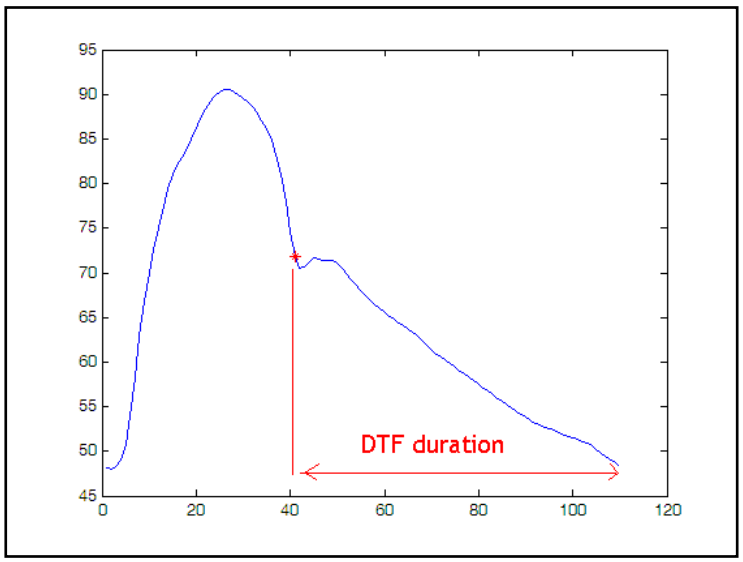

Figure 56. Showing the calculation of diastolic time fraction (DTF) from the central aortic pressure waveform. The second derivative was used to assess the maximum rate of change.

CMR Protocol

A group of 8 normal volunteers (6 males aged 29±8 years) with no known history of cardiac disease were recruited. There was no evidence of conditions such as obstructive lung disease, sick sinus or atrioventricular block that would lead to the contraindication of adenosine administration. Coffee, tea and caffeine-containing drugs were withheld for 24 hours before the investigation. All subjects gave written informed consent, and the local ethics review board approved the study.

Myocardial perfusion CMR was performed on a 3T Philips Achieva® system using a 6 channel cardiac phased array receiver coil for signal reception and a vectorcardiogram for triggering and gating. Subjects had a peripheral cannula inserted in both antecubital fossae, one for administration of a contrast agent and the other for the infusion of adenosine. All perfusion data were acquired in the true short axis of the LV at end-inspiration to minimise respiratory artefacts. The perfusion pulse sequence consisted of a saturation recovery gradient echo method with a repetition time/echo time 3.0ms/1.0ms and flip angle 15°; 5x *k-t* SENSE acceleration was used with 11 interleaved training profiles providing an effective acceleration of 3.8x and a spatial resolution of 1.2x1.2x10mm^3. 3 slices were acquired at each RR interval. The first slice was acquired immediately following the R-wave on the ECG. In order to acquire data during cardiac phases with minimal bulk

cardiac motion, mid-systole and mid-diastole were identified on cine images and the trigger delays for slice two and three set so that acquisition occurred in these cardiac phases. Data were acquired during adenosine-induced hyperaemia (140µg/kg/min) and after a 15minute delay at rest using a dose of 0.05mmol/kg Gd-DTPA (Magnevist®, Shering, Germany) at a rate of 4ml/minute followed by a flush of 20ml Saline. Blood pressure and heart rate were monitored throughout, as was the subject's response to adenosine to ensure that hyperaemic conditions were achieved. Standard dual inversion recovery late gadolinium enhancement images were acquired after 15 minutes to ensure there were no significant areas of scar that may interfere with the analysis.

6.3.2 Exercise Protocol

A specially adapted supine cycle ergometer was used and attached to the sliding table inside the CMR scanner such that the subject could exercise without leaving the table and scanning could occur almost immediately after peak exercise. A standardised exercise protocol was used with increments of 20W each minute for 6 minutes at a rate of 60 rpm[340]. Rate pressure product (RPP) calculated as peak systolic blood pressure x peak HR was recorded at peak exercise.

CMR Protocol

Healthy volunteers without known cardiovascular disease gave informed consent for supine cycle ergometry on the CMR scanner table (Lode, Netherlands). Resting high-resolution perfusion CMR was performed on a 3T Philips Achieva® system using 0.025 mmol/kg Gd-DTPA (saturation recovery gradient echo, repetition time/echo time 2.7ms/0.96ms, flip angle 15°, 5 x k-t SENSE acceleration, 11 interleaved training profiles, WET pre-pulse (angles 120°, 90°, 180°, 140°); delay 100ms, spatial resolution 1.0x1.0x8mm^3, 3 slices acquired at each RR interval, 30 dynamic images). Subjects were then removed from the scanner but remained in a supine position on the table attached to the ECG electrodes and radiofrequency coil. Position on the table was maintained using a specially adapted vacuum cushion. Subjects then underwent a standardised incremental exercise protocol as has been described previously[340]. At peak exercise, the patients were quickly slid back into the scanner

and the perfusion sequence was repeated. After a period of rest for 20 minutes, the exercise protocol was repeated with a further perfusion scan.

6.3.3 CMR Quantification Methods

Data were analysed off-line by means of a commercially available dedicated software package (MASS®, Medis, The Netherlands). The LV myocardium was divided into 6 segments per slice and into an endocardial and epicardial third and signal intensity curves (SI) were generated [see Chapter 2 for a more detailed explanation of methods]. Data generated in MASS were imported to a Fermi Function deconvolution algorithm implemented in Matlab® (The MathWorksInc®, USA). The Fermi deconvolution provided estimates of absolute myocardial blood flow (ml/g/min)[196]. Data are presented as mean ±SD. Myocardial perfusion reserve (MPR) was calculated by dividing peak flow by resting flow values.

6.3.4 Statistical Analysis

Paired *t*-tests were performed on the discrete data and used to examine the difference in means. Multiple comparisons were made using ANOVA. Data are presented as mean ± standard deviation (SD). Coefficient of variation was used to compare inter- and intraobserver differences. A P value of <0.05 was considered significant.

6.4 Results

6.4.1 Adenosine

5 sets of measurements in the 2 patients were taken before and after PCI (see Table 16 below). All data were of suitable quality for full analysis. The adenosine infusion resulted in the predicted fall in central mean arterial pressure (MAP) and an increase in heart rate (HR). These haemodynamic changes resulted in a variation in both the diastolic duration (mean difference 151.9±59.6 ms, P<0.001) and the diastolic time fraction (mean difference 0.04±0.01, P<0.0009).

	Vessel	MAP		HR		Diastolic duration		DTF	
		Rest	*Stress*	*Rest*	*Stress*	*Rest*	*Stress*	*Rest*	*Stress*
1	RCA pre PCI	66.3	61.1	54.3	63.9	695.80	549.29	0.63	0.58
2	RCA post PCI	71.4	66.1	56	64.2	660.91	543.95	0.62	0.58
3	Cx pre PCI	86.3	82.6	51.3	72.6	729.29	485.88	0.62	0.59
4	LAD pre PCI	87.1	85.8	65.8	74.4	562.50	476.52	0.61	0.57
5	LAD post PCI	73.8	76.4	59	73.2	646.25	479.47	0.64	0.59
	Mean	**76.9**	**74.4**	**57.2**	**69.7**	**659**	**507****	**0.62**	**0.58***
	SD	**9.2**	**10.5**	**5.5**	**5.1**	**62.8**	**36.5**	**0.01**	**0.008**

Table 16. Showing the results of the analysis of 5 sets of measurements taken from 2 patients undergoing percutaneous coronary intervention (PCI). All data were recorded at rest and stress during the infusion of i.v. adenosine. MAP =mean arterial pressure, HR =heart rate, DTF =diastolic time fraction. Diastolic duration is measured in milliseconds (ms). *<0.005, **<0.001

A)

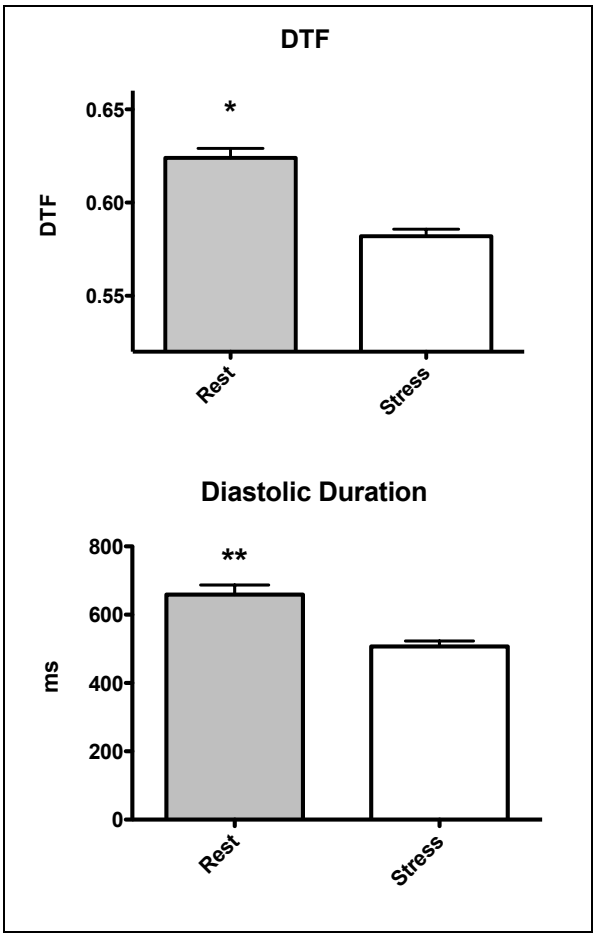

Figure 57. Showing diastolic time fraction (DTF) and diastolic duration (in milliseconds) at rest and during adenosine stress. *P<0.0009, **P<0.001.

All 8 volunteers underwent the protocol and all data was suitable for quantification analysis. Heart rate increased from 63±15 to 85±10 (p=0.01) during hyperaemia. Transmural flow increased from 1.7±0.2 at rest to 4.4±0.4 at peak hyperaemia (p=0.0008). See Figure 59 below. Endocardial flow at rest was consistently higher than epicardial flow across all segments (2.5±0.2ml/g/min vs. 1.9±0.2 ml/g/min p=0.002) with an ENDO/EPI of 1.34±0.2. During hyperaemia there was a reduction in flow heterogeneity between the layers with endocardial flow 5.6±0.6 ml/g/min and epicardial flow 5.2±0.7 ml/g/min respectively (NS) and with a reduced ENDO/EPI of 1.16±0.2 (P=0.03). See Figure 58 below. Mean intra-observer difference of 0.1±0.57 (p=0.68) and a coefficient of variability of 21%. Inter-observer difference was 0.3±0.28 (p=0.13) with a coefficient of variability of 18%.

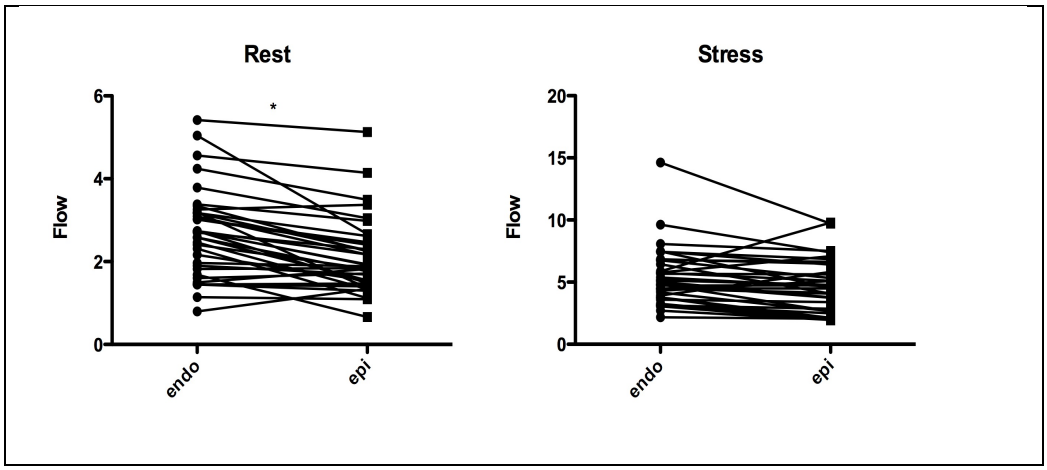

Figure 58. Differences in endo- and epicardial flow at rest and stress. Flow is ml/g/min. *p=0.0025

6.4.2 Exercise

11 subjects (36.3±7.3 years; 6 male) completed two periods of exercise. Of these only 7 were suitable for full quantification analysis of all data. Haemodynamic data is shown in Table 17 below. Resting transmural blood flow was 0.8±0.06 ml/g/min that increased to 2.6±0.4 and 2.5±0.3 ml/g/min during exercise 1 and 2 respectively (P=0.001 rest *vs*. exercise). See Figure 59 below. MPR was 3.3±0.5 for Ex1 and 3.1±0.4 for Ex2. There was an endo- epicardial flow ratio at rest of 1.29±0.2 that reduced to 1.04±0.2 after exercise 1 and 1.07±0.1 after exercise 2 (P= 0.02 *vs*. rest).

6.5 Discussion

At rest there is increased basal blood flow to the subendocardial layer of the myocardium, resulting in an endo-epicardial perfusion gradient. Resting blood flow is predominantly diastolic but as heart rate increases there is increased systolic blood flow. The compressive forces of LV contraction cause impediment of coronary blood flow during systole. This effect is not distributed evenly across the myocardium, however, and a reduction in diastolic time fraction (DTF) with increasing heart rate causes blood to be directed away from the subendocardium to the subepicardial layer resulting in a loss of this perfusion gradient. The present study was able to illustrate these important physiological differences using high resolution CMR perfusion during large muscle exercise *in vivo*.

	Peak Exercise 1				Peak Exercise 2			
Volunteer	**HR**	**% HR_{max}**	**SBP**	**RPP**	**HR**	**% HR_{max}**	**SBP**	**RPP**
1	115	60.53	156	17940	125	65.79	155	19375
2	129	67.89	150	19350	130	68.42	148	19240
3	121	63.68	158	19118	121	63.68	161	19481
4	135	71.05	140	18900	132	69.47	159	20988
5	118	62.11	160	18880	115	60.53	156	17940
6	125	65.4	157	19625	130	70.1	152	20150
7	118	60.9	146	17228	123	63.2	144	17712
Mean	**123**	**64.5**	**152**	**18720**	**125**	**65.8**	**154**	**19269**
SD	**7.1**	**3.8**	**7.3**	**843**	**6**	**3.6**	**6**	**1153**

Table 17. Full haemodynamic data collected at peak exercise. There were no differences in any of the variables between peak Ex1 and peak Ex2. HR = heart rate (bpm); SBP =systolic blood pressure (mmHg); % HR_{max} =percentage of age-predicted peak heart rate attained; RPP =rate pressure product (SBP x HR).

6.5.1 Adenosine Stress Studies

Overall Myocardial Blood Flow (MBF)

The results from the adenosine-CMR part of the study show that k-t SENSE accelerated first-pass perfusion CMR at 3.0 T is an effective method of demonstrating and quantifying myocardial perfusion. The images obtained in the adenosine stress study showed excellent reproducibility and quality. Due to the high spatial resolution of CMR, it was possible to produce detailed images of the subendocardial and subepicardial borders. As a result the physiological differences between the two layers could be demonstrated quantitatively. Basal endocardial flow values were higher than the epicardium, which is to be expected given the dense coronary vasculature in the endocardium that reduces towards the epicardium[372]. This was demonstrated by the ENDO/EPI ratio of 1.34 at rest. During pharmacological stress with adenosine, there is direct vasodilatation of the coronary

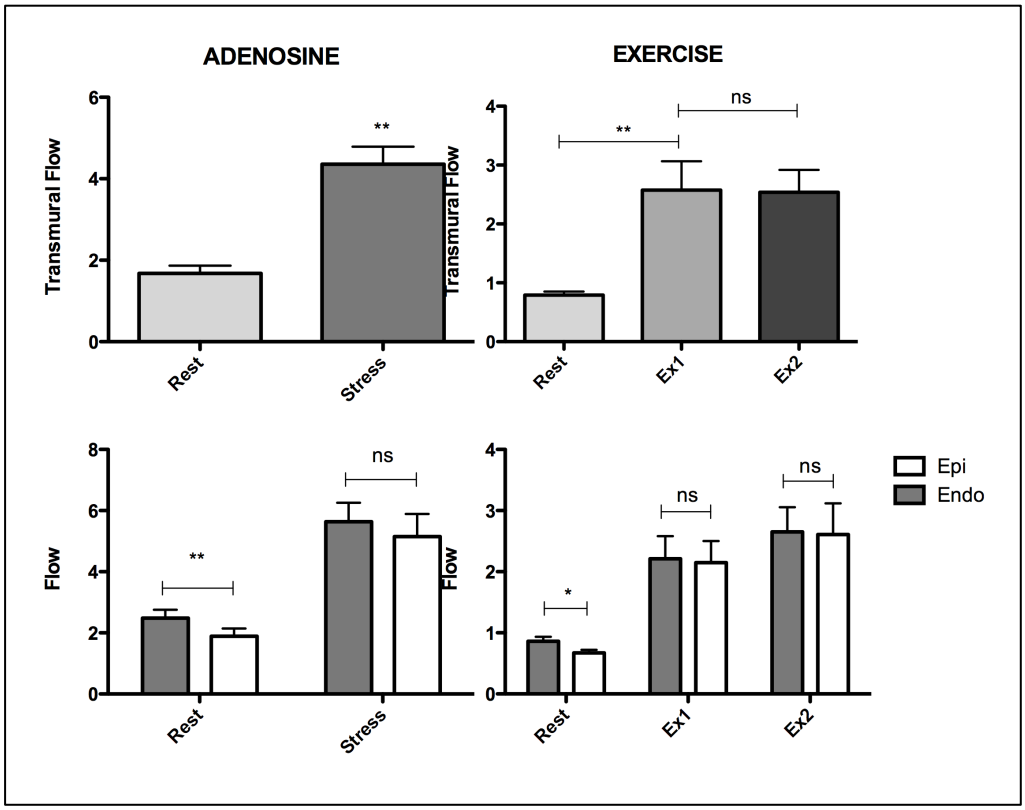

Figure 59. Showing differences in transmural flow and endo- and epicardial flow differences both during adenosine and exercise stress. It can be seen that in both cases there is a significant increase in myocardial blood flow, and that the resting endo-epicardial flow ration is abolished at the increased HR. Flow is measured as ml/g/min. *p=0.005, **p<0.001

vessels, which decreases vascular resistance[165]. Coronary flow increases as a response. In the present study we demonstrated an increase in transmural myocardial perfusion from 1.7±0.2 at rest to 4.4±0.4 at peak hyperaemia (p=0.0008). Few other studies have used quantitative analysis to demonstrate increases in coronary blood flow between rest and stress in first-pass perfusion CMR. Pack et al. compared quantitative myocardial perfusion using CMR imaging with quantitative perfusion using PET[368]. Quantitative analysis for CMR was performed using a deconvolution method similar to that used in the present study. They found a mean rest flow of 1.03 ± 0.76 ml/min/g and a mean stress flow of 2.97 ± 1.59 ml/min/g with first-pass perfusion CMR. In comparison, myocardial perfusion estimates from dynamic ^{13}N-ammonia PET at rest and stress were 0.80 ± 0.24 and ml/min/g 3.04 ± 1.14 ml/min/g respectively. Perfusion estimates were not significantly different between CMR and PET in both coronary arterial regions and in the individual segments. MPR values for CMR and PET were 3.2 ± 1.7 and 3.7 ± 0.7 respectively.

Hsu et al. also used a model of deconvolution to quantify myocardial blood flow in first-pass perfusion CMR[366]. They found a mean flow of 1.02 ± 0.22 ml/min/g at rest and 3.39 ± 0.58 ml/min/g during dipyridamole stress. Absolute myocardial blood flow estimates using PET have yielded similar results. Ibrahim et al. found a mean rest flow value of 0.8 ± 0.2 ml/min/g and a mean value of 2.9 ± 08 ml/min/g during adenosine stress using PET[367]. MPR was 3.9 ± 1.2. Wyss et al. found a mean resting flow value 1.22 ± 0.16 ml/min/g that increased to 5.13 ± 0.74 ml/min/g during adenosine stress[309]. Our rest flow values appear to be slightly higher than reported values. This may be due to background saturation of contrast agent whereby the LV input function is underestimated and thus MBF estimate is larger. However, our adenosine stress values are comparable with the reported ranges. Due to our higher rest flow values, our MPR results were therefore slightly lower then the reported values.

Transmural Flow Redistribution

At the standard doses of adenosine used in the clinical setting (140μg/kg/min) there is often only a relatively small increase in heart rate. Because we wanted to investigate the effects of alteration of DTF on redistribution of transmural MBF it was important first to establish the changes in DTF in response to a standard infusion of adenosine. This was the purpose of the initial stage of the study and it clearly showed significant alterations in diastolic duration and DTF during adenosine-induced hyperaemia, even though there was only a 21% increase in HR. Although we did not specifically measure DTF in either the adenosine-CMR or the exercise-CMR groups, we can assume that with similar increases in HR (even more so in the exercise group) that there would be a corresponding reduction in DTF. The effect of such a reduction is that there would be some redistribution of coronary flow from the subendocardium towards the epicardium[23, 69]. This was reflected in the present study by the subsequent decrease in the ENDO/EPI ratio from 1.34 at rest to 1.16 during adenosine hyperaemia (P=0.03). Christian et al. compared fluorescent microsphere measurements of canine myocardial blood flow with qualitative, semiquantitative, and fully quantitative measurements of first-pass perfusion using magnetic resonance (MR) imaging[293]. They found that CMR full quantitative

assessment underestimated microsphere measurements of MBF. However, they found reductions in the ENDO/EPI ratio with adenosine similar to those in the present study falling from 1.2 to 0.9, and 1.05 to 0.97 for the microsphere and CMR measurements during rest and adenosine respectively. There are few studies examining this in humans. Keijer et al. studied a small group of patients with single vessel coronary disease using perfusion CMR[278]. Despite the use of a standard perfusion protocol achieving an in-plane spatial resolution of 3x2mm (compared to 1.2x1.2 in the present study) they were able to measure a resting ENDO/EPI ratio in normal myocardium of 1.25±0.29. During dipyridamol stress (a similar vasodilator to adenosine), this decreased to 1.08±0.23 (NS). In territories with a significant coronary stenosis the values for the ENDO/EPI ratios were 1.18±0.18 and 0.96±0.21 ($P< 0.0002$). George et al. used multidetector CT perfusion imaging to quantify MBF in patients with and without coronary artery disease[369]. They found ENDO/EPI ratio of 1.12 during adenosine infusion in territories supplied by normal coronary arteries. There were no measurements taken during rest. Like the study by Keijer, they also found that the ENDO/EPI ratio was reduced in territories with significant coronary stenoses where the ratio was 0.91.

6.5.2 Exercise Stress Study

The adenosine studies demonstrated that we were able to detect differences in myocardial transmural flow redistribution consistent with the literature, using *k-t* SENSE accelerated perfusion CMR at 3 T. Because of the more dramatic effect on heart rate it was hypothesised that large muscle exercise would provoke a similar, if not even more significant change in ENDO/EPI myocardial blood flow patterns. Such studies have not been previously carried out.

Absolute Flow Values Reduced Compared to Adenosine

In the present study transmural blood flow increased from 0.8±0.06 ml/g/min to 2.6±0.4 at peak exercise. Although they are still within the normal range from previously published figures[309, 366-368], these values are generally lower than we found with adenosine where the MBF values were 1.7±0.2 at rest increasing to 4.4±0.4 at peak hyperaemia. In the study by Wyss et al. a mean resting flow value

1.22 ± 0.16 ml/min/g increased to 5.13 ± 0.74 ml/min/g during adenosine stress and to 2.35 ± 0.66 ml/min/g during exercise[309]. The reduced exercise flow values were attributed to volunteers not performing exercise to maximal level of effort, and to the fact that images were taken immediately after exercise when heart rate and flow would have fallen fairly rapidly. A similar effect could be seen in the present study. Although in general the subjects achieved around 60-70% of their age-predicted maximum heart rate and they were quickly re-introduced into the scanner, because they were young and fit, there was a rapid decrement in their peak heart rate, such that by the time of scanning (on average less than 1 minute after stopping cycling) this had dropped below their peak. While this might explain the reduced peak flow values compared to the adenosine, however, it does not explain the reduced resting values. One of the major issues may have been the timing of the rest scan. In clinical practice this is conventionally carried out *after* the stress scan and this was the case for the adenosine volunteers. However, when we started the exercise protocol, we found that although peak heart rate dropped rapidly subjects took a long time to return to baseline conditions. Therefore we changed the protocol around so that the rest scan took place first. Although previous data from our department suggests that the effects of this should be minimal [see Chapter 2], it is possible that values for the rest scan in the adenosine protocol therefore may have been generally higher due to the effects of background contrast saturation. In addition, the images in the exercise study were generally noisier than the adenosine scans; increased movement and breathing artefact as well as dark rim, or susceptibility, artefacts associated with increased heart rates made accurate quantification analysis more difficult. Because *k-t* SENSE utilises data under-sampling methods to accelerate scan time it is especially susceptible to any movement that can result in loss of data[222]. The high heart rates also made it more difficult to ensure that the timing of the scan occurred during mid-systole when the myocardium is thickest, the point where mapping of the endo- and epicardial boarders is most accurate. Taken together, these factors may have resulted in less data being available to input into the Fermi deconvolution algorithm resulting in an underestimation of absolute flow values.

Detection of Transmural Flow Heterogeneity

Although the absolute flow values seem to have been underestimated in the exercise study, the relative increases exceeded those with the adenosine. The MPR was 3.3±0.5 for Ex1 and 3.1±0.4 for Ex2, while the MPR for adenosine was 2.6±0.5. Differences between flow in the subendocardium and subepicardium were also detectable in the exercise studies. There was an ENDO/EPI flow ratio at rest of 1.29±0.2 that reduced to 1.04±0.2 after exercise 1 and 1.07±0.1 after exercise 2 (P= 0.02 *vs*. rest). These are similar values to those previously reported, although this is the first time such data has been recorded *in vivo.* Ball et al. found an ENDO/EPI ratio of 1.12-1.33 in various regions of the left ventricle in resting unanaesthetized dogs using tracer microspheres[21]. As the dogs were subjected to increasing levels of exercise, decreases in the ENDO/EPI ratio were observed, with an ENDO/EPI ratio of 0.95-1.14 at maximal exercise. Similarly, Barnard et al. also observed a decrease in the left ventricular ENDO/EPI ratio from 1.29 during rest to 1.03 during exercise in dogs[46].

6.6 Limitations

Both studies involved a small number of patients. Although previous studies have demonstrated the feasibility of k-t SENSE accelerated first-pass perfusion CMR in healthy volunteers and patients[221, 288], reproducibility of subendocardial and subepicardial data need to be explored further in larger samples.

As discussed earlier, the images and data obtained from the exercise stress first-pass perfusion CMR test were often sub-optimal. In 4 out of the 11 volunteers it was not possible to analyse completely all three scans due to excessive artefacts. Data from these subjects were therefore not included in the final analysis. This represents a significant proportion of the population and reflects the difficulties of scanning under such conditions. There is a need to optimize the sequence for physical exercise further focusing on the need to increase the speed of data acquisition and reduction in the incidence of respiratory and other movement-induced artefacts. Potential options that we have considered might include: reconstruction of the

perfusion sequence with *k*t-BLAST and rather than *k*t-SENSE; use of a saturation 'slab' over the anterior chest wall to nullify the signal from the chest which is the most frequent source of artefact in *k*-space; caudal-cranial fold-over direction as opposed to anterior-posterior; a new reconstruction protocol called *k*t-PCA (not available at the time of our studies), which rejects signals that vary too much from the mean of the surrounding tissue and reduces the impact of artefact on the averaged output[335]; use of much lower doses of Gd-DTPA (e.g. 0.004mmol/kg), which avoids potential signal saturation that can occur with higher contrast doses on the second and third perfusion scans. All of these need to be fully tested and then incorporated into an updated scanning protocol but it is hoped that they will substantially improve the quality and consistency of the perfusion images. Further work also needs to be carried out to assess the inconsistency in the absolute flow values measured across the studies.

6.7 Future Work

"Gradientograms"

In the present study, we measured the relationship between endo- and epicardial myocardial blood flow by dividing the myocardium into thirds and comparing mean flows across each of these segments. Although this is a standard technique and used in other studies[278] it is relatively crude in that it does not account for variations in flow *within* each of these segments. Data from the present study was therefore used to describe a new approach for characterization and visualization of regional and dynamic differences in myocardial contrast uptake. Conventional quantitative assessments of myocardial perfusion analyse the temporal relation between the arterial input function and the myocardial signal intensity (SI) curves, thereby neglecting the important spatial relation between the myocardial SI curves. The new method published in *MRM* enables characterisation of sub-endocardial to subepicardial gradients in myocardial perfusion based on a two dimensional, ''gradientogram'' representation, which displays the evolution of the transmural

gradient in myocardial contrast uptake over time in all circumferential positions of the acquired images[290]. This gradientogram allows for direct quantification of the gradient amplitude, the temporal persistence, and circumferential extent of myocardial perfusion defects and it revealed a clear distinction between normal perfusion and inducible ischaemia in patients with coronary arterial disease during adenosine hyperaemia. This analysis has not yet been carried out in the exercise-CMR subjects because, so far, the perfusion images in this group have not been of sufficient quality. However, this works represents an exciting new method to examine in detail the changes in transmural flow that occur in response to stress.

Transmural Flow Redistribution and "Warm-Up": A Potential Mechanism?

In Chapter 5 of this thesis we documented that microvascular resistance falls in response to large muscle exercise in patients with coronary artery disease and angina. This fall in resistance corresponded with an increase in coronary flow velocity and a fall in LV afterload due to a reduction in arterial wave reflection in the aorta. These changes persisted through recovery and into a second exercise period, resulting in a warm-up effect; manifested as increased time to, and greater workload at the point of ECG-ischaemia. Experimental work in animals has shown that with reducing DTF, subendocardial perfusion becomes dependent on a fall in microvascular resistance to maintain diastolic perfusion[336, 342]. These changes become even more critical in the presence of a coronary stenosis, where the resting ENDO/EPI perfusion ration may be attenuated[278, 369] and vasodilator capacity may be already near maximal[60, 69, 336]. It has been suggested that warm-up may result from changes in coronary blood flow. Previous studies have failed to demonstrate changes in overall coronary flow although such studies used outmoded measures of myocardial blood flow such as coronary sinus sampling[103, 104, 345]. It may be that, rather than changes in bulk flow, warm-up arises through more subtle changes in transmural flow redistribution with enhanced subendocardial perfusion attenuating ischaemia. This would be consistent with the changes in microvascular resistance that we reported in the catheter lab studies described in Chapter 5. Bogaty et al. investigated this using SPECT in patients with exertional angina, but they were not able to demonstrate any changes in flow between the myocardial layers[116]; again

this may have been due to imperfect techniques with the poor spatial resolution afforded by SPECT not sufficient to detect such differences.

The techniques developed in this chapter, as well as the exciting advances afforded by the "gradientogram" analysis outlined above, provide a good model to investigate the changes in transmural myocardial blood flow that accompany heavy exercise in patients with ischaemic heart disease. Following these initial promising results in normal volunteers, and after further optimisation of the scanning protocol outlined above, the next stage of my research was to recruit patients with significant coronary arterial disease and angina. Full ethical approval had been obtained for this. Indeed, we got as far as recruiting and scanning a couple of patients, but after this the 3T scanner at St Thomas' underwent a major refurbishment, which in the end lasted 10 months and meant that I was not able to recruit any further patients or conduct any further studies into this part of my PhD research. Now that the scanner is operational once again, this line of investigation into mechanisms of warm-up is being continued by my colleagues, Dr. Kal Asrass and Dr. Rupert Williams, as part of their PhD theses; they have received BHF funding to do so, partly based on the preliminary data provided in this chapter.

6.8 Conclusion

Exercise stress testing remains the most physiological method of inducing myocardial stress. Due to high heart rate and respiratory motion the feasibility of physiological stress in the MR environment has limited its clinical and scientific application, but following the development of high-resolution CMR methods, these responses now can be measured. *k-t* SENSE is associated with improved temporal and spatial resolution of perfusion CMR through acceleration of data acquisition. These results suggest that using *k-t* SENSE we can detect and quantify changes in flow to the different myocardial layers. We were able to demonstrate that at rest endocardial flow was greater than epicardial; and, as heart rate increases, there is an equalisation in flow due to the redistribution of blood secondary to the disproportionate effect of systolic flow impediment on the subendocardial layer.

These data are consistent with the available physiological literature. We are not aware of any previous studies that have documented transmural myocardial flow heterogeneity in response to exercise stress *in vivo*. Although in need of some further refinement, these studies provide a model suited to investigate potential mechanisms of clinically important phenomena such as warm-up angina that may arise through changes in transmural perfusion gradients.

6.9 Acknowledgments

I would like to thank AG for his assistance in the blinded analysis of the DTF data. MI and HT carried out the blinded analysis of the adenosine perfusion data, and RW and HT carried out the analysis of the exercise perfusion data. KA assisted in the recruitment and the exercise volunteer studies. SP, EN, AC and SK provided invaluable advice and assistance in the perfusion analysis. SR assisted in the catheterisation lab measurements and analysis. MM provided overall guidance and support throughout. Dr. Chris Schofield from the Dept. of Medical Statistics, KCL, provided statistical support. I would like to thank the BHF for funding this research. Support was also provided by a grant from the BRC.

7 SYNTHESIS

The purpose of this synthesis is to summarise the major findings and implications of the studies that are the focus of this thesis.

7.1 Aims and Hypotheses of this Thesis

The response of the human heart to ischaemic stress is variable and a variety of potential adaptive mechanisms attenuate myocyte damage and improve performance. Such mechanisms are poorly understood and may include innate myocardial responses, changes in microvascular function and more general systemic haemodynamic adaptations. The main aim of this thesis was to examine some of these adaptive mechanisms to ischaemic stress, using the models of exercise induced myocardial ischaemia and acute myocardial infarction. In the former, we sought to use invasive physiological measurements and high-resolution cardiac magnetic resonance imaging to assess changes in coronary blood flow, central haemodynamics and transmural myocardial perfusion in patients with symptomatic coronary arterial disease. In the latter, we sought to examine the role of *post-conditioning* as a potential therapeutic tool in a randomised controlled trial involving patients undergoing primary percutaneous revascularisation for acute myocardial infarction.

Key Hypotheses Under Investigation in this Thesis

4. The reduction of ischaemia seen on second exercise in patients with coronary artery disease can be explained by changes in central haemodynamics, especially a reduction in central blood pressure causing a reduction in ventricular afterload and enhanced vascular-ventricular coupling.
5. Warm up angina is associated with reduced microvascular resistance and an improvement in subendocardial perfusion on second exercise
6. Postconditioning causes a reduction in infarct size through activation of innate myocardial protective mechanisms

7.2 Summary of the Main Findings

7.2.1 Postconditioning in Acute Myocardial Infarction

Initial clinical results using a postconditioning protocol in the context of primary percutaneous revascularisation (PPCI) have been promising[148, 319], but whether postconditioning results in a long-term sustained attenuation of post-ischaemic injury and infarct reduction rather than simply a delay in inevitable injury is a question still to be determined. The demonstration of such an effect would add significantly to the argument of the existence of intrinsic cardiac protection in ischaemic heart disease patients, where the promise of such a phenomenon based on laboratory studies has perhaps failed to live up to expectations in the clinical setting. The purpose of the initial studies of this thesis was to design and undertake a randomised clinical trial examining these long-term effects. Cardiac magnetic resonance imaging (CMR) was chosen to assess infarct size, both at baseline and at follow-up as it provides unique tissue characterisation of the myocardium with high resolution and reproducibility and without the use of ionising radiation. CMR is also able to track both changes in LV segmental wall thickening and the presence of microvascular obstruction (MVO). It is suggested that by ameliorating the deleterious effects of reperfusion injury in the first minutes following restoration of coronary flow postconditioning will reduce MVO and promote LV recovery over and above the reduction in infarct size alone.

Out of the 33 patients randomised into the study there was a high proportion who dropped out, with 8 being excluded in the postconditioning (PC) arm and 6 excluded in the control arm before the cath lab protocol was completed. There was no suggestion that the PC protocol of re-occluding the vessel with serial balloon inflations was associated with procedural complications and, indeed, it was tolerated very well by the patients. 5 further patients dropped out before the second CMR scan could be performed at 5 month follow-up, including one patient who had a cardiac defibrillator fitted. Such difficulties in recruitment and follow-up greatly hampered our ability to complete this trial.

The main results of the interim analysis of this randomised, prospective study examining the benefits of postconditioning compared to control in a population of patients undergoing primary PCI for acute ST-elevation MI suggest an improvement in tissue perfusion, based on ST-segment resolution on the ECG, but no reduction in infarct size. These results must be treated cautiously as they are not powered to determine any significant differences due to low numbers. Hence the hypothesis that postconditioning causes a reduction in infarct size through activation of innate myocardial protective mechanisms cannot be answered decisively with these data.

7.2.2 High Resolution CMR Perfusion Imaging in Stable Coronary Disease

The principle tools required for the studies involving stable IHD patients were high-speed and high-resolution CMR imaging and invasive dual-sensor coronary measurements in the cardiac catheterisation lab. Both of these involved the development of a specially adapted supine ergometer that would be used to exercise the patients to provoke myocardial ischaemia. For the CMR protocol, data sampling had to be very fast, not only to allow imaging at high heart rates such as during peak exercise but also to allow high-resolution imaging required to determine differences in endo- and epicardial patterns of perfusion. New CMR acquisition strategies that simultaneously take advantage of coil encoding and spatiotemporal correlations, such as *k*-space and time sensitivity encoding (*k*-*t* SENSE), allow considerable acceleration of CMR data acquisition[220]. Scanning at higher field strength of 3-Tesla offers better signal-to-noise ratio with a reduction in artefacts compared to the more standard 1.5-T. The use of such perfusion sequences therefore offered distinct advantages over standard perfusion techniques. However, because there have been only few studies using *k*-t perfusion at 3-T a validation study was first required comparing it's diagnostic accuracy with the invasively measured fractional flow reserve (FFR). This was carried out in a cohort of patients at St Thomas' hospital with stable angina pectoris and single vessel coronary arterial disease being considered for percutaneous revascularisation (PCI). A group of

normal volunteers was also scanned in order to optimise the *k-t* perfusion sequence and to validate the full perfusion quantification methods used in the main study.

The main results of the study showed that high-resolution myocardial perfusion CMR imaging accurately detects functionally significant coronary artery stenosis as determined by FFR using both visual and quantitative analysis of the perfusion data. Measurements of myocardial blood flow obtained from CMR perfusion correlated better with the physiologically based FFR than with anatomical assessment of the coronary angiogram, which is to be expected. Importantly, the data from this study suggested that these CMR methods were robust and accurate with good reproducibility and repeatability, and could be used in the further studies of this thesis.

7.2.3 Synergistic Adaptations in Warm-Up Angina

The mechanisms of the phenomenon warm-up angina remain elusive. Warm-up shares many characteristics with ischaemic preconditioning but also maintains distinct differences, which suggest that other factors may predominate. During repetitive exercise, differences in ventricular afterload, subendocardial perfusion and microvascular resistance that relate to the propagation of waves within the aortic and coronary circulation may play an important role, although such adaptations have never been demonstrated *in vivo.*

In our study population of patients with severe coronary disease warm-up was confirmed on second effort (Ex2). Careful analysis of systemic and coronary haemodynamics during first and second exercise revealed a number of highly significant and interdependent alterations that likely contribute to this effect. Most striking amongst these was a reduction in central aortic pressure augmentation hence reducing left ventricular work. This was accompanied by a reduction in coronary microvascular resistance leading to a higher coronary blood flow velocity and an increased flow-accelerating backward expansion wave at the onset of diastole, reflecting the important interaction of cardiac-coronary coupling and microvascular conduction with respect to enhancing myocardial perfusion. These combined adaptations synergistically served to alleviate the imbalance between

myocardial demand and supply and resulted in the improved performance seen on second exercise. These data are unique and such work has not been previously carried out. They shine light on one of the main hypotheses of this thesis, suggesting that important changes in central haemodynamics, especially a reduction in central blood pressure do cause a reduction in ventricular afterload and enhanced vascular-ventricular coupling. They also support the hypothesis that warm up angina is associated with reduced microvascular resistance, that in turn would be expected to lead to an improvement in subendocardial perfusion on second exercise. To address this issue of enhanced subendocardial perfusion specifically we turn to the last series of studies reported in this thesis.

7.2.4 Transmural Flow Heterogeneity During Exercise

The revealing results from the exercise studies in the catheterisation lab, showing reduced microvascular resistance and enhanced coronary-cardiac interaction on second exercise, strongly suggest that an important component of warm-up results from the transmural redistribution of myocardial blood towards the vulnerable subendocardial layer. This formed the final hypothesis under investigation in this thesis and utilised the high-speed CMR perfusion techniques developed in our earlier studies. To be able to detect such changes *in vivo* at peak exercise represented a considerable challenge, testing our technical capabilities to the limit due to the problems caused by high heart rates and breathing and movement artefacts. Even in healthy volunteers, many iterations and much fine-tuning of the perfusion sequence was required before any meaningful data could be obtained. However, finally we were able to obtain good signals and quantification of myocardial blood flow demonstrated flow heterogeneity during exercise; the first time such data has been acquired during exercise in human subjects. Subsequently, we had started acquiring data from patients with coronary disease with a serial exercise warm-up protocol but unfortunately this coincided with extensive refurbishment and upgrade of the 3T research scanner, which meant that I was not able to carry out any further data collection for the duration of my research time. Therefore, while the changes in microvascular function and increase in the backward-travelling coronary suction wave on second exercise allude to enhanced subendocardial perfusion as a key

element in warm-up in patients with exertional angina, we have not been able to address this question directly from the results of this study.

7.3 Conclusion

The mechanisms of adaptation of the heart to ischaemic stress are complex and likely multifactorial. We were able to demonstrate that the reduction of ischaemia seen on second exercise in patients with stable coronary artery disease is associated with synergistic changes in central and coronary haemodynamics, especially a reduction in central blood pressure causing a reduction in ventricular afterload and enhanced vascular-ventricular coupling. This is also accompanied by a reduction in myocardial microvascular resistance suggesting a generalised reactive hyperaemic vasodilatory response to exercise that results in improved myocardial perfusion and overall performance. Transmural flow redistribution to the subendocardium is likely to play an important role in attenuating myocardial ischaemia on repeat exercise although we await the results of ongoing work. High-speed CMR perfusion imaging using *k*-t acceleration is a feasible tool to investigate these differences, with sufficient spatial resolution to detect transmural flow heterogeneity. Innate myocardial protection, such as that afforded by postconditioning remains a possibility, although the results from this study are inconclusive.

8 PUBLICATIONS AND PRESENTATIONS RELATING TO THIS THESIS

Chapter 1. Introduction

- **Lockie, T**, Nagel, E, Redwood, S, Plein, S. The Use of Cardiovascular Magnetic Resonance Imaging in Acute Coronary Syndromes. *Circulation* 2009;119; 1671-1681
- **Lockie T,** Plein S, Redwood S. Microvascular Obstruction Following Primary Angioplasty: Beyond the Epicardial Artery. *Heart Metab.* 2008;40:26-29

Chapter 2. Methods

- **T Lockie**, D Perera, K de Silva, I Webb, S Redwood. The Impact of Measuring Fractional Flow Reserve on Decision Making in the Cath Lab in an Unselected Cohort of Patients Being Considered for Coronary Revascularisation. *J Invasive Cardiol.* 2010 Sep;22 (9):413-6
- **Tim Lockie,** Masaki Ishiri, Eike Nagel, Mike Marber, Sven Plein. Validation of a Cycle Ergometer High resolution MR Stress Perfusion Technique in Normal Volunteers. *Moderated poster presentation British Cardiovascular Society Scientific Sessions, Manchester June 2010 Heart 2010; 96:A49; doi:10.1136/hrt.2010.196071.3*
- Christian Stehning, **Tim Lockie,** Eike Nagel, Sven Plein. Myocardial T1 During Multiple Bolus Injections. *Oral presentation at ISMRN, Hawaii, USA May 2010*

Chapter 3. Postconditioning in Acute Myocardial Infarction

- A Mather **T Lockie**, E Nagel, M Marber, D Perera, S Redwood, A Radjenovic, A Saha, J Greenwood, Sven Plein. Appearance of microvascular obstruction on high-resolution first-pass perfusion, early and late gadolinium enhancement CMR in patients with acute myocardial infarction. *J of Cardiovascular Magnetic Resonance* 2009, **11**:33-37

- **Tim Lockie**, Ian Webb, Amedeo Chiribiri, Mrin Saha, Rupert Williams, Sven Plein, Divaka Perera, Simon Redwood, Michael Marber. Postconditioning To Reduce Infarct Size Following Acute Myocardial Infarction. ***Best Original Resuscitation Science****, Moderated Poster Session, American Heart Association, Orlando, 2009. Circulation.* 2009;120:S1467-S1468.
- C. Jansen, A.Wiethoff, M. Makowski**, T. Lockie**, A. Chiribiri, R. Razavi, E. Nagel, G.Greil, S. Redwood, D. Perrera, R.M. Botnar Contrast enhanced magnetic resonance imaging of culprit lesions in patients with late presentation myocardial infarction. *Presentation at the AHA, Orlando, 2009; Circulation. 2009;120:S1201-S1220*

Chapter 4. High-Resolution Magnetic Resonance Perfusion

- Motwani M, **Lockie T**, Greenwood JP, Plein S . Accelerated, high spatial resolution cardiovascular magnetic resonance myocardial perfusion imaging. *J Nucl Cardiol. 2011 Oct;18(5):952-8.*
- **T Lockie**, M Ishiwa, D Perera, K de Silva, S Kozerke, M Marber, E Nagel, S Redwood, S Plein. High-resolution magnetic resonance myocardial perfusion imaging at 3 tesla to detect haemodynamically significant coronary stenoses as determined by fractional flow reserve. *Journal of the American College of Cardiology 2010 vol. 57 (1) pp. 70-5*
- ***Winner Young Investigator Award (Clinical Science), SCMR Scientific Sessions, Phoenix, Arizona, Jan2010. Journal of Cardiovascular Magnetic Resonance 2010, 12(Suppl 1):O3***
- Amedeo Chiribiri, Gilion Hautvast, **Tim Lockie**, Andreas Schuster, Boris Bigalke, Luca Olivotti, Simon Redwood, Marcel Breeuwer, Sven Plein, Eike Nagel Transmural perfusion gradient analysis by high-resolution MR versus fractional flow reserve for the assessment of coronary artery stenosis. *Journal of Cardiovascular Magnetic Resonance* 2012, 14(Suppl 1):O90 (1 February 2012)

Chapter 5. Synergistic Adaptations to Warm-Up Angina

- **T.P.E Lockie**, M.C Rolandi, A. Guilcher, D. Perera, K. De Silva, R. Williams, K.N. Asrress, K. Patel, S. Plein, P. Chowienczyk, M. Siebes, S.R Redwood, M.S Marber. Synergistic Adaptations to Exercise in the Systemic and Coronary Circulations that Underlie the Warm-Up Angina Phenomenon*. Circulation 2012 Nov 27;126(22):2565-74*
- *Associated Editorial*: Usman Baber and George Dangas. Exercise Physiology in the Cath Lab: Still Alive and Well! *Circulation. 2012 Nov 27;126(22):2550-2*
- C. Rolandi, **Tim Lockie,** Antoine Guilicher, Divaka Perera, Mike Marber, Simon Redwood, Maria Siebes. The Effect of Warm-Up Exercise on Myocardial Perfusion Studies with Wave Intensity Analysis. *Oral presentation at European Conference of the International Federation for Medical and Biological Engineering, September 14-18, 2011, Budapest, Hungary*
- **Tim Lockie,** Antoine Guilcher, Cristina Rolandi, Divaka Perera, Phil Chowienzyk, Sven Plein, Maria Siebes, Simon Redwood, Mike Marber. Warm Up Angina is Reduced Arterial Wave Reflection and Enhanced LV Relaxation Contribute to Warm-Up Angina. *Presented as moderated poster at British Cardiovascular Society Scientific Sessions, Manchester June 2011 Heart.* ***97****: A28-29. doi:10.1136/heartjnl-2011-300198.41*
- ***Young Investigator Finalist –Advanced Cardiovascular Interventions, British Cardiovascular Intervention Society, London, Jan 2011***
- **Tim Lockie,** Antoine Guilcher, Cristina Rolandi, Divaka Perera, Phil Chowienzyk, Sven Plein, Maria Siebes, Simon Redwood, Mike Marber. The Heart Sucks While the Circulation Complies. *Poster presentation MRS/AMS/RCP meeting for Clinical Scientists RCP Feb 2011*

Chapter 6. Transmural Flow Heterogeneity During Exercise.

- A Chiribiri, G Hautvast, **T Lockie**, A Schuster, B Bigalke, L Olivotti, S Redwood, M Breeuwer, S Plein, E Nagel. Quantitative analysis of transmural perfusion gradients by high-resolution magnetic resonance versus fractional flow reserve for the assessment of coronary artery stenosis severity and location. *Accepted for publication JACC:Imaging July 2012 (in press)*

- G Hautvast, A Chiribiri, **T Lockie**, M Breeuwer, E Nagel, S Plein. Quantitative Analysis of Transmural Gradients in Perfusion CMR Images. *Magn Reson Med*. 2011 Nov;66(5):1477-87
- Asrress KN, **Lockie T,** Williams R, , Biglands J, De Silva K, Radjenovic A, Kozerke S, Nagel E, Chowienczyk P, Marber M, Redwood SR, Plein S. Increased endocardial to epicardial flow ratio present at rest disappears during exercise stress in normal volunteers. *Oral presentation at SCMR, Orlando, Jan 2012. Journal of Cardiovascular Magnetic Resonance* 2012, **14**(Suppl 1):P230 (1 February 2012)
- Asrress KN, **Lockie T,** Williams R, , Lossnitzer D, Jogiya R, Kozerke S, Chowienczyk P, Greil G, Marber MS, Nagel E, Redwood SR, Plein S. The Use of Feature Tracking to Assess Ventricular Strain During Exercise Stress in Normal Volunteers. *Oral presentation at SCMR, Orlando, Jan 2012. Journal of Cardiovascular Magnetic Resonance* 2012, **14**(Suppl 1):P226 (1 February 2012)
- **Tim Lockie,** Hanson Tang, Masaki Ishiri, Kalpa De Silva, Mike Marber, Eike Nagel, Sven Plein. Transmural Flow Heterogeneoity can be Demonstrated in Normal Volunteers Using Full Quantification of *kt*-SENSE Accelerated Myocardial Perfusion at 3Tesla. *Poster presentation at EuroCMR, Florence, Italy, May 2010.*
- **Tim Lockie,** Masaki Ishiri, Eike Nagel, Mike Marber, Sven Plein. The use of a cycle ergometer to calculate myocardial perfusion reserve with kt-SENSE accelerated myocardial perfusion imaging at 3 Tesla. *Presented at SCMR Scientific Sessions, Phoenix, Arizona, USA, Jan 2010. Journal of Cardiovascular Magnetic Resonance* 2010, **12**(Suppl 1):O145

9 REFERENCES

1. Bateman TM, Prvulovich E. Assessment of prognosis in chronic coronary artery disease. *Heart*. 2004;90 Suppl 5:v10-15
2. Heberden J. A letter to dr heberden, concerning the angina pectoris; and an account of the dissection of one; who had been troubled with that disorder. *Medical Transactions, Royal College of Physicians in London*. 1785;3:1-11
3. Kuo L, Davis MJ, Chilian WM. Longitudinal gradients for endothelium-dependent and -independent vascular responses in the coronary microcirculation. *Circulation*. 1995;92:518-525
4. Kuo L, Davis MJ, Chilian WM. Myogenic activity in isolated subepicardial and subendocardial coronary arterioles. *Am J Physiol*. 1988;255:H1558-1562
5. Jones CJ, Kuo L, Davis MJ, Chilian WM. Regulation of coronary blood flow: Coordination of heterogeneous control mechanisms in vascular microdomains. *Cardiovasc Res*. 1995;29:585-596
6. Spaan JA, ter Wee R, van Teeffelen JW, Streekstra G, Siebes M, Kolyva C, Vink H, Fokkema DS, VanBavel E. Visualisation of intramural coronary vasculature by an imaging cryomicrotome suggests compartmentalisation of myocardial perfusion areas. *Med Biol Eng Comput*. 2005;43:431-435
7. Feigl EO. Coronary physiology. *Physiol Rev*. 1983;63:1-205
8. Laughlin MH, Tomanek RJ. Myocardial capillarity and maximal capillary diffusion capacity in exercise-trained dogs. *J Appl Physiol*. 1987;63:1481-1486
9. Richalet JP, Soulard C, Nitenberg A, Teisseire B, de Bovee J, Seroussi S. Myocardial oxygen extraction and oxygen-hemoglobin equilibrium curve during moderate exercise. *Eur J Appl Physiol Occup Physiol*. 1981;47:27-39
10. Suga H. Ventricular energetics. *Physiol Rev*. 1990;70:247-277
11. Jorgensen CR, Gobel FL, Taylor HL, Wang Y. Myocardial blood flow and oxygen consumption during exercise. *Ann N Y Acad Sci*. 1977;301:213-223
12. Sonnenblick EH, Braunwald E, Williams JF, Jr., Glick G. Effects of exercise on myocardial force-velocity relations in intact unanesthetized man: Relative roles of changes in heart rate, sympathetic activity, and ventricular dimensions. *J Clin Invest*. 1965;44:2051-2062
13. Merkus D, Sorop O, Houweling B, Hoogteijling BA, Duncker DJ. Kca+ channels contribute to exercise-induced coronary vasodilation in swine. *Am J Physiol Heart Circ Physiol*. 2006;291:H2090-2097
14. Koch-Weser J, Blinks JR. The influence of the interval between beats on myocardial contractility. *Pharmacol Rev*. 1963;15:601-652
15. Ekstrom-Jodal B, Haggendal E, Malmberg R, Svedmyr N. The effect of adrenergic -receptor blockade on coronary circulation in man during work. *Acta Med Scand*. 1972;191:245-248
16. Jorgensen CR, Wang K, Wang Y, Gobel FL, Nelson RR, Taylor H. Effect of propranolol on myocardial oxygen consumption and its hemodynamic correlates during upright exercise. *Circulation*. 1973;48:1173-1182
17. Poliner LR, Dehmer GJ, Lewis SE, Parkey RW, Blomqvist CG, Willerson JT. Left ventricular performance in normal subjects: A comparison of the responses to exercise in the upright and supine positions. *Circulation*. 1980;62:528-534

18. Horwitz LD, Atkins JM, Leshin SJ. Role of the frank-starling mechanism in exercise. *Circ Res*. 1972;31:868-875
19. Vatner SF, Franklin D, Higgins CB, Patrick T, Braunwald E. Left ventricular response to severe exertion in untethered dogs. *J Clin Invest*. 1972;51:3052-3060
20. Khouri EM, Gregg DE, Rayford CR. Effect of exercise on cardiac output, left coronary flow and myocardial metabolism in the unanesthetized dog. *Circ Res*. 1965;17:427-437
21. Ball RM, Bache RJ, Cobb FR, Greenfield JC, Jr. Regional myocardial blood flow during graded treadmill exercise in the dog. *J Clin Invest*. 1975;55:43-49
22. Nelson RR, Gobel FL, Jorgensen CR, Wang K, Wang Y, Taylor HL. Hemodynamic predictors of myocardial oxygen consumption during static and dynamic exercise. *Circulation*. 1974;50:1179-1189
23. Duncker DJ, Ishibashi Y, Bache RJ. Effect of treadmill exercise on transmural distribution of blood flow in hypertrophied left ventricle. *Am J Physiol*. 1998;275:H1274-1282
24. Kitamura K, Jorgensen CR, Gobel FL, Taylor HL, Wang Y. Hemodynamic correlates of myocardial oxygen consumption during upright exercise. *J Appl Physiol*. 1972;32:516-522
25. Namdar M, Koepfli P, Grathwohl R, Siegrist PT, Klainguti M, Schepis T, Delaloye R, Wyss CA, Fleischmann SP, Gaemperli O, Kaufmann PA. Caffeine decreases exercise-induced myocardial flow reserve. *J Am Coll Cardiol*. 2006;47:405-410
26. Wyss CA, Koepfli P, Mikolajczyk K, Burger C, von Schulthess GK, Kaufmann PA. Bicycle exercise stress in pet for assessment of coronary flow reserve: Repeatability and comparison with adenosine stress. *J Nucl Med*. 2003;44:146-154
27. Heiss HW, Barmeyer J, Wink K, Hell G, Cerny FJ, Keul J, Reindell H. Studies on the regulation of myocardial blood flow in man. I.: Training effects on blood flow and metabolism of the healthy heart at rest and during standardized heavy exercise. *Basic Res Cardiol*. 1976;71:658-675
28. Richmond KN, Tune JD, Gorman MW, Feigl EO. Role of k(atp)(+) channels and adenosine in the control of coronary blood flow during exercise. *J Appl Physiol*. 2000;89:529-536
29. Parks CM, Manohar M. Distribution of blood flow during moderate and strenuous exercise in ponies (equus caballus). *American journal of veterinary research*. 1983;44:1861-1866
30. Parks CM, Manohar M. Transmural coronary vasodilator reserve and flow distribution during severe exercise in ponies. *J Appl Physiol*. 1983;54:1641-1652
31. Cerretelli P DPP. Gas exchange in exercise. *Handbook of physiology. The respiratory system. Gas exchange*. Bethesda; 1987.
32. Harrison MH. Effects on thermal stress and exercise on blood volume in humans. *Physiol Rev*. 1985;65:149-209
33. Messer JV, Wagman RJ, Levine HJ, Neill WA, Krasnow N, Gorlin R. Patterns of human myocardial oxygen extraction during rest and exercise. *J Clin Invest*. 1962;41:725-742

34. Grubbstrom J, Berglund B, Kaijser L. Myocardial blood flow and lactate metabolism at rest and during exercise with reduced arterial oxygen content. *Acta Physiol Scand*. 1991;142:467-474
35. Bache RJ, Dai XZ, Herzog CA, Schwartz JS. Effects of nonselective and selective alpha 1-adrenergic blockade on coronary blood flow during exercise. *Circ Res*. 1987;61:II36-41
36. Bache RJ, Homans DC, Schwartz JS, Dai XZ. Differences in the effects of alpha-1 adrenergic blockade with prazosin and indoramin on coronary blood flow during exercise. *J Pharmacol Exp Ther*. 1988;245:232-237
37. Duncker DJ, Bache RJ. Regulation of coronary blood flow during exercise. *Physiol Rev*. 2008;88:1009-1086
38. Spaan JA, M, Piek JJ, Siebes,. Coronary circulation and haemodynamics. In: Sperelakis Nea, ed. *Heart physiology and pathophysiology*. Academic Press; 2001:19-44.
39. Spaan JA, Siebes, M, Verhoeff, B-J, Piek, JJ. The coronary circulation. In: al KSe, ed. *Interventional cardiology*. McGraw Hill; 2007:25-45.
40. Hanley FL, Messina LM, Grattan MT, Hoffman IE. The effect of coronary inflow pressure on coronary vascular resistance in the isolated dog heart. *Circ Res*. 1984;54:760-772
41. Verhoeff BJ, Siebes M, Meuwissen M, Atasever B, Voskuil M, de Winter RJ, Koch KT, Tijssen JG, Spaan JA, Piek JJ. Influence of percutaneous coronary intervention on coronary microvascular resistance index. *Circulation*. 2005;111:76-82
42. Brandes RP, Schmitz-Winnenthal FH, Feletou M, Godecke A, Huang PL, Vanhoutte PM, Fleming I, Busse R. An endothelium-derived hyperpolarizing factor distinct from no and prostacyclin is a major endothelium-dependent vasodilator in resistance vessels of wild-type and endothelial no synthase knockout mice. *Proc Natl Acad Sci U S A*. 2000;97:9747-9752
43. Spaan JA. Mechanical determinants of myocardial perfusion. *Basic Res Cardiol*. 1995;90:89-102
44. Westerhof N, Boer C, Lamberts RR, Sipkema P. Cross-talk between cardiac muscle and coronary vasculature. *Physiol Rev*. 2006;86:1263-1308
45. Sanders M, White FC, Peterson TM, Bloor CM. Characteristics of coronary blood flow and transmural distribution in miniature pigs. *Am J Physiol*. 1978;235:H601-609
46. Barnard RJ, Duncan HW, Livesay JJ, Buckberg GD. Coronary vasodilator reserve and flow distribution during near-maximal exercise in dogs. *J Appl Physiol*. 1977;43:988-992
47. Downey JM, Kirk ES. Inhibition of coronary blood flow by a vascular waterfall mechanism. *Circ Res*. 1975;36:753-760
48. Spaan JA. *Coronary blood flow: Mechanics, distribution and control*. Dordrecht: Kluwer Academic; 1991.
49. Duncker DJ, Zhang J, Bache RJ. Coronary pressure-flow relation in left ventricular hypertrophy. Importance of changes in back pressure versus changes in minimum resistance. *Circ Res*. 1993;72:579-587

50. Bender SB, van Houwelingen MJ, Merkus D, Duncker DJ, Laughlin MH. Quantitative analysis of exercise-induced enhancement of early- and late-systolic retrograde coronary blood flow. *J Appl Physiol*.108:507-514
51. von Restorff W, Holtz J, Bassenge E. Exercise induced augmentation of myocardial oxygen extraction in spite of normal coronary dilatory capacity in dogs. *Pflugers Arch*. 1977;372:181-185
52. White FC, Roth DM, Bloor CM. Coronary collateral reserve during exercise induced ischemia in swine. *Basic Res Cardiol*. 1989;84:42-54
53. Breisch EA, White FC, Nimmo LE, McKirnan MD, Bloor CM. Exercise-induced cardiac hypertrophy: A correlation of blood flow and microvasculature. *Journal of applied physiology*. 1986;60:1259-1267
54. Laughlin MH, Burns JW, Fanton J, Ripperger J, Peterson DF. Coronary blood flow reserve during +gz stress and treadmill exercise in miniature swine. *J Appl Physiol*. 1988;64:2589-2596
55. Siebes M, Campbell CS, D'Argenio DZ. Fluid dynamics of a partially collapsible stenosis in a flow model of the coronary circulation. *J Biomech Eng*. 1996;118:489-497
56. Mates RE, Gupta RL, Bell AC, Klocke FJ. Fluid dynamics of coronary artery stenosis. *Circ Res*. 1978;42:152-162
57. Kern MJ, Lerman A, Bech JW, De Bruyne B, Eeckhout E, Fearon WF, Higano ST, Lim MJ, Meuwissen M, Piek JJ, Pijls NH, Siebes M, Spaan JA. Physiological assessment of coronary artery disease in the cardiac catheterization laboratory: A scientific statement from the american heart association committee on diagnostic and interventional cardiac catheterization, council on clinical cardiology. *Circulation*. 2006;114:1321-1341
58. Canty JM, Jr., Smith TP, Jr. Adenosine-recruitable flow reserve is absent during myocardial ischemia in unanesthetized dogs studied in the basal state. *Circ Res*. 1995;76:1079-1087
59. Duncker DJ, Bache RJ. Regulation of coronary vasomotor tone under normal conditions and during acute myocardial hypoperfusion. *Pharmacol Ther*. 2000;86:87-110
60. Bache RJ, Cobb FR. Effect of maximal coronary vasodilation on transmural myocardial perfusion during tachycardia in the awake dog. *Circ Res*. 1977;41:648-653
61. Bache RJ, Duncker, D.J. . Coronary steal. *Acc Cur J Rev*. 1994;3:9-12
62. Hoffman JI, Spaan JA. Pressure-flow relations in coronary circulation. *Physiol Rev*. 1990;70:331-390
63. Boudoulas H. Diastolic time: The forgotten dynamic factor. Implications for myocardial perfusion. *Acta Cardiol*. 1991;46:61-71
64. Holmberg S, Serzysko W, Varnauskas E. Coronary circulation during heavy exercise in control subjects and patients with coronary heart disease. *Acta Med Scand*. 1971;190:465-480
65. Holmberg S, Varnauskas E. Coronary circulation during pacing-induced tachycardia. *Acta Med Scand*. 1971;190:481-490
66. Flynn AE, Coggins DL, Goto M, Aldea GS, Austin RE, Doucette JW, Husseini W, Hoffman JI. Does systolic subepicardial perfusion come from retrograde subendocardial flow? *Am J Physiol*. 1992;262:H1759-1769

67. Nabel EG, Selwyn AP, Ganz P. Paradoxical narrowing of atherosclerotic coronary arteries induced by increases in heart rate. *Circulation*. 1990;81:850-859
68. Epstein SE, Talbot TL. Dynamic coronary tone in precipitation, exacerbation and relief of angina pectoris. *Am J Cardiol*. 1981;48:797-803
69. Fokkema DS, VanTeeffelen JW, Dekker S, Vergroesen I, Reitsma JB, Spaan JA. Diastolic time fraction as a determinant of subendocardial perfusion. *Am J Physiol Heart Circ Physiol*. 2005;288:H2450-2456
70. Ferro G, Duilio C, Spinelli L, Liucci GA, Mazza F, Indolfi C. Relation between diastolic perfusion time and coronary artery stenosis during stress-induced myocardial ischemia. *Circulation*. 1995;92:342-347
71. Braunwald E, Sarnoff SJ, Stainsby WN. Determinants of duration and mean rate of ventricular ejection. *Circ Res*. 1958;6:319-325
72. Shaver JA, Kroetz FW, Leonard JJ, Paley HW. The effect of steady-state increases in systemic arterial pressure on the duration of left ventricular ejection time. *J Clin Invest*. 1968;47:217-230
73. Lewis RP, Boudoulas H, Forester WF, Weissler AM. Shortening of electromechanical systole as a manifestation of excessive adrenergic stimulation in acute myocardial infarction. *Circulation*. 1972;46:856-862
74. Merkus D, Kajiya F, Vink H, Vergroesen I, Dankelman J, Goto M, Spaan JA. Prolonged diastolic time fraction protects myocardial perfusion when coronary blood flow is reduced. *Circulation*. 1999;100:75-81
75. Kolyva C, Verhoeff BJ, Spaan JA, Piek JJ, Siebes M. Increased diastolic time fraction as beneficial adjunct of alpha1-adrenergic receptor blockade after percutaneous coronary intervention. *Am J Physiol Heart Circ Physiol*. 2008;295:H2054-2060
76. Aversano T, Becker LC. Persistence of coronary vasodilator reserve despite functionally significant flow reduction. *Am J Physiol*. 1985;248:H403-411
77. Canty JM, Jr., Klocke FJ. Reduced regional myocardial perfusion in the presence of pharmacologic vasodilator reserve. *Circulation*. 1985;71:370-377
78. Gorman MW, Sparks HV, Jr. Progressive coronary vasoconstriction during relative ischemia in canine myocardium. *Circ Res*. 1982;51:411-420
79. Pantely GA, Bristow JD, Swenson LJ, Ladley HD, Johnson WB, Anselone CG. Incomplete coronary vasodilation during myocardial ischemia in swine. *Am J Physiol*. 1985;249:H638-647
80. Heusch G, Guth BD, Seitelberger R, Ross J, Jr. Attenuation of exercise-induced myocardial ischemia in dogs with recruitment of coronary vasodilator reserve by nifedipine. *Circulation*. 1987;75:482-490
81. Laxson DD, Dai XZ, Homans DC, Bache RJ. The role of alpha 1- and alpha 2-adrenergic receptors in mediation of coronary vasoconstriction in hypoperfused ischemic myocardium during exercise. *Circ Res*. 1989;65:1688-1697
82. Pauca AL, Wallenhaupt SL, Kon ND, Tucker WY. Does radial artery pressure accurately reflect aortic pressure? *Chest*. 1992;102:1193-1198
83. Rowell LB, Brengelmann GL, Blackmon JR, Bruce RA, Murray JA. Disparities between aortic and peripheral pulse pressures induced by upright exercise and vasomotor changes in man. *Circulation*. 1968;37:954-964

84. Westerhof N, O'Rourke MF. Haemodynamic basis for the development of left ventricular failure in systolic hypertension and for its logical therapy. *J Hypertens*. 1995;13:943-952
85. Boutouyrie P, Bussy C, Lacolley P, Girerd X, Laloux B, Laurent S. Association between local pulse pressure, mean blood pressure, and large-artery remodeling. *Circulation*. 1999;100:1387-1393
86. Safar ME, Blacher J, Pannier B, Guerin AP, Marchais SJ, Guyonvarc'h PM, London GM. Central pulse pressure and mortality in end-stage renal disease. *Hypertension*. 2002;39:735-738
87. Wilkinson IB, Mohammad NH, Tyrrell S, Hall IR, Webb DJ, Paul VE, Levy T, Cockcroft JR. Heart rate dependency of pulse pressure amplification and arterial stiffness. *Am J Hypertens*. 2002;15:24-30
88. Munir S, Jiang B, Guilcher A, Brett S, Redwood S, Marber M, Chowienczyk P. Exercise reduces arterial pressure augmentation through vasodilation of muscular arteries in humans. *Am J Physiol Heart Circ Physiol*. 2008;294:H1645-1650
89. Sharman JE, McEniery CM, Campbell RI, Coombes JS, Wilkinson IB, Cockcroft JR. The effect of exercise on large artery haemodynamics in healthy young men. *Eur J Clin Invest*. 2005;35:738-744
90. Safar ME, London GM. Therapeutic studies and arterial stiffness in hypertension: Recommendations of the european society of hypertension. The clinical committee of arterial structure and function. Working group on vascular structure and function of the european society of hypertension. *J Hypertens*. 2000;18:1527-1535
91. Murgo JP, Westerhof N, Giolma JP, Altobelli SA. Aortic input impedance in normal man: Relationship to pressure wave forms. *Circulation*. 1980;62:105-116
92. London G, Guerin A, Pannier B, Marchais S, Benetos A, Safar M. Increased systolic pressure in chronic uremia. Role of arterial wave reflections. *Hypertension*. 1992;20:10-19
93. Marchais SJ, Guerin AP, Pannier BM, Levy BI, Safar ME, London GM. Wave reflections and cardiac hypertrophy in chronic uremia. Influence of body size. *Hypertension*. 1993;22:876-883
94. Buckberg GD, Fixler DE, Archie JP, Hoffman JI. Experimental subendocardial ischemia in dogs with normal coronary arteries. *Circ Res*. 1972;30:67-81
95. Murgo JP, Westerhof N, Giolma JP, Altobelli SA. Effects of exercise on aortic input impedance and pressure wave forms in normal humans. *Circ Res*. 1981;48:334-343
96. Armentano RL, Levenson J, Barra JG, Fischer EI, Breitbart GJ, Pichel RH, Simon A. Assessment of elastin and collagen contribution to aortic elasticity in conscious dogs. *Am J Physiol*. 1991;260:H1870-1877
97. Edwards RJ, Redwood SR, Lambiase PD, Tomset E, Rakhit RD, Marber MS. Antiarrhythmic and anti-ischaemic effects of angina in patients with and without coronary collaterals. *Heart*. 2002;88:604-610
98. Marber MS, Joy MD, Yellon DM. Is warm-up in angina ischaemic preconditioning? *Br Heart J*. 1994;72:213-215

99. Yellon DM, Baxter GF, Marber MS. Angina reassessed: Pain or protector? *Lancet*. 1996;347:1159-1162
100. MacAlpin RN KA. Adaptation to exercise in angina pectoris. The electrocardiogram during treadmill walking and coronary angiographic findings. *Circulation*. 1966;33:118-131
101. Jaffe MD, Quinn NK. Warm-up phenomenon in angina pectoris. *Lancet*. 1980;2:934-936
102. Joy M, Cairns AW, Sprigings D. Observations on the warm up phenomenon in angina pectoris. *Br Heart J*. 1987;58:116-121
103. Williams DO, Bass TA, Gewirtz H, Most AS. Adaptation to the stress of tachycardia in patients with coronary artery disease: Insight into the mechanism of the warm-up phenomenon. *Circulation*. 1985;71:687-692
104. Okazaki Y, Kodama K, Sato H, Kitakaze M, Hirayama A, Mishima M, Hori M, Inoue M. Attenuation of increased regional myocardial oxygen consumption during exercise as a major cause of warm-up phenomenon. *J Am Coll Cardiol*. 1993;21:1597-1604
105. Tzivoni D, Maybaum S. Attenuation of severity of myocardial ischemia during repeated daily ischemic episodes. *J Am Coll Cardiol*. 1997;30:119-124
106. Waters DD, McCans JL, Crean PA. Serial exercise testing in patients with effort angina: Variable tolerance, fixed threshold. *J Am Coll Cardiol*. 1985;6:1011-1015
107. Bagger JP. Coronary sinus blood flow determination by the thermodilution technique: Influence of catheter position and respiration. *Cardiovasc Res*. 1985;19:27-31
108. van den Wijngaard JP, Kolyva C, Siebes M, Dankelman J, van Gemert MJ, Piek JJ, Spaan JA. Model prediction of subendocardial perfusion of the coronary circulation in the presence of an epicardial coronary artery stenosis. *Med Biol Eng Comput*. 2008
109. Murry CE, Jennings RB, Reimer KA. Preconditioning with ischemia: A delay of lethal cell injury in ischemic myocardium. *Circulation*. 1986;74:1124-1136
110. Kloner RA, Bolli R, Marban E, Reinlib L, Braunwald E. Medical and cellular implications of stunning, hibernation, and preconditioning: An nhlbi workshop. *Circulation*. 1998;97:1848-1867
111. Li YW, Whittaker P, Kloner RA. The transient nature of the effect of ischemic preconditioning on myocardial infarct size and ventricular arrhythmia. *Am Heart J*. 1992;123:346-353
112. Kloner RA, Yellon D. Does ischemic preconditioning occur in patients? *J Am Coll Cardiol*. 1994;24:1133-1142
113. Maybaum S, Ilan M, Mogilevsky J, Tzivoni D. Improvement in ischemic parameters during repeated exercise testing: A possible model for myocardial preconditioning. *Am J Cardiol*. 1996;78:1087-1091
114. Murry CE, Richard VJ, Jennings RB, Reimer KA. Myocardial protection is lost before contractile function recovers from ischemic preconditioning. *Am J Physiol*. 1991;260:H796-804
115. Bogaty P, Kingma JG, Jr., Robitaille NM, Plante S, Simard S, Charbonneau L, Dumesnil JG. Attenuation of myocardial ischemia with repeated exercise in subjects with chronic stable angina: Relation to myocardial contractility,

intensity of exercise and the adenosine triphosphate-sensitive potassium channel. *J Am Coll Cardiol*. 1998;32:1665-1671
116. Bogaty P, Kingma JG, Guimond J, Poirier P, Boyer L, Charbonneau L, Dagenais GR. Myocardial perfusion imaging findings and the role of adenosine in the warm-up angina phenomenon. *J Am Coll Cardiol*. 2001;37:463-469
117. Correa SD, Schaefer S. Blockade of k(atp) channels with glibenclamide does not abolish preconditioning during demand ischemia. *Am J Cardiol*. 1997;79:75-78
118. Gould KL. Pressure-flow characteristics of coronary stenoses in unsedated dogs at rest and during coronary vasodilation. *Circ Res*. 1978;43:242-253
119. Bolli R. Mechanism of myocardial "stunning". *Circulation*. 1990;82:723-738
120. Murray CJ, Lopez AD. Alternative projections of mortality and disability by cause 1990-2020: Global burden of disease study. *Lancet*. 1997;349:1498-1504
121. Risk stratification and survival after myocardial infarction. *N Engl J Med*. 1983;309:331-336
122. Volpi A, De Vita C, Franzosi MG, Geraci E, Maggioni AP, Mauri F, Negri E, Santoro E, Tavazzi L, Tognoni G. Determinants of 6-month mortality in survivors of myocardial infarction after thrombolysis. Results of the gissi-2 data base. The ad hoc working group of the gruppo italiano per lo studio della sopravvivenza nell'infarto miocardico (gissi)-2 data base. *Circulation*. 1993;88:416-429
123. Pfeffer MA, Pfeffer JM, Lamas GA. Development and prevention of congestive heart failure following myocardial infarction. *Circulation*. 1993;87:IV120-125
124. Simes RJ, Topol EJ, Holmes DR, Jr., White HD, Rutsch WR, Vahanian A, Simoons ML, Morris D, Betriu A, Califf RM, et al. Link between the angiographic substudy and mortality outcomes in a large randomized trial of myocardial reperfusion. Importance of early and complete infarct artery reperfusion. Gusto-i investigators. *Circulation*. 1995;91:1923-1928
125. Fieno DS, Hillenbrand HB, Rehwald WG, Harris KR, Decker RS, Parker MA, Klocke FJ, Kim RJ, Judd RM. Infarct resorption, compensatory hypertrophy, and differing patterns of ventricular remodeling following myocardial infarctions of varying size. *J Am Coll Cardiol*. 2004;43:2124-2131
126. Keeley EC, Boura JA, Grines CL. Primary angioplasty versus intravenous thrombolytic therapy for acute myocardial infarction: A quantitative review of 23 randomised trials. *Lancet*. 2003;361:13-20
127. Christian TF, Schwartz RS, Gibbons RJ. Determinants of infarct size in reperfusion therapy for acute myocardial infarction. *Circulation*. 1992;86:81-90
128. A clinical trial comparing primary coronary angioplasty with tissue plasminogen activator for acute myocardial infarction. The global use of strategies to open occluded coronary arteries in acute coronary syndromes (gusto iib) angioplasty substudy investigators. *N Engl J Med*. 1997;336:1621-1628

129. Lincoff AM, Topol EJ. Illusion of reperfusion. Does anyone achieve optimal reperfusion during acute myocardial infarction? *Circulation*. 1993;88:1361-1374
130. Ragosta M, Camarano G, Kaul S, Powers ER, Sarembock IJ, Gimple LW. Microvascular integrity indicates myocellular viability in patients with recent myocardial infarction. New insights using myocardial contrast echocardiography. *Circulation*. 1994;89:2562-2569
131. Rochitte CE, Lima JA, Bluemke DA, Reeder SB, McVeigh ER, Furuta T, Becker LC, Melin JA. Magnitude and time course of microvascular obstruction and tissue injury after acute myocardial infarction. *Circulation*. 1998;98:1006-1014
132. Park JL, Lucchesi BR. Mechanisms of myocardial reperfusion injury. *Ann Thorac Surg*. 1999;68:1905-1912
133. Yellon DM, Hausenloy DJ. Myocardial reperfusion injury. *N Engl J Med*. 2007;357:1121-1135
134. Hearse DJ, Humphrey SM, Nayler WG, Slade A, Border D. Ultrastructural damage associated with reoxygenation of the anoxic myocardium. *J Mol Cell Cardiol*. 1975;7:315-324
135. Hearse DJ, Humphrey SM, Bullock GR. The oxygen paradox and the calcium paradox: Two facets of the same problem? *J Mol Cell Cardiol*. 1978;10:641-668
136. Hearse DJ, Bolli R. Reperfusion induced injury: Manifestations, mechanisms, and clinical relevance. *Cardiovasc Res*. 1992;26:101-108
137. Zhao ZQ, Vinten-Johansen J. Postconditioning: Reduction of reperfusion-induced injury. *Cardiovasc Res*. 2006;70:200-211
138. Garcia-Dorado D, Ruiz-Meana M, Padilla F, Rodriguez-Sinovas A, Mirabet M. Gap junction-mediated intercellular communication in ischemic preconditioning. *Cardiovasc Res*. 2002;55:456-465
139. Hausenloy D, Wynne A, Duchen M, Yellon D. Transient mitochondrial permeability transition pore opening mediates preconditioning-induced protection. *Circulation*. 2004;109:1714-1717
140. Tomai F, Crea F, Chiariello L, Gioffre PA. Ischemic preconditioning in humans: Models, mediators, and clinical relevance. *Circulation*. 1999;100:559-563
141. Zhao ZQ, Corvera JS, Halkos ME, Kerendi F, Wang NP, Guyton RA, Vinten-Johansen J. Inhibition of myocardial injury by ischemic postconditioning during reperfusion: Comparison with ischemic preconditioning. *Am J Physiol Heart Circ Physiol*. 2003;285:H579-588
142. Kin H, Zatta AJ, Lofye MT, Amerson BS, Halkos ME, Kerendi F, Zhao ZQ, Guyton RA, Headrick JP, Vinten-Johansen J. Postconditioning reduces infarct size via adenosine receptor activation by endogenous adenosine. *Cardiovasc Res*. 2005;67:124-133
143. Kin H, Zhao ZQ, Sun HY, Wang NP, Corvera JS, Halkos ME, Kerendi F, Guyton RA, Vinten-Johansen J. Postconditioning attenuates myocardial ischemia-reperfusion injury by inhibiting events in the early minutes of reperfusion. *Cardiovasc Res*. 2004;62:74-85

144. Mykytenko J, Kerendi F, Reeves JG, Kin H, Zatta AJ, Jiang R, Guyton RA, Vinten-Johansen J, Zhao ZQ. Long-term inhibition of myocardial infarction by postconditioning during reperfusion. *Basic Res Cardiol*. 2007;102:90-100
145. Sun HY, Wang NP, Halkos M, Kerendi F, Kin H, Guyton RA, Vinten-Johansen J, Zhao ZQ. Postconditioning attenuates cardiomyocyte apoptosis via inhibition of jnk and p38 mitogen-activated protein kinase signaling pathways. *Apoptosis*. 2006;11:1583-1593
146. Bolli R, Marban E. Molecular and cellular mechanisms of myocardial stunning. *Physiol Rev*. 1999;79:609-634
147. Couvreur N, Lucats L, Tissier R, Bize A, Berdeaux A, Ghaleh B. Differential effects of postconditioning on myocardial stunning and infarction: A study in conscious dogs and anesthetized rabbits. *Am J Physiol Heart Circ Physiol*. 2006;291:H1345-1350
148. Staat P, Rioufol G, Piot C, Cottin Y, Cung TT, L'Huillier I, Aupetit JF, Bonnefoy E, Finet G, Andre-Fouet X, Ovize M. Postconditioning the human heart. *Circulation*. 2005;112:2143-2148
149. Laskey WK. Brief repetitive balloon occlusions enhance reperfusion during percutaneous coronary intervention for acute myocardial infarction: A pilot study. *Catheter Cardiovasc Interv*. 2005;65:361-367
150. Yang XC, Liu Y, Wang LF, Cui L, Wang T, Ge YG, Wang HS, Li WM, Xu L, Ni ZH, Liu SH, Zhang L, Jia HM, Vinten-Johansen J, Zhao ZQ. Reduction in myocardial infarct size by postconditioning in patients after percutaneous coronary intervention. *J Invasive Cardiol*. 2007;19:424-430
151. Ma XJ, Zhang XH, Li CM, Luo M. Effect of postconditioning on coronary blood flow velocity and endothelial function in patients with acute myocardial infarction. *Scand Cardiovasc J*. 2006;40:327-333
152. Horwitz LD, Fennessey PV, Shikes RH, Kong Y. Marked reduction in myocardial infarct size due to prolonged infusion of an antioxidant during reperfusion. *Circulation*. 1994;89:1792-1801
153. Farb A, Kolodgie FD, Jenkins M, Virmani R. Myocardial infarct extension during reperfusion after coronary artery occlusion: Pathologic evidence. *J Am Coll Cardiol*. 1993;21:1245-1253
154. Miki T, Swafford AN, Cohen MV, Downey JM. Second window of protection against infarction in conscious rabbits: Real or artifactual. *J Mol Cell Cardiol*. 1999;31:809-816
155. Fox K, Garcia MA, Ardissino D, Buszman P, Camici PG, Crea F, Daly C, De Backer G, Hjemdahl P, Lopez-Sendon J, Marco J, Morais J, Pepper J, Sechtem U, Simoons M, Thygesen K, Priori SG, Blanc JJ, Budaj A, Camm J, Dean V, Deckers J, Dickstein K, Lekakis J, McGregor K, Metra M, Osterspey A, Tamargo J, Zamorano JL. Guidelines on the management of stable angina pectoris: Executive summary: The task force on the management of stable angina pectoris of the european society of cardiology. *Eur Heart J*. 2006;27:1341-1381
156. Schwitter J, Wacker CM, van Rossum AC, Lombardi M, Al-Saadi N, Ahlstrom H, Dill T, Larsson HB, Flamm SD, Marquardt M, Johansson L. Mr-impact: Comparison of perfusion-cardiac magnetic resonance with single-photon

emission computed tomography for the detection of coronary artery disease in a multicentre, multivendor, randomized trial. *Eur Heart J*. 2008;29:480-489
157. Zaret BL, Wackers FJ. Nuclear cardiology (2). *N Engl J Med*. 1993;329:855-863
158. Zaret BL, Wackers FJ. Nuclear cardiology (1). *N Engl J Med*. 1993;329:775-783
159. Schinkel AF, Bax JJ, Geleijnse ML, Boersma E, Elhendy A, Roelandt JR, Poldermans D. Noninvasive evaluation of ischaemic heart disease: Myocardial perfusion imaging or stress echocardiography? *Eur Heart J*. 2003;24:789-800
160. Underwood SR, Anagnostopoulos C, Cerqueira M, Ell PJ, Flint EJ, Harbinson M, Kelion AD, Al-Mohammad A, Prvulovich EM, Shaw LJ, Tweddel AC. Myocardial perfusion scintigraphy: The evidence. *Eur J Nucl Med Mol Imaging*. 2004;31:261-291
161. Hachamovitch R, Berman DS, Shaw LJ, Kiat H, Cohen I, Cabico JA, Friedman J, Diamond GA. Incremental prognostic value of myocardial perfusion single photon emission computed tomography for the prediction of cardiac death: Differential stratification for risk of cardiac death and myocardial infarction. *Circulation*. 1998;97:535-543
162. Shaw LJ, Berman DS, Maron DJ, Mancini GB, Hayes SW, Hartigan PM, Weintraub WS, O'Rourke RA, Dada M, Spertus JA, Chaitman BR, Friedman J, Slomka P, Heller GV, Germano G, Gosselin G, Berger P, Kostuk WJ, Schwartz RG, Knudtson M, Veledar E, Bates ER, McCallister B, Teo KK, Boden WE. Optimal medical therapy with or without percutaneous coronary intervention to reduce ischemic burden: Results from the clinical outcomes utilizing revascularization and aggressive drug evaluation (courage) trial nuclear substudy. *Circulation*. 2008;117:1283-1291
163. Weiner DA, Ryan TJ, McCabe CH, Chaitman BR, Sheffield LT, Ferguson JC, Fisher LD, Tristani F. Prognostic importance of a clinical profile and exercise test in medically treated patients with coronary artery disease. *J Am Coll Cardiol*. 1984;3:772-779
164. Lee J, Chae SC, Lee K, Heo J, Iskandrian AS. Biokinetics of thallium-201 in normal subjects: Comparison between adenosine, dipyridamole, dobutamine and exercise. *J Nucl Med*. 1994;35:535-541
165. Sato A, Terata K, Miura H, Toyama K, Loberiza FR, Jr., Hatoum OA, Saito T, Sakuma I, Gutterman DD. Mechanism of vasodilation to adenosine in coronary arterioles from patients with heart disease. *Am J Physiol Heart Circ Physiol*. 2005;288:H1633-1640
166. Knabb RM, Gidday JM, Ely SW, Rubio R, Berne RM. Effects of dipyridamole on myocardial adenosine and active hyperemia. *Am J Physiol*. 1984;247:H804-810
167. Salcedo J, Kern MJ. Effects of caffeine and theophylline on coronary hyperemia induced by adenosine or dipyridamole. *Catheter Cardiovasc Interv*. 2009;74:598-605
168. van Geuns RJ, Wielopolski PA, de Bruin HG, Rensing BJ, van Ooijen PM, Hulshoff M, Oudkerk M, de Feyter PJ. Basic principles of magnetic resonance imaging. *Progress in cardiovascular diseases*. 1999;42:149-156
169. Armstrong P, Keevil SF. Magnetic resonance imaging--1: Basic principles of image production. *Bmj*. 1991;303:35-40

170. Scherzinger AL, Hendee WR. Basic principles of magnetic resonance imaging--an update. *The Western journal of medicine*. 1985;143:782-792
171. Hundley WG, Bluemke DA, Finn JP, Flamm SD, Fogel MA, Friedrich MG, Ho VB, Jerosch-Herold M, Kramer CM, Manning WJ, Patel M, Pohost GM, Stillman AE, White RD, Woodard PK. Accf/acr/aha/nasci/scmr 2010 expert consensus document on cardiovascular magnetic resonance: A report of the american college of cardiology foundation task force on expert consensus documents. *Circulation*. 2010;121:2462-2508
172. Barkhausen J, Ruehm SG, Goyen M, Buck T, Laub G, Debatin JF. Mr evaluation of ventricular function: True fast imaging with steady-state precession versus fast low-angle shot cine mr imaging: Feasibility study. *Radiology*. 2001;219:264-269
173. Jahnke C, Paetsch I, Gebker R, Bornstedt A, Fleck E, Nagel E. Accelerated 4d dobutamine stress mr imaging with k-t blast: Feasibility and diagnostic performance. *Radiology*. 2006;241:718-728
174. Jahnke C, Nagel E, Gebker R, Bornstedt A, Schnackenburg B, Kozerke S, Fleck E, Paetsch I. Four-dimensional single breathhold magnetic resonance imaging using kt-blast enables reliable assessment of left- and right-ventricular volumes and mass. *J Magn Reson Imaging*. 2007;25:737-742
175. Bellenger NG, Burgess MI, Ray SG, Lahiri A, Coats AJ, Cleland JG, Pennell DJ. Comparison of left ventricular ejection fraction and volumes in heart failure by echocardiography, radionuclide ventriculography and cardiovascular magnetic resonance; are they interchangeable? *Eur Heart J*. 2000;21:1387-1396
176. Semelka RC, Tomei E, Wagner S, Mayo J, Caputo G, O'Sullivan M, Parmley WW, Chatterjee K, Wolfe C, Higgins CB. Interstudy reproducibility of dimensional and functional measurements between cine magnetic resonance studies in the morphologically abnormal left ventricle. *Am Heart J*. 1990;119:1367-1373
177. Sechtem U, Sommerhoff BA, Markiewicz W, White RD, Cheitlin MD, Higgins CB. Regional left ventricular wall thickening by magnetic resonance imaging: Evaluation in normal persons and patients with global and regional dysfunction. *Am J Cardiol*. 1987;59:145-151
178. Hoffmann R, von Bardeleben S, Kasprzak JD, Borges AC, ten Cate F, Firschke C, Lafitte S, Al-Saadi N, Kuntz-Hehner S, Horstick G, Greis C, Engelhardt M, Vanoverschelde JL, Becher H. Analysis of regional left ventricular function by cineventriculography, cardiac magnetic resonance imaging, and unenhanced and contrast-enhanced echocardiography: A multicenter comparison of methods. *J Am Coll Cardiol*. 2006;47:121-128
179. Zerhouni EA, Parish DM, Rogers WJ, Yang A, Shapiro EP. Human heart: Tagging with mr imaging--a method for noninvasive assessment of myocardial motion. *Radiology*. 1988;169:59-63
180. Rutz AK, Ryf S, Plein S, Boesiger P, Kozerke S. Accelerated whole-heart 3d cspamm for myocardial motion quantification. *Magn Reson Med*. 2008;59:755-763

181. Garot J, Pascal O, Diebold B, Derumeaux G, Gerber BL, Dubois-Rande JL, Lima JA, Gueret P. Alterations of systolic left ventricular twist after acute myocardial infarction. *Am J Physiol Heart Circ Physiol*. 2002;282:H357-362
182. Paetsch I, Foll D, Kaluza A, Luechinger R, Stuber M, Bornstedt A, Wahl A, Fleck E, Nagel E. Magnetic resonance stress tagging in ischemic heart disease. *Am J Physiol Heart Circ Physiol*. 2005;288:H2708-2714
183. Kramer CM, Rogers WJ, Geskin G, Power TP, Theobald TM, Hu YL, Reichek N. Usefulness of magnetic resonance imaging early after acute myocardial infarction. *Am J Cardiol*. 1997;80:690-695
184. Geskin G, Kramer CM, Rogers WJ, Theobald TM, Pakstis D, Hu YL, Reichek N. Quantitative assessment of myocardial viability after infarction by dobutamine magnetic resonance tagging. *Circulation*. 1998;98:217-223
185. Kramer CM, Malkowski MJ, Mankad S, Theobald TM, Pakstis DL, Rogers WJ, Jr. Magnetic resonance tagging and echocardiographic response to dobutamine and functional improvement after reperfused myocardial infarction. *Am Heart J*. 2002;143:1046-1051
186. Gerber BL, Rochitte CE, Melin JA, McVeigh ER, Bluemke DA, Wu KC, Becker LC, Lima JA. Microvascular obstruction and left ventricular remodeling early after acute myocardial infarction. *Circulation*. 2000;101:2734-2741
187. Baer FM, Voth E, Schneider CA, Theissen P, Schicha H, Sechtem U. Comparison of low-dose dobutamine-gradient-echo magnetic resonance imaging and positron emission tomography with [18f]fluorodeoxyglucose in patients with chronic coronary artery disease. A functional and morphological approach to the detection of residual myocardial viability. *Circulation*. 1995;91:1006-1015
188. Paetsch I, Jahnke C, Ferrari VA, Rademakers FE, Pellikka PA, Hundley WG, Poldermans D, Bax JJ, Wegscheider K, Fleck E, Nagel E. Determination of interobserver variability for identifying inducible left ventricular wall motion abnormalities during dobutamine stress magnetic resonance imaging. *Eur Heart J*. 2006;27:1459-1464
189. Paetsch I, Jahnke C, Wahl A, Gebker R, Neuss M, Fleck E, Nagel E. Comparison of dobutamine stress magnetic resonance, adenosine stress magnetic resonance, and adenosine stress magnetic resonance perfusion. *Circulation*. 2004;110:835-842
190. Schwitter J. Myocardial perfusion imaging by cardiac magnetic resonance. *J Nucl Cardiol*. 2006;13:841-854
191. Schwitter J, Nanz D, Kneifel S, Bertschinger K, Buchi M, Knusel PR, Marincek B, Luscher TF, von Schulthess GK. Assessment of myocardial perfusion in coronary artery disease by magnetic resonance: A comparison with positron emission tomography and coronary angiography. *Circulation*. 2001;103:2230-2235
192. Plein S, Ryf S, Schwitter J, Radjenovic A, Boesiger P, Kozerke S. Dynamic contrast-enhanced myocardial perfusion mri accelerated with k-t sense. *Magn Reson Med*. 2007;58:777-785
193. Gebker R, Jahnke C, Paetsch I, Kelle S, Schnackenburg B, Fleck E, Nagel E. Diagnostic performance of myocardial perfusion mr at 3 t in patients with coronary artery disease. *Radiology*. 2008;247:57-63

194. Cheng AS, Pegg TJ, Karamitsos TD, Searle N, Jerosch-Herold M, Choudhury RP, Banning AP, Neubauer S, Robson MD, Selvanayagam JB. Cardiovascular magnetic resonance perfusion imaging at 3-tesla for the detection of coronary artery disease: A comparison with 1.5-tesla. *J Am Coll Cardiol*. 2007;49:2440-2449
195. Fritz-Hansen T, Hove JD, Kofoed KF, Kelbaek H, Larsson HB. Quantification of mri measured myocardial perfusion reserve in healthy humans: A comparison with positron emission tomography. *J Magn Reson Imaging*. 2008;27:818-824
196. Jerosch-Herold M, Wilke N, Stillman AE. Magnetic resonance quantification of the myocardial perfusion reserve with a fermi function model for constrained deconvolution. *Med Phys*. 1998;25:73-84
197. Selvanayagam JB, Jerosch-Herold M, Porto I, Sheridan D, Cheng AS, Petersen SE, Searle N, Channon KM, Banning AP, Neubauer S. Resting myocardial blood flow is impaired in hibernating myocardium: A magnetic resonance study of quantitative perfusion assessment. *Circulation*. 2005;112:3289-3296
198. Nagel E, Klein C, Paetsch I, Hettwer S, Schnackenburg B, Wegscheider K, Fleck E. Magnetic resonance perfusion measurements for the noninvasive detection of coronary artery disease. *Circulation*. 2003;108:432-437
199. Cullen JH, Horsfield MA, Reek CR, Cherryman GR, Barnett DB, Samani NJ. A myocardial perfusion reserve index in humans using first-pass contrast-enhanced magnetic resonance imaging. *J Am Coll Cardiol*. 1999;33:1386-1394
200. Al-Saadi N, Nagel E, Gross M, Bornstedt A, Schnackenburg B, Klein C, Klimek W, Oswald H, Fleck E. Noninvasive detection of myocardial ischemia from perfusion reserve based on cardiovascular magnetic resonance. *Circulation*. 2000;101:1379-1383
201. Wolff SD, Schwitter J, Coulden R, Friedrich MG, Bluemke DA, Biederman RW, Martin ET, Lansky AJ, Kashanian F, Foo TK, Licato PE, Comeau CR. Myocardial first-pass perfusion magnetic resonance imaging: A multicenter dose-ranging study. *Circulation*. 2004;110:732-737
202. Pennell DJ. Cardiovascular magnetic resonance and the role of adenosine pharmacologic stress. *Am J Cardiol*. 2004;94:26D-31D; discussion 31D-32D
203. Kim RJ, Chen EL, Lima JA, Judd RM. Myocardial gd-dtpa kinetics determine mri contrast enhancement and reflect the extent and severity of myocardial injury after acute reperfused infarction. *Circulation*. 1996;94:3318-3326
204. Kim RJ, Wu E, Rafael A, Chen EL, Parker MA, Simonetti O, Klocke FJ, Bonow RO, Judd RM. The use of contrast-enhanced magnetic resonance imaging to identify reversible myocardial dysfunction. *N Engl J Med*. 2000;343:1445-1453
205. Judd RM, Lugo-Olivieri CH, Arai M, Kondo T, Croisille P, Lima JA, Mohan V, Becker LC, Zerhouni EA. Physiological basis of myocardial contrast enhancement in fast magnetic resonance images of 2-day-old reperfused canine infarcts. *Circulation*. 1995;92:1902-1910
206. Kim RJ, Fieno DS, Parrish TB, Harris K, Chen EL, Simonetti O, Bundy J, Finn JP, Klocke FJ, Judd RM. Relationship of mri delayed contrast enhancement to irreversible injury, infarct age, and contractile function. *Circulation*. 1999;100:1992-2002

207. Fieno DS, Kim RJ, Chen EL, Lomasney JW, Klocke FJ, Judd RM. Contrast-enhanced magnetic resonance imaging of myocardium at risk: Distinction between reversible and irreversible injury throughout infarct healing. *J Am Coll Cardiol*. 2000;36:1985-1991
208. Wu E, Judd RM, Vargas JD, Klocke FJ, Bonow RO, Kim RJ. Visualisation of presence, location, and transmural extent of healed q-wave and non-q-wave myocardial infarction. *Lancet*. 2001;357:21-28
209. Klein C, Nekolla SG, Bengel FM, Momose M, Sammer A, Haas F, Schnackenburg B, Delius W, Mudra H, Wolfram D, Schwaiger M. Assessment of myocardial viability with contrast-enhanced magnetic resonance imaging: Comparison with positron emission tomography. *Circulation*. 2002;105:162-167
210. Wagner A, Mahrholdt H, Holly TA, Elliott MD, Regenfus M, Parker M, Klocke FJ, Bonow RO, Kim RJ, Judd RM. Contrast-enhanced mri and routine single photon emission computed tomography (spect) perfusion imaging for detection of subendocardial myocardial infarcts: An imaging study. *Lancet*. 2003;361:374-379
211. Bondarenko O, Beek AM, Nijveldt R, McCann GP, van Dockum WG, Hofman MB, Twisk JW, Visser CA, van Rossum AC. Functional outcome after revascularization in patients with chronic ischemic heart disease: A quantitative late gadolinium enhancement cmr study evaluating transmural scar extent, wall thickness and periprocedural necrosis. *J Cardiovasc Magn Reson*. 2007;9:815-821
212. Abdel-Aty H, Zagrosek A, Schulz-Menger J, Taylor AJ, Messroghli D, Kumar A, Gross M, Dietz R, Friedrich MG. Delayed enhancement and t2-weighted cardiovascular magnetic resonance imaging differentiate acute from chronic myocardial infarction. *Circulation*. 2004;109:2411-2416
213. Kellman P, Aletras AH, Mancini C, McVeigh ER, Arai AE. T2-prepared ssfp improves diagnostic confidence in edema imaging in acute myocardial infarction compared to turbo spin echo. *Magn Reson Med*. 2007;57:891-897
214. Nandalur KR, Dwamena BA, Choudhri AF, Nandalur MR, Carlos RC. Diagnostic performance of stress cardiac magnetic resonance imaging in the detection of coronary artery disease: A meta-analysis. *J Am Coll Cardiol*. 2007;50:1343-1353
215. Lockie T, Nagel E, Redwood S, Plein S. Use of cardiovascular magnetic resonance imaging in acute coronary syndromes. *Circulation*. 2009;119:1671-1681
216. Plein S, Radjenovic A, Ridgway JP, Barmby D, Greenwood JP, Ball SG, Sivananthan MU. Coronary artery disease: Myocardial perfusion mr imaging with sensitivity encoding versus conventional angiography. *Radiology*. 2005;235:423-430
217. Watkins S, McGeoch R, Lyne J, Steedman T, Good R, McLaughlin MJ, Cunningham T, Bezlyak V, Ford I, Dargie HJ, Oldroyd KG. Validation of magnetic resonance myocardial perfusion imaging with fractional flow reserve for the detection of significant coronary heart disease. *Circulation*. 2009;120:2207-2213

218. Bartunek J, Sys SU, Heyndrickx GR, Pijls NH, De Bruyne B. Quantitative coronary angiography in predicting functional significance of stenoses in an unselected patient cohort. *J Am Coll Cardiol*. 1995;26:328-334
219. Araoz PA, Glockner JF, McGee KP, Potter DD, Jr., Valeti VU, Stanley DW, Christian TF. 3 tesla mr imaging provides improved contrast in first-pass myocardial perfusion imaging over a range of gadolinium doses. *J Cardiovasc Magn Reson*. 2005;7:559-564
220. Tsao J, Boesiger P, Pruessmann KP. K-t blast and k-t sense: Dynamic mri with high frame rate exploiting spatiotemporal correlations. *Magn Reson Med*. 2003;50:1031-1042
221. Plein S, Kozerke S, Suerder D, Luescher TF, Greenwood JP, Boesiger P, Schwitter J. High spatial resolution myocardial perfusion cardiac magnetic resonance for the detection of coronary artery disease. *Eur Heart J*. 2008
222. Kozerke S, Tsao J. Reduced data acquisition methods in cardiac imaging. *Top Magn Reson Imaging*. 2004;15:161-168
223. Plein S, Schwitter J, Suerder D, Greenwood JP, Boesiger P, Kozerke S. K-space and time sensitivity encoding-accelerated myocardial perfusion mr imaging at 3.0 t: Comparison with 1.5 t. *Radiology*. 2008;249:493-500
224. Scanlon PJ, Faxon DP, Audet AM, Carabello B, Dehmer GJ, Eagle KA, Legako RD, Leon DF, Murray JA, Nissen SE, Pepine CJ, Watson RM, Ritchie JL, Gibbons RJ, Cheitlin MD, Gardner TJ, Garson A, Jr., Russell RO, Jr., Ryan TJ, Smith SC, Jr. Acc/aha guidelines for coronary angiography: Executive summary and recommendations. A report of the american college of cardiology/american heart association task force on practice guidelines (committee on coronary angiography) developed in collaboration with the society for cardiac angiography and interventions. *Circulation*. 1999;99:2345-2357
225. Pijls NH, De Bruyne B, Peels K, Van Der Voort PH, Bonnier HJ, Bartunek JKJJ, Koolen JJ. Measurement of fractional flow reserve to assess the functional severity of coronary-artery stenoses. *N Engl J Med*. 1996;334:1703-1708
226. Aarnoudse W, Fearon WF, Manoharan G, Geven M, van de Vosse F, Rutten M, De Bruyne B, Pijls NH. Epicardial stenosis severity does not affect minimal microcirculatory resistance. *Circulation*. 2004;110:2137-2142
227. Fearon WF, Aarnoudse W, Pijls NH, De Bruyne B, Balsam LB, Cooke DT, Robbins RC, Fitzgerald PJ, Yeung AC, Yock PG. Microvascular resistance is not influenced by epicardial coronary artery stenosis severity: Experimental validation. *Circulation*. 2004;109:2269-2272
228. Blows LJ, Redwood SR. Pressure wire in practice. *Heart*. 2006
229. Chamuleau SA, Siebes M, Meuwissen M, Koch KT, Spaan JA, Piek JJ. Association between coronary lesion severity and distal microvascular resistance in patients with coronary artery disease. *Am J Physiol Heart Circ Physiol*. 2003;285:H2194-2200
230. Spaan JA, Piek JJ, Hoffman JI, Siebes M. Physiological basis of clinically used coronary hemodynamic indices. *Circulation*. 2006;113:446-455
231. Pijls NH, Kern MJ, Yock PG, De Bruyne B. Practice and potential pitfalls of coronary pressure measurement. *Catheter Cardiovasc Interv*. 2000;49:1-16
232. Meuwissen M, Chamuleau SA, Siebes M, Schotborgh CE, Koch KT, de Winter RJ, Bax M, de Jong A, Spaan JA, Piek JJ. Role of variability in microvascular

resistance on fractional flow reserve and coronary blood flow velocity reserve in intermediate coronary lesions. *Circulation*. 2001;103:184-187
233. De Bruyne B, Pijls NH, Smith L, Wievegg M, Heyndrickx GR. Coronary thermodilution to assess flow reserve: Experimental validation. *Circulation*. 2001;104:2003-2006
234. Ibrahim T, Nekolla SG, Schreiber K, Odaka K, Volz S, Mehilli J, Guthlin M, Delius W, Schwaiger M. Assessment of coronary flow reserve: Comparison between contrast-enhanced magnetic resonance imaging and positron emission tomography. *J Am Coll Cardiol*. 2002;39:864-870
235. Klocke FJ. Measurements of coronary flow reserve: Defining pathophysiology versus making decisions about patient care. *Circulation*. 1987;76:1183-1189
236. Ng MK, Yeung AC, Fearon WF. Invasive assessment of the coronary microcirculation: Superior reproducibility and less hemodynamic dependence of index of microcirculatory resistance compared with coronary flow reserve. *Circulation*. 2006;113:2054-2061
237. Shimada K, Sakanoue Y, Kobayashi Y, Ehara S, Hirose M, Nakamura Y, Fukuda D, Yamagishi H, Yoshiyama M, Takeuchi K, Yoshikawa J. Assessment of myocardial viability using coronary zero flow pressure after successful angioplasty in patients with acute anterior myocardial infarction. *Heart*. 2003;89:71-76
238. Meuwissen M, Siebes M, Chamuleau SA, van Eck-Smit BL, Koch KT, de Winter RJ, Tijssen JG, Spaan JA, Piek JJ. Hyperemic stenosis resistance index for evaluation of functional coronary lesion severity. *Circulation*. 2002;106:441-446
239. Nijveldt R, Beek AM, Hirsch A, Stoel MG, Hofman MB, Umans VA, Algra PR, Twisk JW, van Rossum AC. Functional recovery after acute myocardial infarction: Comparison between angiography, electrocardiography, and cardiovascular magnetic resonance measures of microvascular injury. *J Am Coll Cardiol*. 2008;52:181-189
240. Siebes M, Verhoeff BJ, Meuwissen M, de Winter RJ, Spaan JA, Piek JJ. Single-wire pressure and flow velocity measurement to quantify coronary stenosis hemodynamics and effects of percutaneous interventions. *Circulation*. 2004;109:756-762
241. Fearon WF, Balsam LB, Farouque HM, Caffarelli AD, Robbins RC, Fitzgerald PJ, Yock PG, Yeung AC. Novel index for invasively assessing the coronary microcirculation. *Circulation*. 2003;107:3129-3132
242. Fearon WF, Farouque HM, Balsam LB, Caffarelli AD, Cooke DT, Robbins RC, Fitzgerald PJ, Yeung AC, Yock PG. Comparison of coronary thermodilution and doppler velocity for assessing coronary flow reserve. *Circulation*. 2003;108:2198-2200
243. Hartley CJ, Cole JS. An ultrasonic pulsed doppler system for measuring blood flow in small vessels. *J Appl Physiol*. 1974;37:626-629
244. Davies JE, Whinnett ZI, Francis DP, Willson K, Foale RA, Malik IS, Hughes AD, Parker KH, Mayet J. Use of simultaneous pressure and velocity measurements to estimate arterial wave speed at a single site in humans. *Am J Physiol Heart Circ Physiol*. 2006;290:H878-885

245. Davies JE, Whinnett ZI, Francis DP, Manisty CH, Aguado-Sierra J, Willson K, Foale RA, Malik IS, Hughes AD, Parker KH, Mayet J. Evidence of a dominant backward-propagating "suction" wave responsible for diastolic coronary filling in humans, attenuated in left ventricular hypertrophy. *Circulation*. 2006;113:1768-1778
246. O'Rourke MF, Gallagher DE. Pulse wave analysis. *J Hypertens Suppl*. 1996;14:S147-157
247. Kelly R, Hayward C, Avolio A, O'Rourke M. Noninvasive determination of age-related changes in the human arterial pulse. *Circulation*. 1989;80:1652-1659
248. Munir S, Guilcher A, Kamalesh T, Clapp B, Redwood S, Marber M, Chowienczyk P. Peripheral augmentation index defines the relationship between central and peripheral pulse pressure. *Hypertension*. 2008;51:112-118
249. Sharman JE, Lim R, Qasem AM, Coombes JS, Burgess MI, Franco J, Garrahy P, Wilkinson IB, Marwick TH. Validation of a generalized transfer function to noninvasively derive central blood pressure during exercise. *Hypertension*. 2006;47:1203-1208
250. Stok WJ, Westerhof BE, Karemaker JM. Changes in finger-aorta pressure transfer function during and after exercise. *Journal of applied physiology*. 2006;101:1207-1214
251. O'Rourke MF, Adji A. An updated clinical primer on large artery mechanics: Implications of pulse waveform analysis and arterial tonometry. *Current opinion in cardiology*. 2005;20:275-281
252. Verbeke F, Segers P, Heireman S, Vanholder R, Verdonck P, Van Bortel LM. Noninvasive assessment of local pulse pressure: Importance of brachial-to-radial pressure amplification. *Hypertension*. 2005;46:244-248
253. Parker KH, Jones CJ. Forward and backward running waves in the arteries: Analysis using the method of characteristics. *J Biomech Eng*. 1990;112:322-326
254. Sun YH, Anderson TJ, Parker KH, Tyberg JV. Wave-intensity analysis: A new approach to coronary hemodynamics. *J Appl Physiol*. 2000;89:1636-1644
255. Khir AW, Parker KH. Wave intensity in the ascending aorta: Effects of arterial occlusion. *J Biomech*. 2005;38:647-655
256. Sun YH, Anderson TJ, Parker KH, Tyberg JV. Effects of left ventricular contractility and coronary vascular resistance on coronary dynamics. *Am J Physiol Heart Circ Physiol*. 2004;286:H1590-1595
257. Parker KH. An introduction to wave intensity analysis. *Med Biol Eng Comput*. 2009;47:175-188
258. Bleasdale RA, Parker KH, Jones CJ. Chasing the wave. Unfashionable but important new concepts in arterial wave travel. *American journal of physiology. Heart and circulatory physiology*. 2003;284:H1879-1885
259. Tonino PA, Fearon WF, De Bruyne B, Oldroyd KG, Leesar MA, Ver Lee PN, Maccarthy PA, Van't Veer M, Pijls NH. Angiographic versus functional severity of coronary artery stenoses in the fame study fractional flow reserve versus angiography in multivessel evaluation. *J Am Coll Cardiol*.55:2816-2821

260. Hughes AD, Parker KH. Forward and backward waves in the arterial system: Impedance or wave intensity analysis? *Med Biol Eng Comput*. 2009;47:207-210
261. Kovacs G, Maier R, Aberer E, Brodmann M, Scheidl S, Hesse C, Troester N, Salmhofer W, Stauber R, Furst F, Thonhofer R, Ofner-Kopeinig P, Gruenig E, Olschewski H. Assessment of pulmonary arterial pressure during exercise in collagen vascular disease: Echocardiography versus right heart catheterisation. *Chest*.
262. Mattingly TW. Postexercise electrocardiogram: Value in diagnosis and prognosis of coronary artery disease. *Fed Proc*. 1962;21(4)Pt 2:98
263. Sowton E, Burkart F. Haemodynamic changes during continuous exercise. *Br Heart J*. 1967;29:770-774
264. Togni M, Gloekler S, Meier P, de Marchi SF, Rutz T, Steck H, Traupe T, Seiler C. Instantaneous coronary collateral function during supine bicycle exercise. *Eur Heart J*.31:2148-2155
265. Bevegard S, Holmgren A, Jonsson B. The effect of body position on the circulation at rest and during exercise, with special reference to the influence on the stroke volume. *Acta physiologica Scandinavica*. 1960;49:279-298
266. Wetherbee JN, Bamrah VS, Ptacin MJ, Kalbfleisch JH. Comparison of st segment depression in upright treadmill and supine bicycle exercise testing. *J Am Coll Cardiol*. 1988;11:330-337
267. Kramer CM, Lima JA, Reichek N, Ferrari VA, Llaneras MR, Palmon LC, Yeh IT, Tallant B, Axel L. Regional differences in function within noninfarcted myocardium during left ventricular remodeling. *Circulation*. 1993;88:1279-1288
268. Grothues F, Smith GC, Moon JC, Bellenger NG, Collins P, Klein HU, Pennell DJ. Comparison of interstudy reproducibility of cardiovascular magnetic resonance with two-dimensional echocardiography in normal subjects and in patients with heart failure or left ventricular hypertrophy. *Am J Cardiol*. 2002;90:29-34
269. Bellenger NG, Davies LC, Francis JM, Coats AJ, Pennell DJ. Reduction in sample size for studies of remodeling in heart failure by the use of cardiovascular magnetic resonance. *J Cardiovasc Magn Reson*. 2000;2:271-278
270. Richard V, Murry CE, Reimer KA. Healing of myocardial infarcts in dogs. Effects of late reperfusion. *Circulation*. 1995;92:1891-1901
271. Baks T, van Geuns RJ, Biagini E, Wielopolski P, Mollet NR, Cademartiri F, van der Giessen WJ, Krestin GP, Serruys PW, Duncker DJ, de Feyter PJ. Effects of primary angioplasty for acute myocardial infarction on early and late infarct size and left ventricular wall characteristics. *J Am Coll Cardiol*. 2006;47:40-44
272. Taylor AJ, Al-Saadi N, Abdel-Aty H, Schulz-Menger J, Messroghli DR, Friedrich MG. Detection of acutely impaired microvascular reperfusion after infarct angioplasty with magnetic resonance imaging. *Circulation*. 2004;109:2080-2085
273. Wu KC, Zerhouni EA, Judd RM, Lugo-Olivieri CH, Barouch LA, Schulman SP, Blumenthal RS, Lima JA. Prognostic significance of microvascular obstruction

by magnetic resonance imaging in patients with acute myocardial infarction. *Circulation*. 1998;97:765-772

274. Wilke N, Jerosch-Herold M, Stillman AE, Kroll K, Tsekos N, Merkle H, Parrish T, Hu X, Wang Y, Bassingthwaighte J, et al. Concepts of myocardial perfusion imaging in magnetic resonance imaging. *Magn Reson Q*. 1994;10:249-286
275. Slutsky RA, Peterson T, Strich G, Brown JJ. Hemodynamic effects of rapid and slow infusions of manganese chloride and gadolinium-dtpa in dogs. *Radiology*. 1985;154:733-735
276. Strich G, Hagan PL, Gerber KH, Slutsky RA. Tissue distribution and magnetic resonance spin lattice relaxation effects of gadolinium-dtpa. *Radiology*. 1985;154:723-726
277. Weinmann HJ, Brasch RC, Press WR, Wesbey GE. Characteristics of gadolinium-dtpa complex: A potential nmr contrast agent. *AJR. American journal of roentgenology*. 1984;142:619-624
278. Keijer JT, van Rossum AC, Wilke N, van Eenige MJ, Jerosch-Herold M, Bronzwaer JG, Visser CA. Magnetic resonance imaging of myocardial perfusion in single-vessel coronary artery disease: Implications for transmural assessment of myocardial perfusion. *Journal of cardiovascular magnetic resonance : official journal of the Society for Cardiovascular Magnetic Resonance*. 2000;2:189-200
279. Wilke N, Jerosch-Herold M, Wang Y, Huang Y, Christensen BV, Stillman AE, Ugurbil K, McDonald K, Wilson RF. Myocardial perfusion reserve: Assessment with multisection, quantitative, first-pass mr imaging. *Radiology*. 1997;204:373-384
280. Ishida N, Sakuma H, Motoyasu M, Okinaka T, Isaka N, Nakano T, Takeda K. Noninfarcted myocardium: Correlation between dynamic first-pass contrast-enhanced myocardial mr imaging and quantitative coronary angiography. *Radiology*. 2003;229:209-216
281. Schwitter J, Debatin JF, von Schulthess GK, McKinnon GC. Normal myocardial perfusion assessed with multishot echo-planar imaging. *Magnetic resonance in medicine : official journal of the Society of Magnetic Resonance in Medicine / Society of Magnetic Resonance in Medicine*. 1997;37:140-147
282. Ding S, Wolff SD, Epstein FH. Improved coverage in dynamic contrast-enhanced cardiac mri using interleaved gradient-echo epi. *Magnetic resonance in medicine : official journal of the Society of Magnetic Resonance in Medicine / Society of Magnetic Resonance in Medicine*. 1998;39:514-519
283. Kellman P, Derbyshire JA, Agyeman KO, McVeigh ER, Arai AE. Extended coverage first-pass perfusion imaging using slice-interleaved tsense. *Magnetic resonance in medicine : official journal of the Society of Magnetic Resonance in Medicine / Society of Magnetic Resonance in Medicine*. 2004;51:200-204
284. Pruessmann KP, Weiger M, Scheidegger MB, Boesiger P. Sense: Sensitivity encoding for fast mri. *Magnetic resonance in medicine : official journal of the Society of Magnetic Resonance in Medicine / Society of Magnetic Resonance in Medicine*. 1999;42:952-962
285. Lee DC, Klocke FJ. Magnetic resonance approaches and recent advances in myocardial perfusion imaging. *Curr Cardiol Rep*. 2006;8:59-64

286. Klocke FJ, Simonetti OP, Judd RM, Kim RJ, Harris KR, Hedjbeli S, Fieno DS, Miller S, Chen V, Parker MA. Limits of detection of regional differences in vasodilated flow in viable myocardium by first-pass magnetic resonance perfusion imaging. *Circulation*. 2001;104:2412-2416
287. Kraitchman DL, Wilke N, Hexeberg E, Jerosch-Herold M, Wang Y, Parrish TB, Chang CN, Zhang Y, Bache RJ, Axel L. Myocardial perfusion and function in dogs with moderate coronary stenosis. *Magn Reson Med*. 1996;35:771-780
288. Lockie T, Ishida M, Perera D, Chiribiri A, De Silva K, Kozerke S, Marber M, Nagel E, Rezavi R, Redwood S, Plein S. High-resolution magnetic resonance myocardial perfusion imaging at 3.0-tesla to detect hemodynamically significant coronary stenoses as determined by fractional flow reserve. *Journal of the American College of Cardiology*. 2010;57:70-75
289. Jahnke C, Nagel E, Gebker R, Kokocinski T, Kelle S, Manka R, Fleck E, Paetsch I. Prognostic value of cardiac magnetic resonance stress tests: Adenosine stress perfusion and dobutamine stress wall motion imaging. *Circulation*. 2007;115:1769-1776
290. Hautvast GL, Chiribiri A, Lockie T, Breeuwer M, Nagel E, Plein S. Quantitative analysis of transmural gradients in myocardial perfusion magnetic resonance images. *Magnetic resonance in medicine : official journal of the Society of Magnetic Resonance in Medicine / Society of Magnetic Resonance in Medicine*. 2011;66:1477-1487
291. Lee DC, Simonetti OP, Harris KR, Holly TA, Judd RM, Wu E, Klocke FJ. Magnetic resonance versus radionuclide pharmacological stress perfusion imaging for flow-limiting stenoses of varying severity. *Circulation*. 2004;110:58-65
292. Axel L. Tissue mean transit time from dynamic computed tomography by a simple deconvolution technique. *Investigative radiology*. 1983;18:94-99
293. Christian TF, Rettmann DW, Aletras AH, Liao SL, Taylor JL, Balaban RS, Arai AE. Absolute myocardial perfusion in canines measured by using dual-bolus first-pass mr imaging. *Radiology*. 2004;232:677-684
294. Christian TF, Aletras AH, Arai AE. Estimation of absolute myocardial blood flow during first-pass mr perfusion imaging using a dual-bolus injection technique: Comparison to single-bolus injection method. *Journal of magnetic resonance imaging : JMRI*. 2008;27:1271-1277
295. Futamatsu H, Wilke N, Klassen C, Shoemaker S, Angiolillo DJ, Siuciak A, Morikawa-Futamatsu K, Suzuki N, von Ziegler F, Bass TA, Costa MA. Evaluation of cardiac magnetic resonance imaging parameters to detect anatomically and hemodynamically significant coronary artery disease. *Am Heart J*. 2007;154:298-305
296. Costa MA, Shoemaker S, Futamatsu H, Klassen C, Angiolillo DJ, Nguyen M, Siuciak A, Gilmore P, Zenni MM, Guzman L, Bass TA, Wilke N. Quantitative magnetic resonance perfusion imaging detects anatomic and physiologic coronary artery disease as measured by coronary angiography and fractional flow reserve. *J Am Coll Cardiol*. 2007;50:514-522
297. Larsson HB, Stubgaard M, Sondergaard L, Henriksen O. In vivo quantification of the unidirectional influx constant for gd-dtpa diffusion across the

myocardial capillaries with mr imaging. *Journal of magnetic resonance imaging : JMRI*. 1994;4:433-440
298. Kurita T, Sakuma H, Onishi K, Ishida M, Kitagawa K, Yamanaka T, Tanigawa T, Kitamura T, Takeda K, Ito M. Regional myocardial perfusion reserve determined using myocardial perfusion magnetic resonance imaging showed a direct correlation with coronary flow velocity reserve by doppler flow wire. *European heart journal*. 2009;30:444-452
299. Vallee JP, Lazeyras F, Kasuboski L, Chatelain P, Howarth N, Righetti A, Didier D. Quantification of myocardial perfusion with fast sequence and gd bolus in patients with normal cardiac function. *Journal of magnetic resonance imaging : JMRI*. 1999;9:197-203
300. Svendsen JH, Efsen F, Haunso S. Capillary permeability of 99mtc-dtpa and blood flow rate in the human myocardium determined by intracoronary bolus injection and residue detection. *Cardiology*. 1992;80:18-27
301. Tong CY, Prato FS, Wisenberg G, Lee TY, Carroll E, Sandler D, Wills J, Drost D. Measurement of the extraction efficiency and distribution volume for gd-dtpa in normal and diseased canine myocardium. *Magnetic resonance in medicine : official journal of the Society of Magnetic Resonance in Medicine / Society of Magnetic Resonance in Medicine*. 1993;30:337-346
302. Cheng CP, Herfkens RJ, Taylor CA. Abdominal aortic hemodynamic conditions in healthy subjects aged 50-70 at rest and during lower limb exercise: In vivo quantification using mri. *Atherosclerosis*. 2003;168:323-331
303. Cheng CP, Herfkens RJ, Taylor CA. Comparison of abdominal aortic hemodynamics between men and women at rest and during lower limb exercise. *J Vasc Surg*. 2003;37:118-123
304. Niezen RA, Doornbos J, van der Wall EE, de Roos A. Measurement of aortic and pulmonary flow with mri at rest and during physical exercise. *J Comput Assist Tomogr*. 1998;22:194-201
305. Hjortdal VE, Emmertsen K, Stenbog E, Frund T, Schmidt MR, Kromann O, Sorensen K, Pedersen EM. Effects of exercise and respiration on blood flow in total cavopulmonary connection: A real-time magnetic resonance flow study. *Circulation*. 2003;108:1227-1231
306. Jekic M, Foster EL, Ballinger MR, Raman SV, Simonetti OP. Cardiac function and myocardial perfusion immediately following maximal treadmill exercise inside the mri room. *Journal of cardiovascular magnetic resonance : official journal of the Society for Cardiovascular Magnetic Resonance*. 2008;10:3
307. Gerber BL, Raman SV, Nayak K, Epstein FH, Ferreira P, Axel L, Kraitchman DL. Myocardial first-pass perfusion cardiovascular magnetic resonance: History, theory, and current state of the art. *Journal of cardiovascular magnetic resonance : official journal of the Society for Cardiovascular Magnetic Resonance*. 2008;10:18
308. Tweedle MF, Hagan JJ, Kumar K, Mantha S, Chang CA. Reaction of gadolinium chelates with endogenously available ions. *Magn Reson Imaging*. 1991;9:409-415
309. Wyss CA, Koepfli P, Mikolajczyk K, Burger C, von Schulthess GK, Kaufmann PA. Bicycle exercise stress in pet for assessment of coronary flow reserve:

Repeatability and comparison with adenosine stress. *Journal of nuclear medicine : official publication, Society of Nuclear Medicine*. 2003;44:146-154
310. Ma X, Zhang X, Li C, Luo M. Effect of postconditioning on coronary blood flow velocity and endothelial function and lv recovery after myocardial infarction. *J Interv Cardiol*. 2006;19:367-375
311. Maisch B. How cardiac cells die--necrosis, oncosis and apoptosis. *Herz*. 1999;24:181-188
312. Gibbons RJ, Valeti US, Araoz PA, Jaffe AS. The quantification of infarct size. *J Am Coll Cardiol*. 2004;44:1533-1542
313. Thiele H, Kappl MJ, Conradi S, Niebauer J, Hambrecht R, Schuler G. Reproducibility of chronic and acute infarct size measurement by delayed enhancement-magnetic resonance imaging. *J Am Coll Cardiol*. 2006;47:1641-1645
314. Choi KM, Kim RJ, Gubernikoff G, Vargas JD, Parker M, Judd RM. Transmural extent of acute myocardial infarction predicts long-term improvement in contractile function. *Circulation*. 2001;104:1101-1107
315. Wu KC, Kim RJ, Bluemke DA, Rochitte CE, Zerhouni EA, Becker LC, Lima JA. Quantification and time course of microvascular obstruction by contrast-enhanced echocardiography and magnetic resonance imaging following acute myocardial infarction and reperfusion. *J Am Coll Cardiol*. 1998;32:1756-1764
316. Armstrong WF, Pellikka PA, Ryan T, Crouse L, Zoghbi WA. Stress echocardiography: Recommendations for performance and interpretation of stress echocardiography. Stress echocardiography task force of the nomenclature and standards committee of the american society of echocardiography. *J Am Soc Echocardiogr*. 1998;11:97-104
317. Bax M, de Winter RJ, Schotborgh CE, Koch KT, Meuwissen M, Voskuil M, Adams R, Mulder KJ, Tijssen JG, Piek JJ. Short- and long-term recovery of left ventricular function predicted at the time of primary percutaneous coronary intervention in anterior myocardial infarction. *J Am Coll Cardiol*. 2004;43:534-541
318. Thibault H, Piot C, Staat P, Bontemps L, Sportouch C, Rioufol G, Cung TT, Bonnefoy E, Angoulvant D, Aupetit JF, Finet G, Andre-Fouet X, Macia JC, Raczka F, Rossi R, Itti R, Kirkorian G, Derumeaux G, Ovize M. Long-term benefit of postconditioning. *Circulation*. 2008;117:1037-1044
319. Masotti M, Freixa, X, Bellera, M, Jimenez, Betriu, A. Is postconditioning usless in acute myocardial infarction? *EHJ*. 2009;30:Abstract Suppl (892)
320. MacRae JM, Sun YH, Isaac DL, Dobson GM, Cheng CP, Little WC, Parker KH, Tyberg JV. Wave-intensity analysis: A new approach to left ventricular filling dynamics. *Heart Vessels*. 1997;12:53-59
321. Silva-Tinoco R, Castillo-Martinez L, Orea-Tejeda A, Asensio-Lafuente E, Orozco-Gutierrez JJ, Vazquez-Diaz O, Rebollar-Gonzalez V. The effect of left ventricular dysfunction on right ventricle ejection fraction during exercise in heart failure patients: Implications in functional capacity and blood pressure response. *Cardiol J*. 2009;16:127-132

322. Koh TW, Pepper JR, DeSouza AC, Parker KH. Analysis of wave reflections in the arterial system using wave intensity: A novel method for predicting the timing and amplitude of reflected waves. *Heart Vessels*. 1998;13:103-113
323. Kerry SM, Bland JM. The intracluster correlation coefficient in cluster randomisation. *Bmj*. 1998;316:1455
324. Guillevin R, Menuel C, Duffau H, Kujas M, Capelle L, Aubert A, Taillibert S, Idbaih A, Pallud J, Demarco G, Costalat R, Hoang-Xuan K, Chiras J, Vallee JN. Proton magnetic resonance spectroscopy predicts proliferative activity in diffuse low-grade gliomas. *J Neurooncol*. 2008;87:181-187
325. Piot C, Croisille P, Staat P, Thibault H, Rioufol G, Mewton N, Elbelghiti R, Cung TT, Bonnefoy E, Angoulvant D, Macia C, Raczka F, Sportouch C, Gahide G, Finet G, Andre-Fouet X, Revel D, Kirkorian G, Monassier JP, Derumeaux G, Ovize M. Effect of cyclosporine on reperfusion injury in acute myocardial infarction. *N Engl J Med*. 2008;359:473-481
326. Pijls NH, van Schaardenburgh P, Manoharan G, Boersma E, Bech JW, van't Veer M, Bar F, Hoorntje J, Koolen J, Wijns W, de Bruyne B. Percutaneous coronary intervention of functionally nonsignificant stenosis: 5-year follow-up of the defer study. *J Am Coll Cardiol*. 2007;49:2105-2111
327. Perera D, Biggart S, Postema P, Patel S, Lambiase P, Marber M, Redwood S. Right atrial pressure: Can it be ignored when calculating fractional flow reserve and collateral flow index? *J Am Coll Cardiol*. 2004;44:2089-2091
328. Cerqueira MD, Weissman NJ, Dilsizian V, Jacobs AK, Kaul S, Laskey WK, Pennell DJ, Rumberger JA, Ryan T, Verani MS. Standardized myocardial segmentation and nomenclature for tomographic imaging of the heart: A statement for healthcare professionals from the cardiac imaging committee of the council on clinical cardiology of the american heart association. *Circulation*. 2002;105:539-542
329. Bland JM, Altman DG. Statistical methods for assessing agreement between two methods of clinical measurement. *Lancet*. 1986;1:307-310
330. Rieber J, Huber A, Erhard I, Mueller S, Schweyer M, Koenig A, Schiele TM, Theisen K, Siebert U, Schoenberg SO, Reiser M, Klauss V. Cardiac magnetic resonance perfusion imaging for the functional assessment of coronary artery disease: A comparison with coronary angiography and fractional flow reserve. *Eur Heart J*. 2006;27:1465-1471
331. Al-Saadi N, Nagel E, Gross M, Schnackenburg B, Paetsch I, Klein C, Fleck E. Improvement of myocardial perfusion reserve early after coronary intervention: Assessment with cardiac magnetic resonance imaging. *J Am Coll Cardiol*. 2000;36:1557-1564
332. Samady H, Lepper W, Powers ER, Wei K, Ragosta M, Bishop GG, Sarembock IJ, Gimple L, Watson DD, Beller GA, Barringhaus KG. Fractional flow reserve of infarct-related arteries identifies reversible defects on noninvasive myocardial perfusion imaging early after myocardial infarction. *J Am Coll Cardiol*. 2006;47:2187-2193
333. De Bruyne B, Pijls NH, Bartunek J, Kulecki K, Bech JW, De Winter H, Van Crombrugge P, Heyndrickx GR, Wijns W. Fractional flow reserve in patients with prior myocardial infarction. *Circulation*. 2001;104:157-162

334. Jerosch-Herold M, Vazquez G, Wang L, Jacobs DR, Jr., Folsom AR. Variability of myocardial blood flow measurements by magnetic resonance imaging in the multi-ethnic study of atherosclerosis. *Invest Radiol*. 2008;43:155-161
335. Pedersen H, Kozerke S, Ringgaard S, Nehrke K, Kim WY. K-t pca: Temporally constrained k-t blast reconstruction using principal component analysis. *Magn Reson Med*. 2009;62:706-716
336. Bache RJ, Schwartz JS. Effect of perfusion pressure distal to a coronary stenosis on transmural myocardial blood flow. *Circulation*. 1982;65:928-935
337. Ylitalo K, Jama L, Raatikainen P, Peuhkurinen K. Adaptation to myocardial ischemia during repeated dynamic exercise in relation to findings at cardiac catheterization. *Am Heart J*. 1996;131:689-697
338. Edwards RJ, Redwood SR, Lambiase PD, Marber MS. The effect of an angiotensin-converting enzyme inhibitor and a k+(atp) channel opener on warm up angina. *European heart journal*. 2005;26:598-606
339. Rutenberg HL. Of pre-loads, afterloads and warm-ups. *Lancet*. 1981;1:272
340. Pina IL, Balady GJ, Hanson P, Labovitz AJ, Madonna DW, Myers J. Guidelines for clinical exercise testing laboratories. A statement for healthcare professionals from the committee on exercise and cardiac rehabilitation, american heart association. *Circulation*. 1995;91:912-921
341. Sarnoff SJ, Braunwald E, Welch GH, Jr., Case RB, Stainsby WN, Macruz R. Hemodynamic determinants of oxygen consumption of the heart with special reference to the tension-time index. *Am J Physiol*. 1958;192:148-156
342. Spaan J, Kolyva C, van den Wijngaard J, ter Wee R, van Horssen P, Piek J, Siebes M. Coronary structure and perfusion in health and disease. *Philos Transact A Math Phys Eng Sci*. 2008;366:3137-3153
343. Savitzky A. Smoothing and differentiation of data by simplified least squares procedures. *Anal Chem*. 1964;36:1627-1639
344. Rothman KJ. No adjustments are needed for multiple comparisons. *Epidemiology*. 1990;1:43-46
345. Redwood DR, Rosing DR, Goldstein RE, Beiser GD, Epstein SE. Importance of the design of an exercise protocol in the evaluation of patients with angina pectoris. *Circulation*. 1971;43:618-628
346. Kitakaze M, Hori M, Tamai J, Iwakura K, Koretsune Y, Kagiya T, Iwai K, Kitabatake A, Inoue M, Kamada T. Alpha 1-adrenoceptor activity regulates release of adenosine from the ischemic myocardium in dogs. *Circ Res*. 1987;60:631-639
347. Wilkinson IB, MacCallum H, Flint L, Cockcroft JR, Newby DE, Webb DJ. The influence of heart rate on augmentation index and central arterial pressure in humans. *The Journal of physiology*. 2000;525 Pt 1:263-270
348. Burkart F, Barold S, Sowton E. Hemodynamic effects of repeated exercise. *Am J Cardiol*. 1967;20:509-515
349. Thadani U, Lewis JR, Manyari D, Boroomand K, Cohen J, West RO, Parker JO. Are the clinical and hemodynamic events during exercise stress testing in invasive studies in patients with angina pectoris reproducible? *Circulation*. 1980;61:744-750

350. Brutsaert DL, Sys SU, Gillebert TC. Diastolic failure: Pathophysiology and therapeutic implications. *Journal of the American College of Cardiology*. 1993;22:318-325
351. de Beer VJ, Bender SB, Taverne YJ, Gao F, Duncker DJ, Laughlin MH, Merkus D. Exercise limits the production of endothelin in the coronary vasculature. *American journal of physiology. Heart and circulatory physiology*. 2011;300:H1950-1959
352. Hambrecht R, Wolf A, Gielen S, Linke A, Hofer J, Erbs S, Schoene N, Schuler G. Effect of exercise on coronary endothelial function in patients with coronary artery disease. *N Engl J Med*. 2000;342:454-460
353. Sambuceti G, Marzilli M, Mari A, Marini C, Schluter M, Testa R, Papini M, Marraccini P, Ciriello G, Marzullo P, L'Abbate A. Coronary microcirculatory vasoconstriction is heterogeneously distributed in acutely ischemic myocardium. *American journal of physiology. Heart and circulatory physiology*. 2005;288:H2298-2305
354. Ylitalo K, Niemela,K, Linnaluoto,M, Valkama,J, Peuhkurinen,K. Evidence suggesting coronary vasodilation as the principal mechanism in the warm-up phenomenon. *American Heart Journal*. 2001;141:e10
355. Kern MJ, Ganz P, Horowitz JD, Gaspar J, Barry WH, Lorell BH, Grossman W, Mudge GH, Jr. Potentiation of coronary vasoconstriction by beta-adrenergic blockade in patients with coronary artery disease. *Circulation*. 1983;67:1178-1185
356. McLaurin LP, Rolett EL, Grossman W. Impaired left ventricular relaxation during pacing-induced ischemia. *The American journal of cardiology*. 1973;32:751-757
357. Sakata Y, Kodama K, Kitakaze M, Masuyama T, Hirayama A, Lim YJ, Ishikura F, Sakai A, Adachi T, Hori M. Different mechanisms of ischemic adaptation to repeated coronary occlusion in patients with and without recruitable collateral circulation. *Journal of the American College of Cardiology*. 1997;30:1679-1686
358. Deutsch E, Berger M, Kussmaul WG, Hirshfeld JW, Jr., Herrmann HC, Laskey WK. Adaptation to ischemia during percutaneous transluminal coronary angioplasty. Clinical, hemodynamic, and metabolic features. *Circulation*. 1990;82:2044-2051
359. Vogel R, Indermuhle A, Reinhardt J, Meier P, Siegrist PT, Namdar M, Kaufmann PA, Seiler C. The quantification of absolute myocardial perfusion in humans by contrast echocardiography: Algorithm and validation. *Journal of the American College of Cardiology*. 2005;45:754-762
360. Merkus D, Houweling B, Mirza A, Boomsma F, van den Meiracker AH, Duncker DJ. Contribution of endothelin and its receptors to the regulation of vascular tone during exercise is different in the systemic, coronary and pulmonary circulation. *Cardiovascular research*. 2003;59:745-754
361. Merkus D, Stepp DW, Jones DW, Nishikawa Y, Chilian WM. Adenosine preconditions against endothelin-induced constriction of coronary arterioles. *American journal of physiology. Heart and circulatory physiology*. 2000;279:H2593-2597

362. Wiley KE, Davenport AP. Nitric oxide-mediated modulation of the endothelin-1 signalling pathway in the human cardiovascular system. *Br J Pharmacol*. 2001;132:213-220
363. Goligorsky MS, Tsukahara H, Magazine H, Andersen TT, Malik AB, Bahou WF. Termination of endothelin signaling: Role of nitric oxide. *Journal of cellular physiology*. 1994;158:485-494
364. McEniery CM, Wilkinson IB, Jenkins DG, Webb DJ. Endogenous endothelin-1 limits exercise-induced vasodilation in hypertensive humans. *Hypertension*. 2002;40:202-206
365. Duncker DJ, Merkus D. Exercise hyperaemia in the heart: The search for the dilator mechanism. *The Journal of physiology*. 2007;583:847-854
366. Hsu LY, Rhoads KL, Holly JE, Kellman P, Aletras AH, Arai AE. Quantitative myocardial perfusion analysis with a dual-bolus contrast-enhanced first-pass mri technique in humans. *Journal of magnetic resonance imaging : JMRI*. 2006;23:315-322
367. Ibrahim T, Nekolla SG, Schreiber K, Odaka K, Volz S, Mehilli J, Guthlin M, Delius W, Schwaiger M. Assessment of coronary flow reserve: Comparison between contrast-enhanced magnetic resonance imaging and positron emission tomography. *Journal of the American College of Cardiology*. 2002;39:864-870
368. Pack NA, DiBella EV, Rust TC, Kadrmas DJ, McGann CJ, Butterfield R, Christian PE, Hoffman JM. Estimating myocardial perfusion from dynamic contrast-enhanced cmr with a model-independent deconvolution method. *Journal of cardiovascular magnetic resonance : official journal of the Society for Cardiovascular Magnetic Resonance*. 2008;10:52
369. George RT, Arbab-Zadeh A, Miller JM, Kitagawa K, Chang HJ, Bluemke DA, Becker L, Yousuf O, Texter J, Lardo AC, Lima JA. Adenosine stress 64- and 256-row detector computed tomography angiography and perfusion imaging: A pilot study evaluating the transmural extent of perfusion abnormalities to predict atherosclerosis causing myocardial ischemia. *Circ Cardiovasc Imaging*. 2009;2:174-182
370. Rembert JC, Boyd LM, Watkinson WP, Greenfield JC, Jr. Effect of adenosine on transmural myocardial blood flow distribution in the awake dog. *The American journal of physiology*. 1980;239:H7-13
371. Berne RM, Rubio R. Regulation of coronary blood flow. *Advances in cardiology*. 1974;12:303-317
372. Sethna DH, Moffitt EA. An appreciation of the coronary circulation. *Anesth Analg*. 1986;65:294-305